THE STRATOSPHERIC RESIDUAL CIRCULATION AS DEDUCED FROM SATELLITE DATA.

STEPHEN REUBEN BEAGLEY

DOCTOR OF PHILOSOPHY

UNIVERSITY OF EDINBURGH

1989

CONTENTS

ACKNOWLEDGEMENTS

I wish to thank all the staff and students of the Meteorology Department at Edinburgh University for the enjoyable time I have spent amongst them all and for the assistance and support they provided during my period of study there. I would like in particular to thank my supervisor Dr R.S.Harwood whose support and interest in my thesis has helped me considerably. I would also like to thank Dr C.N.Duncan for his help and for my first research assistant post which allowed me to finish a large part of this thesis after the end of my grant.

Thanks go also to Dr A.O'Neill from the Meteorology Office at Bracknell for the use of the SSU data. I would also like to thank Dr J.Haigh for the use of the radiative heating code which was used in this study.

This research was funded by the NERC for the first three years of the work.

ABSTRACT

In two-dimensional modelling of the stratosphere, the residual circulation and the TEM equation re-formulation has been put forward as a more satisfactory analysis framework. This thesis uses satellite data principally from the LIMS and SSU instruments to examine the residual circulation for the period December 1978 to November 1979 and investigates what drives the circulation and how the various components and forcing mechanisms vary through the seasons and between the hemispheres. In particular the role of the eddy forcing, both time-averaged and transient, in driving the residual circulation and in the momentum and heat budgets is examined. The residual circulation has been examined in various forms. The circulation is calculated by the use of an omega equation, which is solved for Ψ, the residual streamfunction. The streamfunction being obtained from the momentum, thermodynamic and linear balance equations using a set based upon a quasi-geostrophic assumption suitable for spherical geometry. The linear partial differential equation for Ψ allows the various components of the circulation to be separately calculated and assessed. By this means it was possible to examine the relative importance of the eddy and diabatically forced components of the residual circulation. It was also possible to compare these various circulations together with a 'diabatic' circulation, based upon the approximations described by Dunkerton (1978), and to discuss the consequences upon the heat and momentum budgets, and upon the transport contributions of each of the circulations. Each circulation is a response or atmospheric readjustment resulting from the various forcing mechanisms which are tending to disturb the thermal wind balance of the zonal mean state.

The eddy driven circulations were seen to be important components of the total residual circulations evaluated and provided necessary contributions in the budgets of momentum and heat. The magnitude of the principal eddy forcing term ,D_F, has been shown to be large during several months and so must result in vigorous mixing which for a complete description of the total transport must be parametrized when use of a residual circulation is made in modelling. A number of important variations in seasonal behaviour and differences between hemispheres were observed which could have important consequences upon the transport of tracer quantities.

CHAPTER 1

GENERAL INTRODUCTION

1.1 : INTRODUCTION

Interest in the stratosphere has recently intensified, because of the intriguing complex interaction of chemistry, radiation and dynamics revealed by the analysis of global satellite data sets. The stratosphere has received attention not merely because of the many phenomena found there, but also because of the presence of a host of chemical species whose interaction and transport are of importance to the very existence of biological life on the Earth's surface.

Present interest has also increased because of the recent realization that human activities can possibly have serious effects on the stratospheric balance, which could lead to the deterioration of the protective ozone layer. Our understanding of many of the details of such a scenario where man's input to the stratospheric dynamical-radiative- chemical balance could be important, is poor. Therefore, in order that in the future we can examine such cases, it is necessary for our basic knowledge and modelling capability of the stratospheric circulation and photochemistry to be improved. Then, we can understand the natural system, without the added complication of man's perturbation upon it.

Three dimensional modelling of the whole stratospheric system is a enormous task if it is to include accurately all the interactions and feedbacks involved. Two-dimensional modelling, where the atmosphere is zonally averaged, has in the past provided a less sophisticated but more economical basis for examining the complex interrelationships.

A two-dimensional model averages the data zonally, so producing average latitude-height cross sections of the mean and eddy circulation components. The terms, mean and eddy, come from splitting every quantity in the following fashion.

$$\chi(\lambda) = [\chi] + \chi^{*}(\lambda) \qquad (1.1)$$

Where λ represents longitude, and the zonal mean is defined as

$$[\chi] = \frac{1}{2\pi}\int_{o}^{2\pi} \chi(\lambda)\delta\lambda \qquad (1.2)$$

Using this definition the zonal mean momentum, continuity and thermodynamic equations can be derived from the primitive equations. The equations thus derived however do not constitute a closed system; they contain terms which are mean products of eddy quantities such as $[v^{*}\theta^{*}]$ (the meridional eddy heat flux). These are non-explicit model variables. The resultant transport consists of advection by the Eulerian mean meridional circulation and of meridional and vertical fluxes due to zonally asymmetric motions, the so called eddy fluxes. For example:-

$$\left(\frac{\partial}{\partial t} + [v]\frac{\partial}{\partial y} + [\omega]\frac{\partial}{\partial p}\right)[\chi] = -\frac{1}{c}\left(\frac{\partial c[v^{*}\chi^{*}]}{\partial y}\right) - \frac{\partial[\omega^{*}\chi^{*}]}{\partial p} + [S] \qquad (1.3)$$

Where S is a source function for the quantity χ.

Some of the earliest descriptions of stratospheric transports were based upon observations of the distribution of chemical species. From such observations Brewer in 1949 suggested a circulation with rising motion only in the tropics, and descending motion at extra-tropical latitudes (See Figure F1.1b). Murgatroyd and Singleton (1961) presented the first calculated mean circulation for the middle atmosphere. They derived a circulation very much like the one suggested by the tracer studies, by solving the time and zonal average thermodynamic and continuity equations. The zonal average thermodynamic equation is (1.3) above, with $\chi=\theta$ and $S= Q\theta/c_{p}T$. They included diabatic heating in the thermodynamic equation but neglected the eddy heat flux divergence, thus ignoring the eddy momentum and heat fluxes entirely. The meridional circulation derived from that study is shown in Figure F1.1a. A few years later other observational studies including Vincent (1968)

produced circulations which were quite different from the one derived by Murgatroyd & Singleton (1961) or those deduced by the tracer studies. Vincent (1968) used the time and zonal average mean momentum and continuity equations to obtain the meridional circulation, retaining the eddy terms terms in the former equation. In particular rising motion was suggested at high latitudes in winter. (See figure F1.2a.) This type of circulation can be seen more easily and in more detail in Figure F1.2b from Cunnold et al (1975).

The studies by Brewer (1949) and Murgatroyd & Singleton (1961) are approximately measures of the net motion of individual air parcels, and hence Lagrangian motions, while the motions described by Vincent are mean circulations which are only part of the total transport. The Eulerian mean circulations, for example those of Vincent (1968), are valid circulations but they represent only part of the net transport and do not include the eddy portion of the transport. The mean and eddy transports act against each other and only when combined do we see the real net transport. The net motion is the sum of the mean circulation and the eddy terms. More importantly in the conventional Eulerian framework the net zonally averaged transport is generally the small residual of two large terms of opposite sign. These eddy terms arise due to the presence of wave motions in the stratosphere.

The eddy motions in the stratosphere consist primarily of ultra-long quasi-stationary planetary waves which are confined to the winter hemisphere. Additionally in the equatorial stratosphere there exists a special class of waves whose interaction with the zonal mean-flow produces the quasi biennial oscillation. The extra-tropical waves are not generated by in-situ instabilities. Rather, they appear to be waves generated in the troposphere by various mechanisms including orographic forcing and as a result of land sea contrasts. In addition to these stationary waves, the winter circulation features varying transient planetary waves which may occasionally interact to produce the so-called sudden stratospheric warmings. Consequently wave activity in the stratosphere, both climatologically and during a sudden warming, is primarily a result of waves from the troposphere. The influence of these waves upon the stratosphere and the manner in which they interact with the mean flow is a major area of research in the

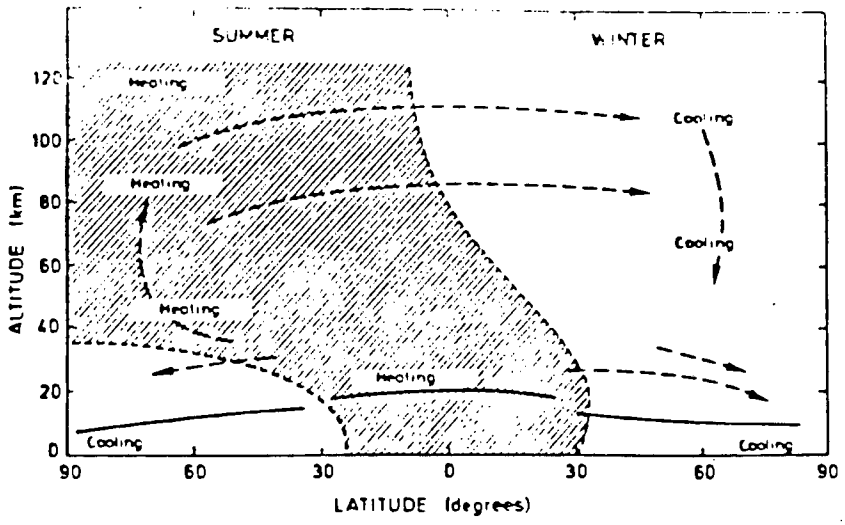

Fig. 1a Meridional circulation based on the study by Murgatroyd and Singleton (1961). From Murgatroyd (1971), copyrighted by Reidel Publishing Company.

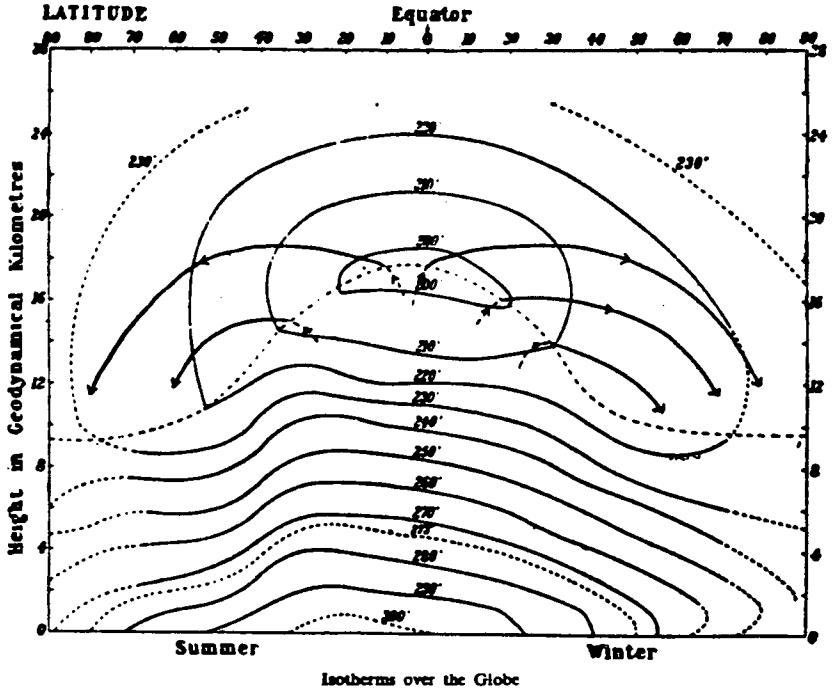

Isotherms over the Globe

FIG. 1b A supply of dry air is maintained by a slow mean circulation from the equatorial tropopause.

Figure F1.1 Meridional circulations of the atmosphere from (a) Murgatroyd (1971) and (b) Brewer (1949).

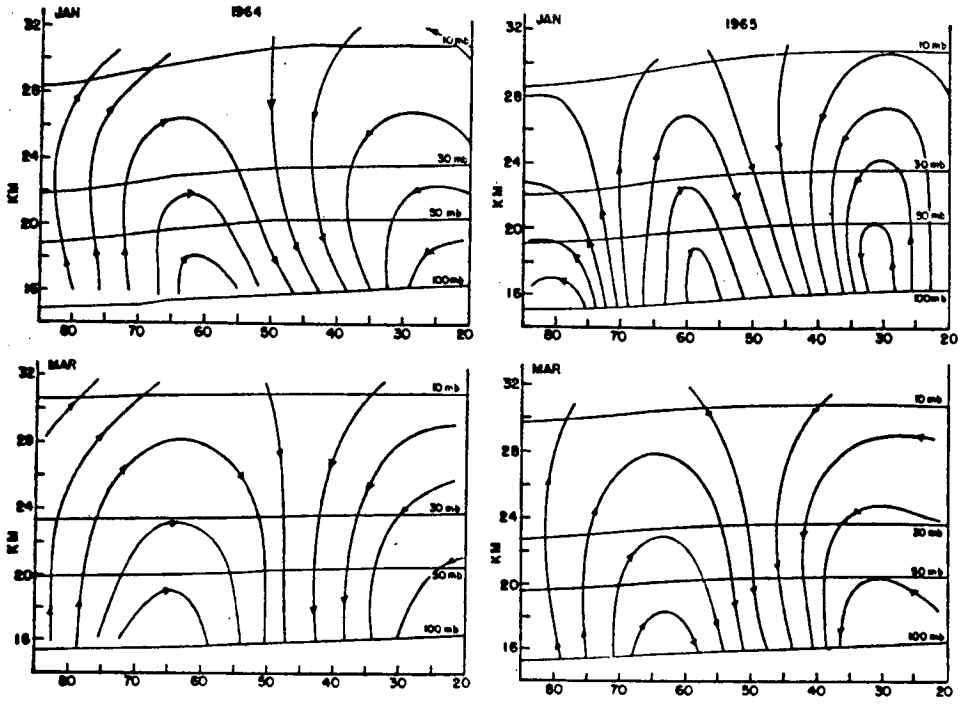

Figure a Flow patterns for mean meridional circulations.

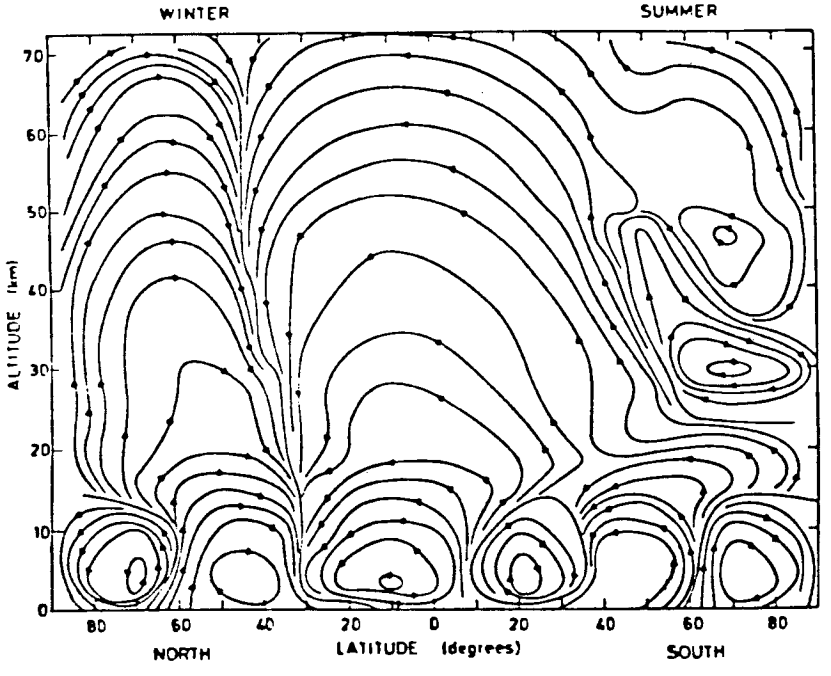

Fig. b Meridional circulation deduced by the theoretical study of Cunnold et al. (1975). (Copyright by the American Meteorological Society).

Figure F1.2 Eulerian-meridional circulations of the stratosphere from (a) Vincent (1968) and (b) Cunnold et al (1975)

stratosphere.

Stratospheric waves approximately satisfy what is referred to as the non-acceleration theorem, which implies no acceleration of the mean flow will occur. This states that if the planetary waves are steady, adiabatic and conservative then the presence of the waves will have no net effect on the mean circulation,(Andrews & McIntyre (1978a & b)). Under non-acceleration wave conditions an equivalent theorem for transport holds, known as a non-transport theorem, implying no net transport of tracer. These theorems describe the atmosphere only under these strict conditions but it is because a large fraction of stratospheric waves approximately satisfy the non-transport theorem that their eddy fluxes are closely balanced by advection due to the Eulerian mean circulation. This mutual compensation of convergences of tracer transport has been clearly illustrated in several numerical general circulation model simulations including Mahlman et al. (1980), showing that regions exist where a very large cancellation occurs; only a small difference is important and acts to produce the net transport. These studies also demonstrated the very important contributions of transient disturbances to the irreversible movement of heat and tracers into the stratospheric polar vortex essential to account for the time-mean structure of the thermal and tracer fields. The non-acceleration theorem, or rather the breakdown of it, provides a means of examination of the net circulation and the effect on the mean-flow due to wave motions. The traditional Eulerian averaging procedure, which is possibly the simplest separation into mean and eddy components, in the mathematical sense, does not measure the net circulation directly. Therefore it is not one of the best means of looking at the total flow. The Eulerian budget terms do not allow an easy interpretation of the net transport and the net heat and momentum budget influences. It would be more useful to find another method which takes explicit account of the near cancellation or eliminates this cancellation internally and only expresses the net transport. The eddy, mean-flow cancellation has long represented a difficulty for two-dimensional descriptions of stratospheric transport. Perhaps most importantly, it suggests that the mean and eddy transports are intimately coupled, and that a proper representation of atmospheric transport must employ an average circulation diagnostic

whose averaging procedure and therefore division of the flow into 'mean' and 'eddy' components is more compatible with the stratospheric circulation itself. The deduction of the qualitative sense of mass transport could instead be described by a Lagrangian viewpoint since the net transport circulation a Lagrangian concept. Such an approach makes the whole theoretical structure of the subject clearer and many workers have concluded that it can provide new insights, since it substantially simplifies and unifies our understanding of wave forcing where non-acceleration is violated. It would be natural to hope that the Lagrangian circulation could be used straight away and without too much difficulty. This is not however possible, as a number of difficulties exist and no immediate practical method of its application is at present viable. For these reasons Edmon et al. (1980) and Dunkerton et al. (1981) proposed the use of a new working variable, defined by Andrews & McIntyre (1976). The new mean meridional circulation's definition is obtained by re-formulating the Eulerian mean equations and including eddy terms in these definitions. The circulation, called the **Residual circulation**, is defined and discussed in detail in chapter 2. The equations thus derived are known as the Transformed Eulerian mean equations. It can be shown to be equal to a Lagrangian circulation in some special circumstances.

1.2 : AIM OF THIS WORK

The description of the wave, mean-flow interaction system and its accompanying meridional circulation poses difficulties in two- dimensional modelling due to its very nature as described above. The alternatives are not to model in two-dimensions and to examine the middle atmosphere by other means, or to find a more satisfactory mean circulation diagnostic system which has not the inherent problems of the traditional method.

The Residual circulation devised by Andrews & McIntyre (1976,1978), is just such a diagnostic. However it is necessary to clarify carefully the picture of what we understand as the residual circulation, by answering some fundamental questions: namely, What contribution does the residual circulation make to the total meridional transport of atmospheric trace species; when is its use valid; and more precisely what exactly does it represent in relation to a true Lagrangian circulation? Also what drives the residual circulation and how does this

vary through the seasons and between hemispheres? Also, what of transience, dissipation, breaking gravity waves and other frictional or sub-scale non-conservative mechanisms? This thesis addresses some of these questions.

The residual circulation is a fairly recent diagnostic and as a result, little is known of its variations and which forcing mechanisms are important to its existence. This thesis examines the residual circulation over a year, decomposing it into its component parts. Using the data obtained from the SSU & LIMS satellite instruments (see chapter 4), and FGGE data for the year December 1978- November 1979, the stratospheric circulation is calculated and hence a year's sequence of the residual circulation is examined and broken up into its component parts. This can be done as the residual circulation can be thought of as being forced by a number of separate mechanisms.

The necessity of parametrization does not disappear with the use of the residual circulation and the size of the remaining eddy terms will show up how important the modelling of such terms is and on what occasions they could be neglected. Parametrization technique and theory has not been dealt with directly in this thesis but the magnitudes of the terms which need to be parametrized are discussed in chapters 5 & 6.

1.3 STRUCTURE OF THE THESIS.

Using an observational study of the residual circulation, the consequences and importance of transient and dissipational effects on the stratospheric circulation and hence upon the transport of tracers are examined.

In Chapter (2) the concept of the residual circulation is introduced and the question of how accurately it is modelled by various approximations is discussed. In Chapter (3) the SSU, LIMS & other data sources will be introduced and their quality and usefulness examined. Then in Chapter (4) an explanation of the calculation method behind the decomposition of the residual circulation undertaken is given, and then goes on to describe some sensitivity tests and the aims of the circulation decomposition process. Chapter (5) will contain the main

results, in the form of various mean meridional circulations over the whole calculation period. In Chapter (6) these results and the other budget terms, together with other mean state and eddy forcing diagnostics, will be combined and used to investigate the transformed Eulerian mean (TEM) budget and the evolution of and importance of the wave, mean interaction effects upon the mean state and mean circulation throughout the study period.

CHAPTER 2

CURRENT DEVELOPMENTS.

2.1 : INTRODUCTION

The distributions of meteorological fields tend to contain a dominant zonal symmetry. This occurs as the planet is a relatively rapid rotating body. This rotation has a major influence upon the meteorological variables resulting in the vertical and latitudinal variations being the most dominant. This fact seen in observations has naturally lead early workers to take advantage of this and to concentrate their diagnosis and theory upon zonal mean quantities. The zonal mean average quantities are achieved by using the most straightforward Eulerian procedure of averaging around latitude circles. Together with the observed feature that the zonal structure is secondary in importance is the fact that the use of a two-dimensional model considerably reduces the scale and complexity of the task of correctly modelling and interpreting the physics, chemistry and dynamics of the atmosphere compared with a full three dimensional approach. The two-dimensional (2D) model therefore can provide a simplier tool to investigate certain aspects of the whole problem of understanding the atmosphere. However the usual 'Eulerian' mean averaging (e.g. with latitude and either height or pressure held constant) leads to a division into 'mean' and 'eddy' quantities which is in many respects artificial and unrelated to physical processes in the fluid. More recently alternative methods of averaging based on Lagrangian concepts have been developed which are more closely related to the fluid behaviour. The formulation of a Lagrangian mean technique for use as a description of the atmosphere has resulted in considerable clarification and improvement in the analysis of the effects of wave activity. The Generalised Lagrangian mean is basically another attempt to successfully subdivide and so identify the turbulent and the mean flow components. This or another alternative sub-division is being sought to provide a coordinate system consistent with the fluid behaviour such that both the changes in the zonal mean wind are directly related to the wave activity divergence and that a wave activity conservation equation can be obtained in this framework under finite amplitude conditions. Some kind of Lagrangian averaging appears

to be a more natural way of defining the mean state of the stratosphere, for use in two dimensional descriptions of models of tracer behaviour. The following sections review some of these methods.

2.2 : THE GENERALISED LAGRANGIAN MEAN. (GLM)

The simplest concept of a Lagrangian average is Stoke's classical idea of taking a time-mean following a single fluid parcel. For a space average, with a Lagrangian mean velocity defined at all points on a field then this idealised concept is not enough. The Generalised Lagrangian mean used, or compromise result, is no longer a pure Lagrangian description, it is a hybrid Eulerian- Lagrangian description of the motion. The GLM developed by Andrews & McIntyre (1978a) is such a Lagrangian description. McIntyre (1980a & b) reviews the general ideas of a Lagrangian viewpoint and the particular definition of the Generalised Lagrangian Mean. This can be described briefly as follows:

A Lagrangian average follows a chosen set of parcels and by averaging over this same set enables the calculation of a net mean flow. Each parcel position is described in terms of the vector fields $\underline{x}$ and $\underline{\xi}$, where $\underline{\xi}$ is a displacement field due to any disturbance in the motion and $\underline{x}$ is the position vector to which the average velocity is uniquely associated. To uniquely 'tie' the quantity obtained by averaging these parcel velocities along their trajectories, to a fixed point in space, a rigorous initial condition is necessary; otherwise the value will not be uniquely associated with just one fixed spatial point and hence parcel set. To achieve this one-to-one relationship between the disturbed parcels and their reference positions necessary for practical usage Andrews & McIntyre (1978a) used at time $t=t_o$ an undisturbed state such that the Lagrangian average and real trajectories intersect. On a sphere this undisturbed set represents a latitude circle. The averaging therefore eliminates any complete oscillatory disturbance component and the average velocity obtained, associated with the point $\underline{x}$, over the chosen actual velocities $u^{\xi}(\underline{x}+\underline{\xi})$ is $[u]^L$, the GLM velocity field. Evaluation of $[u]^L$ allows the motion of the initial undisturbed parcel set to be calculated and so the averaging procedure repeats and in the limit as the time interval over which the disturbance is considered tends to a small value a Lagrangian

velocity field is obtained.

The Lagrangian average can be related to a Eulerian average by defining the Stoke's drift terms $[V]^s$ & $[W]^s$ using equations (2.3) & (2.4).

$$[V]^L - [V] = [V]^s \qquad (2.3)$$

$$[W]^L - [W] = [W]^s \qquad (2.4)$$

The Stoke's drift terms introduced on the right-hand side of (2.3) & (2.4) above describe the difference between the Lagrangian and conventional Eulerian mean averages. These express the correction to the Eulerian mean arising from displacements through disturbance-associated gradients. A 'Stokes correction' can be found for each mean field.

The principal advantage of the Lagrangian viewpoint can be seen by considering the rate of change of a variable X following an air parcel.

$$\frac{DX}{Dt} = Q_x \qquad (2.5)$$

The Eulerian version of the zonal mean of equation (2.5) is:

$$\left(\frac{\partial}{\partial t} + [v]\frac{\partial}{\partial y} + [\omega]\frac{\partial}{\partial p}\right)[X] = \frac{1}{c}\frac{\partial}{\partial y}[v^* X^* c] - \frac{\partial}{\partial p}[\omega^* X^*] + [Q]_x \qquad (2.6)$$

The Lagrangian mean version of (2.5) takes the simple form

$$\left(\frac{\partial}{\partial t} + [v]^L\frac{\partial}{\partial y} + [\omega]^L\frac{\partial}{\partial p}\right)[X]^L = [Q]^L_x \qquad (2.7)$$

This equation has no eddy flux terms on the right, thus avoiding the indirectness of equation (2.6) and the cancellation between the mean and eddy terms. These equations, (2.6) & (2.7), together with the fact that the Lagrangian advective flow will be zero for steady, conservative wave motion, highlight the fact that the effects of wave or eddy motion on net heat and tracer transport are necessarily bound up with departures from conservative motion. These departures entail

the appearance of some quantity $[Q_x] \neq 0$ on the right-hand side of (2.6) and a corresponding $[Q_x]^L$ on the right of (2.7). Thus eddy motions effect $[X]^L$ but only in so far as they promote mixing or other departures from conservative motion(McIntyre (1980)).

Unfortunately the GLM theory cannot be applied straightforwardly to the stratosphere as there are a number of difficulties which prevent its immediate application as a practical diagnostic tool. Conceptual difficulties arise with the practical use of the average because of large parcel dispersion during large amplitude wave events.

2.3 : THE TRANSFORMED EULERIAN MEAN FORMULATION, (TEM).

2.3.1 : DEFINITION OF THE TRANSFORMED EULERIAN MEAN OR RESIDUAL CIRCULATION

The TEM meridional circulation or 'residual circulation' is defined as follows:

$$[v]^R = [v] - \frac{1}{\varrho}\frac{\partial}{\partial \eta}\left(\varrho [v^* \theta^*]/[\theta]_\eta\right) \qquad (2.8)$$

$$[w]^R = [w] + \frac{\partial}{\partial y}\left([v^* \theta^*]/[\theta]_\eta\right) \qquad (2.9)$$

(a) (b) (c)

The transformed Eulerian mean (TEM) equations, of Andrews & McIntyre (1976,1978a) are potentially a marked improvement over the Eulerian system. The TEM approach has a number of practical and conceptual advantages. Firstly it should be closer to the fundamental Lagrangian mean description of the atmosphere than is the standard Eulerian mean formulation and secondly the transformation which defines the residual circulation can always be obtained whereas the Lagrangian mean averaging procedure becomes impractical to apply when waves grow to large amplitude. In the definition of the residual circulation components above, the terms (c) in (2.8) & (2.9), are approximations to the Stokes drift terms in equations (2.3) and (2.4). However the exact relationship between these terms and the degree to which the approximation holds is complex and will be discussed in more detail in section (2.8.1). Since the residual circulation is an approximation to the Lagrangian circulation our attention must be drawn to the examination of the similarities and differences between the Stokes drift terms of equations (2.3) & (2.4), and the (c) terms of equations

(2.8) & (2.9). The transformations which produce the residual circulation components reveal a circulation which incorporates the atmosphere's eddy-mean compensation. This is achieved by subtracting the gradients of the meridional eddy heat fluxes from the Eulerian mean meridional velocities and so the new diagnostic will be closer to the zonally averaged net transport circulation due to the small residue which results from the cancellation between the eddy and mean terms in the Eulerian averaging framework.

The principal flow component of the TEM circulation (in a cartesian and log-pressure coordinate system) is a thermally direct circulation with air rising in regions of net diabatic heating and sinking in regions of net diabatic cooling. (Garcia & Solomon (1983)). This is in marked contrast to the results obtained using the Eulerian mean formulation and it is more in accord with the actual motion of air parcels.

2.3.2 : THE TEM EQUATIONS.

The TEM circulation components, $[w]^R$ and $[v]^R$, contain eddy terms, and by the addition of these terms into the definition of the mean meridional velocities the mean flow equations are simplified considerably, especially when a quasi-geostrophic assumption on a beta-plane is used. i.e.

$$\frac{\partial [u]}{\partial t} - f[v]^R = \frac{1}{\varrho_o} \mathrm{div} F + [F_r]$$

$$= -\frac{\partial}{\partial y}([u^* v^*]) + \frac{f}{\varrho_o} \frac{\partial}{\partial \eta}\left(\varrho_o \left[v^* \frac{\theta^*}{[\theta]_\eta}\right]\right) + [F_r] \qquad (2.10)$$

$$\frac{\partial \theta}{\partial t} + [\theta]_\eta [w]^R = [Q]\left(\frac{p}{p_o}\right)^\kappa \qquad (2.11)$$

The TEM equations retain the advantage of an equation set without eddy flux terms except for unsteady or non-conservative motion. So if non-acceleration conditions hold, the planetary wave motion will have no effect on the mean meridional circulation, or on the distribution of inert chemical constituents. The TEM equations have also the advantages of not depending on any special assumptions concerning wave amplitude, transience or dissipation and if modelled totally can be used to diagnose the mean state changes as well as the transport.

2.4 : EULERIAN OR LAGRANGIAN AVERAGING

As the TEM is not truly Lagrangian in nature, the parcels it averages over are not the same but are changing due to the fixed coordinates. The Lagrangian average fixes its parcels and an average is taken of their changing velocities and properties. Subsequently then a new undisturbed latitudinal ring of parcels at the new position determined by the Lagrangian average velocity, $[u]^L$, is used and so the process repeats. So the residual circulation will generally be different from the Lagrangian because of this fundamental difference in the nature of the averaging process. Only during non-acceleration conditions are the two trivially the same and both equal to zero. Any Eulerian mean is calculated at a fixed point in space and so averages properties of different parcels passing through this chosen point. The subtraction or addition of the 'residual extra terms', terms (c) in equations (2.8) & (2.9), in effect are an attempt to represent the wave displacement of the parcels contribution to the new average measure, although this may not have been the original motivation.

2.5 : THE NON-ACCELERATION THEOREM.

The eddy motions in the stratosphere consist of principally

i) Ultra-long quasi-stationary planetary waves,

andii) Transient planetary waves,

both of which are principally observed in the winter hemisphere. The presence of other waves such as gravity waves and equatorial waves are also important. The influence of these waves upon the stratosphere and the manner in which they interact with the mean flow is a major area of research in the stratosphere. One area of initial difficulty lies in the fact that not all waves have a net effect on the mean-flow. The rather idealised theoretical steady, non-dissipating, conservative planetary waves do not modify the mean-flow and it is only when the waves deviate from the steady, conservative non-dissipating conditions that the waves interact with the mean-flow and decelerate or accelerate the mean-flow. These consequences were first formally stated by Eliassen and Palm (1960) and Charney & Drazin (1961), who produced the non-acceleration theorem. Eliassen & Palm (1960), in a paper on the transfer of energy in stationary mountain (two-dimensional gravity) waves, showed that for

waves of steady amplitude in the absence of dissipation and critical levels, $\varrho_o [u^* w^*]$, the vertical flux of horizontal momentum, is independent of height. Charney & Drazin (1961) showed that it is possible to conclude that the second order changes in the zonal flow vanish identically. Charney & Drazin formalized this as a theorem which states that for stationary, linear, conservative, small amplitude waves outside regions of horizontal shear in the zonal current the second-order changes in the zonal flow are zero. There is no mean-flow variation even in the presence of these waves. They add however that the cases when the conditions for the theorem do not hold appear to be the most interesting, if one is to account for the trapping of energy in the stratosphere when the induced upper atmosphere circumpolar vortices are weak.

Andrews & McIntyre (1976) have produced a generalization to three dimensions of the theorems of Charney & Drazin (1961), Dickinson (1969a) and Holton (1974), on the forcing of the mean-flow, by conservative linear waves. The theorem states that for steady, frictionless, adiabatic, non-dissipating planetary waves of small amplitude propagating in a basically zonal flow, the waves can exist but cannot change the zonal mean fields. Their second-order influences in wave amplitude, the wave induced meridional circulations and the eddy flux convergences due to the waves, exactly cancel. The use of residual circulation and the TEM equations can be further shown as advantageous by considering the equations under the conditions of non-acceleration. The non-acceleration theorem has been already discussed, but here it is worth examining the theorem in more detail with the use of the residual circulation. The relationship between the eddy momentum and heat fluxes and the net effect of the eddies on the zonal mean state, is easiest to see from the transformed mean-flow equations (2.10) & (2.11), presented by Andrews & McIntyre (1976) using the quasi-geostrophic approximation. They show that within the quasi-geostrophic approximation div.F represents the sole internal forcing of the mean state by the wave disturbances. It is then readily seen from equations (2.10) & (2.11) that if div.F, $[F_r]$ and $[Q]$ all vanish the equations result in a steady mean state in which $[u_t]$, $[\theta_t]$, $[v]^R$ and $[w]^R$ are all zero. This is Charney and Drazin's non-acceleration theorem. Thus F is an important wave

diagnostic which has the fundamental advantage that its divergence is zero under non-acceleration conditions.

This simplified explanation of the non-acceleration theorem is further seen through the quasi-geostrophic potential vorticity theory. (Dickinson 1969a). div.F is related to the northward quasi-geostrophic potential vorticity flux in a well known way, and hence (Dickinson 1969a) to the equation governing the zonal mean of the quasi-geostrophic potential vorticity, [q]. For spherical geometry the relationship is simply:

$$\frac{\nabla . F}{a\varrho c} = [v^* q^*_{(m)}] \qquad (2.12)$$

Where the quasi-geostrophic quantity $q^*_{(m)}$, a modified eddy potential vorticity is defined by:

$$q^*_{(m)} = v^*_x - f/c(cu^*/f)_y + f(\theta^*/(\varrho[\theta]_\eta))_\eta \varrho \qquad (2.13)$$

from Palmer (1982).

All dynamical processes through which quasi-stationary Rossby waves influence the mean circulation in the stratosphere and mesosphere can be elucidated through consideration of the potential vorticity conservation. According to the zonal mean quasi-geostrophic potential vorticity equation:

$$\frac{\partial [q]}{\partial t} = - \frac{\partial}{\partial y}[q^* v^*] + [S] \qquad (2.14)$$

Where $v^* = \frac{\partial \psi}{\partial x}$, and ψ is the geostrophic streamfunction.

In the absence of mean sources and sinks ([S]=0), [q] can only be changed if there is a meridional flux of eddy potential vorticity, $[q^* v^*_\psi]$. In other words as shown by Dickinson (1969a), it is necessary to transport potential vorticity by the eddies in order to force a zonal flow. Hence the equality expressed by equation (2.12) illustrates the importance of div.F as a wave, mean acceleration term. If div.F is

zero then the quasi-geostrophic equations permit a steady mean state. Under these conditions $[\omega]$ & $[v]$ are not necessarily zero nor are $[u^* v^*]$ & $[v^* \theta^*]$, and so steady state conditions can arise with non-zero eddy fluxes and Eulerian meridional velocities, which is one reason for some of the interpretational difficulties of early Eulerian studies.

Quasi-stationary Rossby waves not only transport potential vorticity and hence drive changes in the mean-flow, but also transport trace constituents such as ozone. Processes such as transience and dissipation are the primary mechanisms for producing the eddy flux of quasi-geostrophic potential vorticity and their absence results in no forcing of the mean-flow by the waves. In these circumstances a similar non-transport theorem analogous to the non-acceleration theorem can be shown to exist. This also indicates that the net transport of tracer will also suffer from the interpretational confusion of a Eulerian viewpoint with its associated mutually-compensatory eddy fluxes and Eulerian meridional circulation. Calculations of the net transport require alternative viewpoints such as the TEM equations or the generalised Lagrangian mean formalism.

2.6 : THE DIABATIC CIRCULATIONS.

Various authors have presented the point of view that in two-dimensional modelling, the Lagrangian circulation can be approximately represented in their models by the diabatic circulation. e.g. Holton & Wehrbein (1980a), & Matsuno (1980). The diabatic circulation referred to is defined as the circulation which balances the net radiative heating of the atmosphere under steady state conditions. However the diabatic circulation is also a measure of the existence of the various forms of wave, mean interaction mechanisms which influence the stratosphere. Fels (1985) explains the stratospheric interaction and balance (this idea can be traced back at least to Dickinson (1969a)) as a system forced away from radiative equilibrium which is acting 'like a spring' to re-align the atmosphere as a purely radiatively dominated regime but this is stopped by the action of the waves of various scales, including both planetary and gravity waves, which force the atmosphere away from the 'springs relaxed state'. Hence the atmospheric 'spring' remains in a tense and stretched state which gives

rise to diabatic forcing. Without dynamical forcing the atmosphere would have only a small diabatic component changing insolation conditions and so would be close to radiative equilibrium. Therefore the diabatic forcing is present largely due to the dynamics. The diabatic circulation is calculated from a knowledge of the net radiative heating and cooling only. Hence the diabatic circulation is indirectly influenced by eddy forcing.

Early attempts to model the general circulation only used fields of net radiative heating rates to compute the meridional circulation by assuming the adiabatic cooling of the vertical velocity field exactly counterbalanced the radiative heating. This type of model however is based entirely upon the heat balance considerations and no attempt is made to determine whether such a circulation results in a consistent momentum transport balance. In this type of model the eddy fluxes due to planetary waves are neglected.

Holton & Wehrbein (1980a) have examined such a model. They stressed that it is a diabatic circulation not the total Eulerian mean which is being modelled. It is clear from the introduction that the idea is to illustrate to a first approximation, the validity of using this circulation as a description of the Lagrangian total circulation. Holton & Wehrbein (1980a & b), argue for the use of the diabatic circulation as the stratospheric net circulation, based upon the similarity of the non-acceleration condition results, with observed real stratospheric zonal-mean flow profiles.

In the first paper a diabatic (i.e. radiatively driven) circulation is used based upon the assumptions and approximations of Dunkerton (1978); while in the latter, eddy right-hand side terms are included using a highly truncated zonal representation of the wave forcing and a residual circulation is evaluated. The Dunkerton diabatic circulation is similar to that calculated by Muragtroyd & Singleton (1961) but the latter retains the $\delta T/\delta t$ and $v\delta T/\delta y$ terms in its thermodynamic equation when computing their meridional circulation using a combination of the thermodynamic and continuity equations. They found that for

steady solstice conditions to a first approximation the 'other forcing terms' (i.e. non-linear terms and dissipation) in the zonal mean momentum and thermodynamic equations are of secondary importance and that the residual mean vertical velocity just balances the diabatic heating Q and may be identified as the diabatic circulation. Since steady wave solstice conditions are assumed, the eddy fluxes of heat and momentum are neglected. This diabatic circulation can be defined more precisely; as per Dunkerton (1978). This paper showed, using a scale analysis of the thermodynamic equation for similar quiet solstice conditions, that the Lagrangian mean-flow could be approximated using only the diabatic forced residual circulation. Dunkerton's method employs the thermodynamic equation and the equation of continuity as in Murgatroyd & Singleton (1961).

$$\underset{(a)}{\frac{\partial [T]}{\partial t}} + \underset{(b)}{[v]\frac{\partial [T]}{a\partial\varphi}} + \underset{(c)}{(\Gamma_d - \Gamma)[W]} = \underset{(d)}{[Q]} - \underset{(f)}{\frac{1}{\varrho}\frac{\partial}{\partial z}(\varrho_o [W^* T^*])} \underset{(e)}{-\frac{1}{ac}\frac{\partial}{\partial\varphi}([v^* T^*]c)} \qquad (2.15)$$

$$\frac{1}{ac}\frac{\partial}{\partial\varphi}([v]c) + \frac{1}{\varrho_o}\frac{\partial}{\partial z}(\varrho_o [W]) = 0 \qquad (2.16)$$

{equations (2.1) & (2.2) of Dunkerton (1978)}

Equation (2.15) is then simplified using several approximations. Principally these involve assuming solstice conditions (i.e. $\partial[T]/\partial t \approx 0$), which are also considered to involve only steady and conservative waves, as all winter wave activity is assumed to have no effect upon $\partial[T]/\partial t$. It also involves the neglect due to scale considerations of the terms (b) and (f) in equation (2.15). Thus equation (2.15) is reduced to:

$$(\Gamma_d - \Gamma)[W] = [Q] - \frac{1}{ac}\frac{\partial}{\partial\varphi}([v^* T^*]c) \qquad (2.17)$$

Using the definition of the residual circulation (see equations (2.8) & (2.9)) it is possible to write (2.16) & (2.17) as

$$(\Gamma_d - \Gamma)[W]^D = [Q] \qquad (2.18)$$

$$\frac{1}{ac\partial\varphi}([v]^D c) + \frac{1}{\rho_o}\frac{\partial}{\partial z}(\rho_o [W]^D) = 0 \qquad (2.19)$$

Thus we can define an alternative diabatic circulation here labelled as $[W]^D$ & $[v]^D$, which are described by Dunkerton as approximations to the residual circulation $[W]^R$,& $[v]^R$. Thus $[v]^D$ and $[W]^D$ may be obtained directly from a knowledge of the diabatic heating and static stability only. Matsuno (1980) shows that the Lagrangian mean velocities agree fairly well with the velocities expected from radiational balance.

The approximate balance

$$[W]^L = [W]^D = [Q]/(\Gamma_d - \Gamma) \qquad (2.20)$$

then holds in a steady state and appears to be a good approximation under such circumstances. Contrary to this notion Holton & Wehrbein (1980b) examined a residual circulation containing both eddy and diabatically driven components which showed that during conditions of wave damping and transience the simplicity of using the first approximation of the mean meridional circulation, the diabatic circulation, is no longer sufficient to describe the total circulation and the circulation differs significantly from the total circulation observed and modelled. The vertical velocity pattern becomes more complicated involving indirect cells at high latitudes in both hemispheres. The Dunkerton-diabatic form of circulation, is based upon the inherent assumption of rapid readjustment of the atmosphere by any momentum forcing, so that $[u_t]$ and $[\theta_t]$ remain small and the momentum balance takes care of itself. Obviously this type of circulation cannot be used to diagnose the mean state changes and its calculation is based upon a knowledge of [Q] from observational data external to the model. The 'Dunkerton-diabatic' circulation assumes a steady state balance and thereby includes all the eddy effects which are included in the observed data used in its calculation. This diabatic circulation as defined earlier is clearly not the same as the diabatically driven circulation component and the two must not be confused. The basic difference in definition and the physical processes involved in driving the circulations are shown later in this study to produce considerable

differences in the magnitudes of the two circulations.

Pyle & Rogers (1980a) have found that exclusion of eddies in both the calculation of the mean circulation and the trace gas species continuity equations results in a failure to reproduce the observed trace gas distribution. The circulation used in Pyle & Rogers (1980a) is the residual circulation component driven by [Q] only and as such ignores the effects of eddy forcing. The transport of the residual circulation is enhanced over that of a purely diabatically driven circulation, by the effects of transience and dissipation; the enhancement being especially pronounced and the transport being greater, at high latitudes in winter. Ignoring the eddy terms eliminates the need for parametrization and the extra eddy driven component of the circulation. Inclusion of transient and/or damped waves however results in a contribution to the momentum and tracer continuity equations via eddy processes. The TEM quasi-geostrophic eddy momentum term, div.**F**, if retained in equation (2.10), is smaller than its Eulerian counterpart, the eddy convergence term. The size difference is due to the removal of a large portion of the Eulerian fluxes under circumstances where the eddy flux and mean flow convergence's largely cancel. However, Andrews et al (1983) found that div.**F** is not always negligible resulting in a small residual difference between $-[u^* v^*]_y$ and $(f_o [v^* \theta^*]/\theta_p)_p$. In the stratosphere and lower mesosphere of their model the two components did tend to take opposite signs but in the upper mesosphere they tended to be of the same sign. Care must therefore be taken with these statements as a precise knowledge of the real relative sizes of the above components under varied conditions throughout a year say, is not known. In Hess & Holton (1985) it is shown that the approximation of the residual transformation is only helpful in producing a better approximation to the Lagrangian under certain conditions and will under some circumstances fail to improve our interpretation of the dynamics. Events such as sudden warmings do occur, when the zonal-mean flow changes calculated from any of the diabatic circulation budgets will not be the same as the observed zonal-mean flow changes. Under these circumstances both the residual circulation driven only by the diabatic forcing and the 'Dunkerton-diabatic' circulation fail to reproduce the changes in [θ] and [u]. Both $[\theta_t]$ and $[u_t]$

throughout the events are not negligible and so the steady state balance does not always occur. Hence on particular occasions the dynamical influence of the forced wave disturbance contributes significantly. The frequency and seasonal behaviour of these events would therefore be a valuable indicator to the validity of the 'Dunkerton-diabatic' circulation as a first approximation to the residual stratospheric mean meridional circulation.

A final point which makes the use of the 'Dunkerton-diabatic' circulation as a description of the Lagrangian circulation appear more acceptable and which will be expanded upon in more detail later in section (2.9.1), involves the apparent paradox observed by Mahlman et al (1980) who showed that the 'Dunkerton-diabatic' circulation cannot exist independently of the wave mean interaction and non-conservative influences. Thus the 'Dunkerton-diabatic' circulation which is observed to resemble the Lagrangian is partly driven by the deceleration mechanisms. i.e. transience and dissipation. The atmosphere drives a diabatic circulation in order to maintain this new equilibrium. This circulation cannot be explained purely by the radiative diabatic forcing which a model neglecting eddy forcing, and therefore using a diabatically driven component circulation, would use to calculate the mean circulation. Any subsequent predictions of tracers and the mean state from such a model would be incorrect.

2.7 : BREAKDOWN OF THE NON-ACCELERATION THEOREM.

The area of principle interest due to the consequences in terms of transport and forcing is during conditions when the non-acceleration theorem breaks down and a whole host of poorly understood and complex processes are involved. The theory of wave, mean-flow interaction may be described under two grand headings, namely 'wave dissipation' (departures from conservative motion) and 'wave transience' (departures from purely harmonic motion, such as wave growth and decay). Dissipation and transience can arise from several processes e.g. instability, variable wave propagation, wave-wave interaction or interference, and the presence of non-conservative effects. The study of individual mechanisms of breakdown is important and should be undertaken but we are concerned with a general view and subdivision of the individual forcing mechanisms has not been undertaken in this

study.

Consider the time-averaged quasi-geostrophic two-dimensional TEM equations with their eddy flux terms split into time-average and transient flux components.

$$\frac{\partial [u]}{\partial t} - f[v^R] = \underbrace{-\frac{\partial}{\partial y}[u^* v^*]}_{(A)} + \underbrace{\frac{f}{\varrho_o}\frac{\partial}{\partial \eta}\varrho_o\left(\frac{\overline{[v^* \theta^*]}}{[\theta]_\eta}\right)}_{(B)}$$

$$\underbrace{-\frac{\partial}{\partial y}[u'^* v'^*]}_{(C)} + \underbrace{\frac{f}{\varrho_o}\frac{\partial}{\partial \eta}\left(\varrho_o \frac{\overline{[v'^* \theta'^*]}}{[\theta]_\eta}\right)}_{(D)} \qquad (2.21)$$

$$\frac{\partial [\theta]}{\partial t} + [v^R]\frac{\partial [\theta]}{\partial y} + [w^R]\frac{\partial [\theta]}{\partial \eta} = [Q]$$

$$-\frac{\partial}{\partial \eta}\Big(\varrho_o \frac{\partial [\theta]}{\partial y}\Big(\underbrace{[v^* \theta^*]}_{(A)} + \underbrace{[v'^* \theta'^*]}_{(C)}\Big)\Big/\frac{\partial [\theta]}{\partial \eta}$$

$$+ \Big(\underbrace{[w^* \theta^*]}_{(B)} + \underbrace{[w'^* \theta'^*]}_{(D)}\Big)\Big)\Big)/\varrho_o$$

(2.22)

The eddy flux terms on the right hand side of equation (2.21) & (2.22) represent the total effects of wave transience and dissipation. The eddy terms have been split into their time-averaged, terms (A) & (B), and their transient flux components, terms (C) & (D). This separation is intended as a simple means of identifying transience. The transient component is obtained as a perturbation or eddy from a time mean and so the transient fluxes are evaluated as covariances of variable perturbations in time. The transience so calculated is a statistical measure of all unsteady flux contributions and not just as a result of forcing mechanisms which produce or destroy planetary waves and so lead to irreversible heat and momentum transport.

The essential aspect of the theoretical concept of transience which is required to be identified is the component of the time variation which leads to permanent increase in particle dispersion. The partition achieved by the mean and time transient fluxes used in equations (2.21 & 2.22) will not measure just the irreversible transience as described

above. It will only provide an indicator of the degree of variability and therefore extent and importance of the transient mechanisms. The eddy flux separation in equations (2.21 & 2.22) are incorrect due to a number of reasons so that the statistical measures of transience calculated differ from a correct measure of net irreversible transience. Part of this difference arises due to the presence of travelling waves and part is due to the averaging period dividing longer period contributions between the transient and stationary statistical measures components. Any growing or decaying stationary wave is split into a steady and transient components and will contribute to both the steady and transient averaged eddy fluxes. Also, any travelling waves that do occur (even if their occurrence is of slight importance) will be divided, contributing flux to both transient and stationary statistics and so is misinterpreted, being shared between the two fluxes, as above. Also, these statistical values will include trends due to longer term effects such as the variation of diabatic heating as the seasons progress. So, the transient and stationary eddy flux terms represent the influence of all these effects, correct and incorrect contributions, including irreversible transience plus these other additional contributions to the statistics. The values are therefore measures of the time-average and transient eddy flux terms arising because of all the temporal variability present in the atmosphere throughout the month and must be interpreted bearing this in mind. Transience will be measured as the remaining time varying amplitude component of a wave not tied down to any specific mechanisms. i.e. wave propagation, wave-wave interaction, internal gravity waves, etc.

A better separation more consistent with the various mechanisms is needed, at least to complement the present method. No attempt to provide an alternative separation is made in this thesis. It poses the problem of a wrong viewpoint if we cannot understand the driving influences behind these zonally and time averaged statistics.

Observational evidence (Hirota & Sato 1969) indicates that planetary waves in the winter stratospheric hemisphere undergo quasi-periodic oscillations with time scales of the order of two weeks. For winter to summer the seasonal march of the wave activity and the mean zonal

wind is different for the two hemispheres. For such cases the non-steadiness of the waves may significantly influence the wave-zonal flow interaction dynamics in the stratosphere. The neglect of transience and dissipation results in an assumption of complete 'stationarity' of the wave conditions of the wave forcing which by the non-acceleration theorem will not produce changes in the mean state. However the diabatically driven circulation, the only circulation component which arises when this assumption is made, if used in models as an approximate net circulation is not a complete representation of the total net circulation. This is because it is forced only by [Q] and so the circulation and [Q] are not being modified by the eddy forcing which directly and indirectly changes the total circulation as the system evolves. Such a flow, where the momentum forcing is neglected exhibits an imbalance in the momentum equation as there will be a torque due to the diabatically driven meridional circulation component which if div.F is assumed zero will produce large $[u]_t$ significantly changing the zonal wind and hence other mean state fields. This type of modelled flow will eventually tend to an approximate radiative equilibrium temperature and wind structure in a model calculation which contains both momentum and heat balances. The lower stratosphere is not in radiative balance and the presence of waves propagating into the area, including transient waves, act as a source of energy for the region. The temperatures which result from neglecting eddy transports in models are therefore quite different from those observed as such models lack a mechanism to decelerate the zonal winds and so produce a realistic picture. Several studies including Schoeberl & Strobel (1978) state the requirement of some mechanism of deceleration of the zonal winds to explain the real atmospheric structure.

Since conservative stationary waves, the dominant wave motions in the stratosphere, do not accelerate the mean-flow then wave transience and dissipation is important. This may occur on odd occasions or as a small continuous effect. The exact role of transience throughout the year on the mean flow, the meridional circulation and upon the transport of trace species must be investigated either to confirm the assumptions which allow its neglect or to explain its importance and so its incorporation in models of the stratosphere. This means we must fully understand the extent and

importance of transience in influencing not only the mean state but also our chosen meridional circulation diagnostic.

2.8 : THE RESIDUAL CIRCULATION.:

2.8.1: ITS RELATION TO REAL PARCEL MOTIONS.

It is important to consider how accurately the residual circulation models the Lagrangian circulation and to more precisely relate the two circulations. The eddy contributions to $[V]^R$ and $[W]^R$ are approximately Stokes drift terms to a first order in wave amplitude (in the non-acceleration limit). Here we will expand on this statement and attempt mathematically to describe the link between the terms, following Matsuno & Nakamura (1979), Schoeberl (1983), Andrews & McIntyre (1978a & b) and McIntyre (1980a & b).

We can write

$$\chi^{\varepsilon}(x,t) = \chi(x+\varepsilon(x,t),t). \qquad (2.23)$$

In particular $\chi=V$ then the point at $x+\varepsilon$ travels at an actual fluid velocity of V^{ε}. For small amplitude disturbances χ may be expanded using a Taylor's series giving

$$\chi^{\varepsilon} = [\chi] + \chi^{*} + \varepsilon_j \chi_{,j} + 0.5*\varepsilon_j \varepsilon_k [\chi]_{,jk} + O(a^3) \qquad (2.24)$$

The above and following equations use tensor notation where $(\,)_{,i} = \partial(\,)/\partial x_i$ and $(\,)_i$ is tensor notation for a vector and multiple subscripts use the tensor conventions of summation and free indices.

Applying a zonal average operator this becomes

$$[\chi]^{s} = [\varepsilon_j \chi^{*}]_{,j} + 0.5*[\varepsilon_j \varepsilon_k][\chi]_{,jk} + O(a^3) \qquad (2.25)$$

For χ= V and W then Matsuno & Nakamura (1979) have shown that [V] and [W] which are forced by the planetary waves are of $O(a^2)$, in wave amplitude, effects. So the second term on the right is $O(a^4)$ and can be neglected.

Thus

$$[V]^{L} = [V] + [V]^{s} = [V_j] + [\varepsilon_j V^{*}_{,j}] = [V] + [\varepsilon \nabla . V^{*}] \qquad (2.26)$$

Equation (4.5) Matsuno & Nakamura (1979). (Note that the last term on the right of equation (2.26) is only an approximation to the Stokes drift term as it is not correct for sheared flows. See

(see Andrews & McIntyre (1978b)).

The next step in relating the terms involves providing a relationship between $\boldsymbol{\varepsilon}$ and the Eulerian perturbation velocity components. Such a relationship is provided by equation (4.6) in Matsuno & Nakamura(1979). However Matsuno & Nakamura (1979)'s equations are obtained by redefining $\boldsymbol{\varepsilon}$, using the kinematical relation below.

$$\left(\frac{\partial}{\partial t} + \mathbf{V}_o \cdot \nabla \right) \boldsymbol{\varepsilon} = \mathbf{V}(\mathbf{x}+\boldsymbol{\varepsilon}) - \mathbf{V}_o(\mathbf{x}) \qquad (2.27)$$

Equation (2.27) can be compared with the expression of Andrews & McIntyre(1978a).

$$\left(\frac{\partial}{\partial t} + [\mathbf{V}]^L \cdot \nabla \right) \boldsymbol{\varepsilon} = \mathbf{V}(\mathbf{x}+\boldsymbol{\varepsilon}) - [\mathbf{V}]^L(\mathbf{x}) \qquad (2.28)$$

There are a number of differences between equations (2.27) and (2.28). Since $\mathbf{V}'$ is defined as $\mathbf{V}-\mathbf{V}_o$ then $\mathbf{V}_o$ is equivalent to $[\mathbf{V}]$. Of the terms missing from (2.27) $\mathbf{V}^s$ is $O(a^2)$ and $-\mathbf{V}^s.\nabla\boldsymbol{\varepsilon}$ is $O(a^3)$. So $\boldsymbol{\varepsilon}$ is only $O(a)$ accurate in (2.27). This is satisfactory as $\boldsymbol{\varepsilon}.\nabla\mathbf{V}$,(from 2.26), is required only to be $O(a^2)$ accurate. Using equation (2.27) it is possible to write relationships between the displacement fields and the Eulerian perturbation velocity fields. Rood & Schoeberl (1983) have used these and have shown that the meridional Lagrangian velocity components, $[V]^L$ and $[W]^L$, can be written as:

$$[V]^L = [V] + \frac{1}{\rho}\frac{\partial}{\partial z}[\rho V^* \varepsilon] \qquad (2.29)$$

$$[W]^L = [W] - \frac{\partial}{\partial y}[V^* \varepsilon] \qquad (2.30)$$

Thus the correction terms for the Lagrangian and residual circulations can be compared using the eddy thermodynamic equation, to give equation (18) of Rood & Schoeberl (1983), equation (2.31) below.

$$[u^* \phi_z^*] = \frac{-(ko^*[u])^2 N^2 [V^* \xi] + \alpha(f[u]_z [V^* V^*] - N^2 [V^* W^*])}{(\alpha^2 + (ko^*[u])^2)} \qquad (2.31)$$

where α is a Newtonian cooling damping coefficient.

This and subsequent modelling of the circulations in Rood & Schoeberl (1983) indicates the form of the difference between the residual representation of the flow and the real Lagrangian flow during the presence of a dissipation mechanism. Only if $\alpha=0$ is there equality

between the right-hand side of the Lagrangian and residual definitions. (see equations 2.29,2.30 & 2.8,2.9).

This highlights that only under non-acceleration conditions are the residual and Lagrangian circulations equivalent. How rapidly they deviate once the non-acceleration conditions are broken is uncertain. The action of transience and dissipation upon the residual and Lagrangian circulations is different so the residual circulation diverges from the circulation it is attempting to model. It must therefore be realised that the residual circulation and the Lagrangian circulation are not always equivalent. Whenever wave disturbances are growing or decaying rapidly for example the two circulations will be different, so that the residual circulation may not be representative of the parcel motions when transience and/or dissipation are present. The small residual transport may enlargen to a major difference during highly transient events in the presence of dissipation. Extra eddy flux terms above the first order terms which only represent the eddy cancelling terms of the stationary case are required. A model based on the TEM equations, if forced by all sources of eddy fluxes and including eddy parametrization, should provide a good model of the true net transport. The problem lies in our poor representation of these parametrized eddy flux terms and once again the problems of an Eulerian system are reducing the usefulness of the modelling method. One other important point to discover is: to what degree the eddy fluxes during transience and dissipation enlarge the Eulerian cancellation between the mean advection and flux motions, or do they purely result in net transport. A means must be found of identifying what fraction of a transient waves eddy flux terms contributes to producing a net transport and what fraction acts in the manner of steady waves and so acts to drive a cancelling mean circulation. This in other words asks how much do the orbital trajectories of the wave distort from being closed to produce a net drift and how these two motion components (the closed orbits and the drift) translate into the Eulerian eddy flux terms.

A better understanding of the parcel paths during a growing or decaying transient event would give us more information on the nature of the net transport which we are trying to deduce. No amount of

work using an averaging process will reveal the same essential details that should be available from an understanding of the true parcel trajectories without the complication of an averaging process. This was illustrated by Matsuno (1980) whose trajectories for steady planetary waves provide considerable insight into the wave mean cancellation problem. The eddy heat flux during non-acceleration conditions is induced by the elliptical parcel trajectories forced by the vertically propagating planetary waves. It cancels the vertical mean advection, which is also a consequence of the parcel trajectories.

If all the atmospheric forcing is represented correctly then since both the TEM equations and the Lagrangian equations are measuring the same system and events, they should obtain the same result. Any Eulerian representation, if modelled completely by calculating advective and eddy diffusive transport terms in both the tracer budget and the momentum budget equations, will be equivalent to the Lagrangian circulation. Obviously any Eulerian mean transport on its own will not represent the total parcel movement. So once again due to large amplitude events we have a circulation diagnostic which does not in all circumstances describe the air parcel motions. However this error is likely to arise for all zonally averaged circulation diagnostics. Our aim is to minimise the eddy effects and hence errors. The residual circulation is a good step in the right direction as by its definition it reduces the role of the eddy terms in the TEM equations and the consequent equation reformulation.

2.8.2: THE RESIDUAL CIRCULATION: ITS PHYSICAL ROLE IN THE MOMENTUM, THERMODYNAMIC AND ENERGY EQUATIONS.

In this section we consider the residual circulation's role in the momentum, heat and energy balances. It is useful here to note that the wave forcing $\mathrm{div}.\underline{F}/\rho_o$ is a zonally directed body force per unit mass, which shall be referred to hereafter as D. This is equivalent to D_F as used in Dunkerton et al (1981) for spherical coordinates (see appendix A).

The importance of these terms in a full budget analysis should be considered. This equation has not been solved in this thesis but some discussion of the terms involved has been undertaken in chapter 6.

Plumb (1983) compares the traditional energy cycle with one based on the TEM equations. He found that the traditional equations result in an unnecessarily complex description of even simple systems which are straightforward if viewed from the TEM approach. Other workers including Andrews et al. (1983) have found that a combination of the traditional and the TEM diagnostic set approach provides a greater insight than either would if used in isolation. A complete answer to the question of which set, Eulerian or TEM, is more meaningful, appropriate or especially relevant for various atmospheric conditions still remains to be found.

The TEM diagnostic set of which the residual circulation is but a part has been shown by various authors to be a valuable set of tools for gaining insight into the dynamical problems of the atmosphere. It simplifies the forcing interpretation, it provides a clearer measure of the transfer of wave disturbances from one region to another and a mean meridional circulation which does not suffer from the steady wave mean-eddy cancellation.

2.9 TRANSPORT OF TRACE SPECIES:

2.9.1 TRANSIENT EFFECTS.

Studies such as that undertaken by Mahlman, Levy and Moxim (1980) indicate the importance of transient disturbances in producing irreversible transports but they also show that an ambiguity is involved. There appears to be a contradiction in the problem. On time scales longer than a year the net tracer dispersion is controlled by the diabatic circulation which should be a good diagnostic of the transport circulation. The contradiction arises because this long time view implies that complete stationarity is correct but Mahlman, Levy & Moxim (1980) also showed that when viewed instantaneously the polar night jet of their model was continuously reforming and dissipating, with irreversible heat and tracer transport occuring during this transient behaviour. This indicates that the Lagrangian circulation was not capable of being non-zero independent of the transient disturbances. Similarly as

described in Mahlman & Moxim (1978), even though the mid-stratosphere is relatively steady, non-steady contributions are essential to account for the model time-mean structure of the thermal and tracer fields. This can be restated in the following manner as, noted from the description above, the diabatic circulation owes its existence to the past and present history of wave forcing, D_F, which is needed to drive the mean state away from radiative equilibrium and therefore generate the radiative conditions for the existing diabatic circulation.

Furthermore Andrews & McIntyre (1976,1978b) showed that adiabatic inviscid linear wave transience cannot by itself give rise to permanent alteration of the mean-flow. However the results of Matsuno (1971) and Holton & Dunkerton (1978) demonstrate that wave transience in the presence of dissipation can substantially alter mean-flows. This can be explained as Rossby waves become strongly non-linear by the time they reach the middle stratosphere with the result that the breakdown of linear theory leads to a complex flow. The non-linearities occurring generate many scales of motion and cause significant irreversible changes to the large scale mean state. (Juckes & McIntyre 1987). In GCMs the role of wave transience is to excite the dissipative and radiative processes which lead to irreversible tracer transport as well as permanent zonal mean alteration. Such models have also shown that transient effects associated with seasonal flow transitions in the stratosphere can lead to very large de-couplings of the usual mean-cell eddy cancellations typical of mid-winter flow regimes. When reversible events occur the temporary disturbance must be conservative and the mean-flow is left as before. If a very small amount of dissipation is present its effects can interact strongly with the linear transient mean-flow changes that would otherwise be temporary. However Andrews & McIntyre (1978a) also note that although no net mean-flow change is achieved it is possible that these transient fluctuations may produce significant transport.

2.9.2 RECENT DEVELOPMENTS.

The necessity to view the many mechanisms as two 'gross' headings (see equations (2.21 & 2.22)) has been discussed earlier but it is obvious that alternative three dimensional and other perspectives would

give different and possibly better views and interpretations of the forcing and transport mechanisms which are of interest to us. For instance, the use of three dimensional potential vorticity fields and the examination of wave breaking in these fields is a new and important line of research. Clough et al (1985), Leovy et al (1985), & McIntyre & Palmer (1983). This wave breaking is a highly non-linear and transient process and would be seen only as part of the transient contribution in a two-dimensional model. A better separation of the mechanisms involved, by understanding these mechanisms and their relative contributions to two-dimensional fluxes, appears definitely necessary. Ideally the idea of using a hybrid Lagrangian is to obtain a purely mean advective transport measure. One idea is to use the various approximate 'residual circulations' as this advective transport without any extra eddy terms at all. The temptation to find such a single mean advective transport diagnostic is strong but the role of the remaining eddy transport terms in the TEM formulation (primarily driven by transience and dissipation) cannot be ignored out of hand as negligible. A better knowledge of the importance of these eddy terms is necessary if the residual circulation is to be used more successfully. The choice of which circulation diagnostic to use has become very important in determining unambiguously and easily the mechanisms of the transport and the Lagrangian perception of the flow has become a useful one. The residual formulation is a Eulerian diagnostic, and it is a mean-circulation diagnostic which produces the total transport without eddy flux terms (in the manner of a Lagrangian mean circulation) only under strict non-acceleration conditions and so should not be used as a Lagrangian circulation without eddy transport. However the approach has definite advantages if the full TEM equations, (2.10) & (2.11), including the eddy terms are used. In viewing the problem of determining tracer transport it becomes evident that a host of methods and viewpoints are at present all available but in the early stages of development.

A promising new residual formulation uses isentropic co-ordinates. Andrews (1983), Tung (1982) & Mahlman et al (1980). The isentropic co-ordinate is often used as a quasi-Lagrangian coordinate, which improves the conceptual viewpoint of the stratospheric transport and simplifies the interpretation and insights obtained. This type of

Lagrangian orientated diagnostic perspective is likely to see increasing use. A possible combination of potential vorticity and isentropic coordinates as suggested by McIntyre (1980b) may extend this idea further. The problem of choice is quite large and the decision to use any one in particular is a difficult one.

More recently the work and ideas of Plumb & Mahlman (1987) have been presented giving a new clarification of an alternative two-dimensional approach for examining the transport problem. They have produced a transport circulation which is a combination of the Eulerian mean meridional circulation and the advective component of the transport tensor parametrization of the eddy flux terms. This tensor is obtained by assuming a flux-gradient relationship and thereby producing a transport tensor of the coefficients. This can be split into its anti-symmetric and symmetric components which are respectively advective and diffusive in nature. The transport coefficients are defined in terms of Lagrangian parcel statistics and these statistics can be generated from the numerical model. Thus by combining the advective tensor component with the mean circulation it is possible to define a mean transport circulation and the remaining diffusive flux. This circulation differs from the Lagrangian as the diffusive tensor component is not part of the circulation as it is in the generalised Lagrangian mean flow which basically follows the centre of mass of air parcels and so includes all motion influences. The transport circulation and use of the transport tensor clearly provides a satisfactory sub-division of mean and turbulence if the transport tensor coefficients can easily and accurately be calculated. Since the residual is an Eulerian diagnostic it cannot be the same as the Lagrangian circulation and is therefore only an approximation to this concept. Although different the Transport circulation is reasonably approximated by the residual circulation in the stratosphere (Plumb (1986) personal communication, & Plumb & Mahlman (1987)). However, it is not the same circulation as described by the Lagrangian mean velocity, $[u]^L$ of Andrews & McIntyre (1978a), and it is also stressed in Plumb & Mahlman (1987) that neither advection nor diffusion may be neglected in considering the full transport.

CHAPTER 3

3.1: THE RAW DATA SETS.

3.1.1 : THE SSU DATA

The SSU (Stratospheric Sounding Unit) is one of 3 radiometers mounted on the Tiros series of operational spacecraft. Data from these sounders have been available since October 1978 and the series has continued to beyond 1985. The first operational satellite of the series, NOAA-6, was launched in June 1979. The satellites are in sun synchronous orbits, at a height of 850km, providing approximately 14 orbits of data per day. The SSU is the prime sounding instrument of temperature from the tropopause to near 50km. Geopotential heights have been derived and are the basic data set for twelve levels at 1000, 850, 500, 300, 200, 100, 50, 20, 10, 5, 2 and 1 mbar. The data supplied by the meteorological office is from Tiros-N and NOAA-6, the NOAA-6 data being used only for November 1979. The lower atmosphere data used with the SSU derived geopotentials is based upon the lower channels from the HIRS-2 and MSU devices and NMC data.

The weighting functions of the SSU and other instruments are illustrated in figure F3.1. (from Pick & Brownscombe 1981)

The availability of this continuous series of virtually global observations from precisely intercalibrated instruments observing the atmosphere four times a day represents a major advance in monitoring stratospheric temperature.

The geopotential data have been provided with a couple of quality indicators for each date's data in the header information. Using this and examining the data themselves an assessment has been made of their usefulness. The data used cover the period from December 1978 to November 1979 for 12 levels between 1000mbar and 1mbar. From the total data a number of days are not used as they suffer from lost data sections or because of general poor field of view coverage by the satellite scans which results in inaccurate and anomalous features in the derived geopotential fields.

Table T3A illustrates that certain monthly averages are

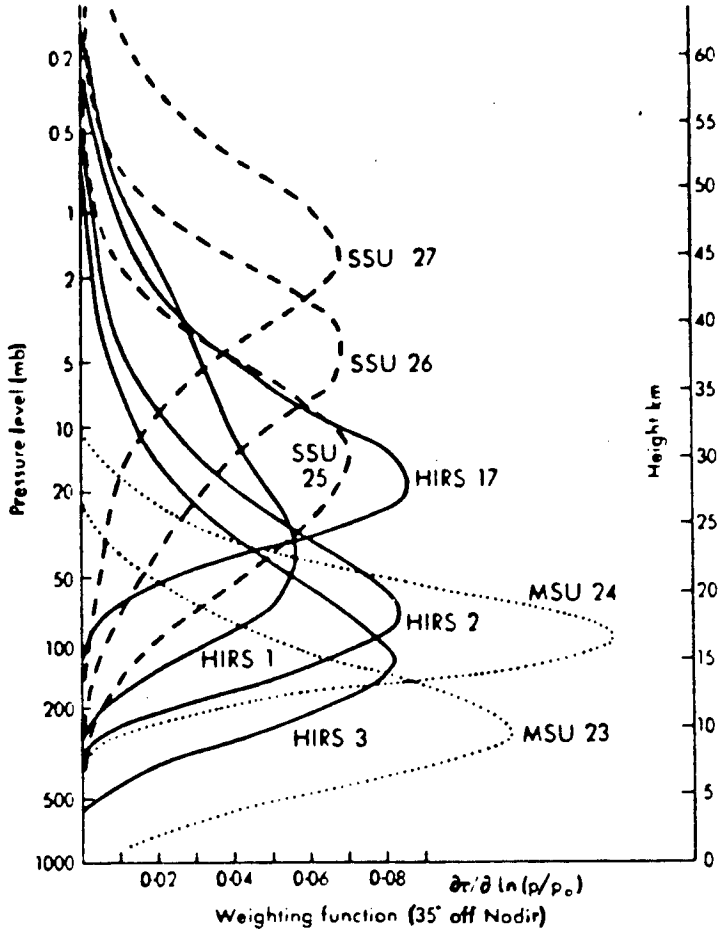

Figure F3.1 The weighting functions of the SSU, HIRS & MSU instruments on TIROS-N and NOAA-6 from Pick & Brownscombe (1981).

Month	Missing data	Poor data	Rejected	Good days
December 1978	1	6	7	24
January 1979	2	4	6	25
Februrary	1	6	7	21
March	1	1	2	29
April	0	1	1	29
May	0	4	4	27
June	3	9	12	18
July	0	22	22	9
August	5	3	8	23
September	9	4	13	17
October	7	3	10	21
November	3	7	10	20
December 1979	3	7	10	21

Table T3a

Table T3a The SSU data quality: Number of days used in the monthly averages and subsequent analysis.

based upon quite low numbers of days of accurate data. The loss of a number of days data was partly due to the fact that the data obtained were subject to operational difficulties. In early December data at 20mbar and above were poor and also throughout the entire flight of Tiros-N the 1mbar data were considered poor because the upper channel was faulty. As a result radiances for retrieval were only available from the channels at 15mbar and 5mbar due to the failure on TIROS-N of channel 27 which will restrict the height range of SSU data used. However the satellite was reported to have worked well otherwise (Pick & Brownscombe 1981). Later examination, of the SSU and LIMS data sets, illustrated by the comparison described in section (4.3.5.8), shows that both monthly averaged and daily diagnostic fields compare well, despite the 'poor' days necessarily neglected from the SSU analyses. It must also be noted that this data set has been successfully used in a number of other studies including Austin & Tuck (1985) and Palmer(1981a & b). Its use was therefore deemed satisfactory despite the 'poor' data days lost.

3.1.2 : THE LIMS DATA SET.

The LIMs experiment on Nimbus 7 used the technique of thermal infra-red limb-scanning to sound the composition and structure of the upper atmosphere. The instrument is a six channel thermal infra-red limb-scanning radiometer. Two channels are centred spectrally in 15μm CO_2 band for sounding the vertical temperature profile, and the others are located at 11.3μm for nitric acid, 9.6μm for ozone, 6.9μm for water vapour and 6.2μm for nitrogen dioxide. Geopotential height is obtained from the temperature profiles on a series of pressure surfaces. The thicknesses between the standard pressure levels were calculated and added to the FGGE 100mbar height to give height fields. The instrument measured vertical profiles of temperature and the concentrations of O_3, H_2O, HNO_3 and NO_2 during the period from late October 1978 until late May 1979. Data were collected day and night over the latitude range from 64°S to 84°N. The LIMS experiment operated virtually without flaw from the time of launch on October 24th, 1978 until it was turned off on May the 28th, 1979. Ozone and temperature values are available at 18 pressure levels, 100, 70, 50, 30, 16, 10, 7, 5, 3, 2, 1.5, 1, 0.7, 0.5, 0.4, 0.2, 0.1, and 0.05mbar. The LIMS data were obtained for use in the study partly in order to

extend the height coverage of the region to be examined and also to provide good geopotential data in the region of 1mbar and above which is possibly suspect in the SSU data. Water vapour measurements were only available up to 3mbar. The other data sets were not used in this study. A brief summary of the accuracy and precision of the results is given in table T3b, overleaf, (from Russell et al 1984).

For a more detailed validation of individual parameters see Gille et al(1984a & b), Russell et al (1984), Remsberg et al (1984) and Leovy et al (1985). Details of the measurements and an overview of the experiment can be found in Russell et al (1984) and Gille & Russell (1984).

3.1.3 : THE FGGE DATA SET.

The FGGE data are the level III-b data, resulting from the operational year of the first GARP global experiment (FGGE) which provided a coordinated concentration of meteorological data from various sources into one extensive set. FGGE data cover the period from December 1978 to November 1979 inclusive with a grid spacing of 1.875 degrees in both the latitude and longitudinal directions. Data supplied on pressure levels are available from the surface to 10mbar. The data are global in coverage and data is provided several times daily.

The FGGE temperature and wind data was used only at the lower boundary, 1000mbar (η=0), of the relaxation grid and to calculate $[\theta]_\eta$ at 850mbar. The higher resolution available with the FGGE data in the lower troposphere allowed a more accurate evaluation of the temperature gradient at 850mbar. The FGGE geopotential was also used at 850mbar as the SSU tape values at this level proved anomalous in early calculations. An extrapolation routine was used to fill in data points when the 850 and 1000 mbar data intersected the ground. Topographic height values were substituted in at these points. This was not a large problem as the 1000mbar values were used for the boundary fluxes only.

Accuracy and precision of LIMS results.

Quantity	Estimated accuracy	Precision
T	=<2K	<0.2-0.6K
O_3	16-41%	<0.25 ppmV
H_2O	18-36%	<0.25 ppmV
HNO_3	17-45%	<0.15 ppbV
NO_2	20-50%	<0.25 ppbV

(at p=< 1 mb.)

variation over height range.

Table T3b
from Russell et al (1984)

Table T3b Accuracy and precision of the LIMS results from Russell et al (1984)

3.1.4: THE SBUV DATA SET

Monthly averaged SBUV ozone data were used when LIMS daily ozone was unavailable. The Solar Backscattered Ultra-violet (SBUV) instrument on NIMBUS 7 was operational throughout the period November 1978 to October 1979 and a global coverage was available for the following pressure levels 506.63, 179.12, 89.56, 43.78, 22.39, 11.19, 4.6, 2.8, 1.4, 0.7, 0.35 & 0.17 mbar. These ozone values are tabulated in McPeters et al (1984) for 10° latitude bands from 80°S to 80°N. For months which had no 80° observations, the 70° values were substituted. These monthly averaged fields were extrapolated onto the study grid. (see chapter 4) The absence of the winter high latitude values does not affect the main calculations as the data is missing for the polar night and so the solar absorption calculations are not affected by the 'poor' ozone values extrapolated to fill in for these regions.

3.2 : DATA COMPARISON.

3.2.1: DATA QUALITY ASSESSMENT

The data have been examined by sampling a number of days from the total in order to assess their quality on both the 'good' and 'poor' days identified in terms of the field of view coverage and in comparison with other data sets.

Firstly hemispheric contour maps were produced from the SSU data for sample days at 300, 50 and 10 mbar, of the geopotential height. These were compared with FGGE charts for the same period. Qualitatively the lower level data appeared in very good agreement, with only antarctic and arctic values giving obvious differences. Large obvious differences were evident in the 10mbar data on 'poor' days, where a 'poor' day is defined by the low quality of satellite data coverage for each location, as indicated by the quality control information provided with each days geopotential field data. See figures F3.2 and F3.3 for some comparisons of the SSU, LIMS and FGGE data fields. These figures are discussed below in section (3.2.2). The 10mbar data level is the maximum height for which a comparison can be made between FGGE and the SSU data. Sample 'poor-days' examined were subject to unrealistic geopotential field structures which persisted throughout the stratosphere down to 50mb (affecting the

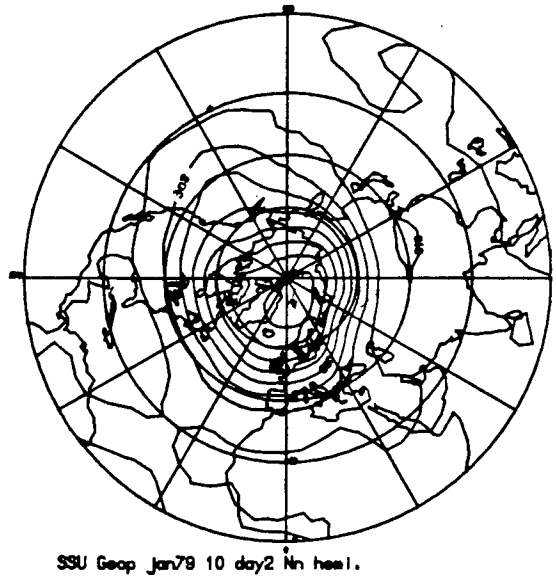

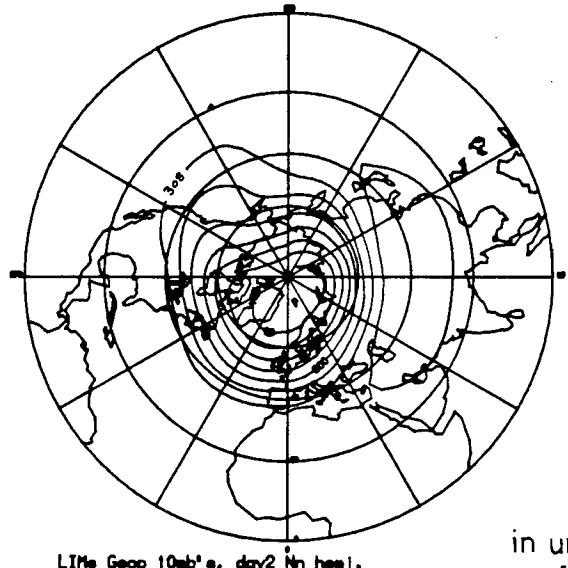

in units of 10^2 m

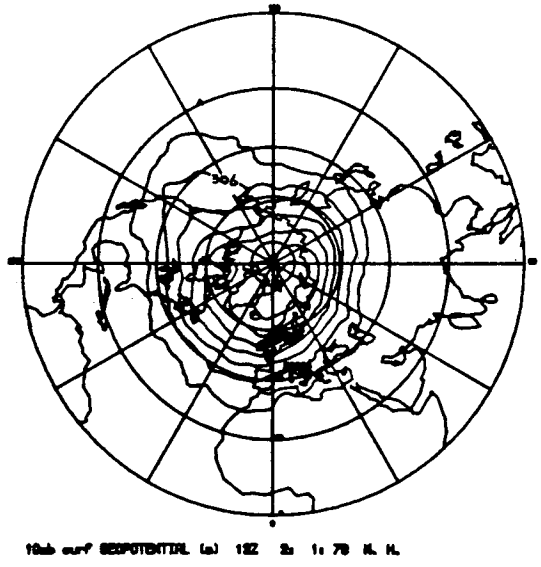

Figure F3.2 A comparison of (a) SSU, (b) LIMS and (c) FGGE northern hemisphere geopotential fields for the 2nd of January 1979 at 10mb, with contour units of 400 m.

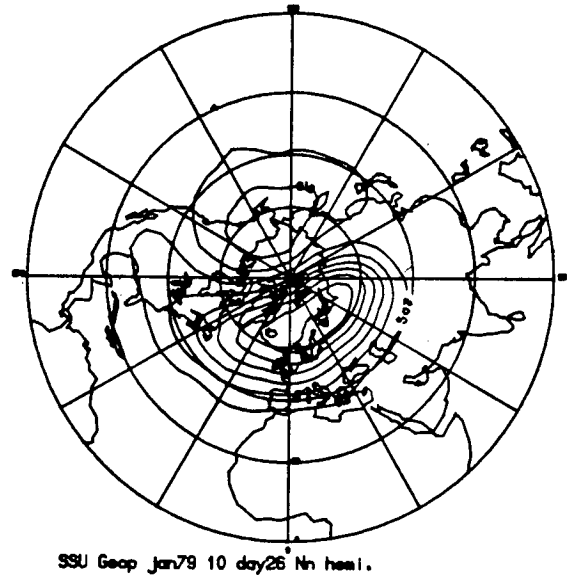

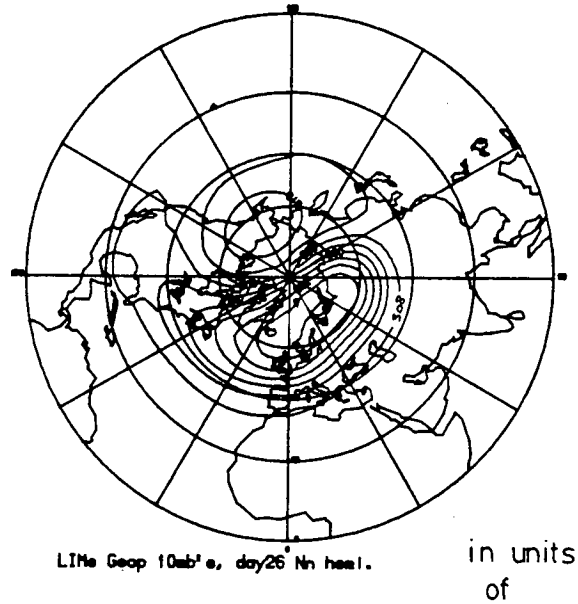

in units of 10^2 m.

Figure F3.3 as F3.2 except for the 26th of January.

data at 20mb and above). These structures were especially obvious in the southern hemisphere where the expected approximately zonally symmetric fields were replaced by erroneous geopotential data. These observed problems were clearly not just because of the upper channel fault and occurred throughout a substantial depth of the stratospheric data. Thus in order to remove the chance of such errors in the subsequent calculations all such bad days were removed from the monthly analysis.

3.2.2: GEOPOTENTIAL HEIGHT COMPARISONS

A direct qualitative comparison was made on a small sample of geopotential surfaces, between the data from SSU, LIMS and FGGE. Figure F3.2, for example, shows the 10mbar geopotential fields for the northern hemisphere on the 2nd of January 1979 and figure F3.3 the same for the 26th of January 1979.

The main wave pattern or vortex in the northern hemisphere is strikingly seen in all three fields, though the FGGE map shows considerably more high wavenumber detail (or noise). The location and magnitude of the low minimum for instance is similar for all three maps, except that the SSU and LIMS minimum are lower in magnitude and slightly more displaced from the pole over the Barents sea compared with the FGGE data. However at latitudes less than 40^{o}N the correspondence is less, and in equatorial regions the smoother surface makes the comparison more difficult and the finer detail more important. As a result the geopotential maps for this area do not compare well. In the southern hemisphere (not shown) the three fields show quite different patterns, especially in the mid-latitudes where the SSU shows a structure different to the LIMS map. Here again the very nature of the smoother summer geopotential field introduces the problem of requiring a more accurate resolution of the patterns to gain the same correspondence between the fields as we had in the northern hemisphere. The problem is less pronounced on the 26th of January 1979 and the finer wave structure in the southern hemisphere can in part be identified on both the SSU and LIMS maps.

A considerably more detailed analysis and comparison of various satellite data sources and fields has been edited by Rodgers (1983),

including the LIMS and SSU data sets. It concludes that significant differences are observed between the various data fields examined which are explained by the different methods, instruments and retrieval procedures used. So the above differences are to be expected and not necessarily identified as being wrong without further independent analysis programs to study the problem.

Following the further analysis of the conclusions in Rodgers(1983) together with the observed differences in the two data sets from the sample days examined it appears that some of these differences are inevitable consequences of the different observing systems and problems associated therewith and so must be accepted as uncertainties in the basic data set which cannot be resolved more accurately by this study.

3.3 : CONCLUDING REMARKS.

The final data used consisted of a mixture of data sources. Initially the fluxes of momentum and heat were computed from the merged SSU and LIMS geopotential data but this combination lead to sharp unobserved gradients at the interface of the data. Consequently the momentum and heat fluxes were computed separately for each data set and the resulting merging of the fluxes proved less problematical and the gradients at the region of data overlap were not seen to be significant in adding erroneous contributions to the D_F evaluated. The spatial coverage of the data in space is also not complete in some regions, arising from missing data portions and also as certain data sets are not global or cover the year chosen exactly. For instance the LIMS and SBUV data do not cover the entire globe and are used where possible as explained in chapter 4. The combination of the SBUV, SSU and LIMS data is not ideal but it does provide data of sufficient quality covering the majority of the globe over the period of interest. Since the intention of the study was to examine the whole stratosphere, data was necessary to cover the majority of this region. Also the method used requires for reasonable results data a few scale heights above the region of interest, therefore the combination of data was essential to fulfill the aims of the thesis. The sensitivity of the solutions obtained in the region of interest to the combined data described above is also discussed in

chapter 4. The sample comparisons show in general that the main qualitative vortex features are seen in all three of the geopotential surface data fields compared. But the lower latitudes of the northern hemisphere and the finer details of the southern hemispheric fields show poorer comparisons. However the comparisons between the data sets used and others in other analyses of various satellite data sources have noticed that some of the differences may be inevitable due to uncertainties in the basic data quantities, different measurement techniques and their associated problems.

As a result of these uncertainties comparisons and sensitivity tests were undertaken on the merged data set and these are described in sections 4.3.3.2 and 4.3.5.8 of chapter 4. The combination of the data sets did produce differences but, as discussed later in section 4.3.5.8, the qualitative nature of the circulations diagnosed remain largely unchanged. Consequently it was concluded that the years data set was satisfactory for use in the subsequent analysis (by means of further comparisons of the resulting diagnostics derived, between the data sets and with other authors results). The result has been to provide some confidence in the results and to allow the analysis to be completed for the period of interest over the majority of the globe.

CHAPTER 4

4.1 : AN OBSERVATIONAL STUDY.

It is evident that a better understanding of the residual circulation transformation is an important aim. The residual circulation remains a fairly new diagnostic and as such its seasonal behaviour, various component parts and its comparison with other circulations used in two-dimensional modelling are areas which have not been extensively analysed. So using the SSU and LIMS data covering the period December 1978 to November 1979, I have examined the global residual circulation in detail for a period of one year. In this chapter the method used to obtain the residual circulation will be presented and described. The details of the technique will be accompanied by a description of some of the sensitivity tests and checks made in order to assess the areas and possible magnitudes of the uncertainties involved in using this method, and from the use of the data.

There are a huge number of questions which arise from the problem of the TEM circulation. How large, relatively and in absolute terms are the transient and dissipational forcing components, what is transience and dissipation and how do they act? How often, and for how long do these terms have significant influences on the TEM? What does the residual circulation look like over a whole year and how is it related to the Lagrangian circulation? What happens to the residual circulation during a warming event, and how does it combine within the wave forcing in the momentum budget to influence the mean-flow acceleration?

The method used to obtain the residual circulation allows for the separation of the circulation into various components: a diabatically forced component, a part due to transient eddies, another due to stationary waves, and forcing from internal and external fluxes. A year's data analysis of the eddy terms important in the calculations has also been produced to improve our understanding of the residual circulation.

4.2 : THE RESIDUAL STREAMFUNCTION CALCULATION.

4.2.1 : THE BASIC EQUATIONS.

The residual circulation will be evaluated by obtaining an omega equation which when combined with the residual circulation's streamfunction definition can be expressed as a partial differential equation for the streamfunction, Ψ. This method has been chosen as it allows an examination of the separable circulation components forced by the eddy fluxes, both transient and steady, and the diabatic forcing. These are not totally independent as the diabatic forcing is dependent on the existence of past wave forcing, but the separation of the streamfunction allows the computation of a circulation component independent of the diabatic forcing, the eddy forced circulation, (Al-Ajmi, Harwood & Miles). The partial differential equation obtained from the omega equation, equation (4.16), may be solved with suitable boundary conditions for the various streamfunction components to Ψ, giving the residual circulation which maintains thermal wind balance, between the zonal wind and the zonal mean temperature gradient, against the perturbing effects of heating and eddy fluxes, (Harwood & Pyle (1975)). Thus the component circulations computed using this method do correspond to definite physical processes responsible for disturbing the geostrophic balance of the zonal mean state. The identification and analysis of the various component circulations is an important aim of this thesis. Another reason for prefering the use of an omega equation for evaluating Ψ is that the omega equation provides a diagnostic equation for $[v]^R$ and $[w]^R$ in terms of an instantaneous geopotential field, having eliminated the time derivative terms, (Holton (1979)). The use of the continuity equation together with one of either the momentum or thermodynamic equations, equations (4.1 & 4.2), to obtain the circulation does not allow any separation of the derived circulation into components and also uses time derivatives in the computation method which must be numerically approximated.

A full primitive equation set would seem to be the best and most accurate basis for calculating the physics and dynamics of the residual circulation. However, a solution for the mean circulation is impossible when the mean state is inertially unstable, (Harwood & Pyle (1975)).

One method of avoiding this difficulty is to use a more approximate equation set. The system of equations used was the simplest version of the quasi-geostrophic system which is applicable to a spherical horizontal region, Holton (1975):

$$\frac{\partial}{\partial t}\nabla^2\psi = -J(\psi, \nabla^2\psi + f) + \nabla\left(f \nabla \cdot \left[\frac{\partial \chi}{\partial p}\right]\right) + \nabla \cdot (\underline{F}_r \times \underline{k}) \qquad (4.1)$$

$$\frac{\partial \theta}{\partial t} = -J(\psi, \theta) + \sigma_e \omega + \frac{Q}{c_p}\left[\frac{p}{p^s}\right]^K \qquad (4.2)$$

where $\omega = \nabla^2 \chi = \frac{Dp}{Dt}$, $\sigma_e = -\frac{\partial \theta}{\partial p}$

ψ, is the quasi-geostrophic streamfunction

& $-\frac{\partial \chi}{\partial p} = X$ the velocity potential,

such that $v_i = \nabla X$

F_r = Frictional force,

Jacobian, $J(a,b) = \nabla a . (\nabla b \times \underline{k})$

These express the thermodynamic and momentum balances of the circulation of an atmosphere moving above a spherical rotating earth. The equations were derived and shown to be energetically consistent, by Lorenz (1960).

Equation (4.1) is similar to the beta-plane quasi-geostrophic vorticity equation, as described by Holton (1979), but with several important differences:

i) f is not in any term approximated by f_o.

ii) The irrotational velocity component, U_i, is retained and results in two extra terms: the ageostrophic meridional advection of the planetary vorticity and a part of the divergence term. These modifications to the beta-plane quasi-geostrophic approximation set also influence the form of the balance equation necessary to keep the equations energetically consistent. The full balance equation has the form.

$$\nabla^2 (\phi + 1/2 (\nabla\psi)^2) = \nabla . ((f + \nabla^2 \psi) . \nabla\psi) \qquad (4.3)$$

Equation (4.3) expresses a rather complicated non-linear relationship between ϕ and ψ. The so called linear balance equation (4.4 below), is obtained when the non-linear terms are considered small compared with the linear terms. This simple filtered model is still quite accurate outside the tropics (Holton (1979)).

$$\nabla^2 \phi = \nabla (f \nabla\psi) \qquad (4.4)$$

This reduction of the balance equation to linear terms, reduces the vorticity equation to the form.

$$\frac{\partial \xi}{\partial t} + v_n . \nabla (\xi + f) + v_i . \nabla f + f \nabla v_i = 0 \qquad (4.5)$$

For a spherical earth according to Lorenz (1960) we require to use equation (4.4) as our balance equation, from which the thermal wind relationship can be derived as:-

$$-\frac{R}{p}\left[\frac{p}{p_o}\right]^{\kappa} \nabla^2 \theta = \nabla \left[f \nabla \frac{\partial \psi}{\partial p} \right] \qquad (4.6)$$

Which is the reduced version of equation (30) of Lorenz (1960). This set of equations will be the basic relationships which will determine the residual circulation.

4.2.2 : DERIVATION OF THE MERIDIONAL STREAMFUNCTION.

Using the equations (4.1) to (4.6), the residual meridional velocity streamfunction can be derived. Equations (4.1) and (4.2) are divided into a zonally averaged portion, denoted by square brackets, plus the deviation from the zonal average, denoted by a star.

$$\psi = [\psi] + \psi^* \quad , V = [V] + V^* \qquad (4.7)$$

The zonally averaged equations can be written as

$$\frac{\partial^2}{\partial y^2}[\psi] = -\frac{\partial}{\partial y}[v^* \nabla^2 \psi^*] + \frac{\partial [\omega]}{\partial p} - [v_i]\nabla f \qquad (4.8)$$

$$\left[\frac{\partial \theta}{\partial t}\right] + [v_i][\theta_y] + [\omega_i][\theta_p] = -[v^*_n \frac{\partial \theta^*}{\partial y}] - [\omega_i{}^* \frac{\partial \theta^*}{\partial p}] + [Q] \qquad (4.9)$$

The equations are next written in terms of spherical co-ordinates with the two poles as the limits of the horizontal co-ordinate. The meridional residual circulation is defined as:

$$[\omega^R] = [\omega] + \frac{1}{c}\frac{\partial}{\partial y}\left[\frac{[v^* \theta^* c]}{[\theta_p]}\right] \qquad (4.10)$$

$$[v^R] = [v] - \frac{\partial}{\partial p}\left[\frac{[v^* \theta^*]}{[\theta_p]}\right] \qquad (4.11)$$

Making use of the two continuity equations for the divergent and non-divergent parts of the velocity, the thermodynamic and vorticity equations in spherical co-ordinates are:

$$\frac{\partial}{\partial t}(c[\theta]) + c[v_i][\theta_y] + c[\omega_i][\theta_p] = -\frac{\partial}{\partial y}[v^*_n c\theta^*] - \frac{\partial}{\partial y}[v^*_i c\theta^*] - \frac{\partial}{\partial p}[\omega_i{}^* c\theta^*] + c[Q] \qquad (4.12)$$

$$\frac{\partial}{\partial t} c[\xi_n] = -\frac{\partial}{\partial y} f c[v_i] - \frac{\partial}{\partial y} c[v_n{}^* \xi_n{}^*] = -\frac{\partial}{\partial y} f c[v_i] - \frac{\partial}{\partial y}(cM) \qquad (4.13)$$

If we integrate these two equations with respect to $y=a\psi$, then using the zonal mean balance and hydrostatic equations, we can after considerable manipulation, (including a transformation of the vertical co-ordinate from geometric height to $\eta=-\log(p/p_o)$, a log-pressure co-ordinate,) restate the problem in terms of a partial differential equation for the residual circulation's streamfunction.

The residual circulation's streamfunction is defined as:

$$[v^R] = \frac{1}{pc}\frac{\partial}{\partial \eta}(p\Psi) \tag{4.14}$$

$$[w^R] = -\frac{1}{c}\frac{\partial}{\partial y}(\Psi) \tag{4.15}$$

The full PDE for the streamfunction, Ψ, used is as follows:

$$\begin{aligned}
&-\frac{f^2}{c}\frac{\partial^2 \Psi}{\partial \eta^2} + \frac{f^2}{c}\frac{\partial \Psi}{\partial \eta} - A_1 p\frac{\partial [\theta]}{\partial y}\frac{\partial}{\partial y}\left(\frac{\Psi}{c}\right) \\
&+A_1 p\frac{\partial [\theta]}{\partial y}\frac{\partial}{\partial y}\left(\frac{1}{c}\frac{\partial \Psi}{\partial \eta}\right) + \frac{A_1}{c} p\frac{\partial^2}{\partial y^2}[\theta]\left(\frac{\partial \Psi}{\partial \eta} - p\Psi\right) \\
&-A_1 p\frac{\partial}{\partial y}\left(\frac{1}{c}\frac{\partial [\theta]}{\partial \eta}\frac{\partial \Psi}{\partial y}\right) \\
&= \frac{1}{c}\left\{ \frac{f}{a}\left\{\frac{\partial}{\partial \eta}\left(\frac{1}{\varrho_0}\frac{\partial}{\partial \eta}\left(a\varrho_0\left[v^*\frac{\theta^*}{[\theta_\eta]}\right]fc\right) - \frac{1}{c}\frac{\partial}{\partial y}\left(ac^2[u^* v^*]\right)\right)\right\} \right. \\
&\quad -A_1 pc\frac{\partial}{\partial y}\left(\frac{\partial [\theta]}{\partial y}\frac{\partial}{\partial \eta}\left(\left[v^*\frac{\theta^*}{[\theta_\eta]}\right]\right) - \frac{\partial [\theta]}{c\partial \eta}\frac{\partial}{\partial y}\left(c\left[v^*\frac{\theta^*}{[\theta_\eta]}\right]\right)\right) \\
&\quad \left. -A_1 pc\frac{\partial}{\partial y}\left(\frac{1}{c}\frac{\partial}{\partial y}\left(c[v^*\theta^*]\right) + [Q]\right) \right\}
\end{aligned}$$

$$= \frac{1}{c}\left[\frac{\partial}{\partial \eta}\left[fD_F\right] - A_1 pc\frac{\partial}{\partial y}\left[\frac{1}{\varrho_0}\times\frac{\nabla [\theta]}{}\cdot div\left[\varrho_0\left[v^*\frac{\theta^*}{[\theta_\eta]}\right]\right]\right]\right.$$

$$\left. -A_1 pc\frac{\partial}{\partial y}\left[\frac{1}{c}\frac{\partial}{\partial y}\left[c[v^*\theta^*]\right] + [Q]\right]\right] \tag{4.16}$$

The right hand side forcing terms, all of which are important, arise due to the presence of the diabatic and eddy flux terms in the equations (4.12) and (4.13), which are the heat flux, momentum flux and diabatic heating which drive the meridional circulation. The diabatic forcing occurs due to various contributions including: latent heat release, boundary heating and radiational heat input arising due to the varied atmospheric absorption qualities of its different gases. The fluxes, on the other hand, are due to the presence of wave perturbations forced from below on the otherwise zonal flow in both hemispheres. It is the variation, origin and relative importance of

these terms which is of great interest. The equation obtained is elliptic if $\partial\theta/\partial p < 0$ i.e. a statically stable atmosphere, and

$$\frac{4\,|\theta_p|\,f^2}{A_1\,\theta_y^{\,2}} > 1 \qquad (4.17)$$

Where $A_1 = R/p_o\,(p/p_o)^{K-1}$.

Using typical scale order values e.g. $\theta_p \approx 2.10^{-3}$ [K/Nm^{-2}], $\theta_y \approx 1.10^{-6}$ [Km^{-1}], $A_1 \approx 0.3 - 0.3.10^{-2}$ [$m^3 kg^{-1} K^{-1}$] & $f \approx 10^{-4}$ [s^{-1}], then it is seen that the value of the left hand side of equation (4.17) is $\approx O(10 - 10^4)$.

The partial differential equation, equation (4.16), is thus solvable under such conditions and so we have a diagnostic equation for the residual circulation via the streamfunction Ψ. Note Ψ here is defined as the meridional streamfunction for the residual circulation, see equations (4.14) & (4.15) above and Appendix A, equation (XXIV). Equation (4.16) is analogous to the omega equation of the beta-plane quasi-geostrophic equation set, being a diagnostic equation for the vertical motion field dependent upon the horizontal velocities and geopotential gradients of the atmosphere.

4.3 : THE FORCING TERMS.

4.3.1 : THE BASIC PROBLEM.

Using SSU, LIMS and FGGE data sets, geostrophic velocities, thicknesses and hence potential temperatures can be evaluated. Using these plus ozone and water vapour from the LIMS data set and a diabatic heating rate evaluation method, (see later section 4.3.4), it is possible to evaluate the forcing terms for the streamfunction calculation. With these known for all points on a global, zonally averaged grid a relaxation method, the successive over-relaxation method (SOR), has been used to solve for Ψ for a number of different forcing cases, including (i) full forcing, (ii) diabatic forcing only, (iii) transient eddy forcing only, (iv) stationary or time-averaged eddy forcing only, and various combinations thereof. These residual circulations will then be compared with their Eulerian counterparts, calculated from the streamfunction definition.

$$\Psi_E = \Psi^R + \frac{c[v^*\theta^*]}{[\theta]_\eta} \qquad (4.18)$$

where Ψ_E is the Eulerian circulation's streamfunction and hereafter Ψ^R will be referred to as Ψ.

The partial differential equation, (4.16), as derived in section 4.2.2 allows a simple separation of the circulation components which are driven by the various forcing mechanisms represented by the right hand side terms of the equation, of the form $L\{\Psi\} = R_Q + R_T + R_S$, where L is the elliptic operator, R_Q represents the term involving [Q], R_T represents the terms involving transient eddy fluxes, and R_S represents the terms involving stationary or time averaged eddy fluxes. As the equation is linear Ψ can be written as:

$$\Psi_R = \Psi = \Psi_Q + \Psi_T + \Psi_S \qquad (4.19)$$

The boundary conditions are similarly linearly split with Ψ_S and Ψ_T specified as the time-average and transient flux components of equation (4.19) at the lower boundary and set to zero on all other boundaries. Ψ_Q is set to zero on all boundaries thus satisfying equation (4.18). Ψ_Q can be thought of as the component of the residual circulation driven by [Q], Ψ_T as the component driven by the transient eddy forcing and Ψ_S as the component driven by the stationary eddy flux forcing terms. It is also useful to define $\Psi_A = \Psi_S + \Psi_T$ as the streamfunction for the total eddy forced residual circulation component.

4.3.2 BOUNDARY CONDITIONS AND FINITE DIFFERENCE FORM.

The successive over-relaxation numerical method, SOR, was used to solve the differential equation and so a finite difference form of the equation and the coefficients of all the terms in equation (4.16) were calculated and tested. The grid was based on data covering 16 levels in the vertical over the whole meridian from 90°S to 90°N in 36 intervals of 5 degrees each. A zero Eulerian vertical velocity was taken as the upper and lower boundary conditions. i.e. $\omega^R = -\partial/\partial y\,(c[v^* \theta^*])$, and so to calculate the residual circulation, eddy fluxes were needed at the ground. Also at the upper lid $\omega=0$ was assumed. This upper lid is placed at $\eta=12.0$ ($\approx$ 84km), well above the

top of the area of interest, the stratosphere. See Figure F4.1 and sections 4.3.6.2 and 4.3.6.5 below, where this choice is shown not to affect significantly the region of interest. This is done in order to minimise the effect of this artificial boundary condition. The satellite data used does not extend to this height and so the data for the levels η=9.75 to η=12.0 have been extrapolated from below where data are available. For all three quantities extrapolated in this manner the profile was assumed to relax to zero at the upper level or lid. The data profile is determined by using a quadratic functional extrapolation between the lower data profile and the upper assumed zero level. Monthly averaged climatological temperature values taken from Barnett & Corney (1985) were used at the upper lid, η=12.0. There are fourteen internal points in the vertical. At both poles the streamfunction, Ψ, was assumed zero.

At the equator equation (4.16) has a singularity and it is necessary to evaluate the streamfunction by some other method. This singularity is removeable however, for operating on (4.9) with $\partial/\partial\varphi$ and setting

$$\left[\frac{\partial\theta}{\partial y}\right] = 0 \quad \& \quad \frac{\partial^2}{\partial t \partial y}[\theta] = 0 \qquad (4.20)$$

we obtain equation (4.21).

$$\frac{1}{c}\left\{-[\theta_\eta]\left[\frac{\partial^2\Psi}{\partial y} + \frac{\partial\Psi}{\partial\eta}[\theta_{yy}]\right] - \frac{\partial\Psi}{\partial y}[\theta_{y\eta}]\right\} = \frac{\partial}{\partial y}\left(H_e/c + [Q]\right) \qquad (4.21)$$

This equation is parabolic. It replaces equation (4.16) at the equator only. These two equations for the equatorial column and the rest of the atmosphere were then written in finite difference form and re-manipulated.

Thus for each $\Psi_{i+r,i+s}$ where r=0,1,-1 & s=0,1,-1, (see appendices B & D) the coefficients of the finite difference equation and right hand side terms were evaluated, see Appendix B equations ((xxxv)-(xxxix)). Using these approximate forms of the partial differential equations the SOR method was used iteratively to solve for Ψ numerically at all points on the grid. Iteration was continued until

the residues between the left hand side and right hand side terms of the method were below 1.10^{-5} s^{-1}. For the full equations, right hand side terms and coefficients used see Appendix B.

4.3.3 :EVALUATION OF THE EDDY FORCING TERMS.

4.3.3.1 BASIC DATA MANIPULATION.

The momentum and heat fluxes and mean state necessary to calculate the terms and coefficients of equation (4.16) above have been derived in the following manner using the geopotential data of the SSU, LIMS and FGGE data sets, covering the period December 1978 to November 1979. As all three sets are not available over the entire period concurrently, certain months are necessarily less accurate as a result of the assumptions used to complete the year's analysis. Both SSU and LIMS geopotential height fields are used as the basic data set. NMC data from 850mbar to 100mbar, SSU from 100mbar to 1mbar, and LIMS from 70mbar to 0.1mbar. A combination of the geopotential data fields before any velocity or temperature calculations were undertaken proved to lead to problems with the derived fluxes at the geopotential data overlap region. The fluxes of heat and momentum were thus calculated for each data set separately and then simply overlapped on the regular grid by averaging the data at the levels η= 3 to η=4.5.

Prior to the calculation of the potential temperature field and the geostrophic velocities from this data set several data quality checks have been used. The SSU data from TIROS-N is subject to problems because of the loss of the upper channel. A number of days during the period contain poor data, as a result of the retrieval providing poor coverage for these days, although only SSU data for 'good' days are used in this study. All days with missing data above 50mb and/or with a large number of gridpoints with poor coverage are not used at all. Therefore one restriction of the results is that the different months considered are calculated on different month lengths depending upon the number of rejected days in any particular month (See section (3.1.1), Table 3A.) For example December 1978 has 13 bad SSU days and so its average is based upon the remaining 18 days of data. A more detailed discussion of the data sets is presented in Chapter 3. For the LIMS data geopotential fields are available for every day of the

month unlike the SSU data and the averages are based upon every day of each month.

For the LIMS data after the geopotential has been reconstructed from the fourier coefficient data it is checked for missing data points which are flagged on the original tape. These are then replaced by interpolation using neighbouring points along a line of latitude. Only the top and bottom levels i.e. 100mb & 0.05mb appear to have a large proportion of missing data points and neither level is used in the analysis. The LIMS geopotential data is then extrapolated onto the whole 90N - 90S meridional cross section by using a quadratic interpolation scheme with assumed symmetry across both poles (due to the zonal averaging of the data at a later stage.) Since LIMS data only extends from 84N to 64°S this will lead to errors at these unknown regions. The polar data is further replaced with a smooth extrapolation at 85°N-90°N, & 70°S- 90°S. (see section 4.3.6.7) The basic layout of the use of the various geopotential fields over the chosen grid is illustrated in Fig F4.1. However note that the polar cap south of 64°S represents only 8 per cent of the surface area of the globe.

Thus daily geopotential data from NMC & SSU from 850mb to 1mb and from LIMS from 70mb to 0.1mb is used. The potential temperature is then calculated at the pressure mid-points of the thicknesses between two geopotential levels, while the geostrophic velocities are calculated from 500mb at the original pressure levels. This was done as the original geopotential data was retrieved from temperature values and thicknesses built up from them. Calculation of the temperatures at the same pressure levels as the velocities lead to erroneous vertical temperature profiles. These irregular data sets were then interpolated on to a regular vertical grid in log pressure coordinates, the SSU and LIMS fluxes being combined only after the fluxes of each have been evaluated on the regular grid.

$$\eta = -\ln\left(\frac{p}{p_o}\right) \qquad (4.22)$$

The values from pressures 850mb to 0.1mb have been interpolated onto

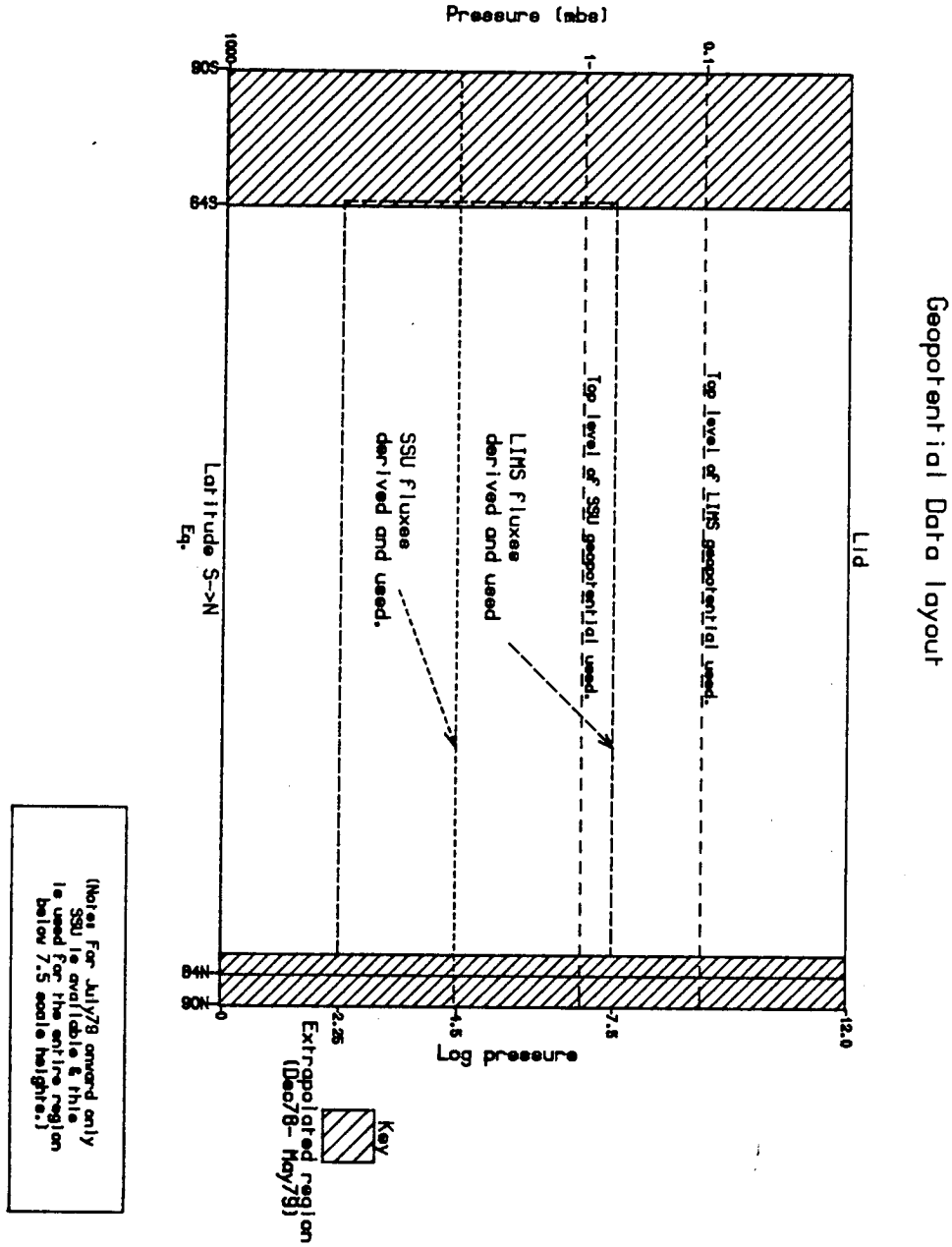

Geopotential Data layout

Figure F4.1 Schematic layout of the geopotential data sources used showing latititudinal and height restrictions.

a log pressure grid ranging from η=0.75 to η=9.75. The top level generated (η=9.75) is above the top data supplied but it is not used.

Thus

$$\overline{[u^* v^*]}\ ,\ \overline{[v^* \theta^*]}\ ,\ \overline{[u^* \cdot v^* \cdot]}\ \&\ \overline{[v^* \cdot \theta^* \cdot]} \qquad (4.23)$$

are all calculated initially on the regular η log pressure grid.

Both the eddy momentum and heat fluxes have been averaged over each months data available. All eddy quantities have been split into their monthly time-average and transient flux terms, the intention being to use this division to gain insight into the variability of the forcing (principally due to eddies) and so examine the role of transience and non-conservative mechanisms upon the residual circulations calculated. However it is important not to confuse this statistical eddy quantification of transience with the theoretical eddy definition (see Andrews & McIntyre (1976) for details of the definition). See section (2.7)

It is important to realise that since the data have been averaged over monthly periods the fluxes achieved will not separate out stationary and transient wave activity alone. The lack of full separation has already been discussed in more detail in section 2.7.

4.3.3.2 DATA COMPARISON

To verify the raw data and data manipulation techniques a number of comparisons between the evaluated values and those from other sources of observations were made. The following comparison was undertaken partly in order to assess the validity and accuracy of the data combination (also discussed in chapter 3) of the LIMS and SSU data sets. This was done only for sample cases due to the large quantity of data. The following cases will be discussed:

i) Some monthly averaged eddy flux cross sections.

ii) Some daily eddy flux field comparisons.

iii) The zonal mean quantities.

iv) EP-flux & divergence diagnostic comparisons.

As the eddy flux fields are the principal data used in the later calculations, except for the diabatic heating rates which will be discussed later, it is important to examine the quality and accuracy of the fluxes obtained. Figures F4.2a-d show the total eddy heat and momentum fluxes as calculated for the months December 1978 and January 1979. These can be compared with figures F4.3a-d from NCAR for the same periods, Hamilton (1982). Comparison of the momentum fluxes for December 1978 reveals a poor agreement between the two sets of values. The SSU & LIMS calculated fluxes are considerably larger and peak higher in the atmosphere than those revealed in the NCAR analyses. Similarly in January 1979 our data show a peak in the momentum flux at $\approx$ 1 mbar which is almost twice the NCAR value. In terms of the heat fluxes obtained the comparison is considerably better. Both exhibit a maximum at approximately 75°N and 1mbar, though the magnitude is slightly different. The lower maxima at 65°N & 20mbar on the other hand are directly comparable. For January 1979 again the similarity is much better than for the momentum fluxes. Both figures showing a northward transport maxima at 70°N & 2mbar, though lower in the atmosphere in the NCAR analysis and of a larger magnitude.

It is clear that the momentum values achieved using the combined SSU and LIMS data sets compared with the NCAR analyses are very different. In fact there appear major differences which will greatly affect the following analysis of the residual circulation. Other sources (Rodgers 1983) however do indicate that various data fields produce differences in the calculated fields of eddy momentum flux and independent analyses using several data sources will be the only way to lead to the solution of problem of identifying the real flux values and explaining the reasons for the observed differences between the different data sets.

Thus to further verify the fluxes achieved using the LIMS data, daily fluxes for two days, the 2^{nd} and 26^{th} of January were calculated as these could be compared with values achieved using the same basic data set and published in the 'Report on the workshops on comparison of data and derived dynamical quantities during northern hemisphere winters' Rodgers (1983). The factor of two difference

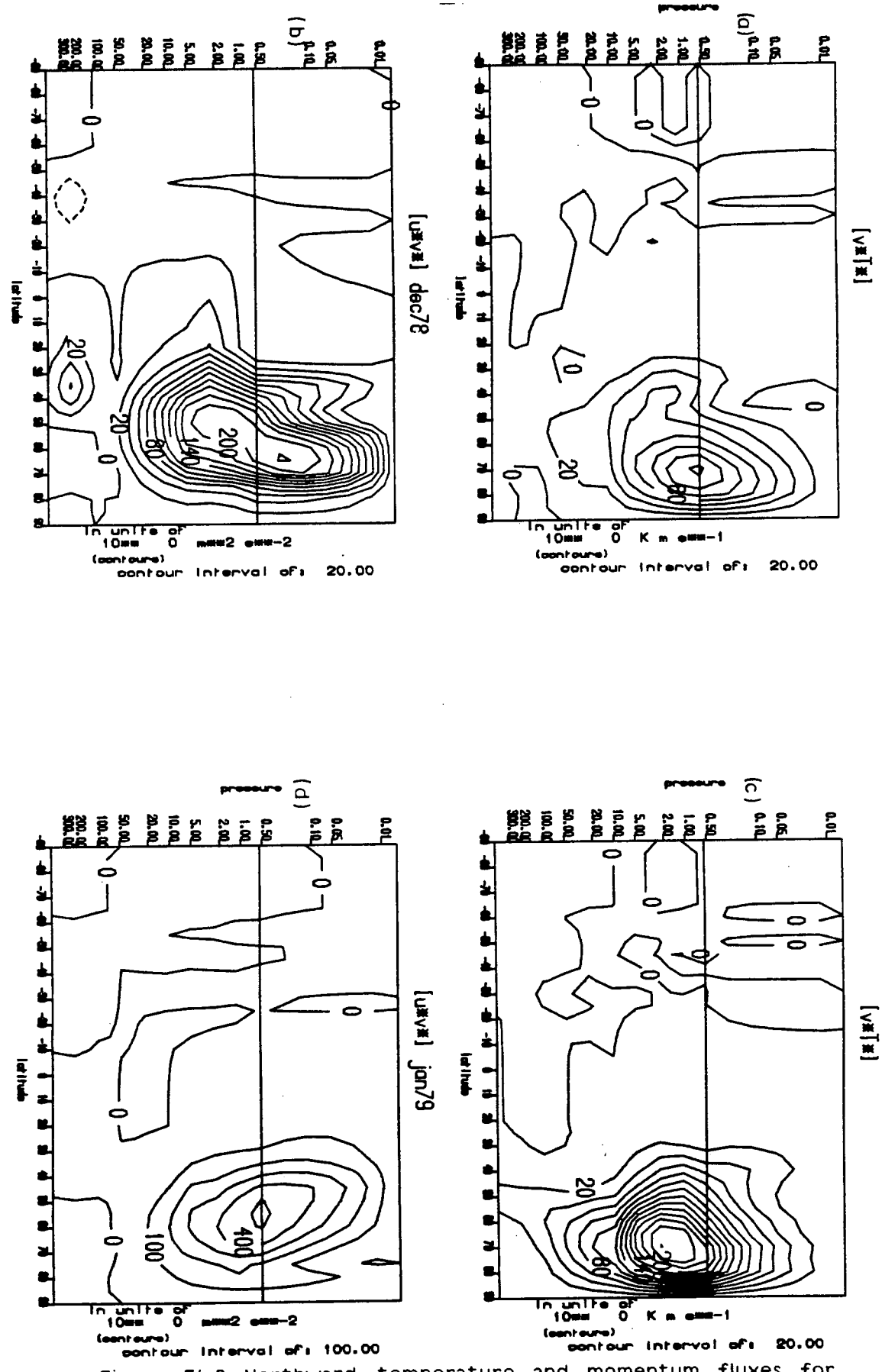

Figure F4.2 Northward temperature and momentum fluxes for December 1978 and January 1979 calculated from the combined LIMS and SSU data sets. The line at 0.6 mb indicates the top of the region of real flux values computed. (solid lines positive, dashed lines negative.)

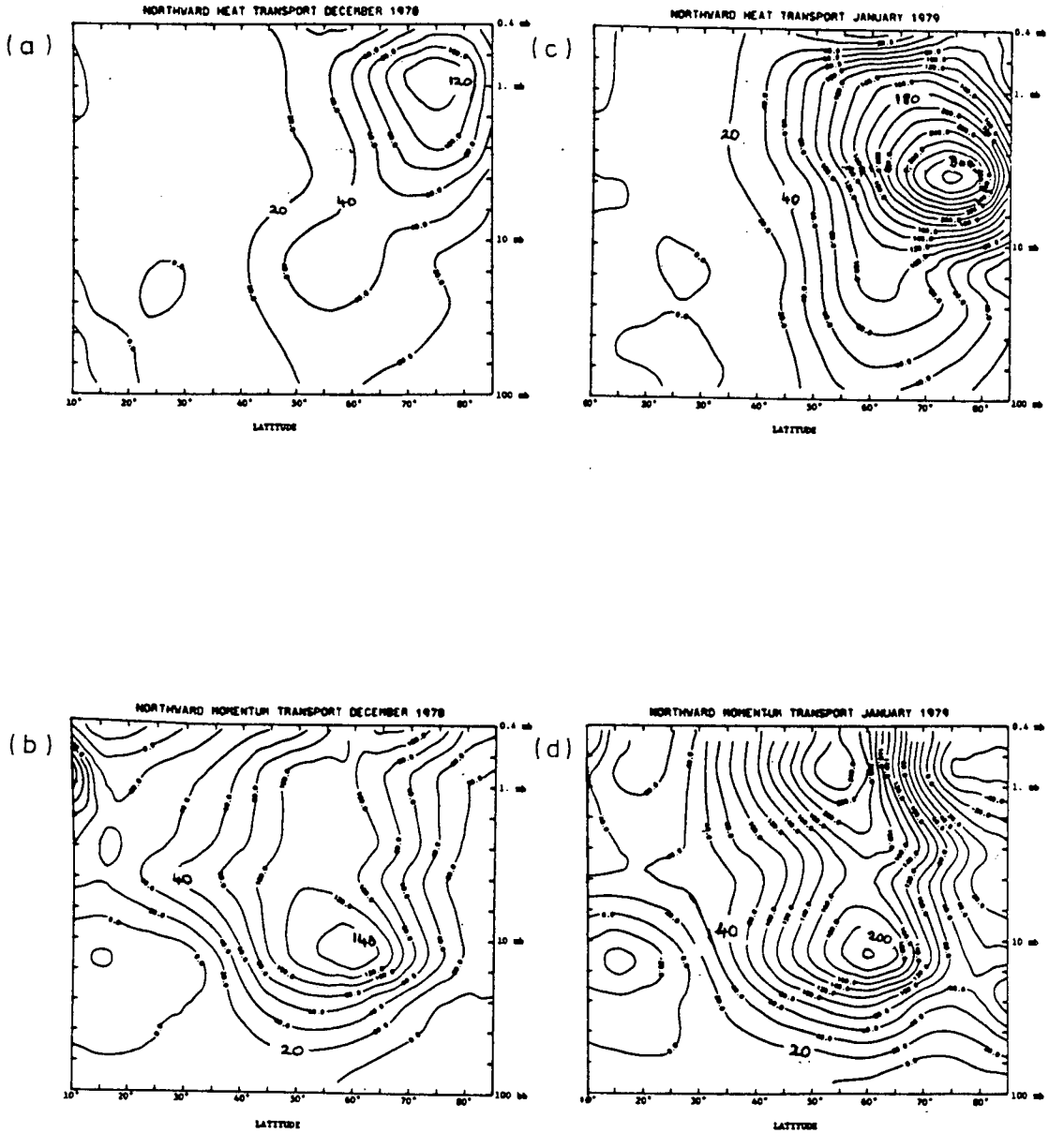

Figure F4.3 Daily northward Temperature and momentum fluxes for December 1978 and January 1979 from NCAR, Hamilton (1982). Contour intervals of 20 K ms^{-1} & 20 $m^2 s^{-2}$ for $[v^* T^*]$ and $[u^* v^*]$ respectively.

between these two sets of flux results (shown in figure's F4.4a-d & F4.5a-d) is due to an error in the Oxford calculation (Rodgers : Personal communication). This shows that the calculation technique was correct and the daily fluxes were reproducible. It would appear then that the differences between the monthly averaged LIMS and NCAR fluxes are possibly due to the differences between the instruments and not an error in the subsequent manipulation procedure used in this thesis.

Zonal fields such as [T] and [U] were also compared during these two months for the two days alone and for the monthly averaged fields. For December 1978 and January 1979 the monthly averaged zonal mean wind and temperature fields were compared with the NCAR values (Hamilton 1982) for the same months. The zonal mean temperature fields compare very well except at high latitudes at about 1 to 0.5 mbar where the NCAR values remain lower than the LIMS values. The zonal mean wind likewise compares well, but the LIMS data underestimates the jet maximum in comparison with the NCAR analysis, while also at about 0.5mbar the LIMS data shows a closing of the jet maxima in the upper stratosphere during January which is not evident in the NCAR analysis.

In order to check the forcing terms namely the EP-flux divergence a comparison was made with some results in February 1979, in two papers by Palmer (1981a) and Butchart et al (1982) which are based upon the same SSU data set. Consequently as the data is the same this is not an independent comparison but just a confirmation of the computation procedure. Diagnostic calculations of the circulation, mean state and forcing of the stratosphere were obtained for several special one day analyses, being based upon SSU data only initially as this was the only data available at the time.

The mean zonal wind field for February the 17^{th} is shown in Figure F4.6a & g from Butchart et al (1982) for the northern hemisphere between 100mbar and 1mbar. This can be compared with Figure F4.7a & c below.

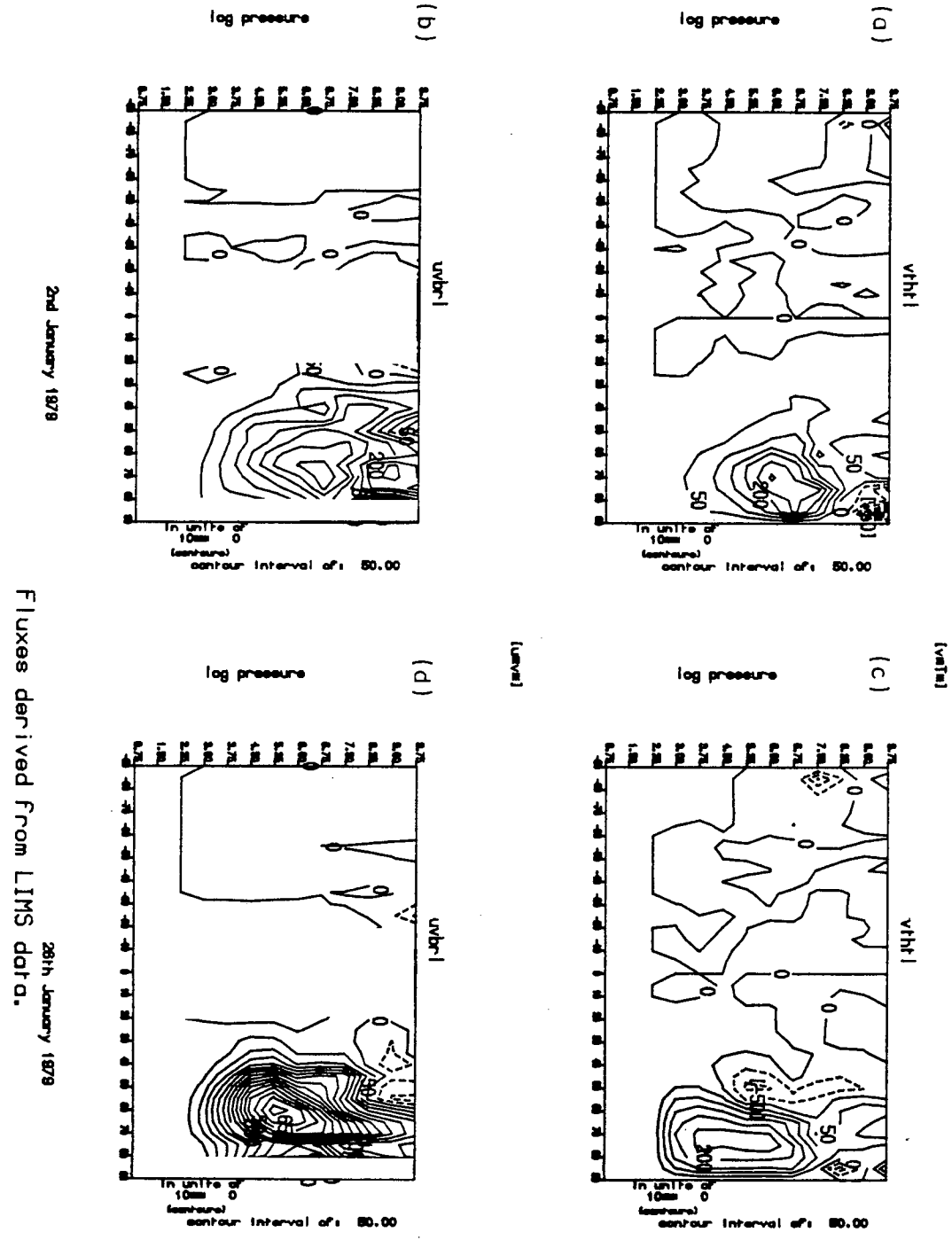

Figure F4.4 Daily northward temperature and momentum fluxes derived, during this study, from LIMS data for the 2nd & 26th of January 1979. (solid lines positive, dashed lines negative.)

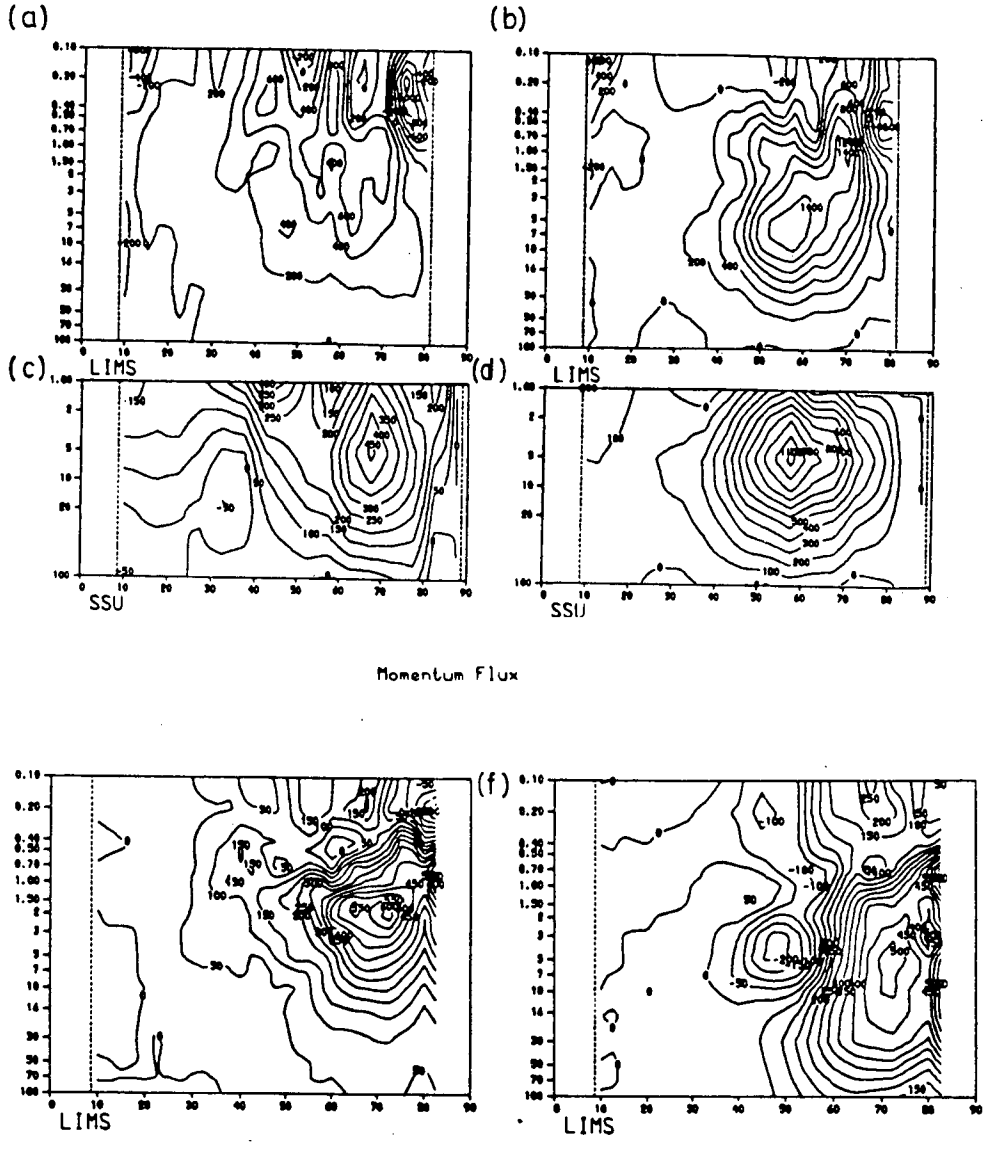

Figure F4.5 Daily northward temperature and momentum fluxes derived from LIMS and SSU data from Rodgers (1983). Contour intervals of (a)&(b) $200 m^2 s^{-2}$, (c) $50 m^2 s^{-2}$, (d) $100 m^2 s^{-2}$ and (e)&(f) 50 Kms^{-1}.

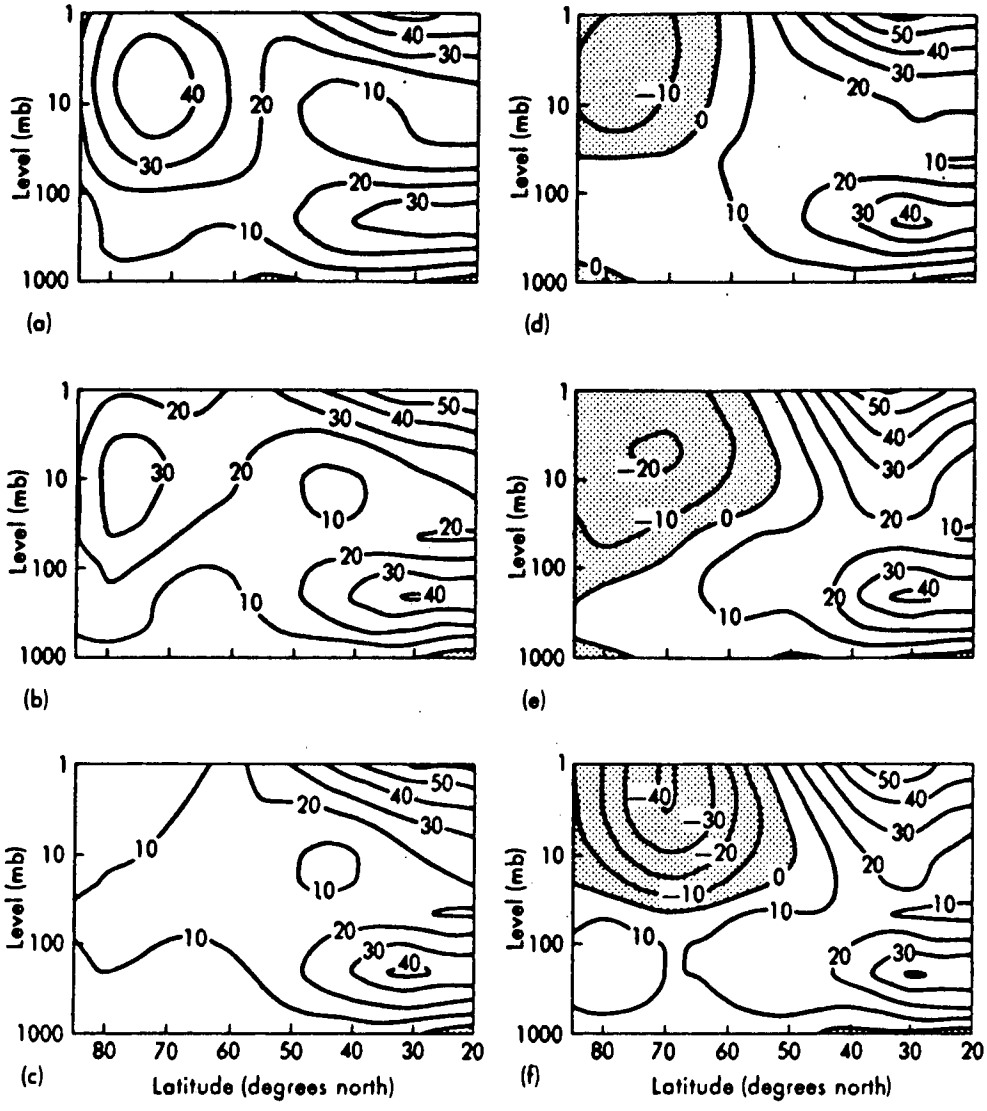

Meridional cross section of zonal mean wind velocity (m s^{-1}). Regions of easterly winds are stippled: (a) 17 February, (b) 19 February, (c) 20 February, (d) 21 February, (e) 23 February, and (f) 27 February.

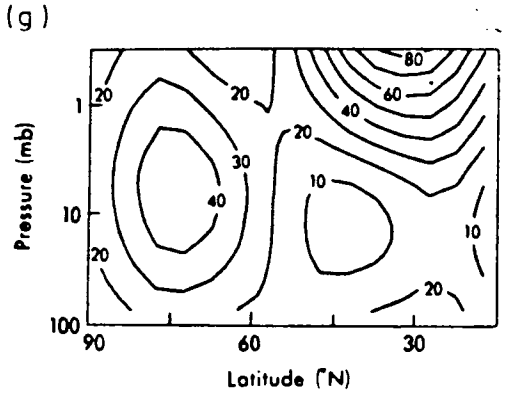

Figure F4.6a-g Meridional cross-sections of zonal wind velocities (using contour intervals of 10 $m s^{-1}$) from Palmer (1981a) & Butchart (1982).

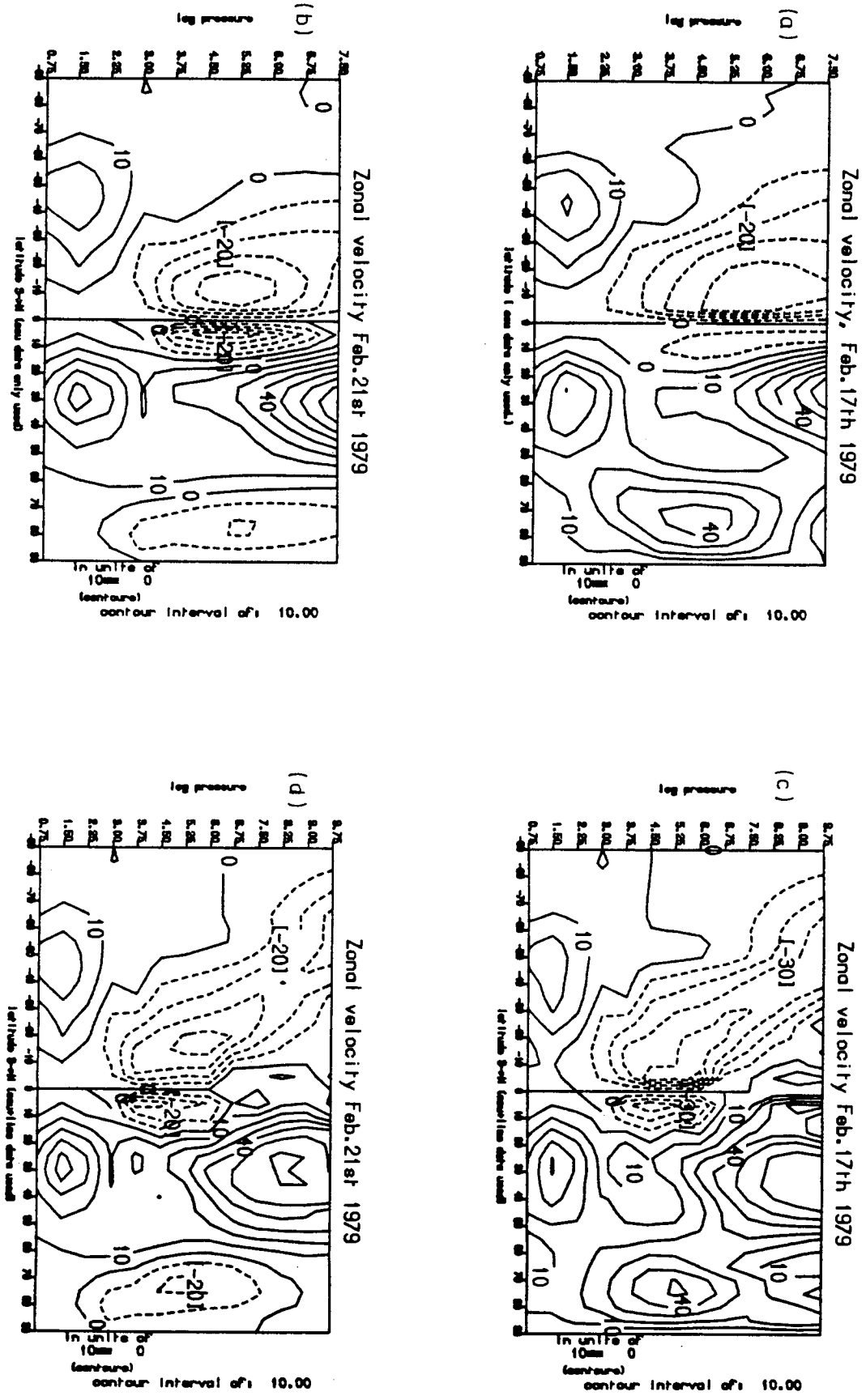

Figure F4.7 Meridional cross-sections of zonal wind velocity ($m\,s^{-1}$), calculated (as geostrophic velocities) during this study, for the 17^{th} & 21^{st} of February 1979 derived from SSU & LIMS data.(solid lines westerly, dashed lines easterly.)

The comparison is good both in terms of magnitudes and structure. More importantly a comparison can be made between the forcing diagnostics calculated by Palmer, Butchart et al and this study. Figure F4.8 shows four diagrams illustrating the eddy forcing by plotting the EP-flux and divergence for the 17^{th}, (a) & (b) and the 21^{st}, (c) & (d), from the two papers Palmer, (a) & (c), and Butchart et al, (b) & (d). However the diagnostics used in the two papers are not exactly equivalent.

The EP-flux F has units (kg m s^{-1}), while the contours of B where

$$B = \frac{\partial F}{\partial y}(y) + \frac{\partial F}{\partial z}(z) \qquad (4.24)$$

are in units of kg s^{-2}. These units are chosen on a (y,z) plane so that only when div.F is non-zero (and so consequently there is divergence or convergence) do the F vectors exhibit divergence or convergence. Without this scaling the vectors may appear to show divergence when there is none present in reality. This study however like Dunkerton et al (1981) has chosen to represent F and div.F on a (φ,η) plane. (Dunkerton et al uses a φ,z plane but the essential difference is in the use of φ rather than y.) This gives F units of kg m^2 s^{-2} and Δ_η, the equivalent of B on a φ,η plane, has units of kg m^2 s^{-2} = J.

Since

$$\int \nabla . F \, dV = \int \Delta_\eta d\varphi d\eta \qquad (4.25)$$

Palmer has used a better method still, as he plots D_F or A,(see figures F4.8a &c), as he refers to it. (i.e. the zonally averaged body force per unit mass acting on the mean state.) Table T4.a shows a sample comparison of the various forms of divergence of the EP-flux used by the various authors considered.

Note: Values marked by being underlined are quoted values from calculations or were read from the diagrams (and as such are less precise.) All the other values have been converted from these observed values using the relations.

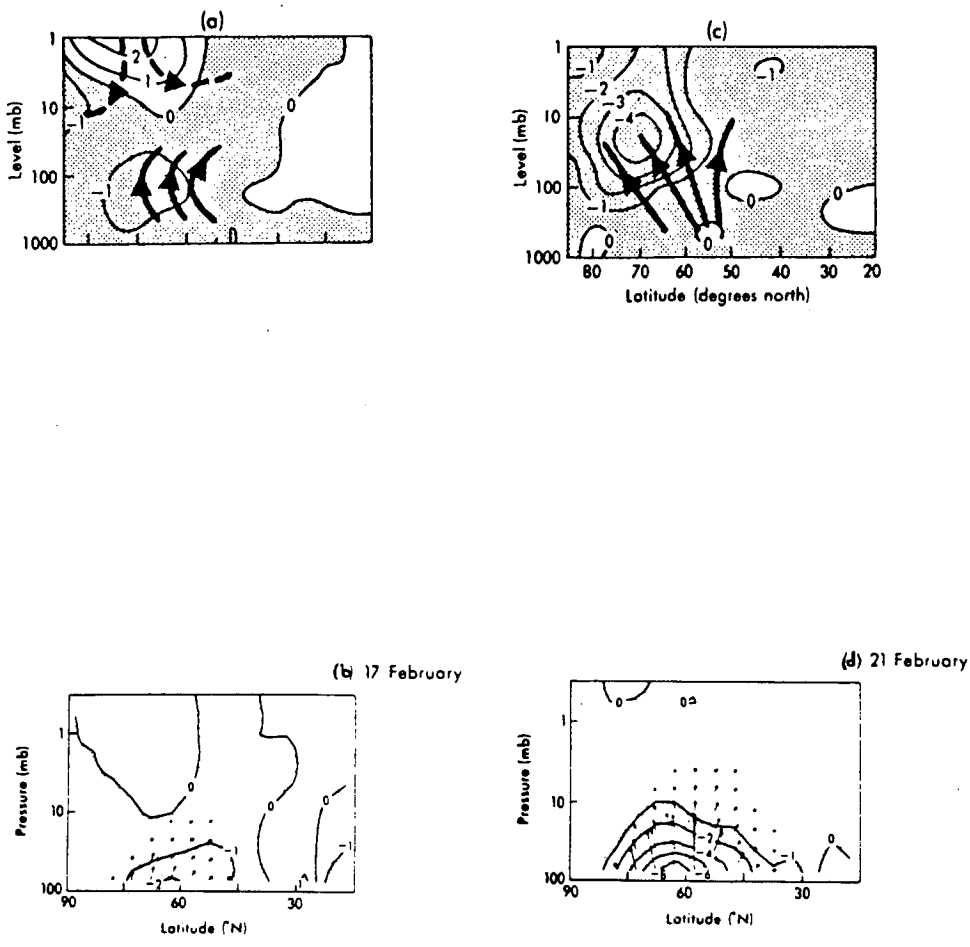

Figure F4.8 Wave forcing diagnostics for the 17th (a) & (b), and the 21st (c) & (d), of February 1979 from Palmer (1981a), (a) & (c), and Butchart et al (1982), (b) & (d). Figures (a) & (c) show contours of D_F in units of 10^{-4} ms^{-2} with some integral curves of F. (negative values are stippled.) While figures (b) & (d) show contours of B labelled in units of 10^{8} kgs^{-2} with EP-Flux vectors which are defined and scaled as per Butchart et al (1982) page 479.

A sample data comparison at 60 N, 100mbs.

	B (kgs^{-2})	$\Delta\eta$ $(kg\ m^2s^{-2})$	D_{F_ϕ} (ms^{-2})	$\nabla \cdot F$ $(kgm^{-1}s^{-2})$
Butchart et al	-2.10^8	-1.10^{19}	$-0.3\ 10^{-4}$	-10.0
Palmer	$-11\ 10^8$	-5.10^{19}	$-1.0\ 10^{-4}$	-54.1
Beagley	$-9\ 10^8$	-4.10^{19}	$-0.9\ 10^{-4}$	-48.7

Note: underlined values are observed values taken from the figure, non-underlined are calculated from these using the relations (4.25).

Table T4a A sample data comparison at 60° N, and 100mb, on the 17th of February, between this study using SSU data only, Palmer (1981a) and Butchart et al (1982), of some EP-Flux divergence quantities.

$$F_{(y)} = 2\pi a F_{\varphi} c$$

$$B = 2\pi a \nabla . Fc$$

$$\Delta = 2\pi a^2 \nabla . Fc$$

$$\Delta_{\eta} = 2\pi a^2 H \nabla . Fc$$

$$D_F = \frac{1}{a\varrho_o c} \nabla . F$$

(4.26)

The values of D_F and Δ_{η} calculated from the SSU data set compare very favourably with the results of Palmer (1981a). A repitition of the analysis was undertaken for the 21^{st} of February 1979. The new values of D_F for the 17^{th} and 21^{st} of February using the combined LIMS and SSU data set are shown together with the D_F derived using only the SSU data in figure F4.10. Here as on the 17^{th} the results compared well with the Palmer values and also compared better with the Butchart et al (1982) results. Only at below 100mbar was the forcing pattern significantly different, as can be seen from figures F4.8a-d,F4.9a-d & F4.10a-d. With the inclusion of the LIMS data set to extend and improve the height resolution of the calculations a second set of analyses for the 17^{th} and 21^{th} was undertaken. For these analyses the zonal mean velocity profile remained basically the same and it appears to have improved the region where poor data at upper levels were used in the SSU analysis case. The comparison of the acceleration diagnostics however illustrates a major difficulty in all data results and which has been unresolved in this thesis. The reliability of the results that follow in this thesis must be considered with the uncertainties described above in mind. The variation introduced, some of which are present due to current data quality inadequacies, however is not sufficient to invalidate the conclusions described in the later chapters.

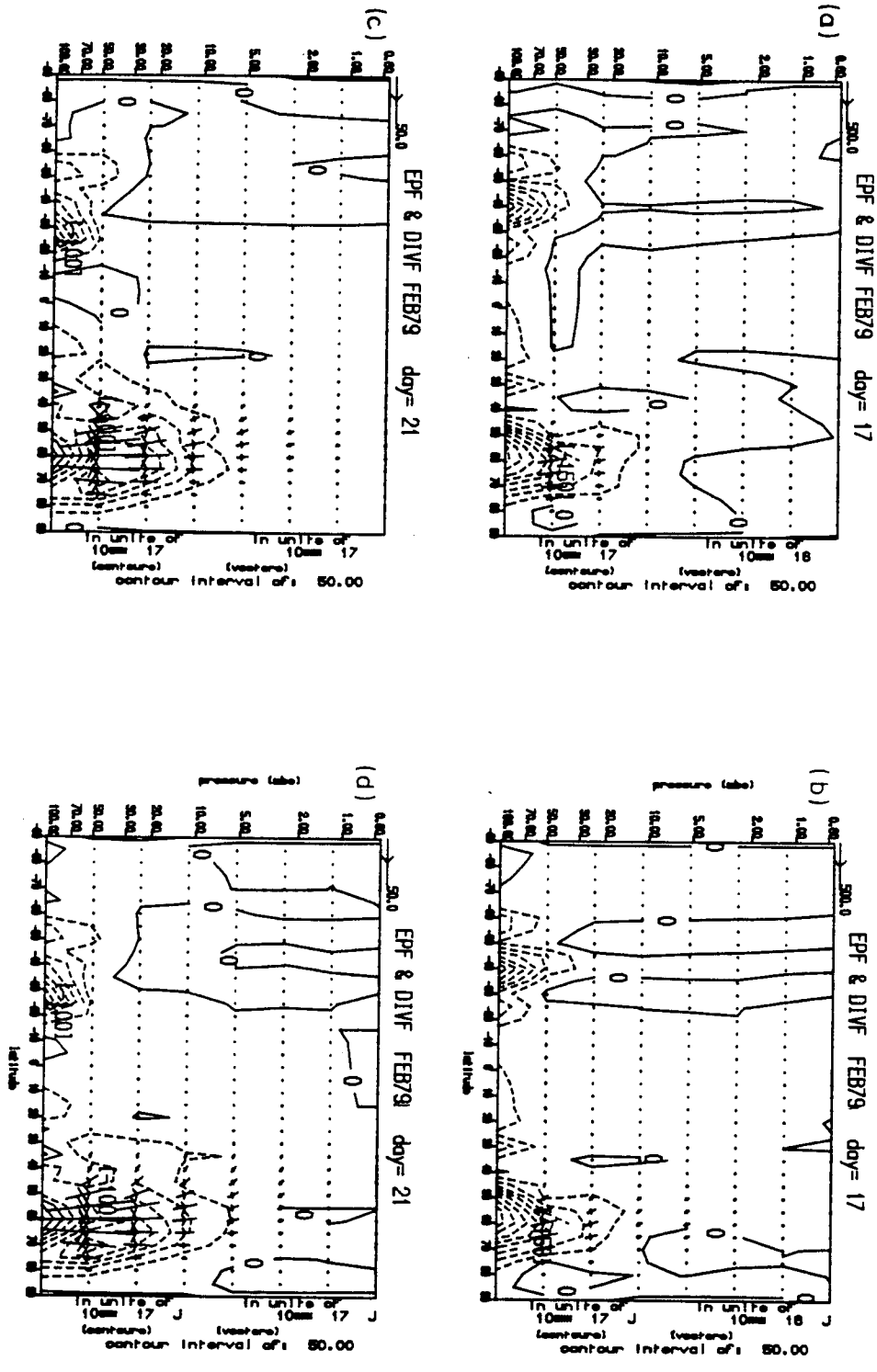

Figure F4.9 Contours of Δ_η (J), see text for definition, combined with EP-flux vectors for: (a) the 17th of February 1979 using SSU data only, (b) the 17th using LIMS+ & SSU combined data, (c) the 21st using SSU data only and (d) the 21st using LIMS & SSU combined data. The arrow scales are such that a vector whose length is the horizontal distance 10° on the diagram represents a value of $(5\pi/18)n$ of F^φ in {J} & a vector whose length is the vertical distance 1 interval of η represents a value n of F^η in {J}; where n is the scale arrow magnitude at the top right of the figure multiplied by the vector scale factor at the left edge (top) of the diagram. F^φ, F^η & Δ_η are defined as in Appendix C. $n= 500.10^{16}$ (J).

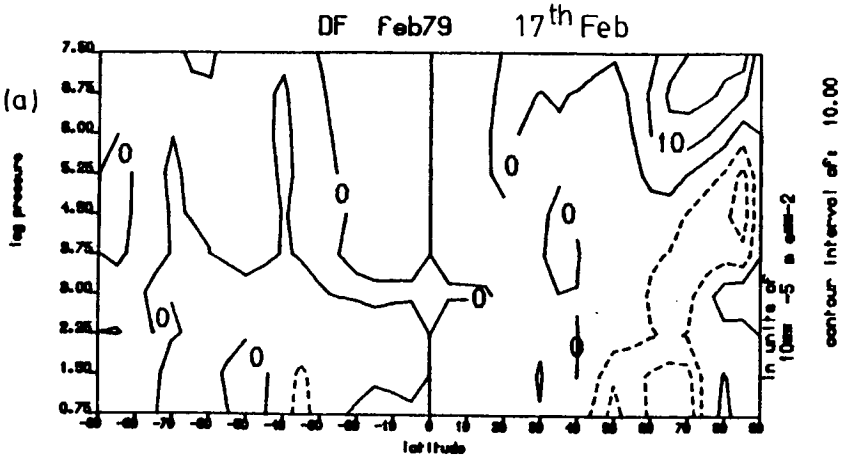

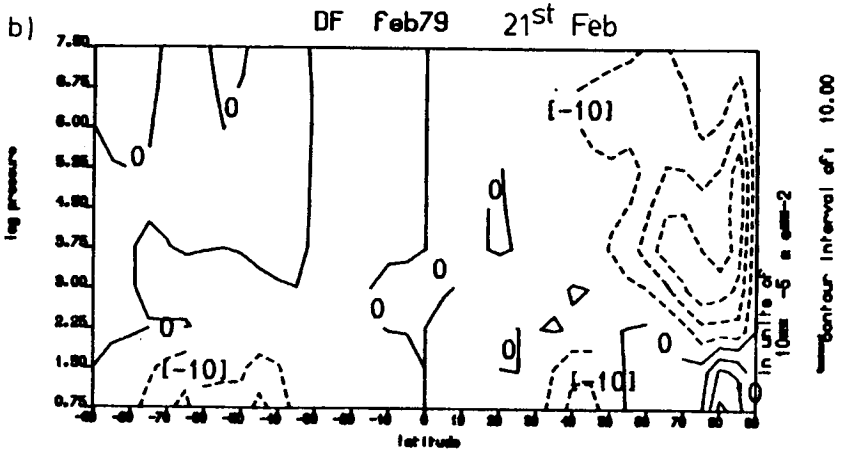

(SSU only.)

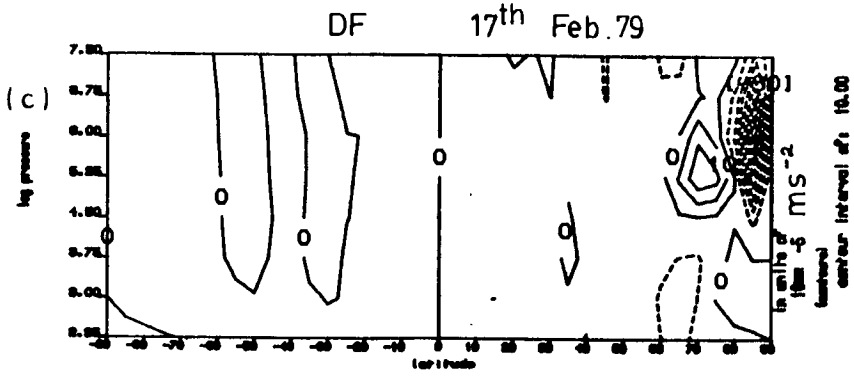

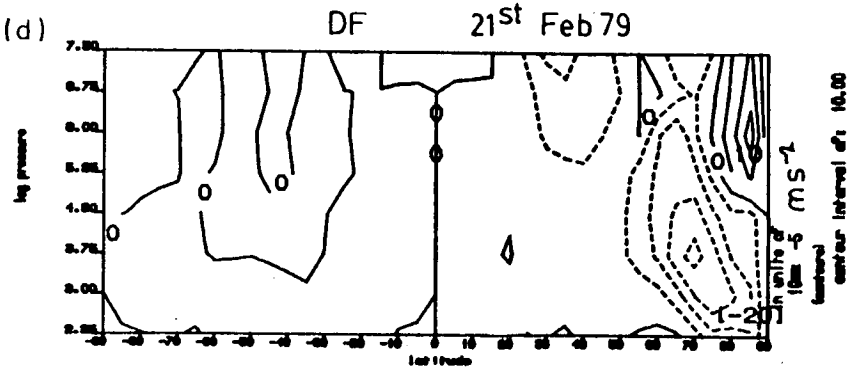

(SSU+LIMS)

Figure F4.10 Contours of D_F for the 17th and 21st of February 1979 based upon SSU and combined SSU+LIMS geopotential height data. Contour units of 10.10^{-5} ms^{-2}

For the 17th of February the two versions of EP-flux and divergence representations are very similar except for the positive divergence region at 2-3 mbar at high latitudes in the northern hemisphere. The major deceleration region is illustrated by the plot of D_F for the combined data in figure F4.10c, which shows above 10mbar a very large region of negative acceleration. Palmer's results and the evaluation of D_F using the SSU data only shown in figure F4.10a both show a much smaller negative feature. It appears that the sharp gradient with latitude of the momentum flux at 75-80^{o}N is responsible for the large convergence and divergence values of D_F in this region. A number of reasons can be put forward for these large values being caused in error including; the finite difference scheme, the data at 85^{o}N being poor, the extrapolation to the pole of the LIMS geopotential data being inaccurate or more probably due to the use of geostrophic momentum fluxes at this latitude which may be inadequate for accurate calculations of the EP-flux and divergence. The comparison of the D_F values is much more favourable away from 80-85^{o}N showing the pattern of forcing is more consistent with the Palmer (1981a) and Butchart et al (1982) results.

For the 21st of February the same problem is evident, with two changes most prominent in figure F4.10d compared with figure F4.10b. The most obvious change between figures F4.10b and F4.10d is the positive region of acceleration at 2-3mbar in figure F4.10d which is not present at all in either the SSU only (see figure F4.10b) or Palmer's values. The other large difference between figure F4.10b & d is the magnitude of the convergence region at 70^{o}N, $\approx$ 20mbar, this has a higher maximum value in figure F4.10d than in F4.10b. However F4.10b is an underestimate of the value seen in figure F4.8 from Palmer(1981a) and F4.10d is closer to the maxima shown in figure F4.8 from Palmer (1981a). Consequently the convergence region at 70^{o}N,$\approx$ 20mbar has been brought closer to Palmer's results by including the LIMS data but the divergence is still very high at 85^{o}N as on the 17th of February.

To check the significance of these large (and possible erroneous) values upon the residual circulations a sensitivity test has been undertaken, See section (4.3.6.7).

The combination of the LIMS and SSU data sets was assessed as part of the above discussion and it is clear from the daily data illustrated in figure F4.10 that the two data sets include important differences and so their combination will introduce some extraneous gradients. However most of the difficulties appear to be confined to the very high latitudes in the winter hemisphere, and figures F4.2, F4.3 and F4.9 show that the monthly averaging reduces the differences inherent in the two data sets to an acceptable and usable level. The LIMS fluxes are seen to be stronger than their SSU counterparts and so the overlap is not perfect. Consequently some sensitivity tests have been undertaken, which are described in section 4.3.5.8, to try and determine the influence of the differences introduced by the combined data upon the circulations derived.

The comparisons made, clearly indicate that important differences are present between the results considered but that this is a common problem to all studies, (Rodgers 1983), which arises because of the differences inherent in the various observed data sets used to evaluate the subsequent diagnostics.

4.3.4 : THE DIABATIC HEATING RATES

4.3.4.1: CALCULATION METHOD.

In order to calculate the diabatically driven circulation, the zonally averaged diabatic heating rates are required. The radiative heating rates used were estimated by using a scheme supplied by Dr Haigh. This calculation requires temperatures, ozone, water vapour and cloud amounts.

If a highly detailed model calculation of individual bands and lines were used in its entirety then even a simple atmospheric problem would be beyond the scope of most computers and the economics of time and expense exorbitant. Thus methods are required which treat correctly the essential statistics of the problem and allow large data sets to be examined usefully within a reasonable research period and at a reasonable cost. The Haigh (1984) routine produces a heating rate principally driven by:

i) the rate of heating due to solar absorption.

ii) the rate of cooling by thermal radiation.

The Haigh (1984) radiation scheme is split into its 'long-wave' and 'short-wave' components. In dealing with the infra-red, (IR), radiative transfer, several simplifying approximations were made to Schwarzchilds equation. A full description of the details are presented in Haigh(1984). The IR region is divided into five spectral regions and only three gases are considered. These principle bands of the gases are considered to be the only significant contributors to the stratosphere. The bands used were 0-555cm^{-1} for H_2O, 555-775 cm^{-1} for H_2O & CO_2, 775-960 cm^{-1} for H_2O, 960-1080 for O_3 and 1080-2200 cm^{-1} for H_2O. For the IR calculation a fine grid of 1.25 km is used to provide a smooth representation of the transmission differences in the stratosphere. The logarithm of the mixing ratios are interpolated linearly between the vertical coordinate levels for each gas, and absorber amounts and mass-weighted pressures are calculated for each vertical sub-interval for each gas and hence a matrix of transmissions is constructed for each spectral interval. The Planck function is then integrated over wavenumber and then linearly interpolated between the model levels. The upward and downward fluxes can thus be obtained at each grid point by a numerical solution of the integrals in the approximate Schwarzchilds equation used. The Haigh (1984) scheme's heating rate is then calculated from the divergence of the net upward flux.

Water vapour, CO_2, CH_4, nitrous oxide and molecular oxygen all have absorption bands in the near infra-red. The transfer of thermal radiation by these bands can be considered negligible, but their absorption of solar radiation makes a significant contribution to the radiative balance of the stratosphere. The Rodgers (1967) approach is used by Haigh (1984), together with the analytical expressions of the Curtis-Godson approximation to obtain the heating rates due to this absorption of the solar radiation.

For the absorption of solar ultra-violet and visible radiation by O_3 and O_2 the method of Strobel (1978) was used. The sum of the above contributions gives the net radiative heating used throughout the stratosphere and is only modified in the troposphere, see below.

Temperatures were obtained from the LIMS values and calculated from the SSU geopotential data. Figure F4.11 shows the various regions of data coverage. The ozone is predominantly provided from LIMS data but SBUV data obtained from McPeters et al (1984) is also used in the lower atmosphere. Water vapour data are only available from the LIMS data. During the months when no LIMS water vapour was available a crude constant water vapour height profile, constant with latitude and month, was used for all the SSU months from June to November 1979. A comparison for May 1979 was made of the effect of the use of these data compared with the LIMS water vapour values. The circulation differences which were observed were not significant, the most noticeable differences which arose occurred in the evaluation of [Q] in the lower stratospheric low latitudes where the cooling was over-estimated due to the lack of the more accurate water vapour values. Water vapour data for the lowest levels in the troposphere are estimated using an assumption of 50 percent saturation. All LIMS data must be extrapolated to the poles. Carbon dioxide is assumed to be uniformly mixed with a mixing ratio of 330 ppm.

The diabatic heating calculation routine did not provide information for the troposphere and so in the lower troposphere the values for the radiative heating were prescribed following the values suggested by Haigh (1984). The radiative cooling of the troposphere has been taken as a constant 1.5 degrees per day in the lower two levels (η=0.25 and η=0.5) and a value of 0.75 degrees per day at the third (η=0.75). These are then combined with sensible and latent heat release values estimated from climatological data taken from Newell et al (1969).

The extrapolation of the various data fields resulted in some anomalous negative concentrations. These occur only rarely and high in the stratosphere where the magnitudes of ozone and water vapour approach zero. In such cases the concentration has been assumed very small and its sign changed and the magnitude multiplied by 10-4. Where temperatures are missing a substitution has been made from adjacent data points; a smoothing routine calculates an average value from the adjacent latitudinal points.

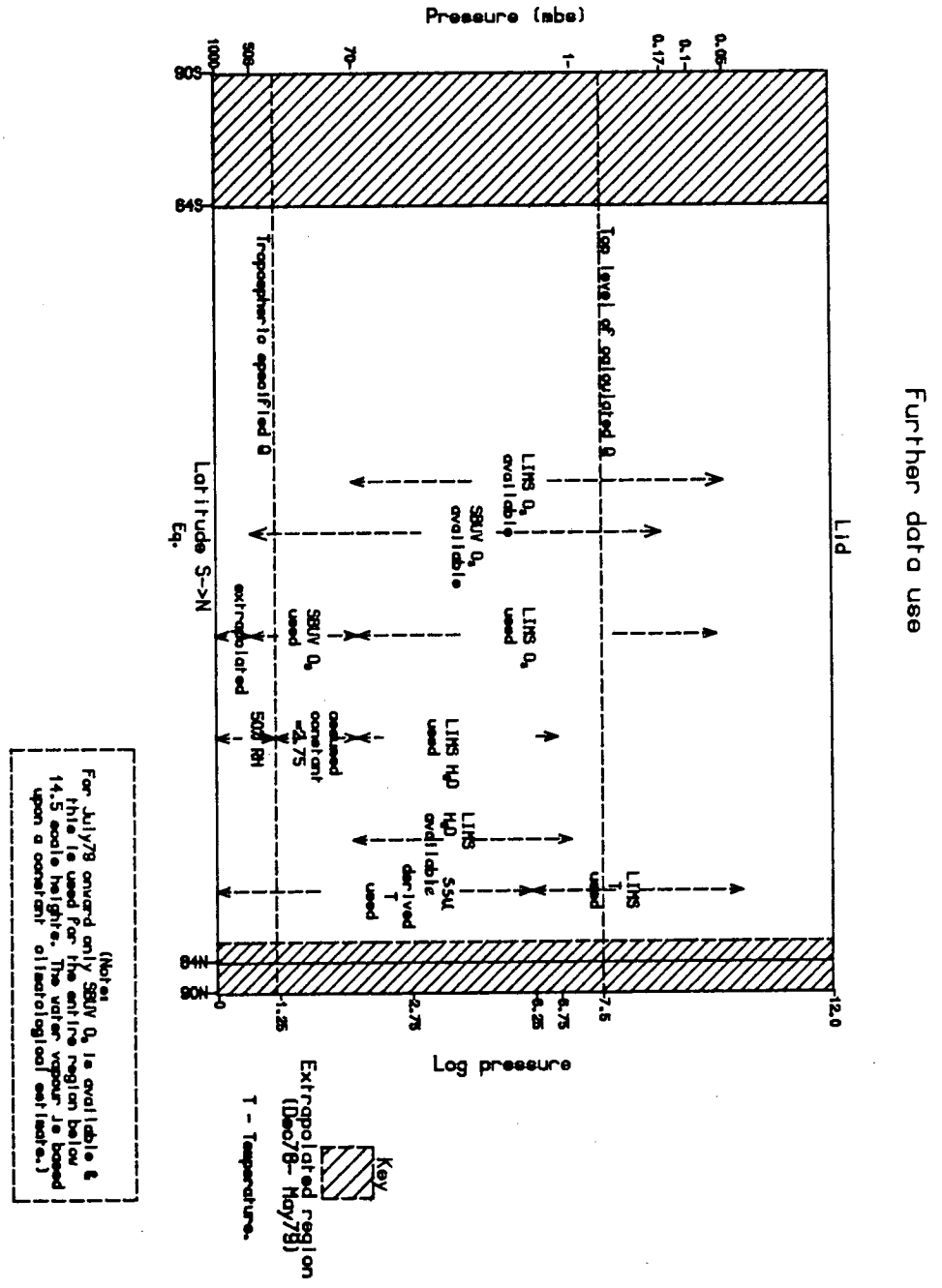

Figure F4.11 Schematic diagram showing the other data sources used over the analysis region to illustrate their spatial and temporal extent.

This diabatic heating routine calculates [Q] only up to log pressure η=7.75, i.e. p$\approx$ 0.4 mbar. Above this level the heating is reduced smoothly to zero. An experiment, see section (4.3.5.5) & figures F4.16a-d), has been undertaken showing that the solution below 1 mbar is not sensitive to the method of extrapolation.

4.3.4.2: THE HEATING RATES- A COMPARISON.

The diabatic heating rates for December, March, June and September are shown in Fig F4.12. These have been obtained using SSU, LIMS, SBUV and climatological data sets as explained above. These can be compared with a variety of different diabatic heating rate evaluations including; in Murgatroyd & Singleton (1961), Crane et al (1980), Haigh (1984) and more recently Kiehl & Solomon (1986). The values that are available are qualitatively similar but the various radiative calculation procedures and different data sets result in quantitative differences of both heating and cooling rates which are considerable.

Comparison of the LIMS [Q] for December, January and February evaluated by Kiehl & Solomon (1986), (see figures 8b-d), with the rates evaluated in this study and illustrated by the examples in figure F4.12, is fairly good qualitatively while the peak polar coolings and warming values are larger in this evaluation and the equatorial-tropical middle atmospheric values are weaker. This region exhibits small values of [Q] as it is close to radiative equilibrium and therefore is sensitive to error. The quantitative problems in the southern hemisphere polar region for the LIMS months are illustrated by the December case in Figure F4.12 which shows the large heating rates in the upper stratosphere at latitudes 90^{o}S- 65^{o}S. The maximum value of $\approx$ 4-5^{o}C/day at 2mbar is well in excess of a similar calculation in Pawson (1987) using the same data which shows a southern hemispheric cooling of only 2^{o}C/day at this level. The discrepancies may be occuring because of the necessity for data extrapolation and the use of climatological temperatures at these latitudes (due to the use of the LIMS data set) which has not in this study been sufficiently accurate in order to prevent anomalous results. Comparison of the months after the end of the LIMS period can be made with the northern hemisphere rates in Crane et al (1980). In June the diabatic heating

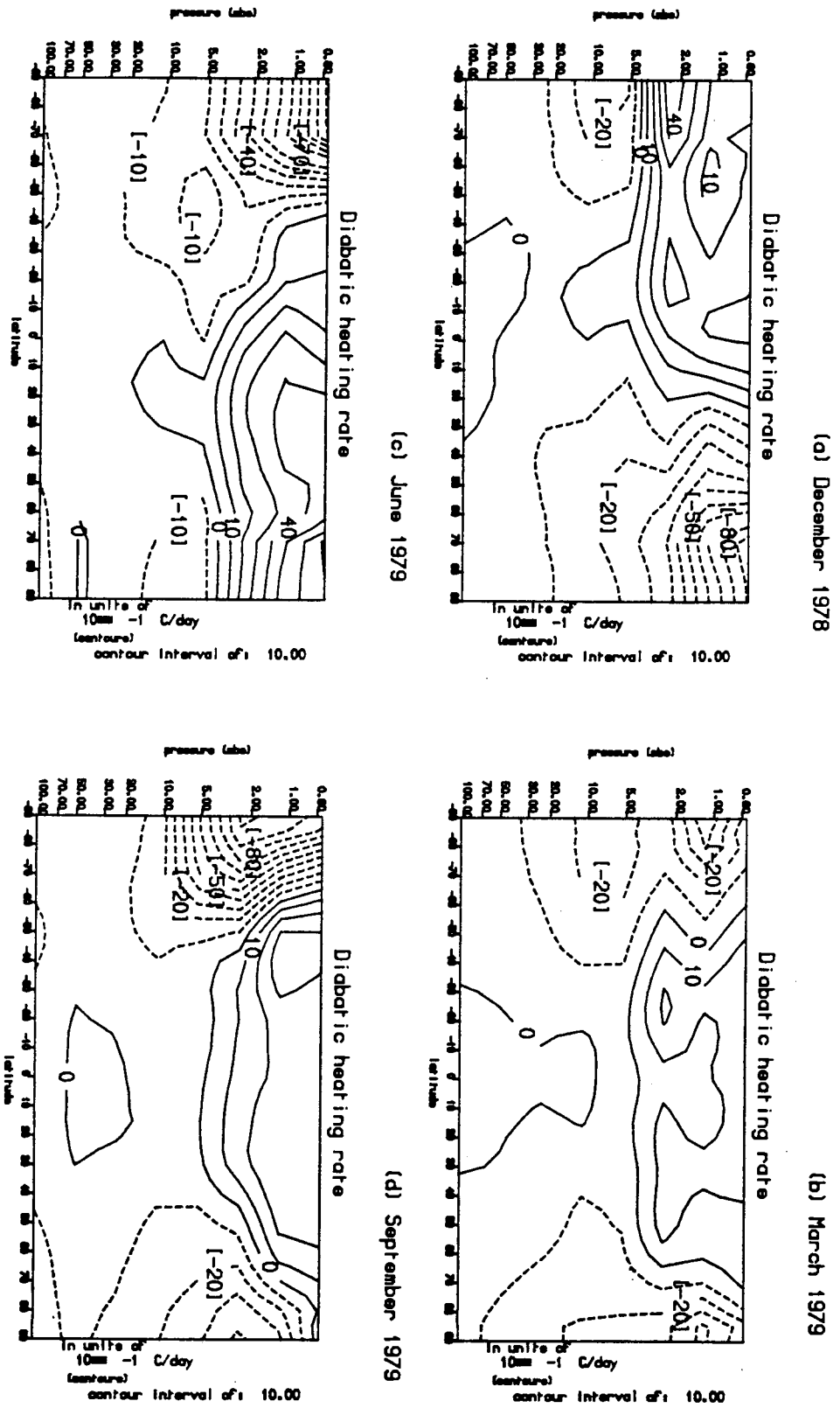

Figure F4.12 Example diabatic heating rates, [Q], deduced for: (a) December 1978, (b) March 1979, (c) June 1979 & (d) September 1979.

rates, (see figure 6 of Crane et al (1980)), suggest an over-estimation of the heating by the SSU data. This most probably arises because of the problem of poor temperature estimates in the upper stratosphere because of the loss of the upper TIROS-N channel throughout this period. This over-estimation in June by the SSU based [Q] values is also found when comparing the rates evaluated for the same months but using SSU instead of LIMS data when this comparison was possible, i.e. from December 1978 to May 1979. However the comparison in September shows a fairly good agreement between the values in Crane et al (1980) with only a slight overall increase in [Q] values compared with the larger differences seen in the earlier months.

It is clear that there is considerable variability inherent in this calculation and this must be borne in mind in the analysis and interpretative comparison of this flow component. Clearly, as commented upon by G.Brasseur (personal communication, 1987), in regions where the [Q] values are small such as the lower stratosphere the uncertainties involved in the evaluation of [Q] due to the different radiation schemes and data sources and errors will produce significant effects upon the diabatically driven circulations derived.

4.3.5 : SENSITIVITY TESTS

In order to assess possible errors from various sources, a number of sensitivity tests were performed. The following 8 tests were undertaken.

i) The effect on the flow of the lower boundary assumption.

ii) The influence of the upper data extrapolation upon the flow.

iii) The effect of the equatorial data extrapolation.

iv) The lower boundary finite difference scheme.

v) The Upper diabatic heating extrapolation.

vi) An Ozone perturbation test.

vii) Eddy flux polar data extrapolation.

viii) Differences between data sets.

4.3.5.1 : THE LOWER BOUNDARY ASSUMPTION.

Since the problem is posed as an elliptical boundary value problem, the boundary conditions used will be important to the solution. It was assumed in the method that [w]=0 at η=0. This cannot always be justified, since the standard Eulerian streamfunction is not quite zero at sea level, if only because of topographical effects. It is necessary therefore to test the importance of this assumption upon the flow and the likely error it may cause, plus the effect of possible errors in the fluxes and potential temperature gradients at the ground which appear in the boundary condition, equation (4.17). As [w]=0 is assumed at the lower boundary, equation (4.17) where Ψ_E=0, expresses the value of the streamfunction used at the boundary. The following variants upon the flux magnitude at the lower boundary were used to assess the differences produced.

a) Flux calculated from FGGE data at 1000mbar.

b) Flux as (a) doubled.

c) Oort & Rasmusson (1971) climatological Northern hemisphere heat fluxes used.

Figure F4.13 illustrates the three residual circulations computed using the three variants above. At first glance the velocities appear to remain virtually unchanged in general appearance; even the 200 per cent variant leaves the flow qualitatively very similar in the region of interest, between η=2.25 and η=7.5. These may however be slightly deceptive as an illustration of the changes. Figure F4.14 a&b shows the vector differences between the variants (a) & (b) and (a) & (c). The latter is expected to be a better estimate of the possible errors involved in specifying the lower boundary condition correctly since the FGGE data provides a reasonable alternative estimate of the fluxes whereas the doubling variant exaggerates the errors expected considerably. It can be seen that these extra components will not significantly affect the circulations calculated except in the winter eddy-active mid-latitudes near and below the tropopause. Variant (b) does show that important changes of $[v]^R$ and $[w]^R$ can occur throughout the depth of the stratosphere if such an error source were to occur. So it is important to use accurate values for the lower boundary fluxes and this is partly why FGGE data were used in

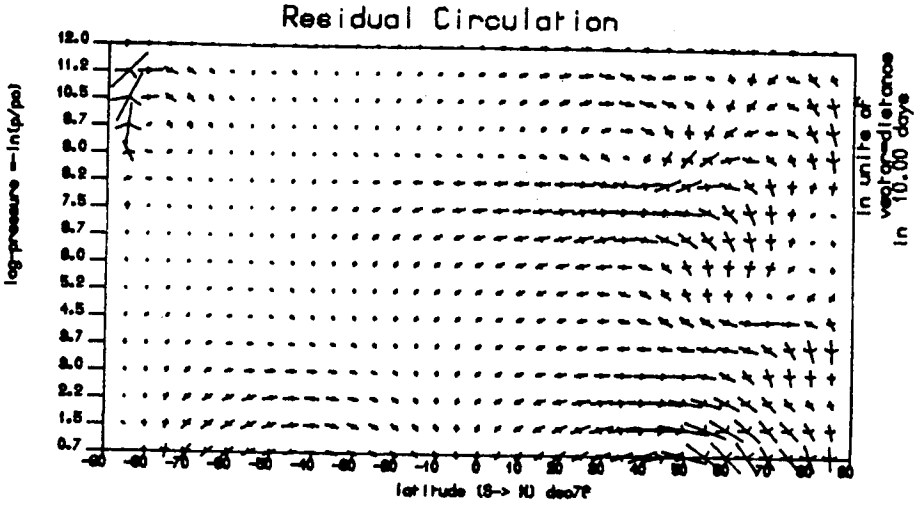

(a) 200% lower boundary Flux Forcing.

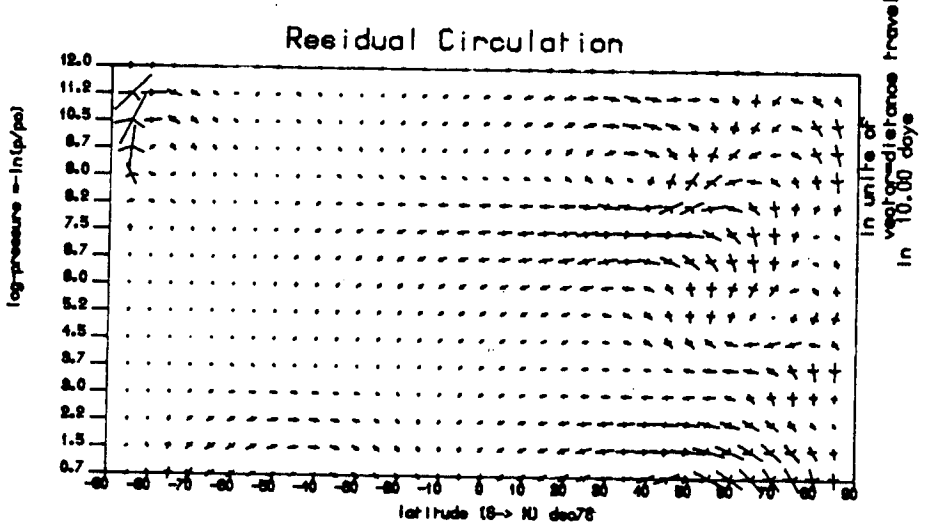

(b) 100% lower boundary Flux Forcing.

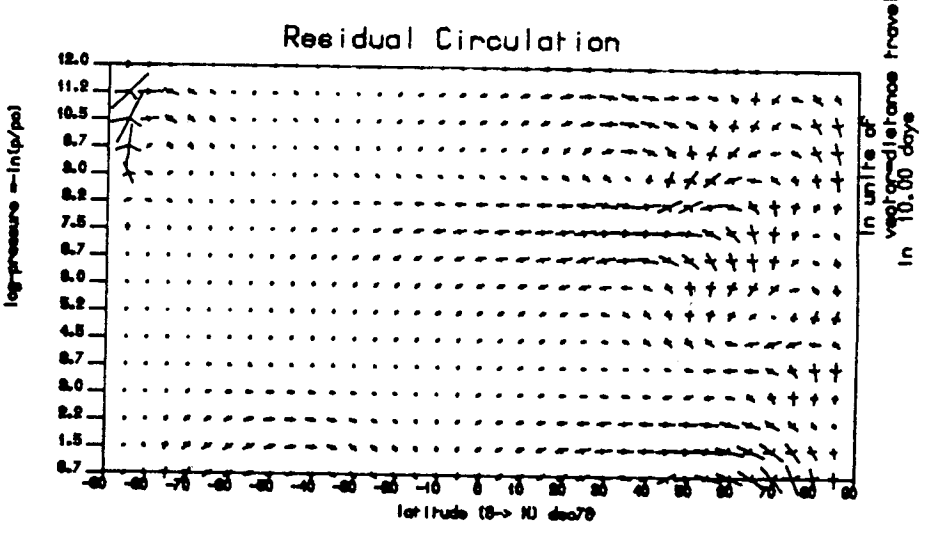

(c) Variant (a) lower boundary Forcing.

Figure F4.13 Eddy driven residual circulations for December 1978 using: (a) a 200 percent estimate of $[v^* \theta^*]$ in the lower boundary condition specification, (based upon FGGE data), (b) $[v^* \theta^*]$ as calculated from FGGE data & (c) $[v^* \theta^*]$ taken from Oort & Rasmussen (1971).

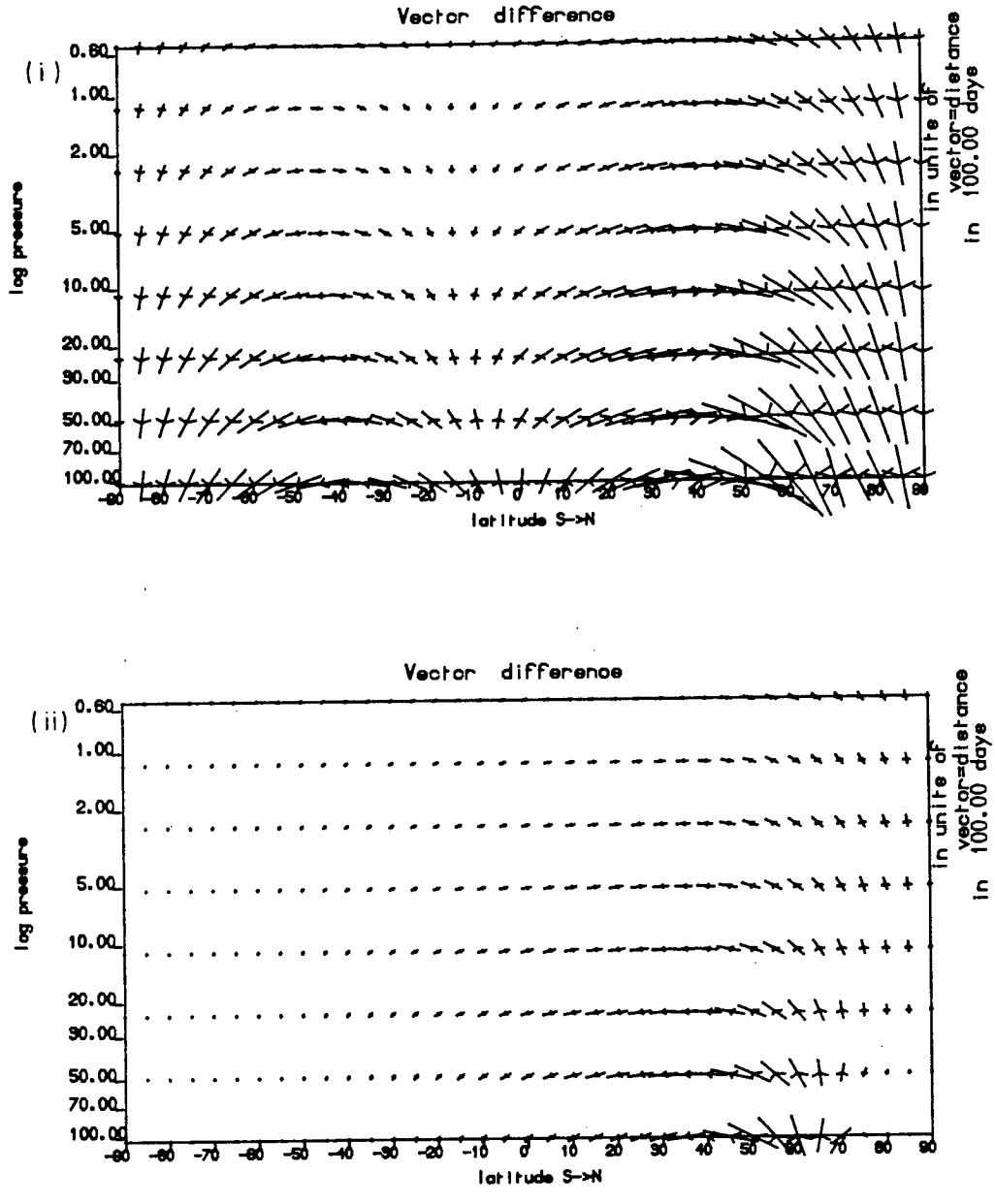

Figure F4.14 A vector difference diagram showing the velocity differences between(i)variants (a) & (b) and(ii)(c) & (b), for the lower boundary condition sensitivity test.

this study. Obviously the tropospheric solution ($\eta < 2.25$) was considerably affected and also the southern hemisphere where the internal forcing was weak.

The main features forced by the internal forcing of the eddy fluxes and diabatic heating appear robust and remain unchanged despite the variations forced at the lower boundary. However error in the velocity magnitudes will result from the uncertainty in the lower boundary assumption, but this will be insufficient to invalidate the general conclusions.

4.3.5.2 : THE UPPER DATA EXTRAPOLATION.

Since all the data at and above $\eta=9.75$ on the grid has been extrapolated, it is important to assess the effect of this upon the region of interest and to ascertain which of several possible extrapolations should be used to minimise the error due to the use of the extrapolation. The influence of the upper boundary condition was assumed as part of the extrapolation tests used and will not be tested separately. It was assumed that the eddy flux forcing profile above the top of the data at approximately 50-60 km tends to zero at the lid level $\eta=12.0$. The variants of upper data profiles used for the tests were as follows:

i) Real flux data used up to $\eta = 9.75$; above this the data were smoothed to zero at the lid.

ii) Real flux data were used up to $\eta = 9$; above this the data were smoothed to zero fluxes at the lid.

iii) Real flux data were used up to $\eta = 8.25$; above this the data were smoothed to zero fluxes at the lid.

iv) Constant fluxes used above $\eta = 7.5$.

Note: variants (i) to (iv) above were applied purely to give different flux functions or distributions above the top of the region of interest, i.e. $\eta > 7.5$.

All these extrapolations used a quadratic interpolation routine which filled in the flux profile between the top two levels of real data and the assumed zero value at the lid.

Figures F4.15a-d show the residual flows computed using the four extrapolations. Of the four versions (iv) produced the largest difference from any of the others in terms of $[v]^R$ within the region of interest, but even in this extreme case the percentage difference was in general less than 10 per cent. Of the other three extrapolations the maximum percentage difference between any two was ≈ 2 per cent. This is a positive indication that the decision to move the lid to η=12.0 and to extrapolate the missing data in between was satisfactory and unlikely to introduce large errors in the flow in the region of study.

It would appear that the choice of upper extrapolation and the influence of the upper boundary assumption is not a major source of error in the flow field. In examining the possible extrapolations of the eddy fluxes it is important to realise that it is the gradients of the fluxes in φ and η which must be 'modelled' best in our extrapolation if the residual circulation is to be dealt with satisfactorily in these regions above the real data.

4.3.5.3 : EQUATORIAL SMOOTHING.

Since for the equatorial region the geostrophic winds are inadequate and at the equator no winds can be found by the above quasi-geostrophic method due to the singularity, 1/f, a smoothing of the eddy flux data fields across the region (20S - 20N) was undertaken. Various forms of smoothing were used and their affect upon the circulation considered. No changes of the flow occurred of a magnitude sufficient to effect any subsequent interpretation even in tropical regions.

4.3.5.4 : THE LOWER BOUNDARY FINITE DIFFERENCE SCHEME.

It was observed that the flow calculated was far more sensitive to the finite difference approximation used to calculate the divergence at the lower boundary than for instance the lower boundary condition. The use of a one sided difference scheme was highly inappropriate due to the sharp reversal of EP-flux divergence to convergence in the lower troposphere, as p decreases, which is observed (figure 5, Edmon et al (1980)). Without the added information of the η=0 eddy fluxes the scheme failed to represent the large wave activity source in the

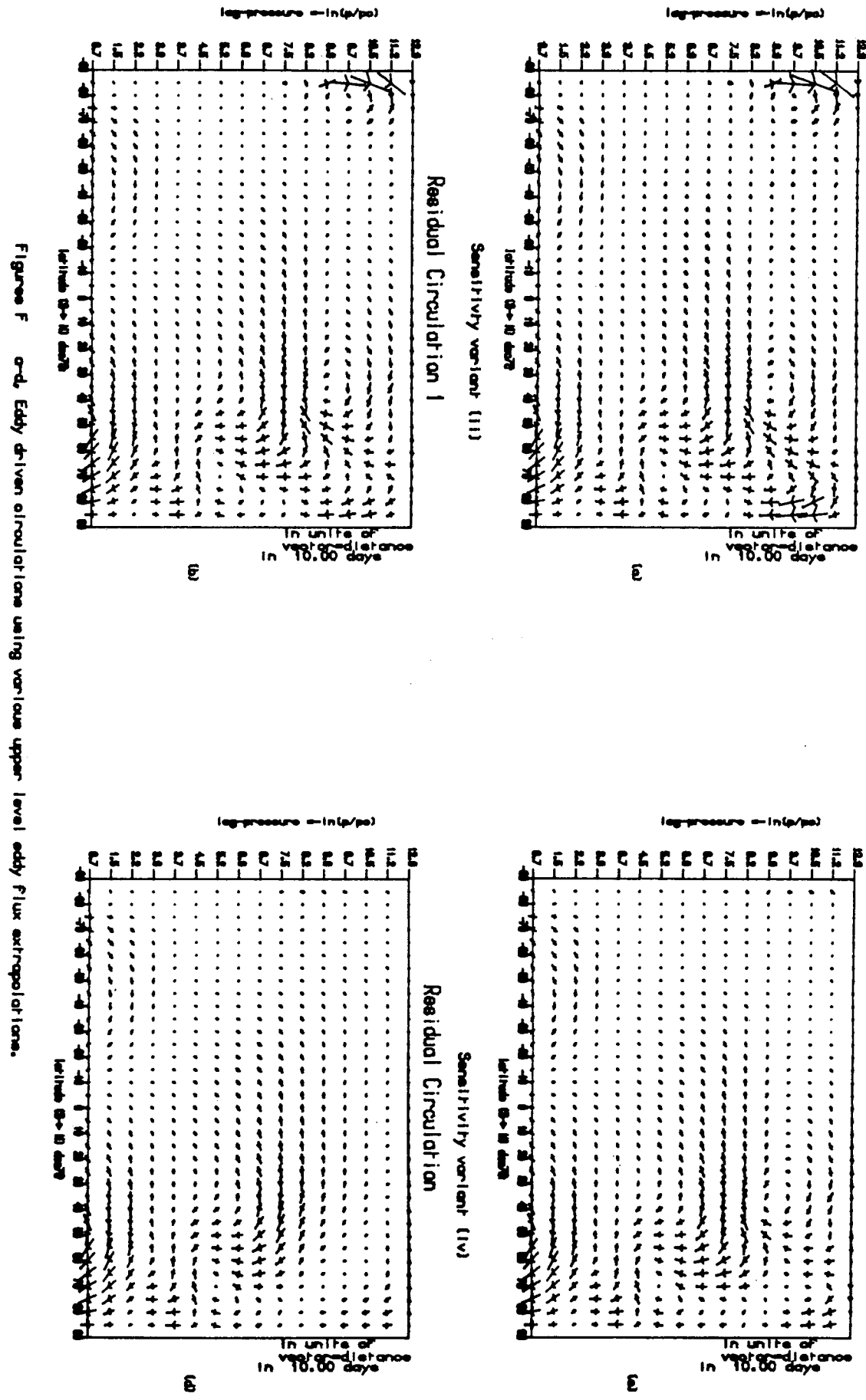

Figures F a-d, Eddy driven circulations using various upper level eddy flux extrapolations.

Figure F4.15 Eddy driven circulations using various upper level eddy flux extrapolations variants (i) to (iv) as above.

lower troposphere due principally to orographic and differential surface heating. It was important therefore to use a central difference scheme for the evaluation of the vertical gradients in calculating the EP-flux divergence at the lowest internal gridpoint, η=0.75, which requires a knowledge of the eddy heat fluxes at η=0. To do this heat fluxes derived from FGGE data were used, and these were also necessary for the lower boundary specification of Ψ.

4.3.5.5 : UPPER DATA DIABATIC HEATING RATE EXTRAPOLATION.

It is necessary to extrapolate the diabatic heating rates above 0.4 mb. Several variants of extrapolation were tested including:

i) Smoothed [Q] from top of real data at p≈ 0.6 mbar (η=7.5) to lid p≈ 0.006 mbar (η=12.0).

ii) Constant [Q] above p≈ 0.6 mbar, (η=7.5).

iii) as i) but smoothed to cooling of 1 K/day at lid.

iv) [Q] was first extrapolated to η=8.25, (p_λ~0.26 mbar), and then this data set was assumed as the top of the 'real' data and smoothed as (i).

From the various extrapolations used, a rough assessment of the possible differences introduced by any one method can be obtained. Since variants (ii) and (iv) use extrapolations which are likely to result in questionable values then in these cases the errors obtained are likely to be high. The values achieved showed that the region η=8.25 to η=7.5, the top of the region of interest does appear to be significantly affected by the choice of upper data extrapolation and that large percentage differences indicate possible large errors. See Figures F4.16a-d. Below this region the influence of even the most extreme variant used diminishes to ≈ < 2 per cent. It is important to note however that the results indicate that the area of sharp gradient in velocity in the upper stratosphere which occurs in all the extrapolations, due to the large diabatic forcing at these levels, can result in large differences in velocity. This occurs as the various extrapolations shift the position of the gradient which leads to differences as large as 50- 60 per cent in terms of the magnitude of $[v]^R$ if the worst variant differences are taken as indicators. However outside the region of the sharp gradient in velocity a value of ≈ 25-30 per cent or lower, may be more typical. It is clear from

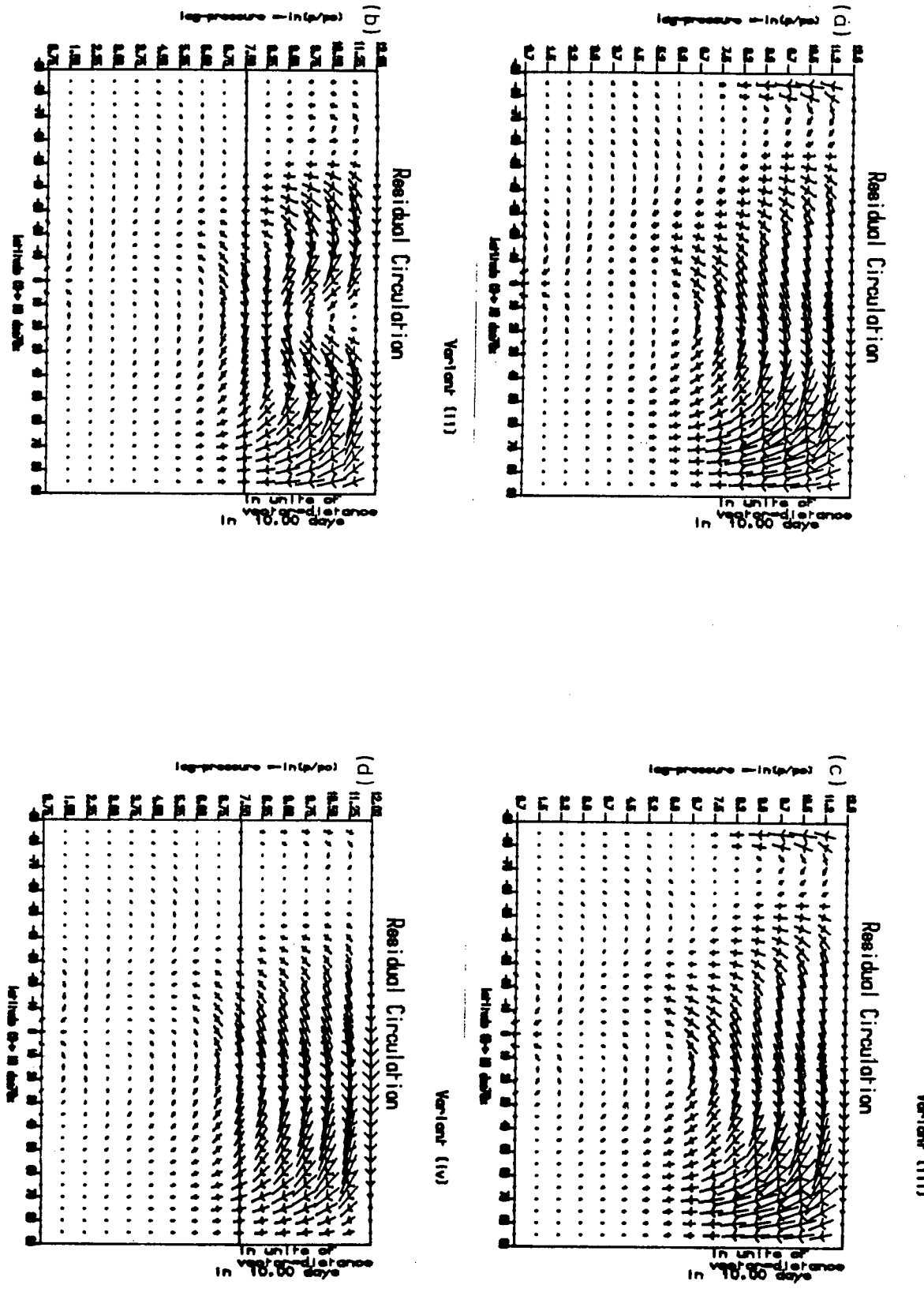

Figure F4.16 Diabatically driven residual circulations using various upper data heating rate, [Q], extrapolations: variants (i) to (iv) see above.

equation (4.16) that it is the gradients of [Q] in φ and η which are important in driving the diabatically forced component of the circulation and so the extrapolation of [Q] was undertaken with this in mind.

It would appear then that the extrapolation of diabatic heating above the region of interest will introduce significant errors in the upper levels η=6 to η=7.5 if the worst variants are taken as indicators of possible errors present.

4.3.5.6 : UNCERTAINTY IN THE OZONE DATA.

Since the LIMS and SBUV ozone data are subject to some possible error, one necessary test was to consider the consequences upon the resulting residual velocity fields. Values from Remsberg et al (1984) suggest a possible 15 per cent upper limit uncertainty in the measurement of the ozone concentration and so this order of deviation was applied to the ozone field by reducing the concentration by 15 per cent and assessing the impact upon the diabatic heating and residual circulation. The results show a qualitatively similar residual flow but [Q] has changed considerably and quantitative comparison of the velocities reveals some large differences in $[v]^R$ for instance where the vertical gradient of velocity is sharp. See Figures F4.17a & b. This variation is likely therefore to be one of the major sources of error in the flow calculation, due to the uncertainty in our knowledge of a basic data field. However the circulation component driven by these errors indicates that the velocity differences remain small except near $\approx$ 0.6mbar i.e. at the top of the region of interest where at this level the root mean square percentage error is $\approx$ 11 percent. Only near the ground does the root mean square error rise above this and here the diabatically driven velocities are very small anyway. The differences likely to occur at the top of the region of interest must therefore be taken note of and considered in the later analysis.

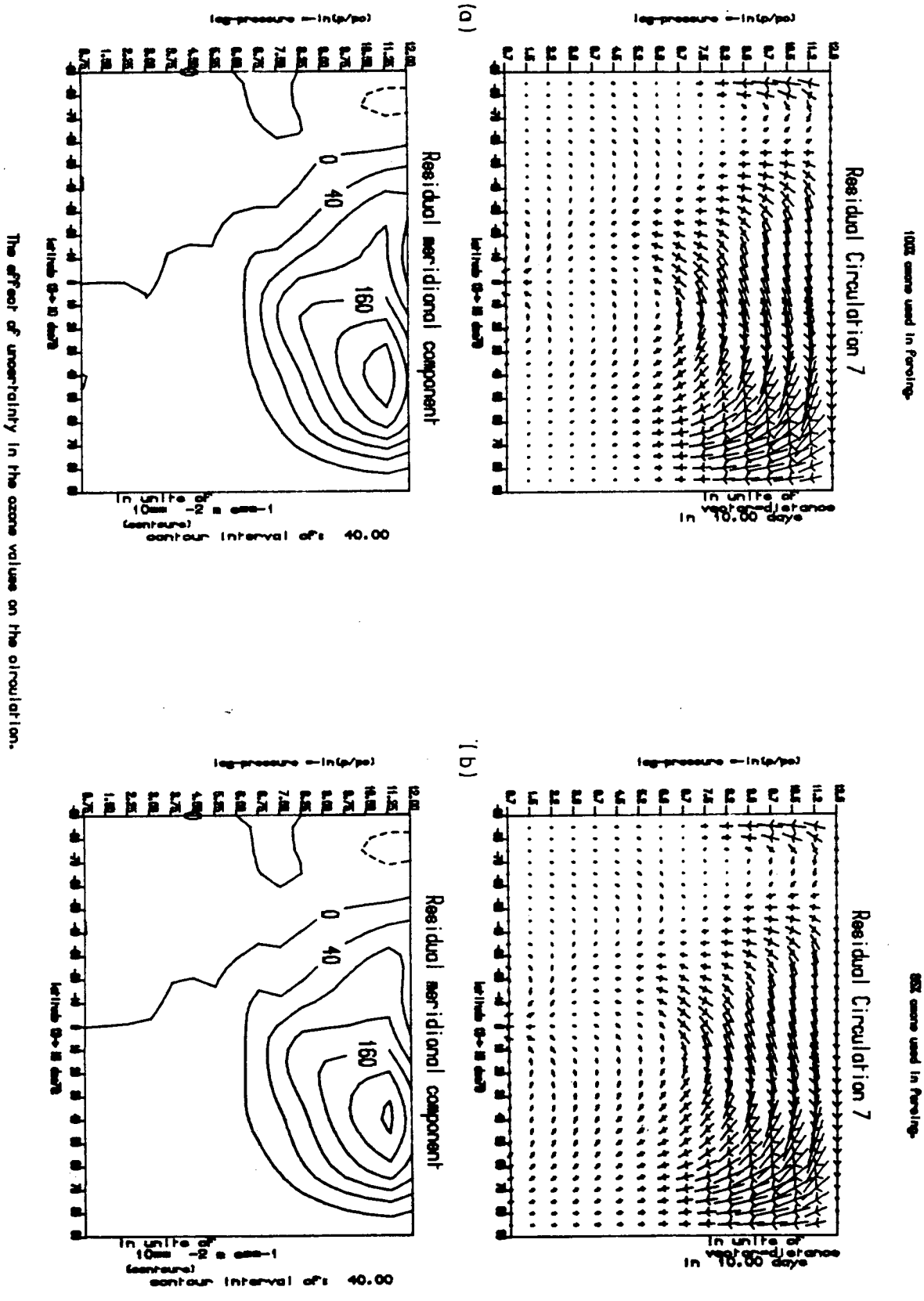

Figure F4.17 The diabatically driven residual; (a) circulations, and (b) the $[v]^R$ component in ms^{-1} using 100 percent and 85 percent Ozone concentrations in the evaluation of [Q]. (negative contours are dashed.)

4.3.5.7 :THE EDDY FLUX POLAR DATA EXTRAPOLATION.

The eddy flux calculated from the LIMS data exhibited very large divergence peaks at 85° N, so it was decided to smooth these features. To test for the significance of this correction and the effect of the various extrapolation models upon the final results the following variant tests were undertaken.

i) Data unsmoothed at >80° N & >65° S.

ii) Flux assumed proportional to cos(φ) poleward of 65° S and 80° N.

iii) Flux assumed proportional to $\cos^2(\varphi)$ poleward of 65° S and 80° N.

Note that these extrapolations do not alter the average divergence of the polar cap, since the total EP-flux across 80° N latitude is unchanged and so by Green's Theorem the volume integral of the divergence of F remains constant.

The three smoothed momentum and heat flux cases resulted in the eddy driven circulations shown in Figures F4.18a-c. Comparison reveals that all extrapolations have little effect on the resulting streamfunction and circulations derived therefrom. The second variant was used subsequently in all the main analyses.

Additional to the above extrapolations several further tests were applied to examine in more detail the influence on the final circulations of what are clearly anomalous forcing features in excess of $2\text{-}4.10^{-4}$ m s**-1 at 85° N. Whatever the reasons for these problem features, their degree of influence on the residual circulations is an important result to ascertain.

Three further polar smoothing variants were used for comparison.

(a) Forcing term D_F unsmoothed.

(b) Forcing assumed to produce solid body acceleration at 85-90° N.

(c) No forcing at 85° N and 90° N.

Note: In all these and subsequent calculations of D_F variant (ii) for test (4.3.5.7) was applied.

Linear cosine(latitude) factor extrapolation used.

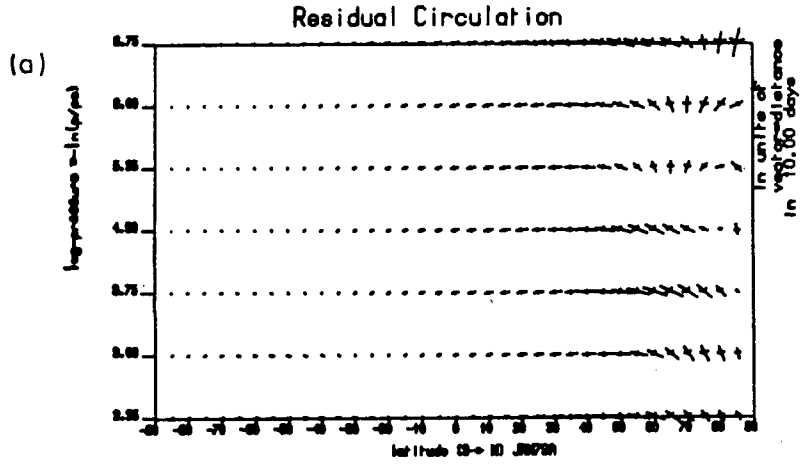

Linear cosine(latitude) squared factor extrapolation used.

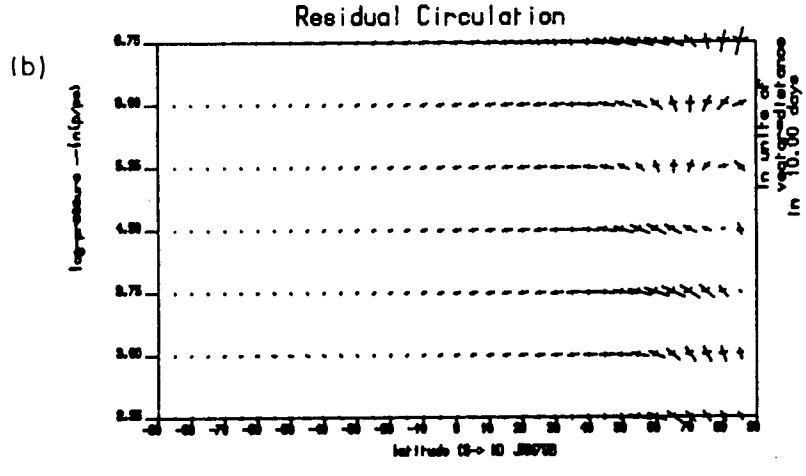

Data unsmoothed at >85N & >84S.

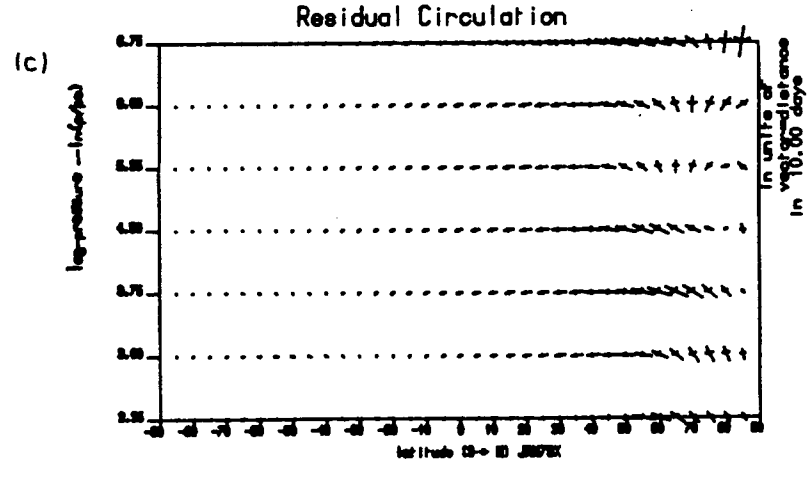

Figure F4.18 Eddy driven circulations using the variants (a),(b) & (c) for the smoothing of the polar eddy flux data.

Using variant (a) as a control for comparison variants (b) and (c) were used as alternatives to examine the influence of the anomaly forcing values upon the circulations driven by the eddy forcing. Variant (b) is a crude but plausible alternative assumption that near the pole the atmosphere is taken to be in a state of solid body rotation. This implies that $[u]$ and so $\partial[u]/\partial t$ is proportional to $\cos(\varphi)$ near the pole and so suggests D_F is proportional to $\cos(\varphi)$. This enables the body forcing term, D_F, at 85°N to be calculated from the relation:

$$D_F\Big|_{(85^\circ N)} = D_F\Big|_{(80^\circ N)} \frac{\cos(\varphi_{85})}{\cos(\varphi_{80})} \qquad (4.27)$$

Figures F4.19a-c show the three eddy driven circulations which result when the three variants are considered. It is clear, since the differences between the three plots are small, that the effect of the extreme forcing values is local and fairly small. The reduction of the large divergence at 85°N has the effect of diminishing the indirect cell seen in the upper stratospheric high latitudes of Figure F4.19c but not removing it entirely. This would indicate that these anomalous values at 85°N do not seriously alter the circulations computed and do not appear to invalidate their realism. The actual magnitude of the forcing term, D_F, at 85°N is dependent upon the eddy momentum flux at 80°N. It is possible that these very large values of D_F arise due to the use of geostrophic eddy fluxes (rather than eddy fluxes derived from the real velocities), which at high latitudes are likely to be inadequate for use in the calculation of the quasi-geostrophic EP-flux divergence, as shown by Robinson (1985) and Andrews (1985). However as will be described later in this thesis (in particular see section 5.4.1), $D_F > 0$ is observed in other observational studies e.g. Geller et al (1983) and there are a number of possible physical explanations for its origin. Further investigation of the reasons for these forcing values and their effects will be discussed in Chapters 5 & 6.

(a) No forcing at 85N.

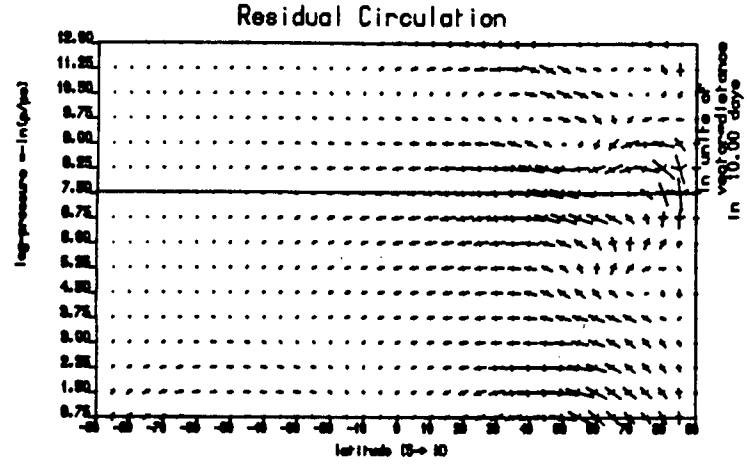

(b) Solid body rotation assumed at 85N.

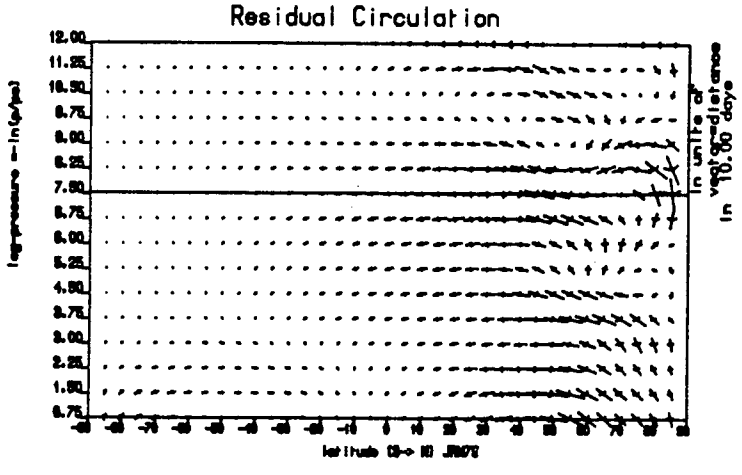

(c) Forcing unamended.

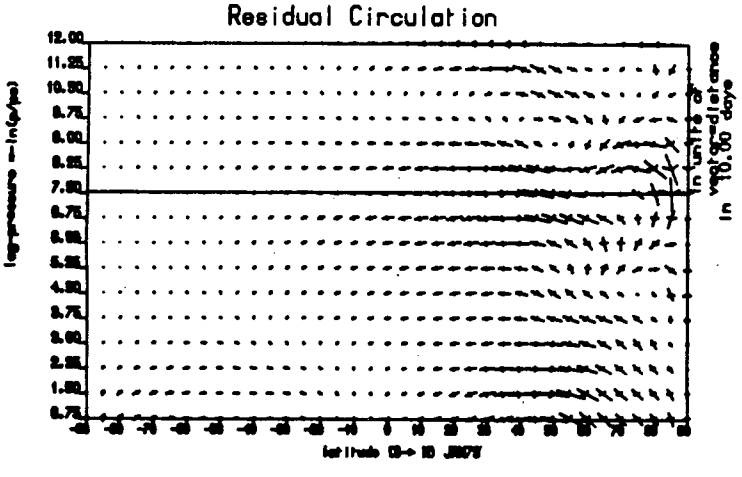

Figure F4.19 Eddy driven circulations produced using variants (a), (b) and (c) of flux extrapolation to test the effect of the anomalous forcing at 85°N.

4.3.5.8 : DIFFERENCES BETWEEN THE LIMS AND SSU DATA SETS.

Comparisons were made between the same months circulations and heating rates using LIMS ozone & geopotential and using SBUV ozone and SSU geopotential. For the months December to May all diagnostics and forcing variables were re-evaluated without the use of LIMS data and so using the SSU geopotentials, CIRA climatological upper level temperatures, SBUV ozone profiles and the climatological water vapour profile. Both the eddy and diabatic forcing terms necessary for the evaluation of the residual streamfunction changed due to the use of this alternative data set.

The magnitudes of [Q] changed quite significantly in the high latitudes in the upper two levels of the data and a lesser redistribution of [Q] values occurred as a consequence of the different temperature, ozone profiles and therefore of radiation budgets in the diabatic heating calculation, throughout the atmosphere. The largest differences occurred in polar regions, $>80^{\circ}$, and were principally due to the larger positive peak magnitudes seen in the SSU based values of [Q] evaluated in the upper stratosphere and lower mesosphere. Differences of $\approx 5^{\circ}C$ occurred, i.e. southern polar region at $\approx$ 1 mbar. More generally changes of $\approx <2^{\circ}C$ were evident and in mid-latitudes and in the lower atmosphere the differences were much less. These differences will obviously have important repercussions on the heat budget analyses and upon the circulations forced by them. Figures F4.20 & F4.21 illustrate the residual circulation and diabatic heating rates for the month of April, using respectively SSU & SBUV in Figures F4.20a & F4.21a and the LIMS/SSU combination in Figures F4.20b & F4.21b.

These differences occurred in all of the six months which could be tested. Below 5mb however the changes in $[v^{R}]$ and $[w^{R}]$ are smaller. The major changes occur due to the faster polar sinking at the stratopause. This increases the horizontal wind by up to 0.1 ms^{-1} and enhancing the ascent and descent in high latitudes above 5mbar for example in December by $\approx(1.10^{-7}s^{-1})$.

(a) Diabatic heating rate using SSU & CIRA temperatures.

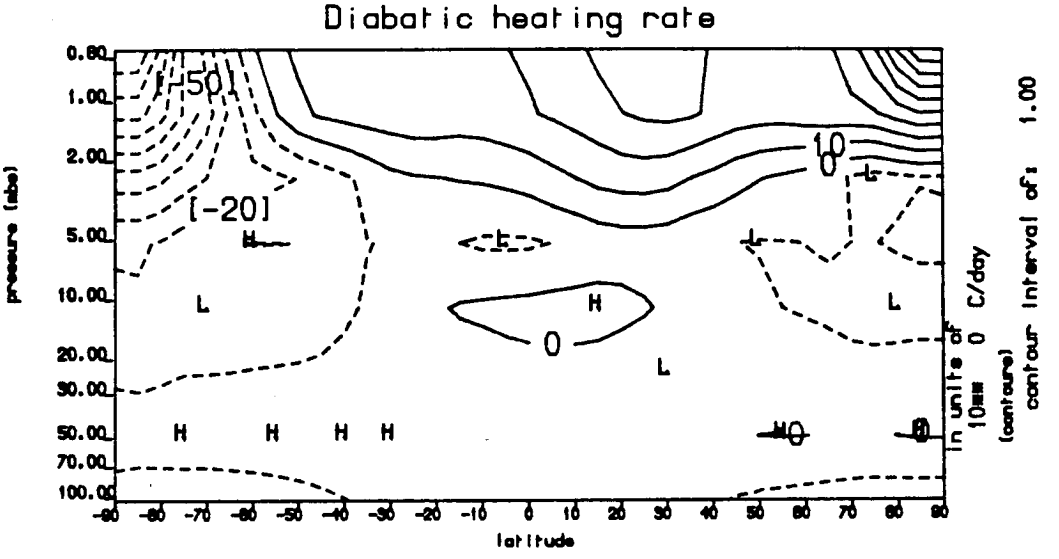

(b) Diabatic heating rate using SSU & LIMS temperatures.

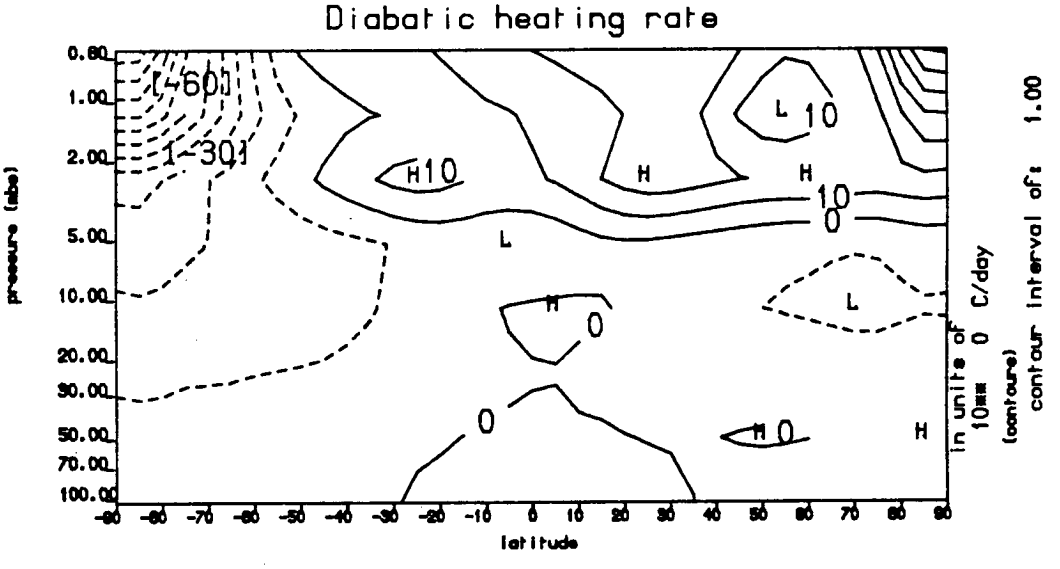

Figure F4.20 Diabatic heating rates for April 1979 using (a) SSU, SBUV & CIRA data, compared with using (b) LIMS and SSU data.

(a)

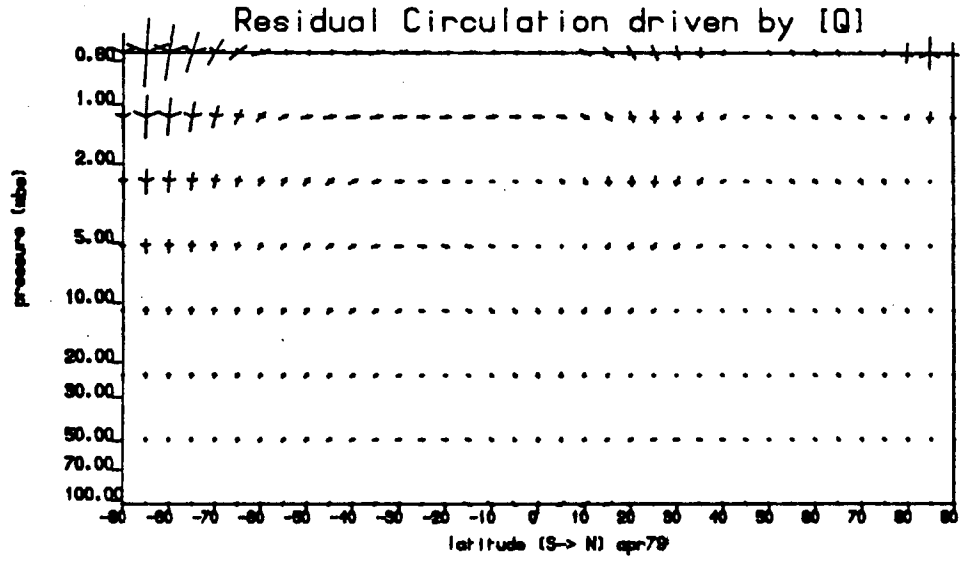

(b)

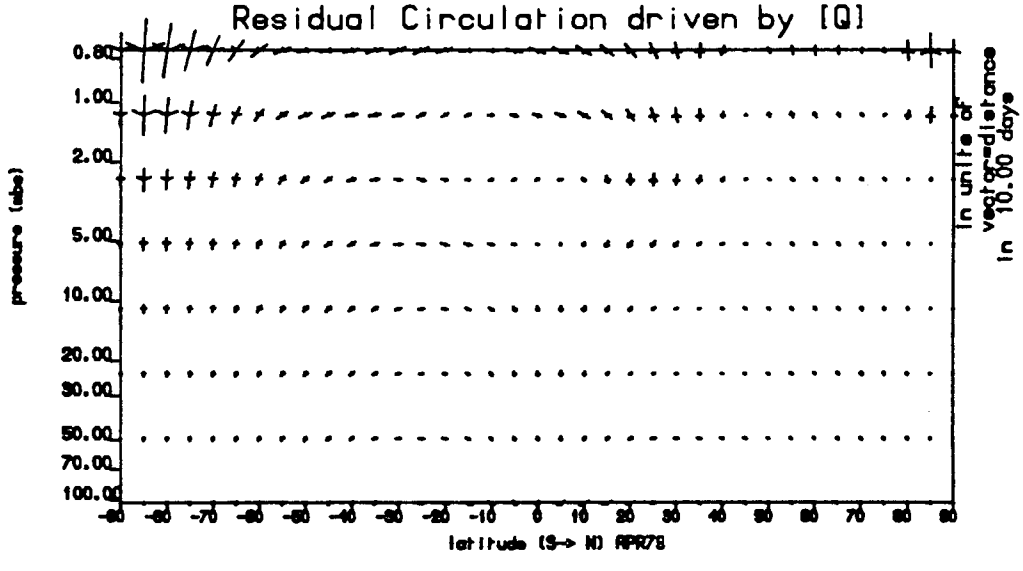

Figure F4.21 Diabatically driven residual circulations for April 1979 using: (a) SSU,SBUV, & CIRA data, and (b) LIMS & SSU data.

The changes because of the eddy driving term, D_F, were also noticeable. The SSU data exhibit a smaller magnitude divergent region in high latitudes but its spatial extent remains basically unchanged. However the maximum D_F of $12.10^{-5} ms^{-2}$ shifts poleward and drops by half when the SSU is used compared with the LIMS geopotentials.

The combined effects of the above changes in [Q] and D_F upon the 'fully forced residual circulations' is illustrated by figure F4.22, which show the flow pattern for the two data variants used. The maximum average differences in $[v]^R$ and $[w]^R$ in an area excluding the polar regions, $>75^o$, and excluding above 5mbar, were found to be: $[v]^R = \approx 0.035\ ms^{-1}$ & $[w]^R = \approx 1.5.10^{-8} s^{-1}$. These changes are obviously important and result in qualitative changes in D_F and [Q] which are very significant to the momentum and heat budget considerations and the assessment analysis in chapter 6. However the changes are relative to the SSU data used and are not necessarily absolute error values, since the SSU values above 2 mbar are subject to error and uncertainty (see chapter 3). These values are estimates of the accuracy of the results but do not strictly indicate error in the LIMS geopotential data and the derived flux quantities etc. Variations here are very important in any hemispheric difference analysis because of the change in the data set used after May 1979 when the LIMS data are no longer available.

The quantitative differences to the flow, especially in high latitudes and above 5 mbar, are not negligible and are therefore important, but as can be seen from Figure F4.22 the resulting effect upon the qualitative nature of the circulations, for all the six months tested, remains largely unchanged and the basic flow features and structure is retained. In certain months the variant, as illustrated in figures F4.22(a) compared with (b), where the SSU and SBUV data are used rather than being combined with the LIMS data, tends to reduce any high latitude reversals close to the north pole and also produces significantly larger vertical velocities at high levels, with air descending into the polar night. Although the magnitude variations are disappointing, the flow remains qualitatively stable despite the influences and differences described above. As a result the direct flow structure and the enhanced poleward cell in the winter

(a)

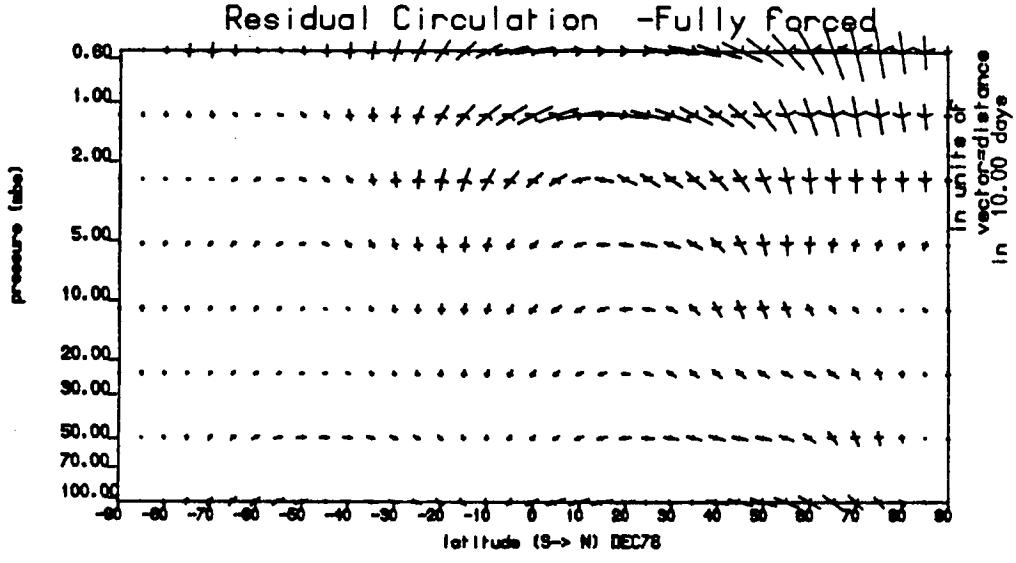

(b)

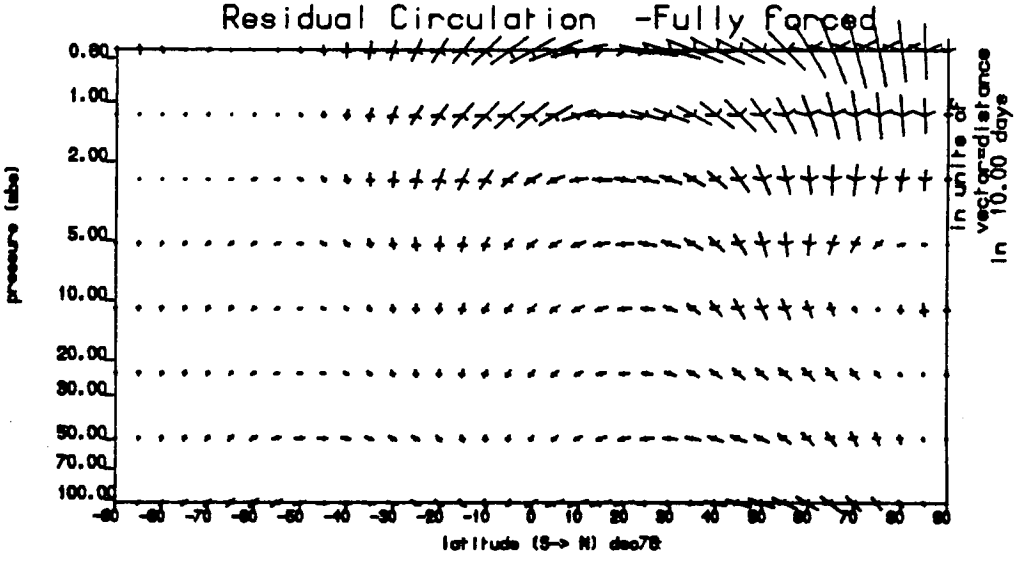

Figure F4.22 Fully forced residual circulations for December 1978 using (a) SSU, SBUV & CIRA data and (b) LIMS & SSU data.

hemisphere, due to eddy forcing, of the residual circulation, are retained in all the sensitivity tests of the circulations attempted.

4.4 : A QUANTITATIVE ASSESSMENT OF THE CIRCULATIONS.

In order to check the circulations a comparison was made between typical velocity values quoted by various sources with the calculated values from this study. The values examined including those shown in Table T4b, are from various model and calculated circulations including Harwood & Pyle (1980), Rogers & Pyle (1984), Crane et al (1980) who calculated Eulerian circulations, Dunkerton (1978) who calculated a Lagrangian circulation, Al-Ajmi, Harwood & Miles (1985) who calculated residual circulations. They show that although considerable variability between the various circulation measures and therefore uncertainty in the velocities exist, the circulations derived and described in this study are of a similar form and order of magnitude. Only an order of magnitude comparison is possible as the circulations are all of different types and based upon different years data, moreover the different circulation types can be qualitatively very different in form. However it is also possible to highlight the differences in the various types and furthermore the new residual circulations calculated for the whole year using modern satellite data can be compared with the other circulation diagnostics discussed above. [V] compares very well between the various sources, except that some circulations have the strong upper stratospheric diabatically driven circulation at a higher altitude in the atmosphere than seen in the circulations presented in this thesis, i.e. Murgatroyd & Singleton (1961) (1 ms^{-2} at $\approx$ 55km compared with $\approx$ 1.2 ms^{-1} $\approx$ 50km. from this study.) The absence of this feature in the present study is likely to occur because of the inability to include the effective forcing by breaking gravity waves. The momentum deposition from the gravity wave breaking is important in driving a major component of the meridional circulation at these levels. The present study values are in general in excess of the other velocities in high latitudes but compare better and are of relatively smaller magnitudes in the middle latitudes. The vertical velocity in the present study are large in comparison with those in other studies in high latitudes (>=75^{o} N.). The values of [w] in January and February peak at approximately 20mms^{-1}, at about 50km, (not shown but can be illustrated in Figure F5.5a which is the Eulerian circulation calculated in

Sample stratospheric velocity magnitudes.

	V ms^{-1}	W mms^{-1}	V present	W study	Comments
Crane et al. (1980)	1 - 3	7	1.6	10	Winter 0.3mb Eulerian
Harwood & Pyle (1980)		3-4		3	December 8mb Eulerian
Dunkerton (1978)	0.7-1.0	5-7	1.6-2.0	3-6	Winter 50km. Lagrangian
Al-Ajmi et al. (1985)	3		1.0		July 2mb. Residual
Pyle & Rogers (1984)	0.6	0.5-1.5	0.5	1.7-3.3	March 50km. Residual

Table T4b A Comparison table showing sample stratospheric velocity magnitudes for the present study and other sources.

this study for December) compared with values more typically of 4-6 mms^{-1} from the other sources. The difference in magnitude of the [w]'s described may arise because of the highly active eddy forcing conditions occuring in these months, see figures F6.17-F6.19, which will tend to drive a large descent over the northern polar region, but it could also be related to the problem of the large flux values obtained when using geostrophic velocities and subsequently large horizontal gradients in the heat and momentum fluxes close to the pole. The large gradients in the momentum flux will via equations (4.16) and (4.17) produce a large $[w]^R$ and hence [w] near the pole in these months. The discussion and comparison of the various circulations above can at best only be an order of magnitude check and is therefore only a low order test. It is not surprising therefore that there are a number of differences between the circulations considered above. Therefore, based upon this simple check only, the differences observed from this comparison are not sufficient to suggest that the circulations are significantly unrepresentative of the mean meridional circulations as identified by the other sources and so offer some confidence in the validity of the circulations calculated. However this short discussion also serves as an introduction of the major differences and similarities between the old circulations compared with the residual circulation in the present study which have been derived for a whole year, allowing a seasonal examination of a circulation which is closely related to a 'transport circulation' description of the stratosphere.

4.5 : SUMMARY

Chapter 4 has provided a detailed description of the method used to evaluate the residual circulations and shows via the sensitivity tests presented and data comparisons, the regions of inevitable uncertainty which are present due to the procedure and data used. As has been seen by other studies the variability of diagnostics between data sets used covering the same time period is a difficulty which must be accepted as inherent at present. The tests also indicate that the circulations will not be significantly affected by these uncertainties and that a degree of confidence can be carried on to the analysis and interpretation of the circulations which will be described in Chapter 5. In chapter 5 the method described above will be used with the data described in chapter 3 to examine the residual circulation and the

problems discussed in chapter 1. The following methods of analysis will be used in chapters 5,6 & 7. Firstly the total circulation calculated from Ψ_R will be examined in order to assess the evolution and major variations of the residual circulation and their consequences in terms of advective transport. The role of each of the separable forced circulation components will be examined by the separate analysis of the individual streamfunctions as defined in section (4.3.1) above. This allows a direct assessment of the role of the diabatic heating, transient eddies and stationary eddy forcing mechanisms in producing advective transport. For comparison with the residual circulations and to examine the relative roles of each circulation type the 'Dunkerton-diabatic' and Eulerian circulations has also been calculated, thus providing alternative descriptions of the mean meridional circulation and allowing their direct comparison for the same conditions. Together with this analysis of the circulations, the forcing terms will be examined in terms of their influence upon the momentum and heat budgets in chapter 6. This allows a description of the seasonal variations of the eddy terms used and their importance in transporting momentum and heat. The mean state and eddy forcing terms will also be examined in terms of the TEM. viewpoint using $\mathbf{F}$ and D_F to determine the influence of the eddy forcing in modifying the existing equilibrium conditions. The calculation and analysis of both the transient and steady components of the flux terms will enable an examination of their relative magnitudes during periods of quiet and vigorous wave activity giving one year's assessment of the degree of atmospheric variability in the various diagnostics presented over the year. An examination will be made of the dynamical features of the two hemispheres thus providing valuable insight into the nature of the stratospheric circulations, throughout a whole years data, and examining the influence of the seasonal variations.

CHAPTER 5

5.1: INTRODUCTION

In chapter 4 equation (4.16) was derived which enabled the evaluation of the residual streamfunction Ψ. It also allowed, being linear, Ψ to be split into the various components Ψ_Q, Ψ_T, & Ψ_S as defined in section (4.3.1). In the following sections this method of separation will be used to examine and compare the residual circulations calculated from each of these streamfunctions together with their Eulerian equivalents, monthly Dunkerton-diabatic circulations as defined in section (2.6) and a meridional circulation associated with a simulated Semi-annual oscillation in the equatorial stratosphere.

5.2: THE FULLY FORCED RESIDUAL CIRCULATION.

In this section the residual circulation evaluated from Ψ_R as defined in section (4.3.1) will be described. The circulation is referred to as the 'fully-forced' residual circulation as Ψ_R is calculated from equation (4.16) with the use of all the forcing terms. Obviously, despite the name, certain physical forcing mechanisms, such as the effects of gravity waves and equatorial waves, are not included in this representation of the residual circulation. The fully-forced residual circulations for the twelve months covering December 1978 to November 1979 are shown in figures F5.1-F5.4. The following descriptive assessment of the circulation diagnostic will be used as an overview of the year to introduce and illustrate certain features in terms of hemispheric and seasonal variations in the flow fields observed.

Firstly the seasonal cycle is clearly shown, as the main upper stratospheric pole to pole flow from the summer to winter hemispheres, shifts and changes direction. In December to February, see figure F5.1, the flow is strongly northward in the upper levels but extends only from 30°S to 90°N. In March, see figure F5.2a, the single flow breaks up into two equator to pole cells almost symmetrical about the equator. Then in April and May, see figures F5.2b & c, the picture has reversed with the upper winds flowing to the south pole.

Here again the main cell does not extend across the entire hemisphere, with a weaker flow existing further north than 25°N. By June, see figure F5.3a, in the upper stratosphere and above there are signs of a single-cell from pole to pole but the mid stratosphere still contains a weaker equator to pole summer hemispheric cell, with flows toward the north pole at 60°N at all levels in the stratosphere in both June and July. In August the summer hemisphere once again exhibits a weak flow toward the north pole. In contrast during September the circulation consists of two equator to pole cells throughout the depth of the atmosphere below ≈ 50km similar to those observed in March. This then develops through October until November, when the single-cell from south to north is dominant. Within this progressive seasonal cycle the flow exhibits other interesting features. These include the development of indirect cells at high latitudes in the mid-stratosphere. In December, January, July and possibly February the indirect cells are important large flow variations additional to the main direct cell pattern and they result in a movement away from the pole between 70° and 90°, and a confluence of the flow and downwelling at about 50-60°. In other months such as June and May, although there is no ascent in high latitudes, the descent has diminished considerably compared with at 50-60°. Apart from these high latitude features the flow structure is fairly simple.

Examination of the seasonal cycle of the Eulerian mean stratospheric flow throughout the year, on the other hand, reveals it is nowhere so simple and symmetrical as was seen for the residual circulation, see figure F5.5. The Eulerian mean-meridional circulation exhibits large indirect Ferrel cells throughout the stratosphere in December, January and February. Then through March to June the mid-stratospheric flow is very weak in both hemispheres, while the upper stratospheric thermally direct pole-to-pole cell returns in June but is also weak from March to May by comparison, with high latitude horizontal velocities being only of the order of 0.2 ms^{-1} compared with ≈ 1-2 ms^{-1} in January and February. Only by July does the flow return to magnitudes approaching those of the winter months, this time exhibiting a three cell structure in the southern hemisphere, with a weak direct cell close to the pole, (in the lower stratosphere only), an indirect cell between and another direct cell from the equatorial

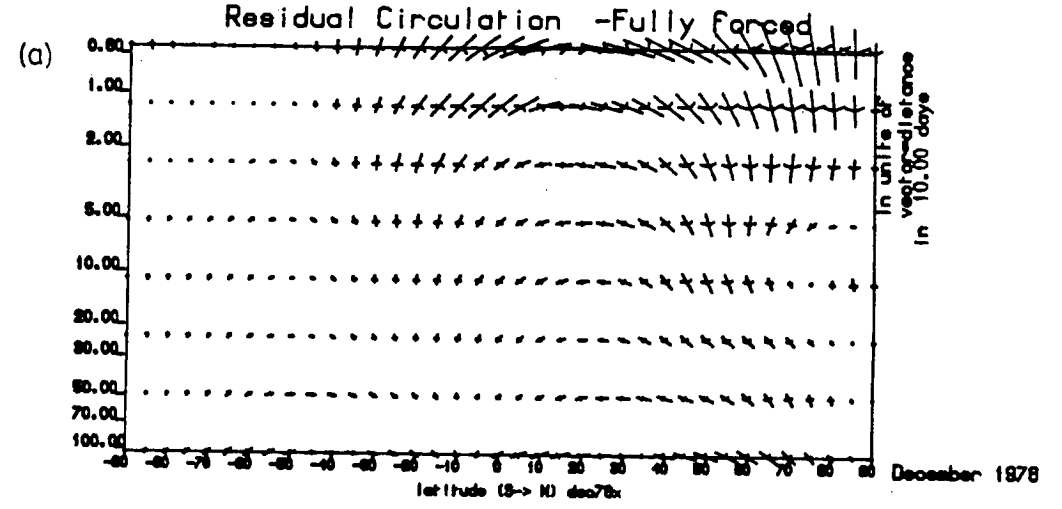

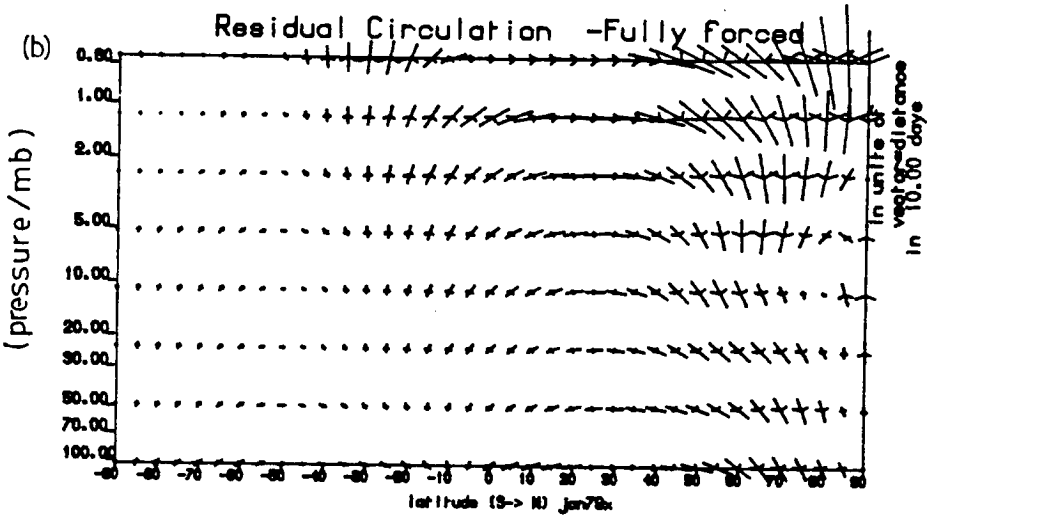

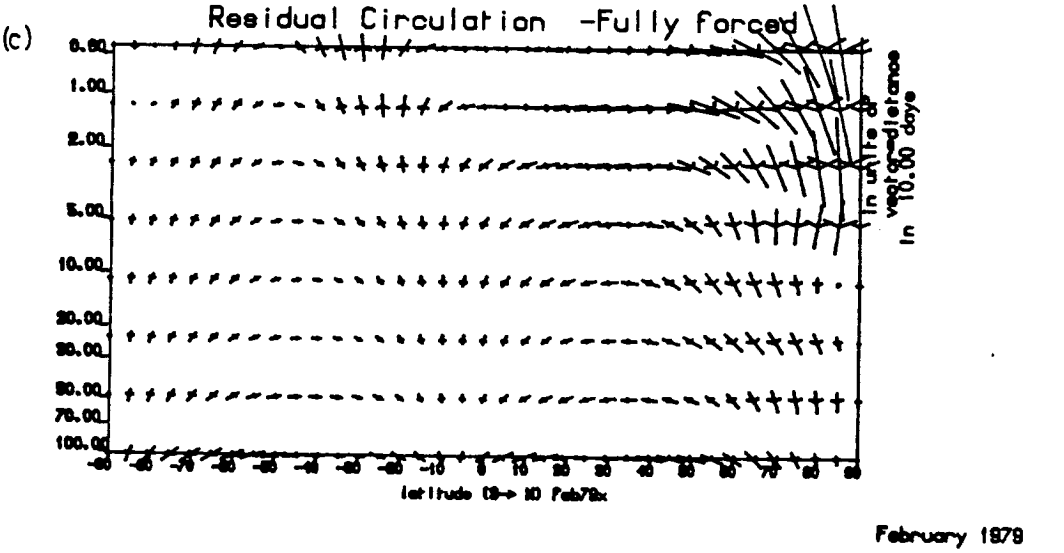

Figure F5.1 The monthly averaged 'Total residual circulations' for (a) December 1978, (b) January 1979, (c) February. Each vector represents the distance travelled by an air parcel in 10 days.

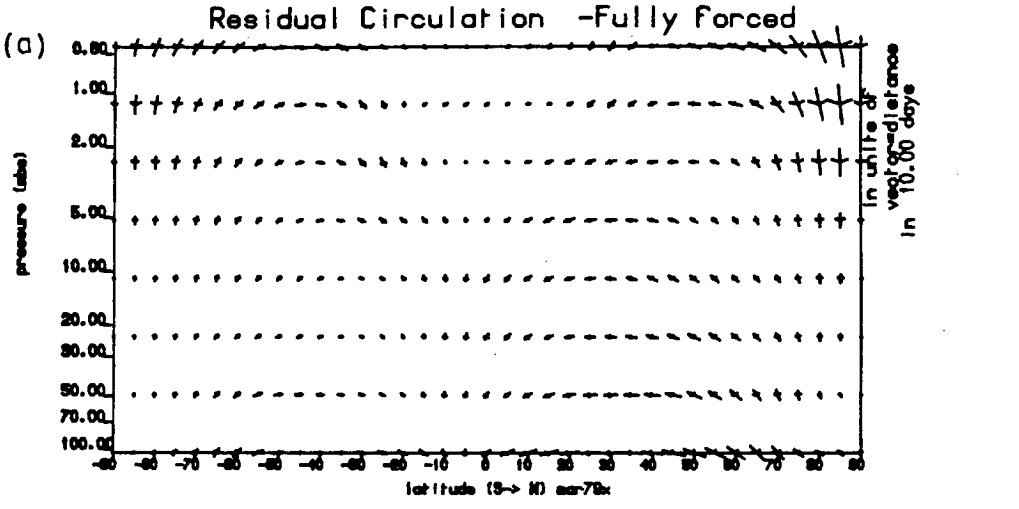

March 1979

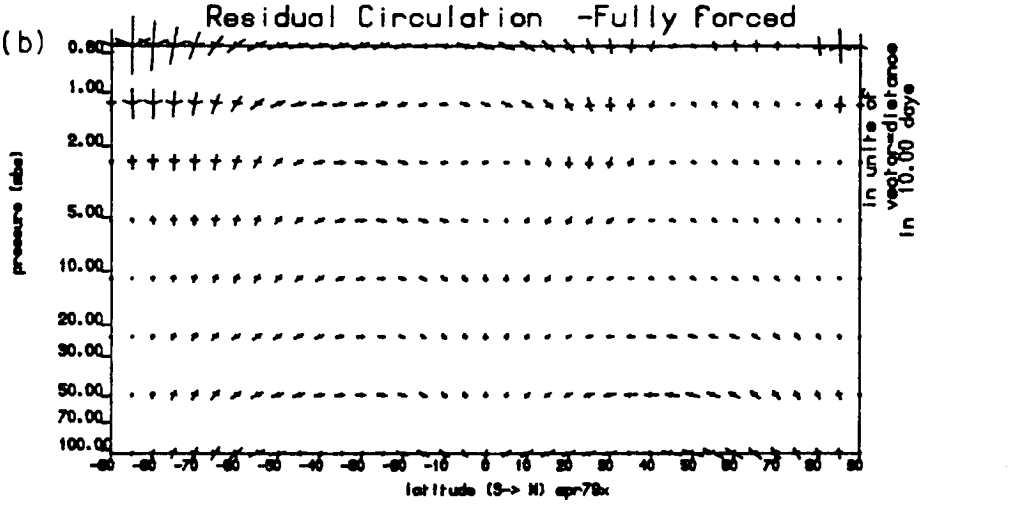

April 1979

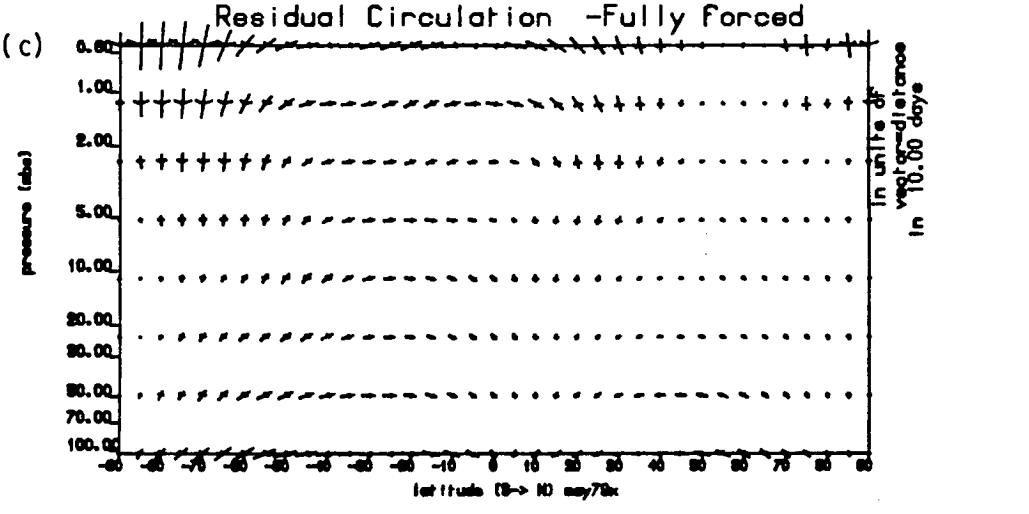

May 1979

Figure F5.2 as F5.1 except for: (a) March, (b) April & (c) May.

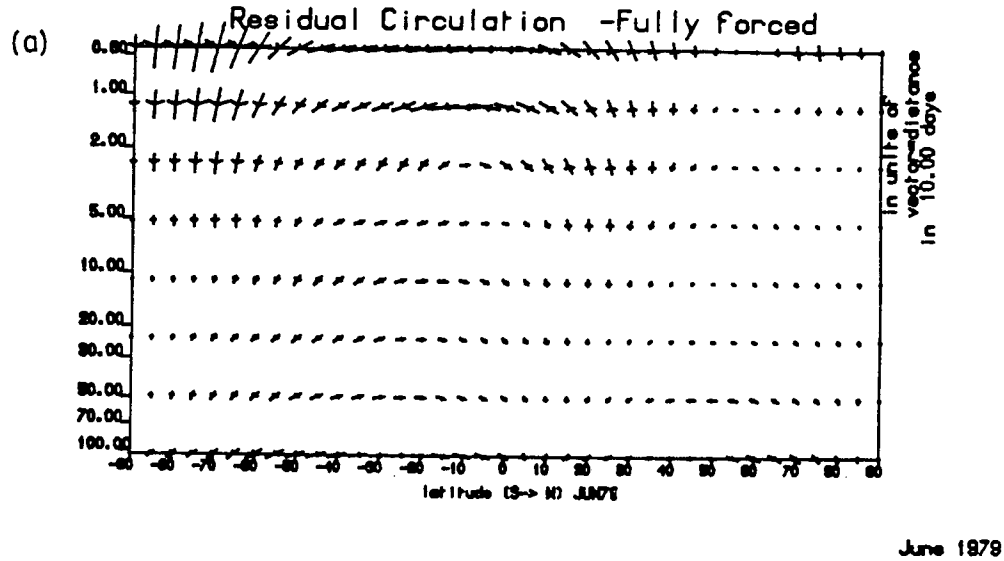

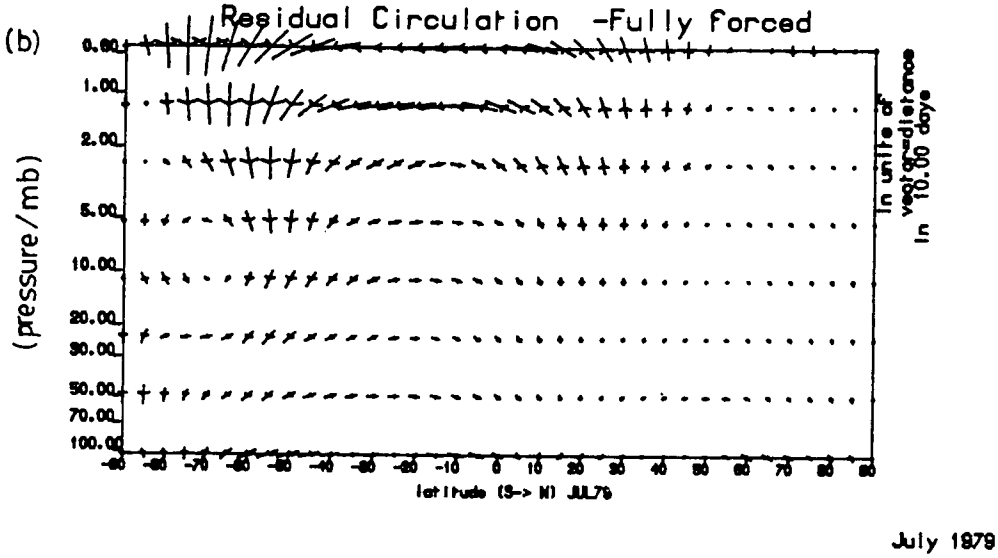

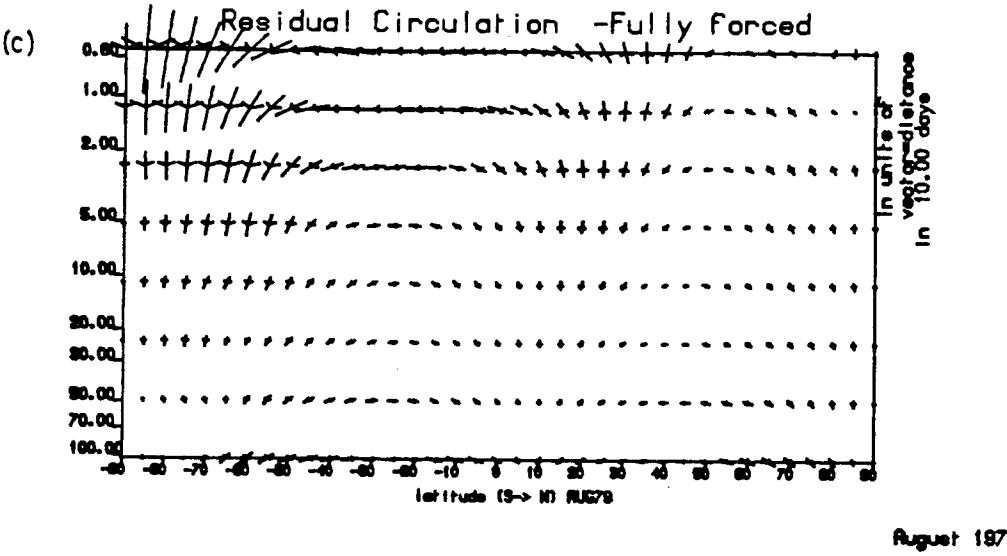

Figure F5.3 as F5.1 except for: (a) June, (b) July & (c) August.

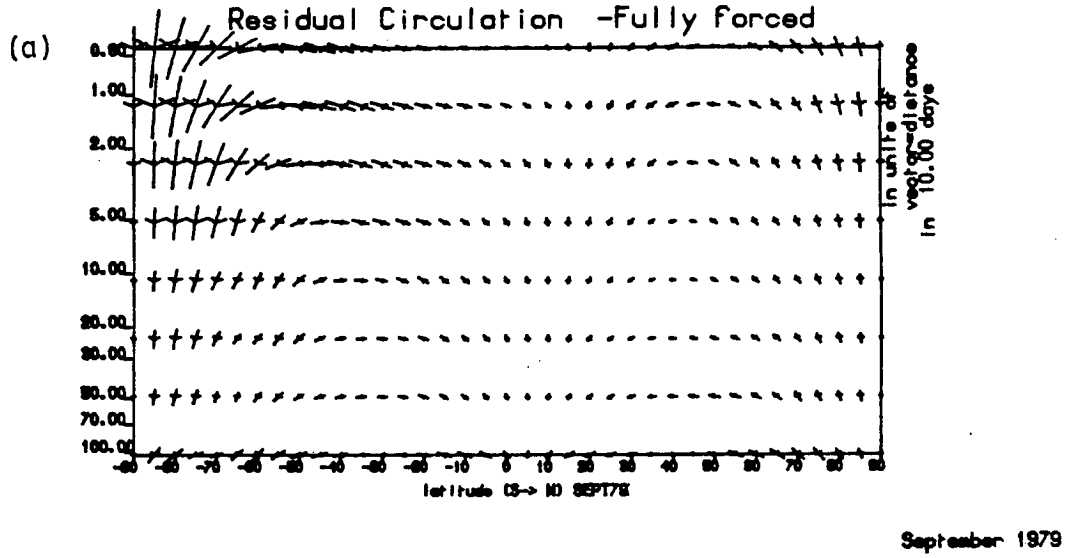

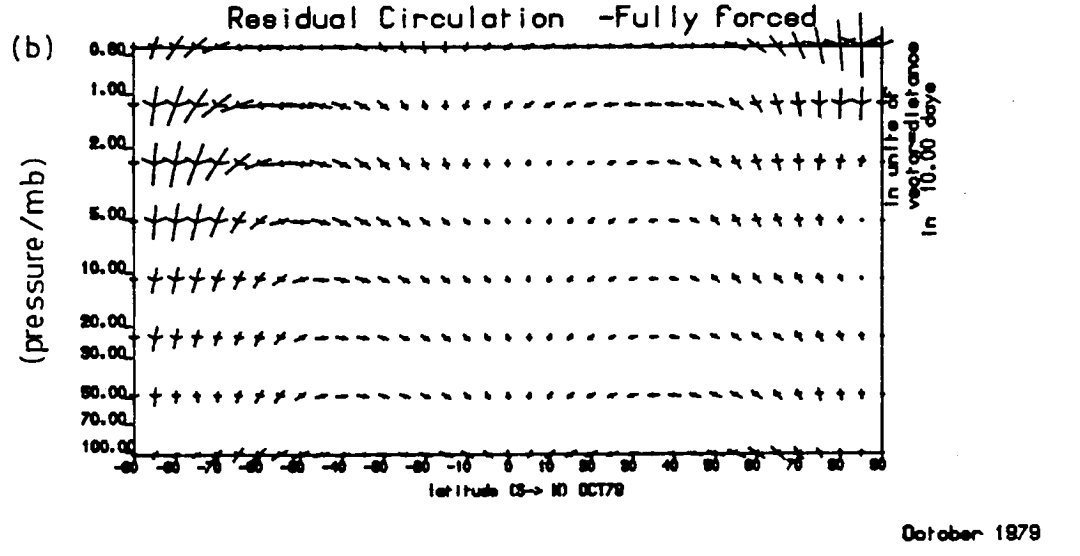

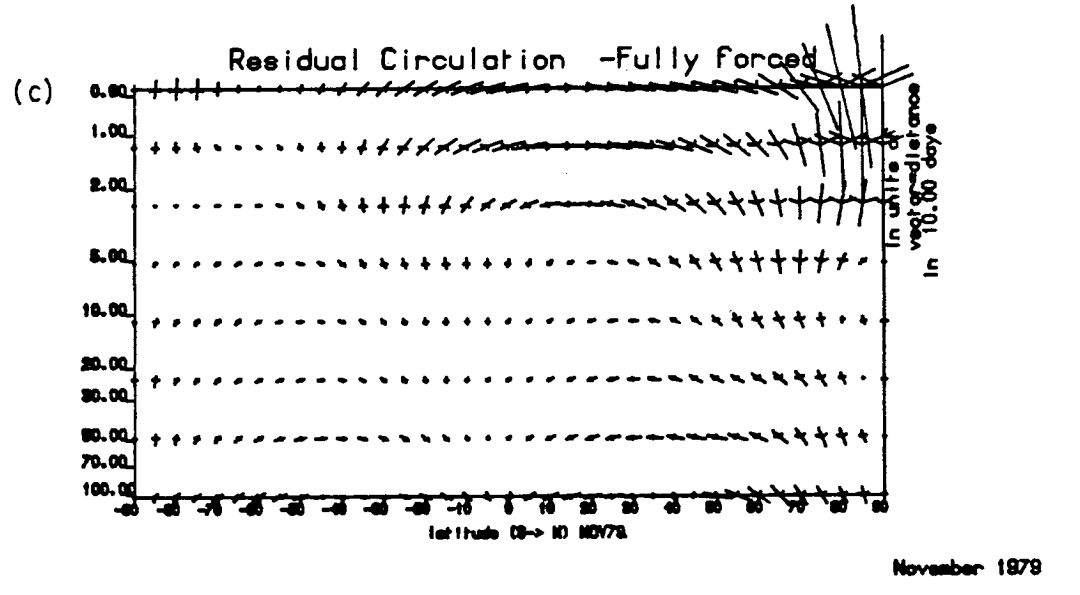

Figure F5.4 as F5.1 except for: (a) September, (b) October & (c) November.

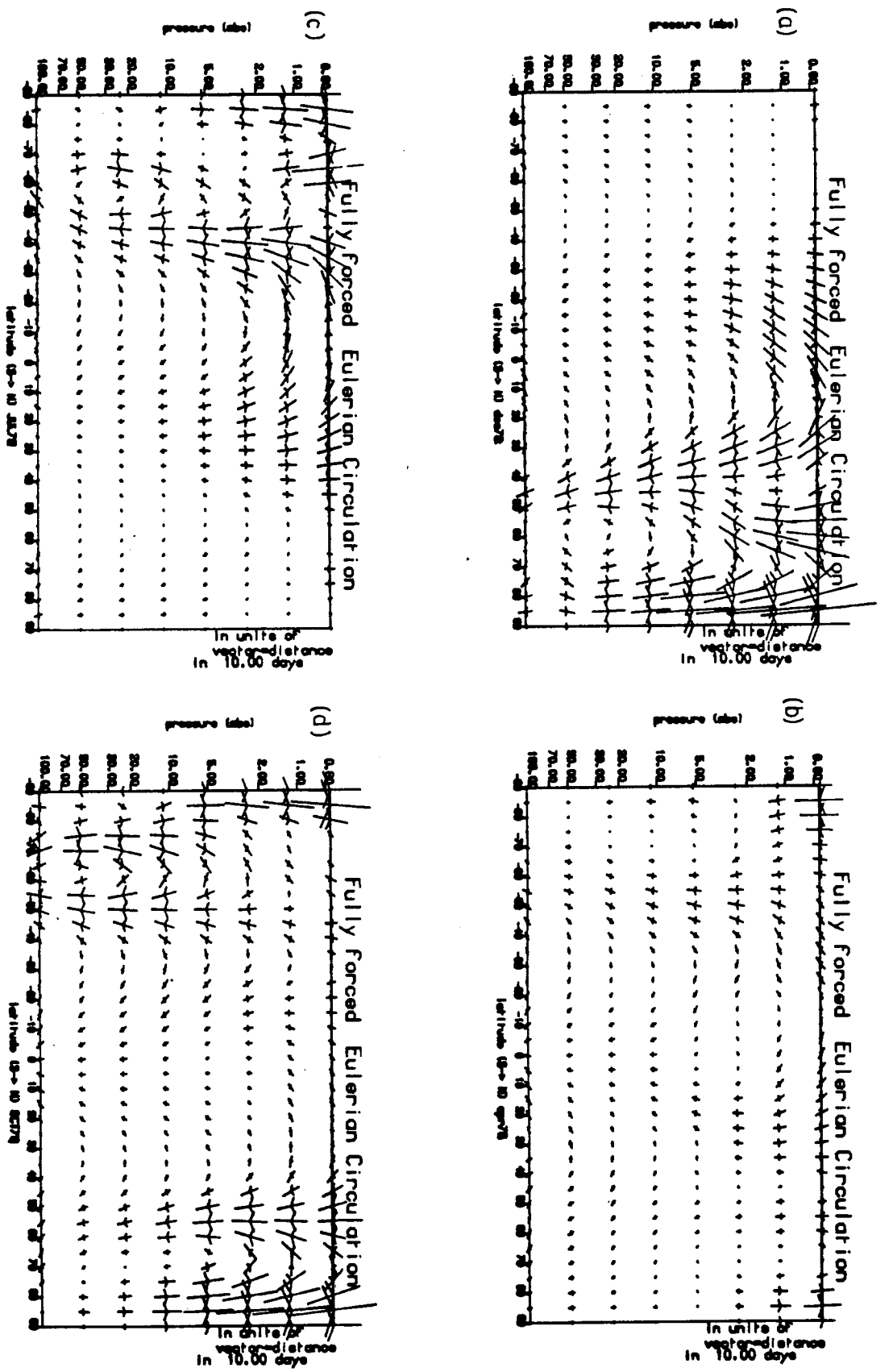

Figure F5.5 The Eulerian mean meridional circulations for : (a) December 1978, (b) April 1979, (c) July 1979, & (d) October 1979.

region south to 40^{o} S. Then in September and October the southern hemisphere circulation reverts to a two-cell stratosphere reminiscent of the equinox flow. From July onwards all southern hemisphere active months have a weak direct cell which occurs in the lower stratosphere close to the pole. In November the southern hemisphere flow has weakened substantially and the system reverts to a winter two-cell northern hemisphere similar to December. It is interesting to note that in contrast to the maximum residual meridional component velocities, (in mid-latitudes), of $\approx 1.6ms^{-1}$ and $1.4.10^{-6}s^{-1}$ in February, the Eulerian circulation exhibits maxima of $\approx 2.5ms^{-1}$ and $3.5.10^{-6}s^{-1}$, also in February.

5.3: INTERHEMISPHERIC DIFFERENCES IN THE RESIDUAL CIRCULATION.

It is possible by examining the circulations only, to gain some insight into part of the transport, which arises due to advection by the residual circulation. However the calculations here of the residual circulations cannot fully deal with the question of the relevance of the flow to the real 'transport circulation', describing the total transport effect of the flow, unless further comparative work is done using these circulations in tracer models along with a consistent parametrization of the eddy transport, and an extensive photochemical representation.

Since the circulation is being examined for its ability to explain the real 'net transport' in the stratosphere it is useful to consider the fully forced circulation for the year and using a purely advective mean circulation, consider the influence of this circulation upon the transport of a tracer. For chemical tracers with sufficiently long chemical lifetimes compared with the meridional transport times, the dynamics must play an important role in the distribution of the chemicals. This is illustrated by ozone whose latitudinal and seasonal variations include a maximum abundance in the region of least production. Firstly the circulation is basically similar to the Brewer-Dobson circulation and so is consistent with the statement that tracers such as ozone require dynamical transport by a circulation of this type. Secondly, the mid-latitude confluent regions of the flow in both spring and winter hemispheres may also be important in helping to explain the spring maxima of ozone and differences between the

hemispheres in terms of latitudinal cross sections. The hemispheric asymmetry in the observed total ozone distribution, (figure F5.6), is generally presumed to be due to differences in the stratospheric dynamics of the two hemispheres. To investigate the effect of the calculated residual circulations in this thesis upon the ozone distribution an examination has been made which highlights the flow differences between the hemispheres and then compares these with the qualitative variations in the ozone redistribution seen in the SBUV total ozone column. A common data set was used for the whole year (SSU data for the winds and temperatures and SBUV data for the ozone), to remove any differences which may arise due to the use of the combined data set as described in Chapter 4, LIMS and SSU, used elsewhere in the main study. Therefore the following description is based upon circulations derived for the whole year using the SSU & SBUV data combination. However the description which follows is illustrated by the total years circulations (which are evaluated using the combined LIMS & SSU data) in figures F5.1 to F5.4, (the circulations computed using the SSU & SBUV data combination only are not shown), and diagrams showing the hemispheric differences, based on the SSU & SBUV data combination only, shown in figures F5.7 & F5.8. Figures F5.7 & F5.8 are obtained by subtracting the reflection about the equator of one month, from its seasonal hemispheric counterpart. These figures are computed using SSU geopotential data only throughout the whole year.

The circulations of December (figure F5.1a) and June (figure F5.3a) are very similar and only small differences are evident (see figure F5.7a) , the upper stratospheric cell being slightly stronger at ≈ 0.6mbar and above in December, flowing in a single-cell from pole to pole. The comparison between January and July, seen in figure F5.7b, is far more significant. The January winter hemisphere exhibits far larger high latitude velocities (i.e. $>65^{\circ}$) whereas the July descent is more extensive across the meridional cross-section and is stronger in the upper and middle stratosphere out to ≈ 25° in the winter hemisphere. Comparing February and August, as seen in figure F5.7c, the most significant difference occurs in the lower stratospheric high latitudes with a much larger flow down into the north polar region in February compared with the equivalent August winter flow into the

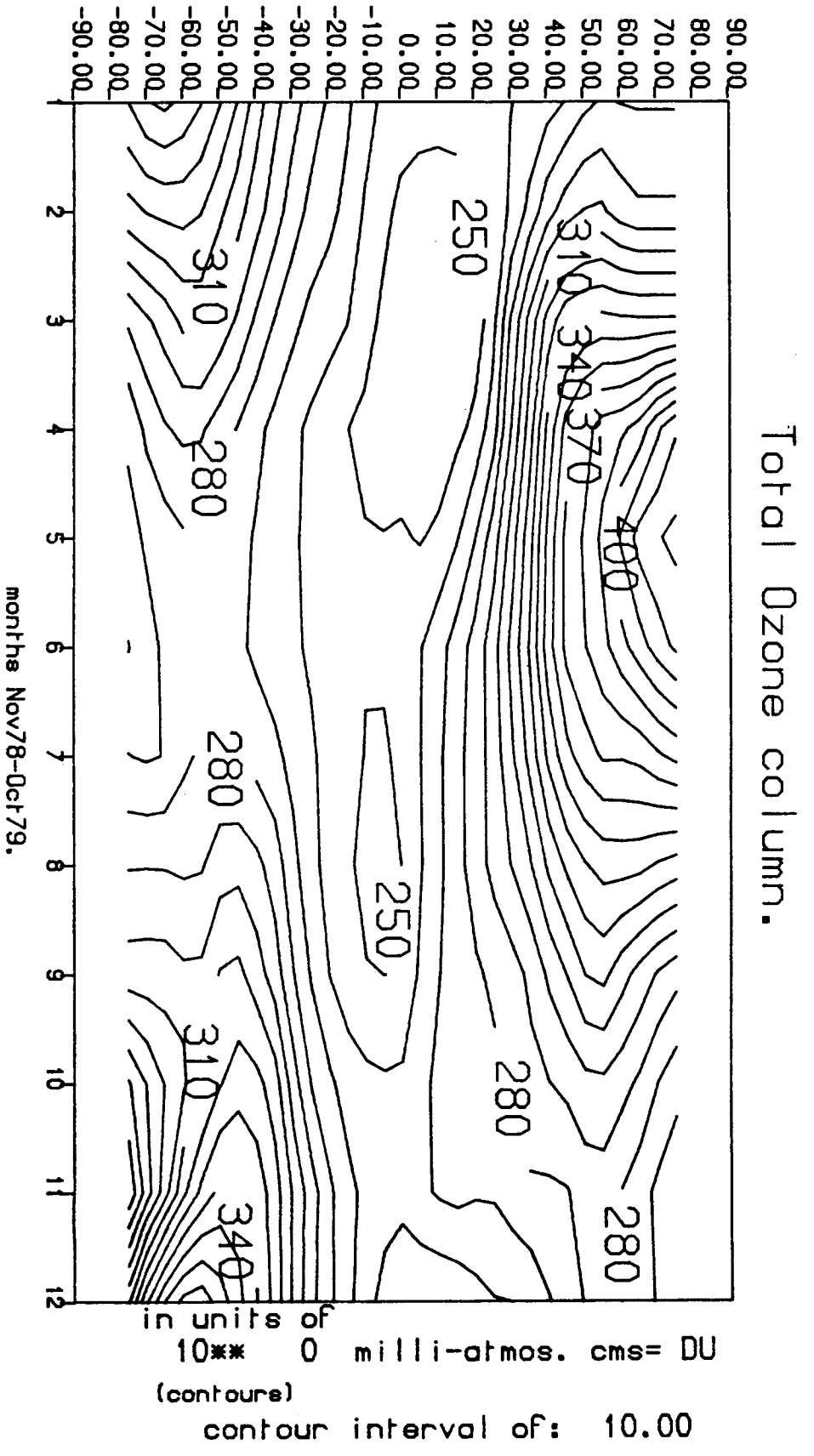

Figure F5.6 The total ozone column, in Dobson units, calculated from the SBUV data set, through November 1978 to October 1979.

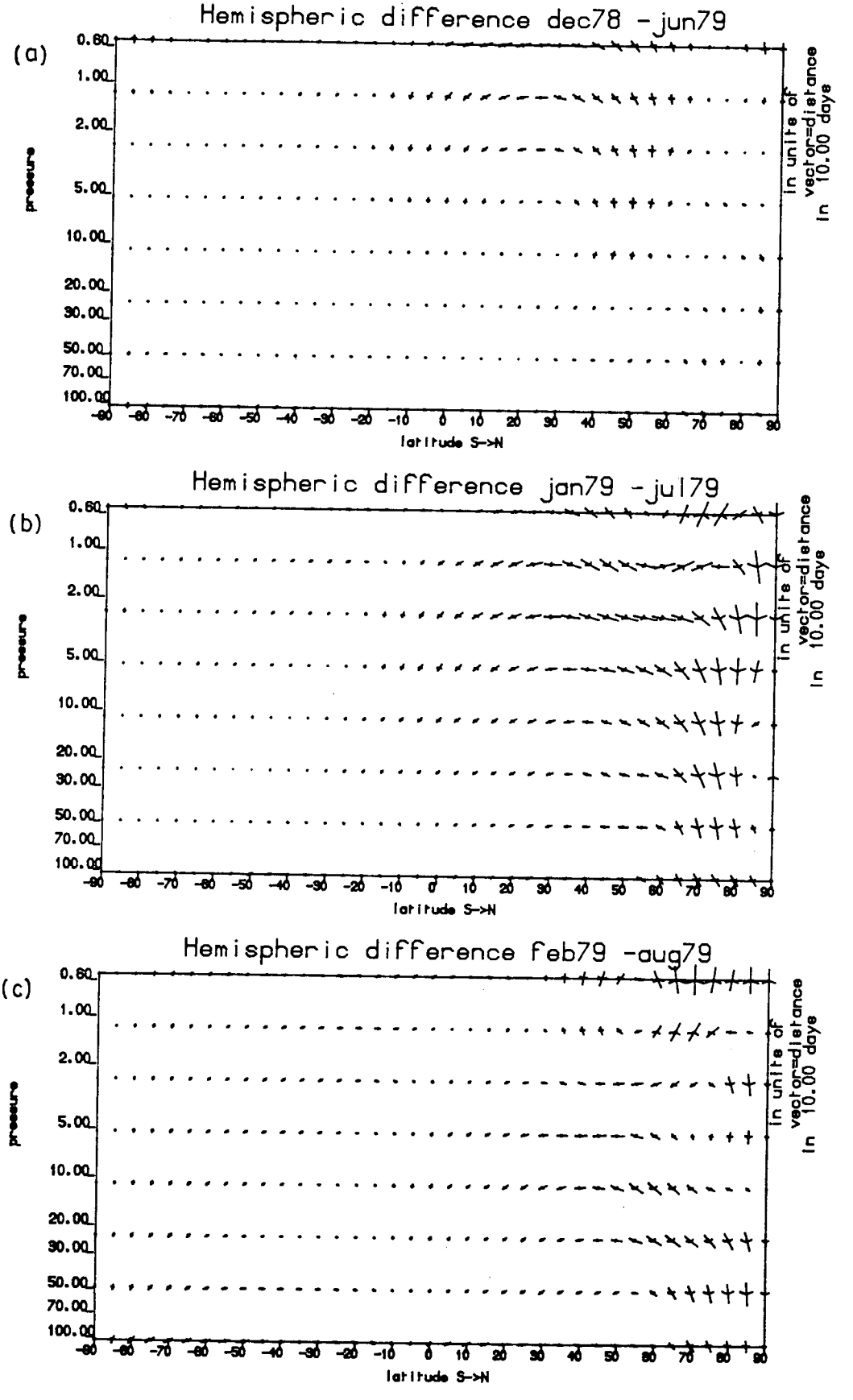

Figure F5.7 The velocity difference between month (1) and the reflection of month (2) about the equator, for (a) December 1978(1) & June 1979(2), (b) January 1979(1) & July 1979(2) and (c) February 1979(1) & August 1979(2). Vector scaling as per F5.1

south pole. This flow descends into the polar regions from mid-latitudes at ≈ 10mbar as well as in the form of a vertical descent from the polar mid-stratosphere. A comparison of March and September,(as seen in figure F5.8a), reveals a weaker flow in the March spring hemisphere compared with the September spring hemisphere throughout the stratosphere, the difference being most pronounced in the upper stratosphere & latitudes > ≈ 70°. Comparing April and October, see figure F5.8b, shows a larger October spring hemispheric flow than in April. The autumn hemispheres are very similar. In November and May the picture is similar to February and August. Figure F5.8c shows the November autumn hemispheric flow is stronger than that of May especially at high latitudes in the upper stratosphere but it is also more extensive in terms of the latitudinal cross-section, i.e. to ≈ 50° in the mid-stratosphere and ≈ 40° in the upper stratosphere.

The hemispheric differences in the flows seen above should imply characteristic features in the tracer distributions. The large flow and confluence of the flow in the northern hemisphere winter, especially during January and February in the lower stratosphere in high latitudes compared with the southern hemisphere might be expected to lead to a larger concentration of tracers at the north pole and give a concentration maximum closer to the pole than its southern hemisphere equivalent. As a result during January and February any dynamically influenced tracer would tend to be concentrated at high latitudes, > 65° of the lower stratospheric northern hemisphere in greater quantity than during the months July to August in the southern hemisphere. In mid-latitudes the differences are not so clear and it appears that during these winter months the vertical velocities are about equivalent in magnitude, although the horizontal velocities are still larger in the northern hemisphere winter. As a consequence, the lower stratospheric mid-latitudes should show none of the large differences in total ozone concentration expected in high latitudes. In the early spring the pattern of expected accumulation of ozone due to advective transport switches hemispheres in high latitudes, as the northern hemispheric flow during March and April becomes considerably weaker than the descending flow into the southern hemisphere polar region during September and October. Throughout early spring therefore the flow

patterns imply a greater concentration of tracer throughout the southern hemisphere but particularly confined to >60°S. However it must be noted that the magnitude of the equinoctial circulation has dropped significantly in relation to the winter months above and so the tracer transport is reduced.

These deductions from the flow differences can be compared with the total ozone distribution illustrated in figure F5.6. derived from the SBUV ozone profiles (see Section 3.1.4). Firstly in the northern hemisphere the main ozone maxima lies at high latitudes, >70°N, and is growing throughout the months of November to March reaching its maxima in this spring month. In the southern hemisphere the maxima is also growing during the winter months of June to September in mid-latitudes, ≈ 40-60°S, and in higher latitudes, ≈ 60-70S, during October and November. This shift of the maxima during the year, which only occurs in the southern hemisphere, can also be possibly explained by the residual circulation's seasonal evolution. In June and July the flow tends to descend into mid-latitudes and only later in September and October does the descent region shift into high latitudes on the same scale as in the northern hemisphere winter. Finally in November the circulation decays and is replaced by the equinoctial cell only. Also the timing of the maxima of ozone in both the northern and southern hemispheres seems to coincide with major changes in the circulations throughout a year. Similarly the timing of the minima at high latitudes is coincident with the beginning of the change in flow, such that the eddy driven cell diminishes in the active hemisphere and begins to develop in the opposite hemisphere and the whole circulation switches direction. The meridional poleward flow and descent into the northern polar region increases and develops from September onward until its decay after February, while the southern hemisphere ozone minimum occurs in April which is the first month of the dominant phase of the meridional circulation in the southern hemisphere.

Thus the general explanation of the positions of the ozone maxima can be in part described by the above reasoning based on hemispheric differences in the residual circulations over the year. This assessment

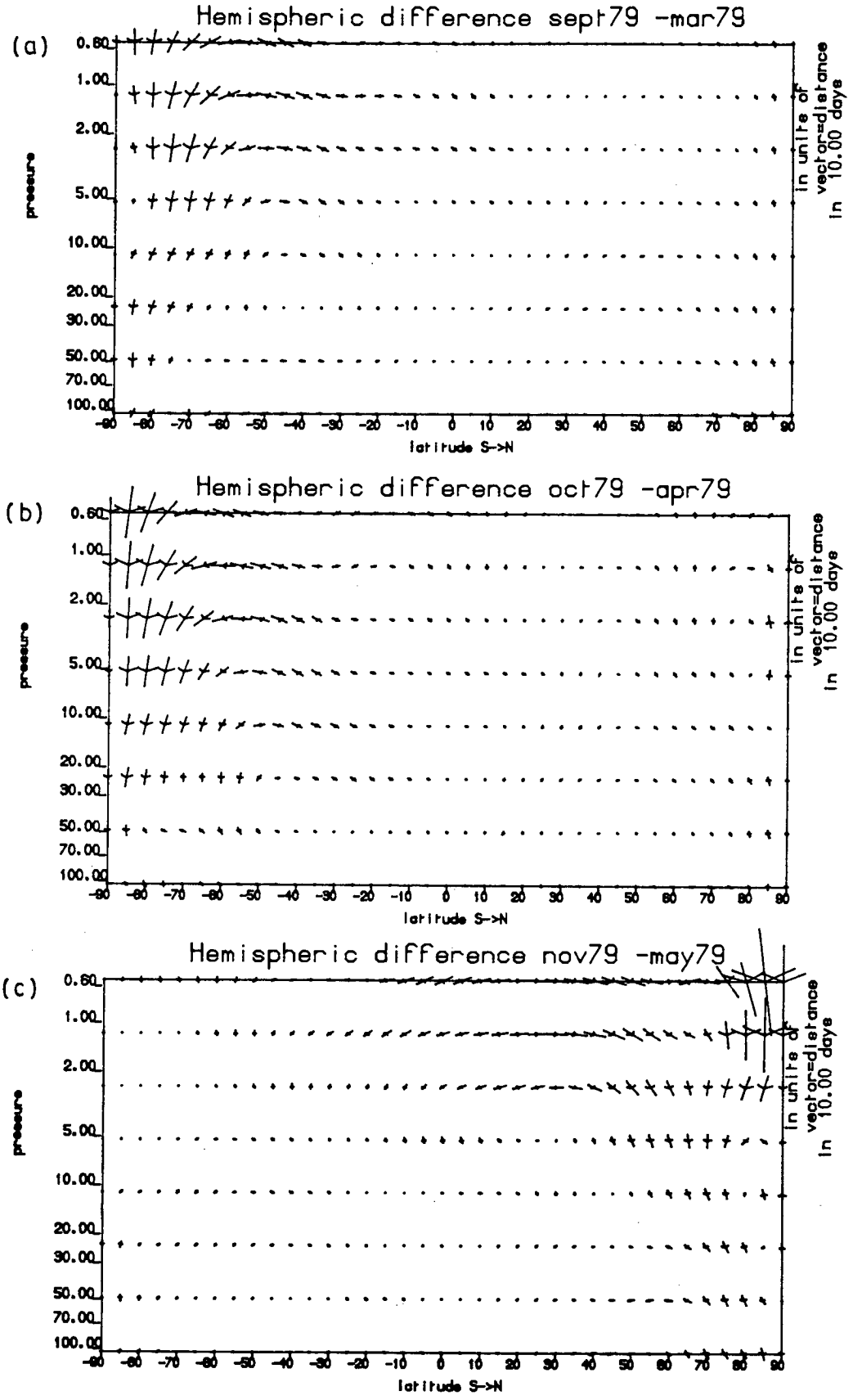

Figure F5.8 as F5.7 except for (a) September 1979(1) & March 1979(2), (b) October 1979(1) & April 1979(2) and (c) November 1979(1) & May 1979(2).

is based only upon qualitative evidence of the circulations advective transport and before any definite statements can be made a more rigorous analysis is necessary. The analysis described above is insufficient to draw definite conclusions since; tracer redistribution and accumulation assessed by eye may be misleading, the uncertainty in the data sets must result in caution and because no attempt has been made to estimate the role of important sources and sinks and eddy transports, both dynamical and chemical. The above conclusions must be taken with these qualifications in mind. To fully analyse the influence of the residual circulation's advective contribution on the tracer evolution the equivalent TEM tracer continuity equation, (5.1) below, to equation (2.6) must be used.

$$\underset{a}{\frac{\partial}{\partial t}[\chi]} + \underset{b}{[v]^{R}\frac{\partial}{\partial y}[\chi]} + \underset{c}{[w]^{R}\frac{\partial}{\partial \eta}[\chi]} = \underset{d}{-\nabla.\underline{F}} + \underset{e}{[S_x]} \qquad (5.1)$$

where $F_y = [v^* \chi^*] - [v^* \theta^*][\chi]_\eta / [\theta]_\eta$

and $F_\eta = [w^* \chi^*] + [v^* \theta^*][\chi]_y / [\theta]_\eta$

The above zonally averaged TEM continuity equation for the variable χ still retains eddy terms, term d. It is this re-formulated eddy term which has been neglected in the tracer redistribution analysis above. In a complete analysis of the tracer redistribution, the use of just the advection by the residual circulation is insufficient to describe the total transport. An extension of this qualitative assessment was attempted by undertaking a number of simple experiments (not shown here) in which the change in ozone concentration due to the advective transport by various of the monthly averaged circulations was evaluated. These showed an agreement in the sense of redistribution by the fully-forced residual circulation and the diabatically driven circulations, but not the 'Dunkerton diabatic circulation'. However the actual magnitudes involved were very different from the values of ozone change obtained for the month by simply subtracting the two monthly ozone fields. This discrepancy in magnitude was to be expected as the experiments described above were basically very crude and therefore unlikely to

give accurate magnitudes. Add to this that only a small section of the region of atmosphere considered is likely to be dynamically controlled, the region poleward of 60°N in winter and below $\approx$ 35-40km. Also below $\approx$ 20km. the ozone concentration is likely to be considerably influenced by the transport resulting from synoptic wave activity (cyclones and anti-cyclones) in the troposphere. Clearly this experiment had a number of major limitations but it also indicated, as did the qualitative analysis above, that the general sense of the fully-forced residual circulations, appears consistent with the observed redistribution of ozone.

5.4 : SEPARATION OF THE CIRCULATION INTO ITS COMPONENTS.

Having examined the 'fully-forced' residual circulation obtained from Ψ_R in the section above, it is interesting to examine next the component parts of this circulation and to assess the importance and role of each of the various forcing components during the year. This can be done by looking at the circulations calculated from Ψ_Q, Ψ_T, Ψ_S and $\Psi_A=(\Psi_T + \Psi_S)$, the diabatically driven component, the transient eddy and stationary eddy and total eddy forced components of the residual circulation respectively, which sum up to Ψ_R. These components are strictly speaking not independent but as explained in chapter 4 the separation into components allows a sense of seeing how the instantaneous meridional circulation is being produced. Each component corresponds to a physical process allowing physical interpretations and arguments for their existence to be made which is not possible by other methods. The split into components driven by the EP-fluxes and by the diabatic heating allows us to see how the temperature is modified away from the radiative equilibrium mean state.

Before such a description is presented along the lines of section (5.2) it is necessary to clarify what exactly the various right hand forcing terms and their subdivision means in physical terms, to ascertain what the physical mechanisms are which drive each component. So in section (5.4.1), these will be discussed; then in sections (5.4.2) & (5.4.3), the component circulations will be examined and analysed.

5.4.1 : SEPARATION OF THE FORCING TERMS.

Because of the monthly average used on all the forcing terms the 'non-acceleration' circumstances of atmospheric forcing are irrelevant to the present study. The reason is that when averages are performed over 30 days, the mean diabatic term, [Q], becomes important in the time-averaged dynamics (Andrews et al (1983)). For long time-averages the balance will be

$$\frac{1}{f_o}\left(\nabla.\underline{F}+[X]\right)_y = -\langle[v]^R\rangle_y = \langle[w]^R\rangle_p$$

$$= \langle[Q]/[\theta]_p\rangle_p \qquad (5.2)$$

where the $\langle..\rangle$ brackets is a time average defined as

$$\langle..\rangle = 1/\tau_a \int_t^{t+\tau_a} (..)\,dt$$

where τ_a is the averaging period, as described in Andrews et al (1983).

Thus where $[u_t]$ is small (and provided [X] is small, where [X] is any mean non-conservative force), D_F ($\alpha\ \nabla.\underline{F}$) will provide the necessary balance for the coriolis torque induced by the forcing [Q]. The state of balance suggested highlights the fact that the whole system is highly interrelated, with part of the radiative induced flow present because of the eddy activity. Therefore the residual component, Ψ_Q, is attributable to the forcing by [Q], but the magnitude of [Q] is largely determined by the existence of the eddy motions, Fels (1985). There would be very little [Q] if there were no eddies and had never been any eddies in the stratosphere. In this sense as discussed in chapter 4 and earlier above Ψ_Q is not independent of the eddy forcing as it is driven by the existing mean diabatic forcing which in turn is forced by previous eddy wave events.

It must also be noted that the zonal average quantity [Q] will not totally represent the total effect of the diabatic heating, Q, because of the non-linear dependency of Q upon the temperature and absorber amounts. The difference arises because [Q] used in this study is evaluated from a knowledge of zonal average measures of temperature

and absorber quantities. However to be calculated in full it should if possible be evaluated from a knowledge of the three dimensional fields of temperature, T, and absorber quantities and so include the non-linear correlations between T and the absorber amount.

The principal eddy forcing term, D_F, drives the major fraction of the transient and stationary components, Ψ_T & Ψ_S. However, D_F is not the only eddy term used to force Ψ_S and Ψ_T which are the response to all the eddy forcing terms in equation (4.16). Extra to D_F are the eddy terms which arise from the thermodynamic equation, (2.22). This equation retains the eddy term normally neglected when the equations are formulated in terms of quasi-geostrophic approximation ~~on a beta-plane~~ and therefore when the eddy forcing term is described in this study, the eddy forcing is chosen so as to include the effects of both the eddy terms in the right-hand side of equation (4.16).

The time-average and transient separation splits the eddy forcing, so that the transient wave activity component can be partly identified and its role and variability in forcing the residual circulation examined. This definition or mathematical means of obtaining transient eddies is refering to motions which deviate from the time-average flow field, so it will include any time varying aspect of the asymmetric deviations from their zonal average values, e.g. $\chi^{*\prime}$, (driven principally by wave activity or at least described as such.) of the u,v and T fields. Consequently there are mechanisms quite different from wave propagation which can contribute to D_F, through F, in particular for large stationary eddies in the troposphere where quite substantial fluctuations in θ^*, the potential temperature, can be induced diabatically. By this means a contribution is made to D_F due to non-conservative motion, giving rise to $[v^* \theta^*]$ quite independent of wave propagation, (Edmon et al (1980)). Many processes must be occurring and thus the divergences and EP-flux vectors achieved are a statistical sum of these. Only by means of modelling studies can a separation be made so that a way of elucidating the role and importance of each separable mechanism is possible. Therefore Ψ_S is forced by the time-averaged stationary eddy flux contribution to D_F. This will contain the average effect of the wave activity over the

month due to the presence of atmospheric conditions resulting in the breakdown of non-acceleration. This will be non-zero because of the time-average effect of a number of mechanisms including mechanical damping, dissipation, non-conservative forces, irreversible transience, wave-wave interactions and the interactions between these mechanisms, which each contribute to the statistical sum which is the eddy flux term. The 30 day average should ensure that the reversible linear transience (described by the time-average of $\partial A/\partial t$, where A is a measure of wave activity) will be a negligible contributor to div.F and so D_F. On the otherhand growth, decay and nonlinear transience, which may be reversible or irreversible, will, compared with reversible transience as described above, have a net effect as its average will be non-zero. The component streamfunction Ψ_T is forced by the transient eddy flux contribution to D_F, which contains influences from a number of transient mechanisms both linear and non-linear. As explained in chapter 2 the measure of transience given by these terms is different to the concept used in the theory and mathematical description of planetary wave breaking, wave dynamics and wave, mean-flow interaction theory. And it is the effect of transience in producing irreversible transport of potential vorticity and tracer constituents which we wish ideally to isolate and which signifies 'true' transience, however in this study this is not achieved. The forcing of Ψ_T will arise due to the variability of the flux contributions over the month, an indicator of the variations in wave flux due to wave transience and non-conservative mechanisms.

With these versions of the 'stationary eddy' , 'transient eddy' and diabatic forcing terms as a basis, the analysis of the component circulations will be undertaken.

Both the transient and stationary components of the eddy forcing are a result of divergence and convergence of the wave activity seemingly, according to a simple use of linear wave theory, indicating in-situ wave generation plus net outward propagation and net inward propagation plus dissipation, respectively, from the particular areas under consideration. However the use of purely linear wave theory to explain D_F and the orientation of the EP-flux vectors, is inadequate due to the importance of significant non-linear dynamics and non-wave

like synoptic circulations, O'Neill & Pope (1988). Alternatively the divergence might also be induced by ageostrophy or by non-linear effects (Andrews 1987). One explanation of the convergence of F can result due to transience, simply showing where the waves are arriving and being dissipated. However in general the interpretation of divergent region of EP-fluxes are not so easily tied to one mechanism. A recent further explanation of regions of divergence in high latitudes is described in O'Neill & Pope (1988). Here a signature of a dipole structure in D_F, similar to structures seen in observational studies including Geller et al (1983), and Hartmann et al (1984), can occur as a result of the widening of the buckling zone consequent upon the phenomena referred to as 'wave breaking' by McIntyre & Palmer (1983). The widening is occuring during a strong wave forcing event involving non-linear dynamics and entrainment of potential vorticity. The dipole in D_F has an origin in the formation of a localised jet seen in the synoptic pattern, O'Neill & Pope (1988) figure 17, on the poleward flank of the developing anticyclone which is pulling out the buckling zone or tongue of high potential vorticity from the main vortex. Hence D_F is merely the two-dimensional representation of the effects of these three dimensional synoptic features. As indicated above the wave flux derived is a statistical 'net' description of a number of processes. The time-averaging process also introduces the possibility that the value D_F will split the forcing of a single event between say two monthly averaged calculations. This will obviously occur if the total wave-forcing event does not start and finish within the first and last day of the monthly average. By the above means a possibly reversible event will contribute to D_F. This will therefore be misinterpreted as a net effect of the atmosphere during these months. One useful indicator of the validity of the divergent regions and hence the consequent circulations they induce is an examination of the directions of the EP-flux vectors. A fuller examination of the forcing terms is undertaken in Section (6.3). The accuracy of some divergent regions observed in the data is open to some doubt, but divergent fluxes in long term averages are not impossible. In general however the interpretation of such features derived from divergent F_G in the polar and sub-polar stratosphere must be carefully considered.

5.4.2 : A COMPARISON OF THE COMPONENT CIRCULATIONS.

The separated circulations obtained from Ψ_Q, Ψ_T, and Ψ_S are illustrated for each month in figures F5.9 to F5.20. In December, (see figure F5.9), the principal flow in the upper stratosphere is due to the Ψ_Q but in the mid-stratosphere, for p<5 mbar, Ψ_T is large and drives an indirect cell forcing the flow away from the pole between p≈ 5 and p ≈ 11 mbar. Ψ_T appears only to be important in the upper stratosphere and very near the tropopause, producing downward motions near the pole and therefore enhancing the diabatically driven flow. In the southern hemisphere all the flow components are weak except for Ψ_T which has an equator to pole flow again in the lower stratosphere at p ≈ 105 to 50 mbar. In January, (see figure F5.10a-c), Ψ_S is the dominant component in high latitudes driving a significant direct cell as well as the indirect cell which is primarily due to forcing by this term only. The very large vertical velocities calculated from this eddy forcing seem excessive. In the high latitudes of the mid-stratosphere, Ψ_A contributes significantly to the total circulation. In February, (see figure F5.11a-c), at high latitudes throughout the stratosphere Ψ_T has a circulation component equal to if not of greater magnitude than that due to Ψ_Q. Ψ_T is the only component to exhibit an indirect cell in the upper stratosphere high latitudes. Again it is only the transient eddy driven equator to pole flow which is significant in terms of eddy forcing in the southern hemisphere. This feature was not so evident in January.

In March, (see figure F5.12), Ψ_A has rapidly diminished while Ψ_Q has changed to a two-cell equator to pole equinoctial flow pattern, with both Ψ_S and Ψ_T being important only in the lower stratosphere and very close to the north pole. In April, (see figure F5.13a-c), the picture is similar, with the eddy components having become very small except in the lower stratosphere. The transient wave forcing in the lower stratosphere is the more vigorous, Ψ_S being very small. So the transient eddy driven equator to pole lower stratospheric cells are the only significant eddy driven circulation components during this month. Figure F5.14 shows May is very similar to April except that the lower stratospheric cells have weakened, while in June, (see figure F5.15), the only change appears to be that the transient wave activity is

increasing in the southern hemisphere and extending higher in the atmosphere as in April.

In July, (see figure F5.16), the pattern changes considerably and all three circulation components are important. The flow is a combination of a weak poleward diabatically driven flow above the southern hemisphere pole with strong descent in the upper and mid-stratosphere, plus a reversal imposed by eddy forcing as a result of both transient and time-averaged eddy forcing. These combine to produce an apparently confluent flow in mid-latitudes in the middle to lower stratosphere. The upper stratosphere is still dominated by Ψ_Q and this extends down to ≈ 2.5 mbar, where the transient and steady eddy components drive indirect cells which extend out to 45-40°S producing confluence at 45°S. Once again in the mid and lower stratosphere the eddy driven flow is as large as the diabatically driven component. In August, (see figure F5.17a-c), Ψ_S vanishes leaving only a fairly extensive transient eddy contribution to combine with the diabatically driven circulation. In particular, in the mid-stratosphere, Ψ_T acts to enhance the single-cell of Ψ_Q. Again the lower stratosphere in both hemispheres is dominated by transient eddy driven equator to pole flows, since Ψ_Q here has virtually vanished below 20 mbar.

In September, (see figure F5.18a-c), the time-averaged component returns, principally in the southern hemisphere high latitudes, but also contributing an upper influx from equatorial regions. Ψ_Q is again exhibiting a two-cell equinoctial structure but the eddy forced components are not. Ψ_T, although less significant, is more widespread and at 70-40°S is more important in the middle and lower stratosphere than either other component. In October, (see figure F5.19a-c), the flow pattern is similar but Ψ_Q is shifting to a northward single-cell dominance while the eddy forced components remain active in the southern hemisphere only. Ψ_S is again large throughout the depth of the stratosphere at 70-90°S, while Ψ_T is much weaker but tends to produce a confluent flow pattern in the mid-stratosphere at ≈ 60°S, which is not evident in either of the other components. Once again the lower stratosphere has the two transient eddy-driven equator to pole cells. Finally, as seen in figure

F5.20a-c, in November the main single cell of Ψ_Q has shifted over to the northern hemisphere winter regime, but only above ≈ 1.5 mbar. Also the eddy activity has changed hemispheres. Again the upper stratospheric Ψ_S vertical velocities are very large, while in the mid-stratosphere the Ψ_S includes an indirect cell. However Ψ_T is again restricted to the lower stratospheric cells, which are virtually continuous throughout the year. This eddy activity is mainly confined to high latitudes, i.e. $>50^\circ$ N.

The above description provides a year's sequential evolution of the separated components of the flow. This basis can be used to highlight periods and features of the flow where particular circulation components play important roles.

Of the months described March to June stand out as the only months during the year observed when the eddy forcing throughout the majority of the stratosphere was not significant. Only in the lower stratosphere/upper troposphere is there any significant eddy driven flow. On all other months the results produced indicated some form of residual circulation driven by the eddies which was not negligible. In contrast to the very weak eddy driven circulations during March to June the remaining months exhibited several strong eddy driven circulation features.

Throughout the year it is evident that the existence of strong divergence of the EP-flux, (see figures F6.17-F6.28), results in the appearance of a distinct flow pattern, with equatorward flow near the pole and well defined cells above and below this. So in the above descriptions of indirect cells it appears necessary to have positive divergence in the high latitudes to drive such a circulation component. In all cases observed where a region of divergence occurred in high latitudes, principally in the upper stratosphere, this characteristic circulation component was generated. Usually this was also associated with a strong positive gradient in the vertical of the EP-flux divergence. i.e. $\partial/\partial\eta(D_F)>0$ and large. Strong convergent regions which occurred without any significant divergent regions present, were seen to be associated with a circulation with a strong poleward and downward cell component. However the upper branch expected was

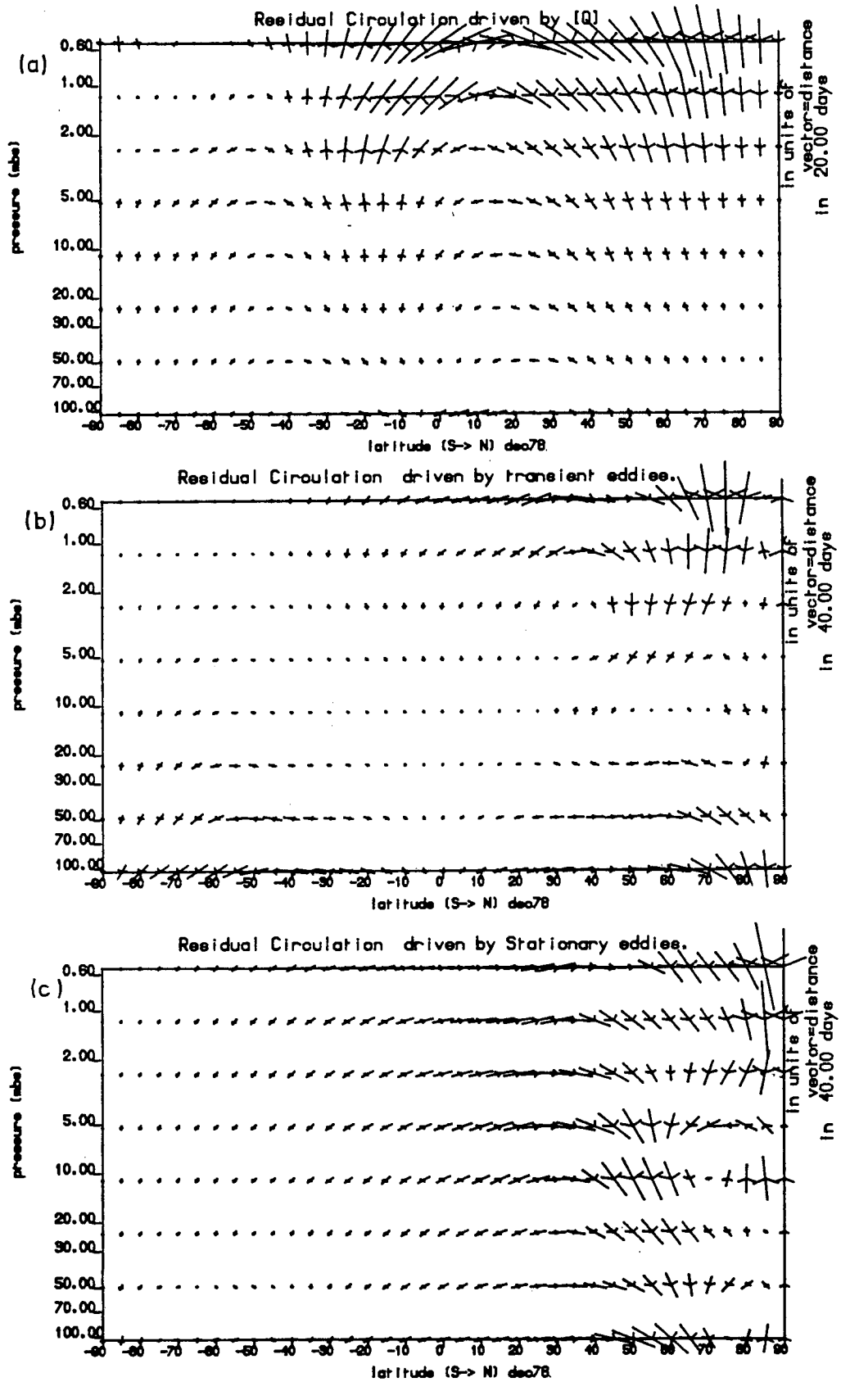

Figure F5.9 The residual component circulation's driven by (a) [Q], (b) the Transient eddy flux forcing terms, & (c) the Time averaged (or stationary wave) eddy flux forcing terms, for December 1978. Vector scaling as figure F5.1

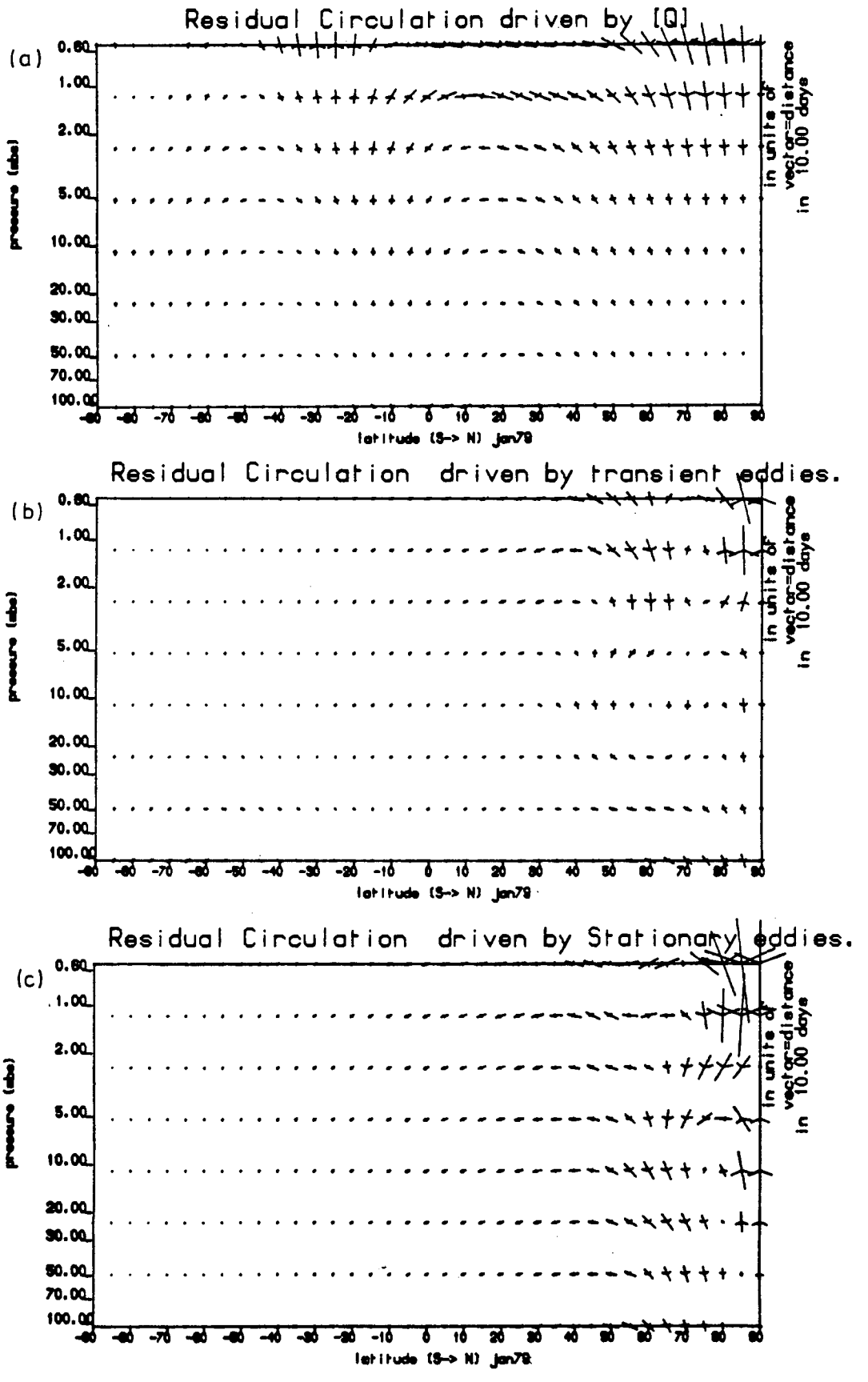

Figure F5.10 as F5.9 except for January 1979

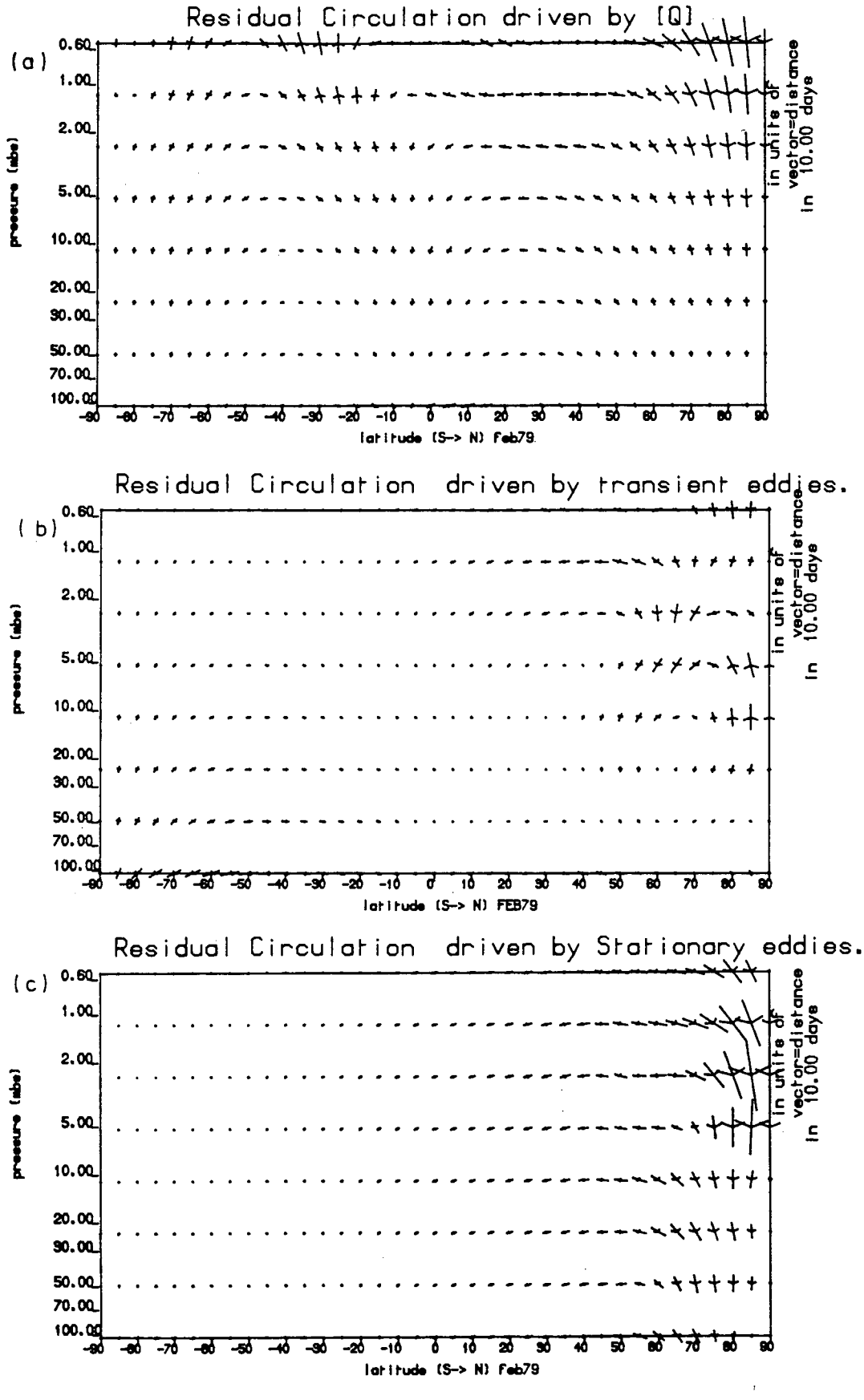

Figure F5.11 as F5.9 except for February

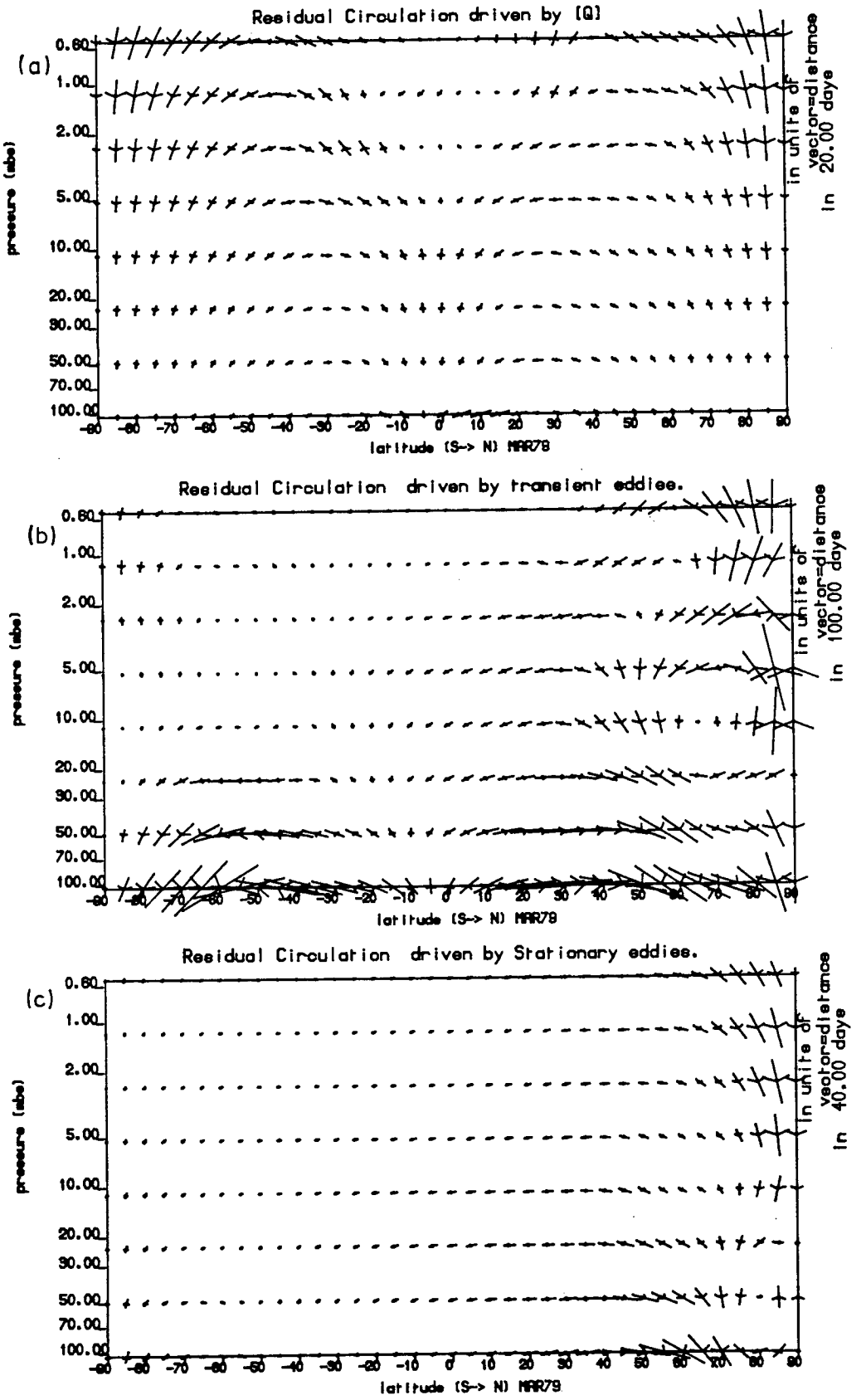

Figure F5.12 as F5.9 except for March

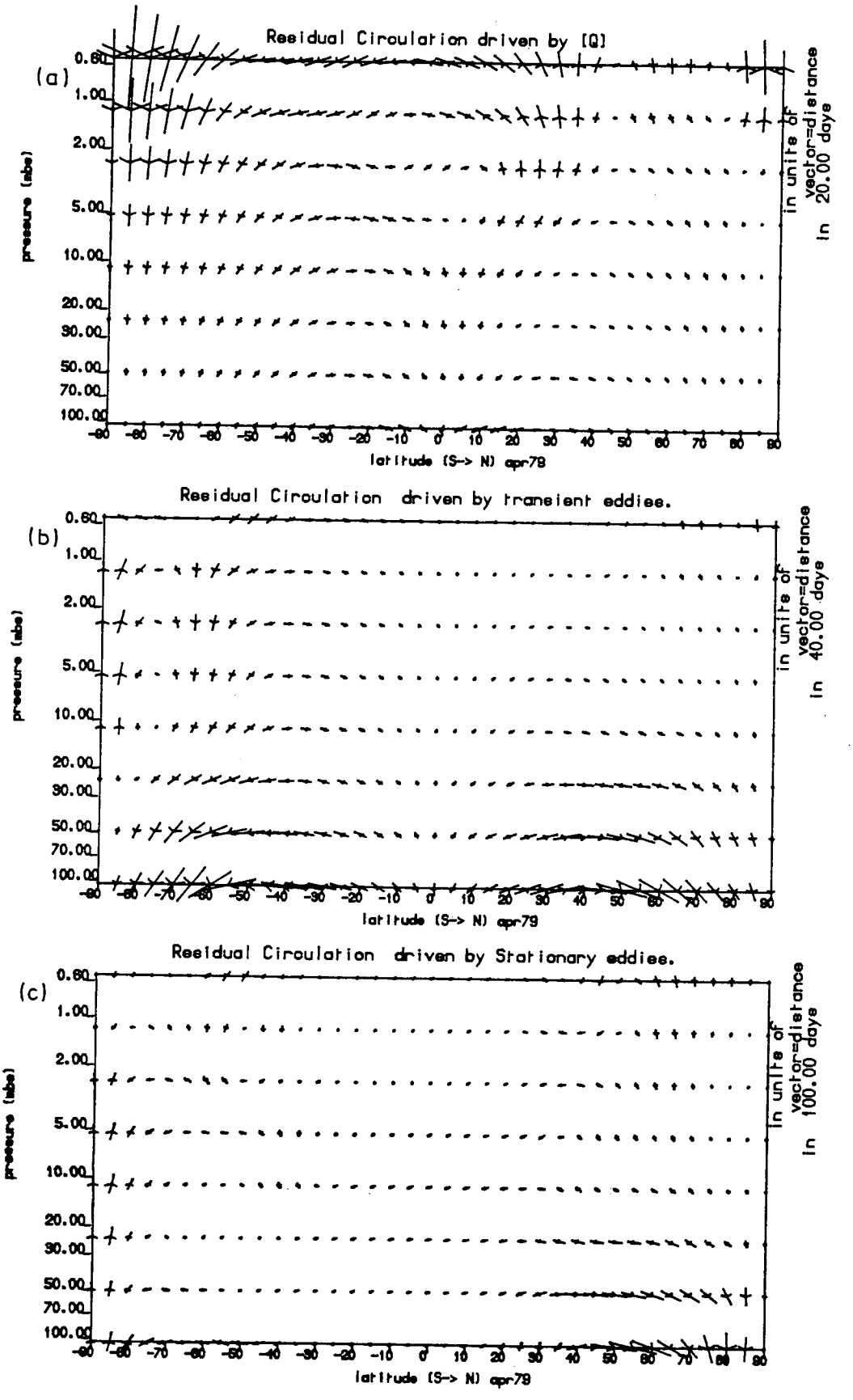

Figure F5.13 as F5.9 except for April

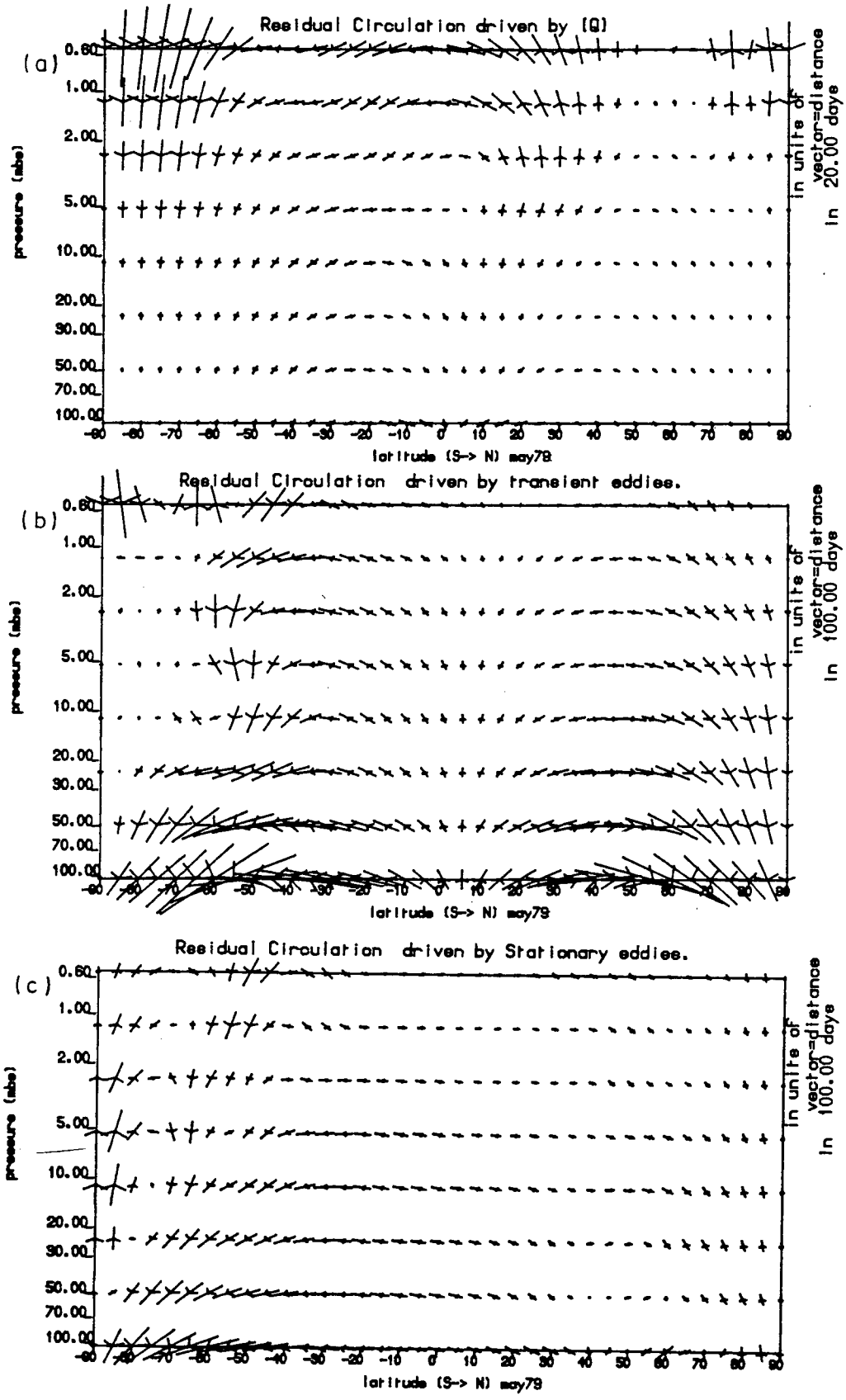

Figure F5.14 as F5.9 except for May

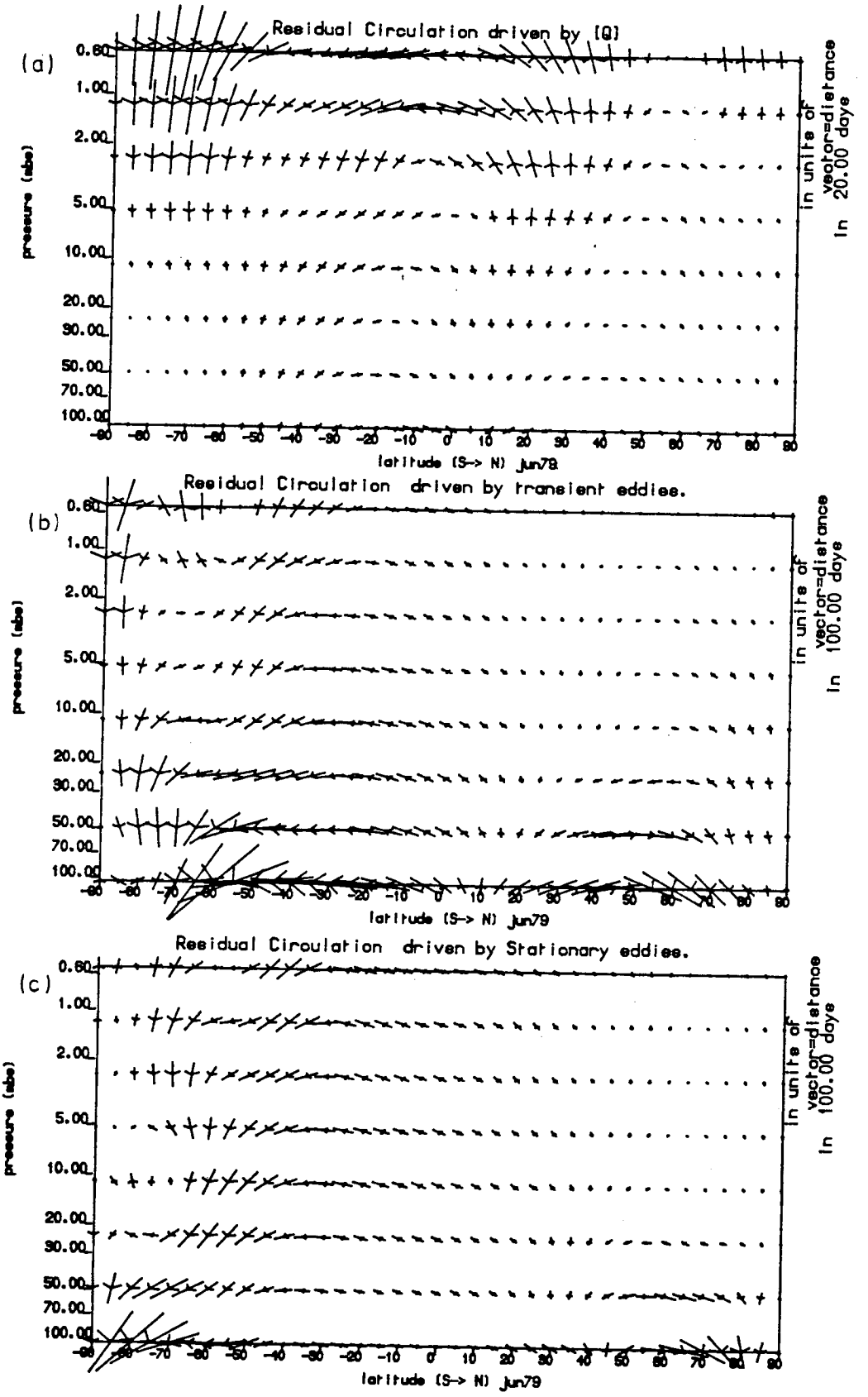

Figure F5.15 as F5.9 except for June

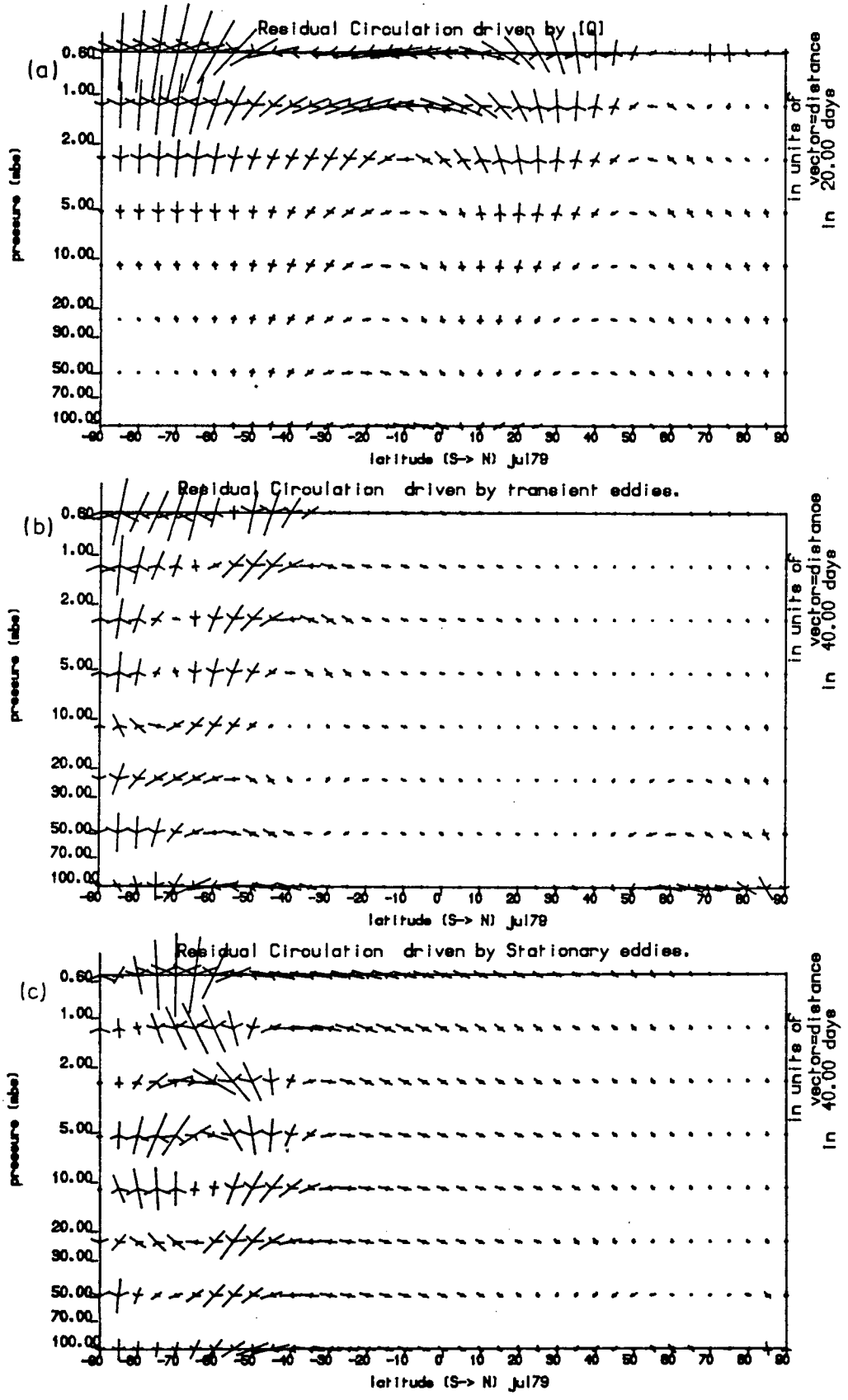

Figure F5.16 as F5.9 except for July

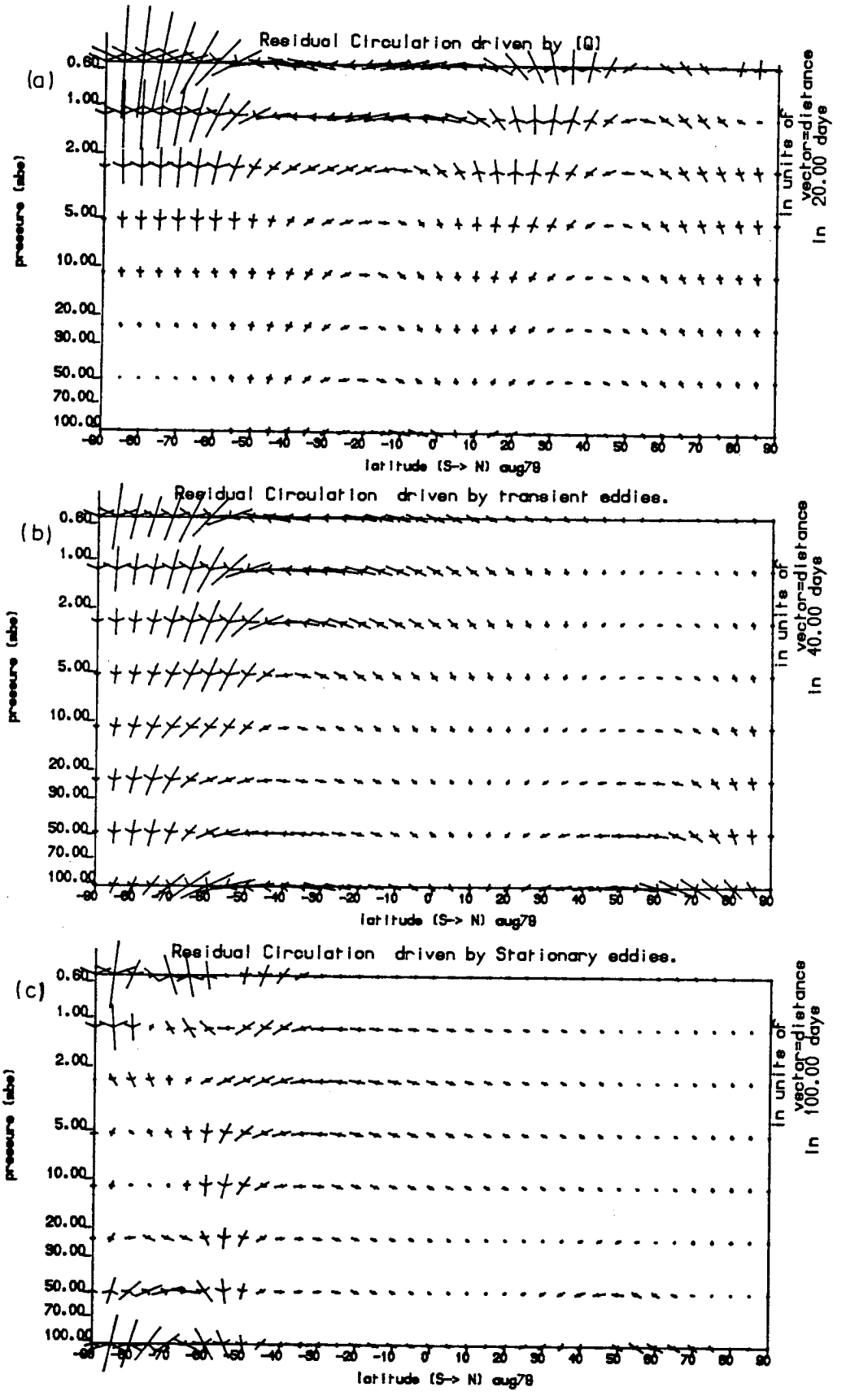

Figure F5.17 as F5.9 except for August

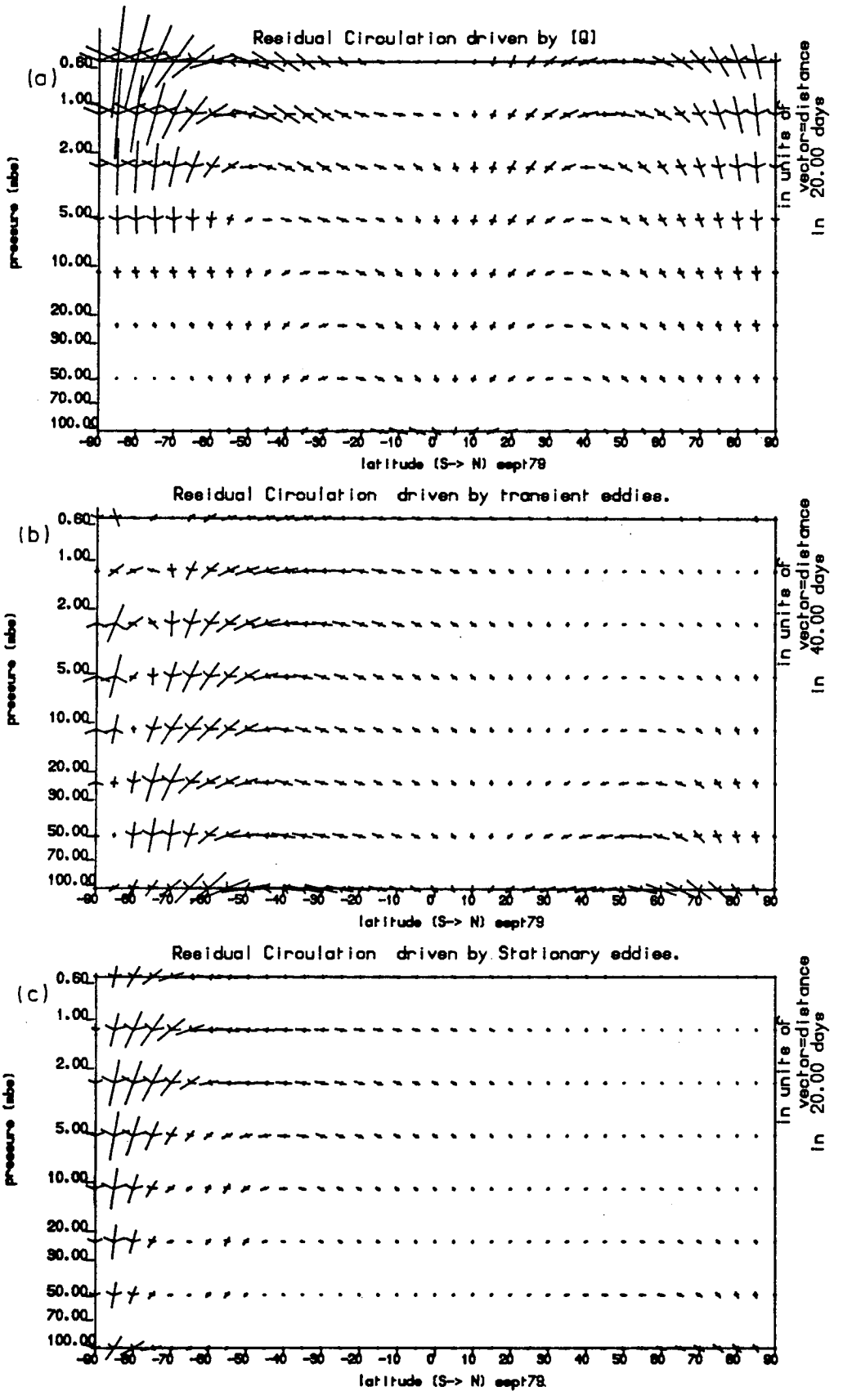

Figure F5.18 as F5.9 except for September

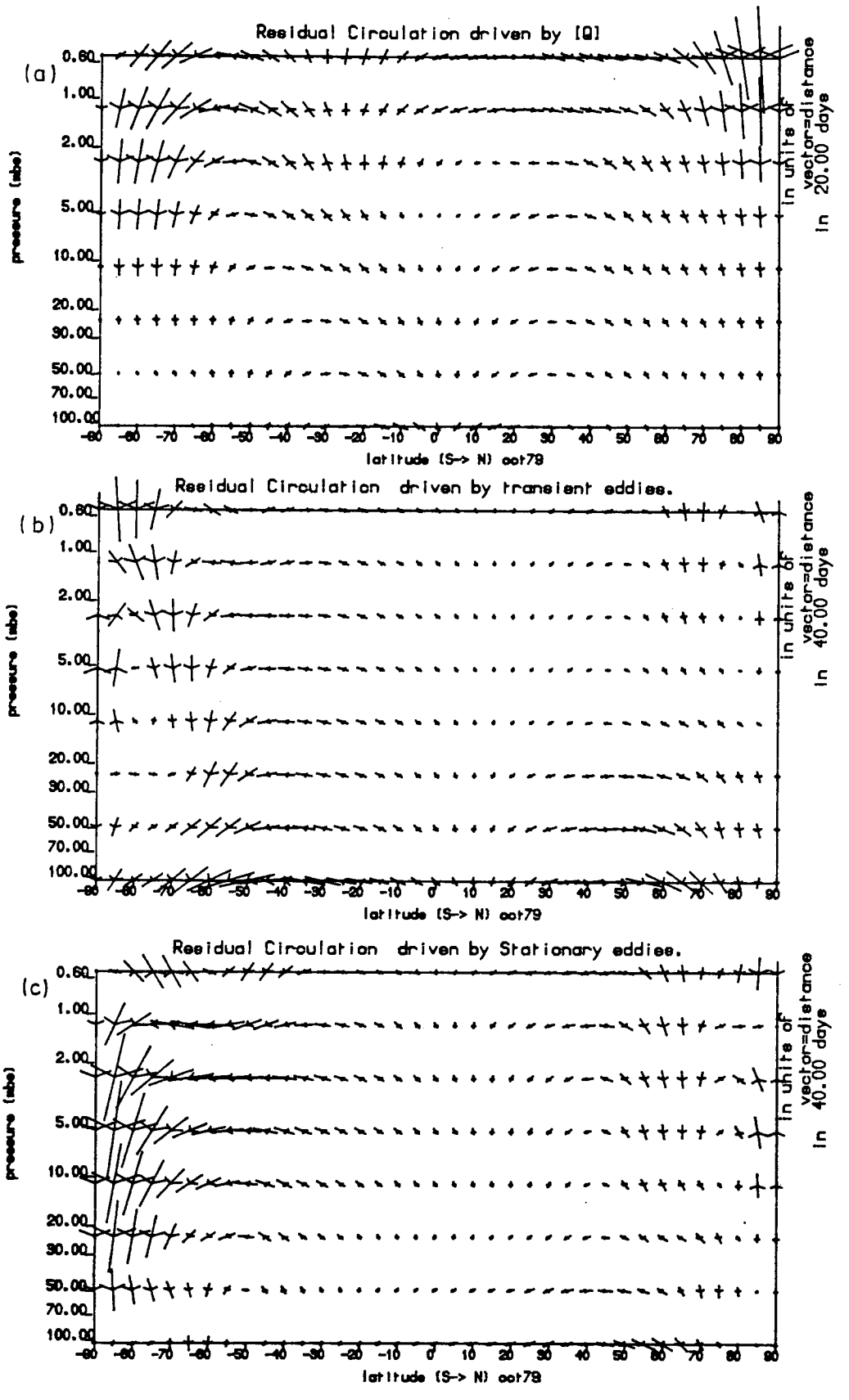

Figure F5.19 as F5.9 except for October

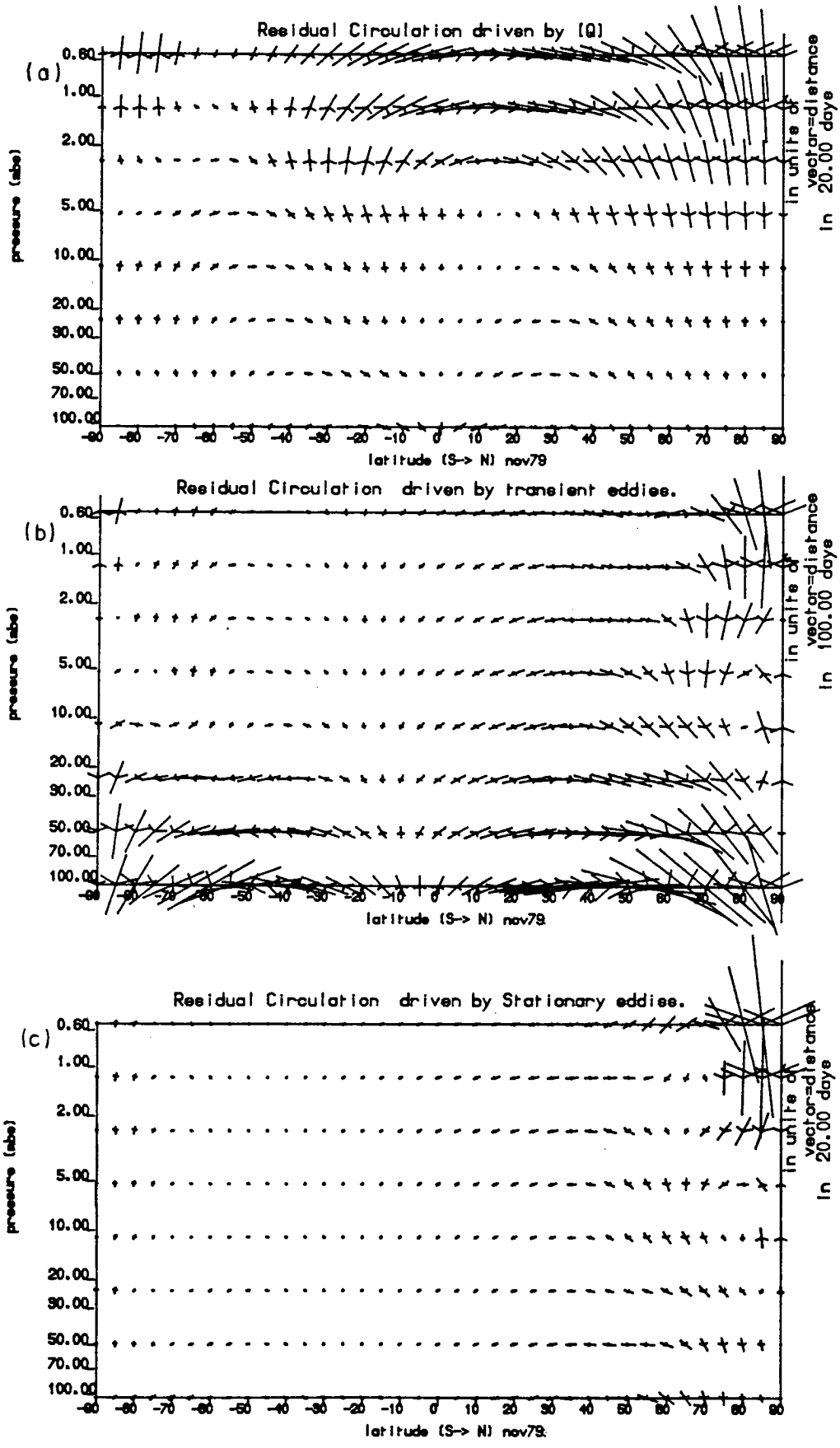

Figure F5.20 as F5.9 except for November

very much weaker or above the top of the 'real' data region. The absence of an upper cell occurred in a number of months where the convergence was predominant throughout the stratosphere and its maxima was high in the upper stratosphere. This forcing pattern therefore was responsible for the second type of general distinct eddy driven circulation component which showed a strong flow acting in cooperation with the existing diabatically driven circulation, to enhance the poleward flow. These two basic components describe idealised descriptions of the flow structures which are more complex in the real atmosphere. However in the months of February, March and October for instance striking examples of the latter circulation component described above can be seen (See figures F5.1,F5.2 & F5.4) and it appears that the flow is predominantly driven by the stationary wave flux forcing when in this particular form. See figures F5.11,F5.12 & F5.19.

The two main circulation components will obviously have important repercussions upon the budgets of heat, momentum and tracers in the stratosphere. Most striking is the large confluent, downward and poleward flow which occurs in both the daily analyses in February (see section 5.6) and its averaged counterpart in the monthly averaged February circulation, see Figures F5.1 & F5.11. Such a circulation has been deduced and analysed on a daily basis by Dunkerton et al (1981) and Palmer (1981b). This component is evident in February, August, September and October and is clearly eddy driven (see Figure F5.9-F5.20), and will result in an adiabatic response which will warm the pole. Thus as explained by Dunkerton et al (1981) the warming is largely an adiabatic response to a wave induced torque on a very large vertical scale. Not surprisingly because of the events which occurred during February, this month exhibits the largest flow branch of this type from the year's analysis.

5.4.3 : THE SEMI ANNUAL OSCILLATION. (SAO)

In the main study of the residual circulation in this thesis the effects of equatorial dynamics have been neglected as both geostrophic fluxes and the use of the quasi-geostrophic equations are inadequate in equatorial regions. In order therefore to examine the transport consequences of the unique circulation features such as the SAO in equatorial regions, an empirical approach is necessary. The recent measurements of tracer fields reveal a 'double peak' in certain constituent concentrations, the origin of which may be linked to the two-dimensional circulation associated with the forcing of the SAO in the zonal wind. Gray & Pyle(1986) have investigated ways in which the SAO could be introduced into present models so that the meridional circulation component thereby added can improve the transport description in equatorial regions. They introduced an empirical SAO representation and examined the resulting meridional circulation. However the description by Gray & Pyle(1986) is not an attempt to study the mechanism of the SAO but rather it is the use of a parametrization of the forcing in order to look at the influence of the circulation thereby induced on stratospheric tracers. This section describes briefly the results produced in this study by using a similar empirical SAO representation, as in Gray & Pyle (1986). Since these effects are not included in the circulations derived and discussed in the main part of this thesis, this work, a repitition of the Gray & Pyle experiment, has been undertaken to assess the effects these extra circulations have upon the conclusions derived from the main study results. To include an SAO simulation a westerly momentum forcing is added by specifying an additional term, assumed to be mainly produced by Kelvin waves, in the zonal component of the momentum equations. The easterly momentum required is not explicitly forced as it is expected to occur due to the non-linear advection of easterly momentum from the summer hemisphere. The wave motions which are assumed to produce the momentum forcing were assumed to play no other role in Gray & Pyle's model i.e. including diffusive mixing etc. The additional westerly momentum is produced by an empirical representation, whose peak magnitude is fitted to a suitable data value. The maximum forcing of westerly momentum was applied at the end of February and August, while negative forcing, the easterly phase,

was set to zero. Using an approximate version of the forcing function in Gray & Pyle (1986) the sharp gradient and consequent peak peripheral upward velocities of Gray & Pyle's results were not obtained. The failure to model the Gray & Pyle forcing function exactly was most likely as a result of the poorer vertical resolution used in the present study compared with their model. However the sinking in equatorial regions was found to be very close to the values quoted in Gray & Pyle (1986). Figures F5.21 & F5.22 show the 'fully-forced' residual circulations for March, excluding and including the SAO driven component respectively, which as described in Section 5.2, was a quieter month in terms of eddy activity. Even in this peak SAO month during quiet conditions for the rest of the circulation components, it requires close examination to identify the modification in the flow field as a result of the SAO forced circulation. This is highlighted in Figure F5.23 which uses a vector scaling of 100 days compared with the 10 day scaling found adequate on other circulation diagrams. Based upon this magnitude comparison it is clear that the SAO circulation would act as a gradual accumulative effect in terms of transport modification rather than an instantaneous flux which dominates the equatorial flow.

5.5 : A COMPARISON OF SEVERAL STRATOSPHERIC MEAN MERIDIONAL CIRCULATIONS.

A direct comparison was made of several alternative meridional circulations for the stratosphere. These were :

i) A fully forced residual circulation.

ii) A diabatic circulation calculated using Dunkerton (1978)'s approximations.

iii) A fully forced Eulerian circulation.

The idea of the comparison was to examine each circulation directly to determine their differences and to highlight these differences to possible two-dimensional model users. No means of assessing the validity of each as an approximation to the Lagrangian flow was possible.

In general over the year the circulations were significantly different in a number of aspects. Firstly the Dunkerton circulation has a much stronger flow in both [v] and [w] components above 10 mbar,

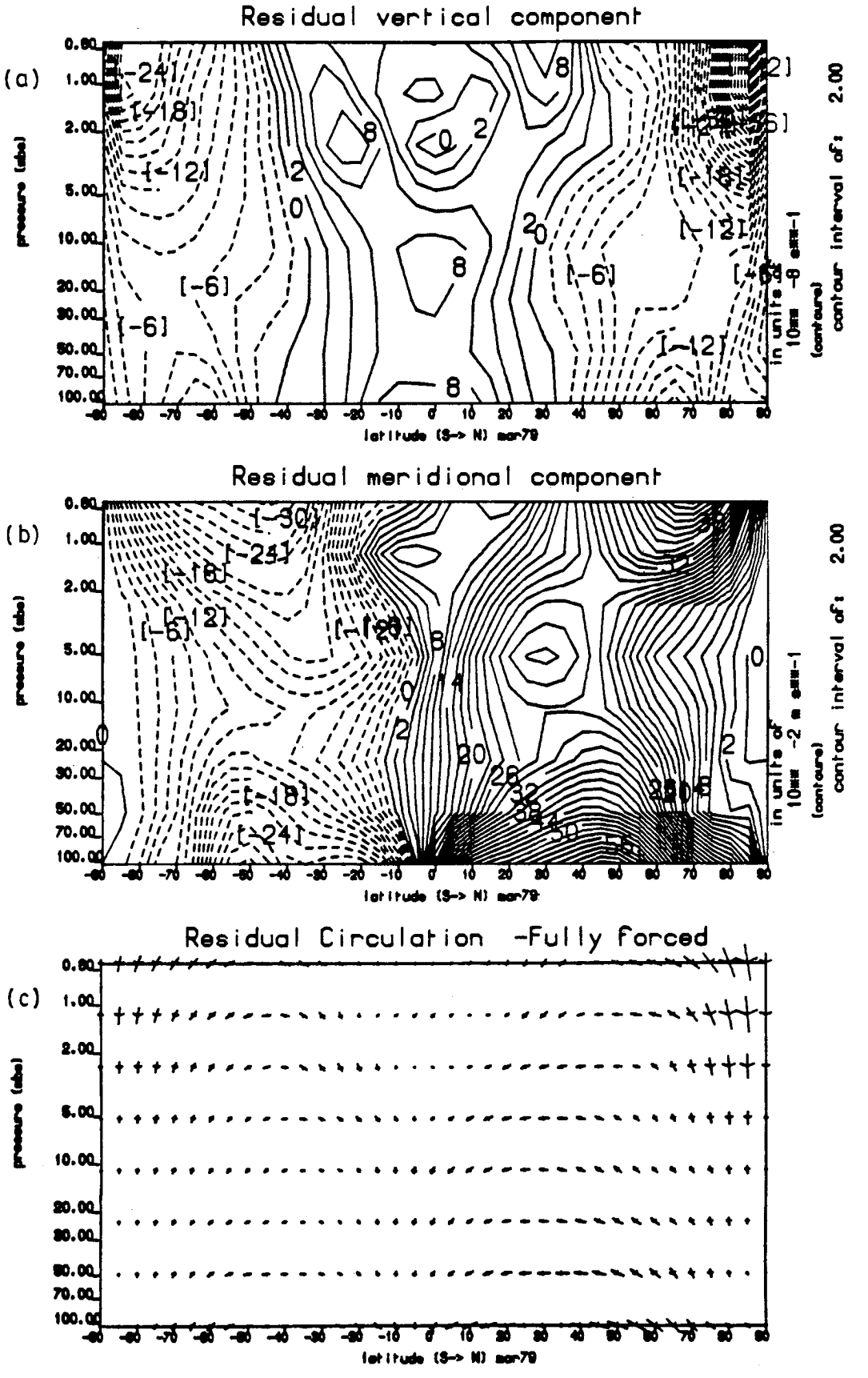

Figure F5.21 The 'Total residual circulation for March 1979. Its velocity components, (a) $[w]^R$ in s^{-1}, (b) $[v]^R$ in ms^{-1} and the circulation, where the vectors are velocity and represent the distance travelled by an air parcel in 10 days. (dashed lines are negative.)

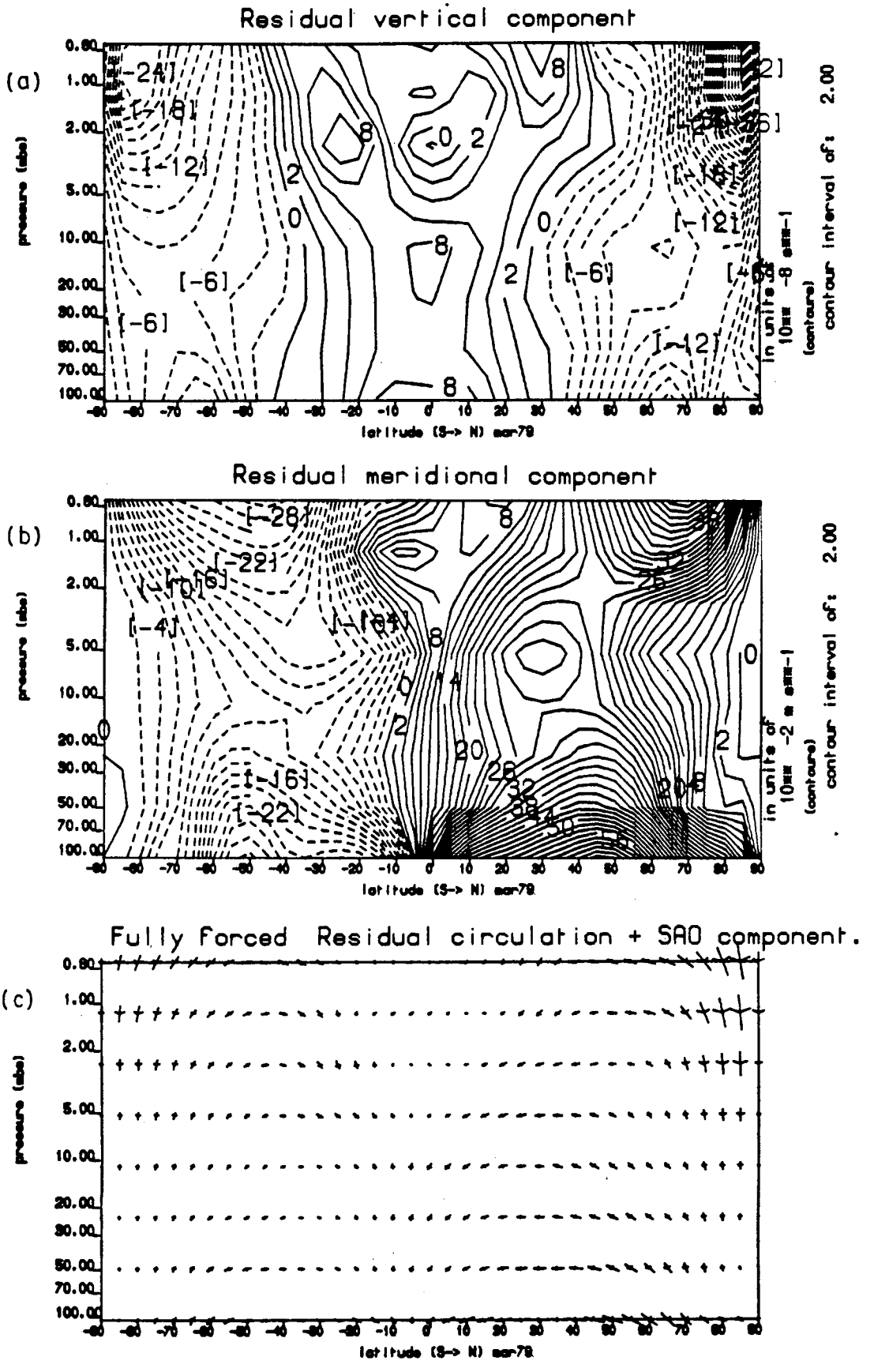

Figure F5.22 The 'Total residual circulation' for March 1979 including an SAO simulated forced component. otherwise as F5.21

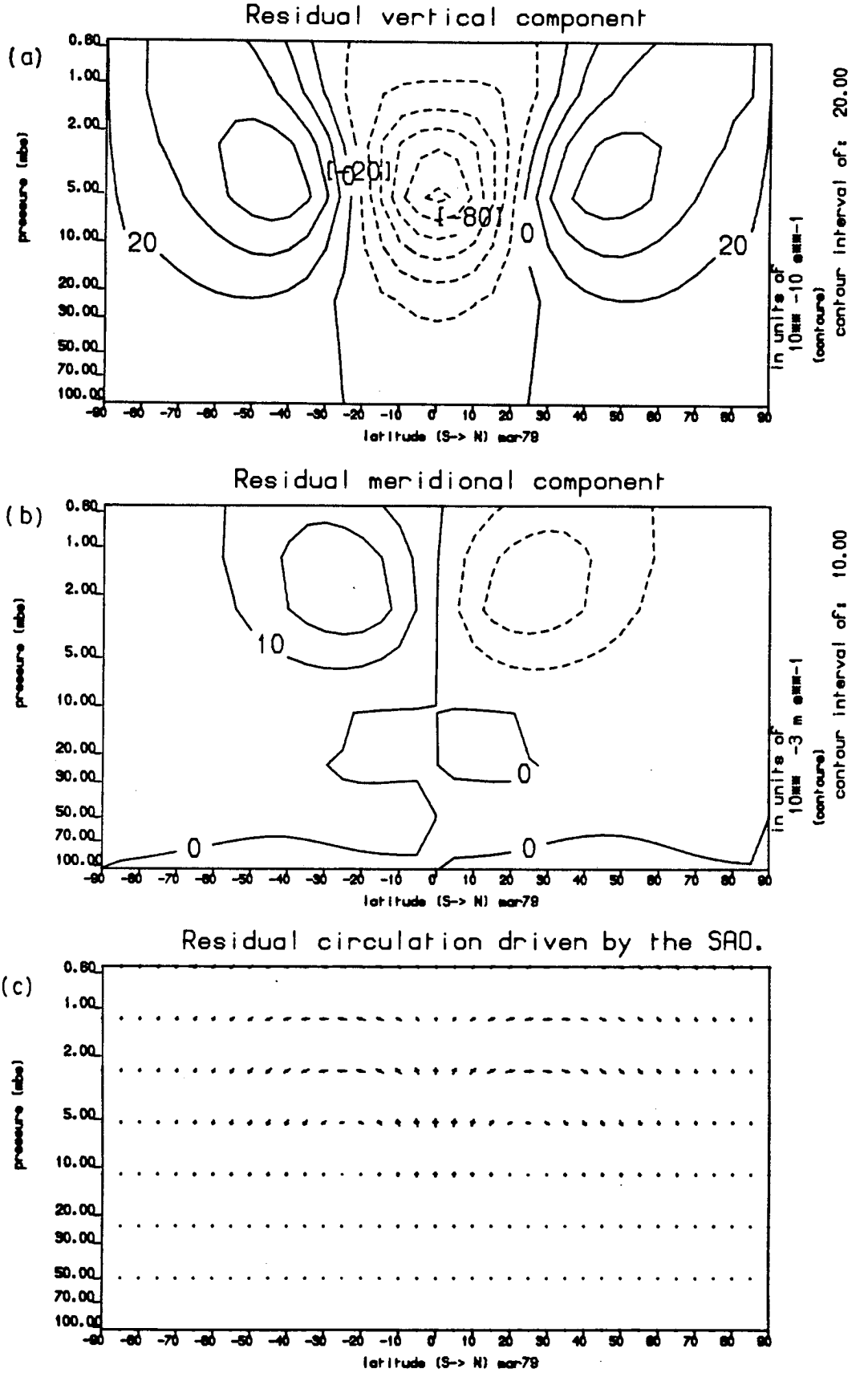

Figure F5.23 The SAO forced component of the residual circulation for March 1979. Its velocity components (a) $[w]^R$ in s^{-1}, (b) $[v]^R$ in ms^{-1} and the circulation, where the vectors are velocity and represent the distance travelled, scaled to the diagram, in 100 days. Note change in scale from figures F5.21 & F5.22.

throughout the year and neither the 'full residual' circulation nor the diabatically driven component thereof have magnitudes similar. Secondly the lower stratospheric-tropospheric flow at p≈ 105mbar extends slightly further equatorward than in the diabatic circulation in high latitudes compared with a stronger horizontal poleward flow in both hemispheres shown in the fully-forced residual circulation. The lower stratospheric-tropospheric flows and the indirect cells in high latitudes during active winter months were features only of the fully-forced residual circulation as explained in section (5.1 & 5.3). Another difference is that the Dunkerton circulation is much more active, see figure F5.24, in the middle stratosphere than any of the other circulations. In the quieter months when the eddy activity, as measured by the Eulerian eddy fluxes, is small, the lower atmosphere below ≈ 5mbar is very similar in all circulations except the Eulerian, see figures F5.24,F5.1-5.4 & F5.5. In the period June to August the summer lower stratosphere is again the only area of agreement between the circulations. In the high latitudes and upper stratosphere where all the velocities are stronger than at lower pressure levels the flows are once again very different.

If the residual circulation driven by [Q] was used as the only circulation component then the flow would be considerably modified compared with the advection implied by the fully-forced residual circulation, not only because of the absence of the eddy driven reversed cells which occur in high latitudes but also because throughout the active hemisphere the eddy forcing drives flows which combine with the diabatic forced circulation. These enhance the single-cell component so it is strong enough to produce the atmospheric balance, which is required to maintain equilibrium and restore thermal wind balance after the modification of the zonal mean state as a result of eddy deceleration. Only in the months such as March, April, May and June do the eddy conditions prevail such that a diabatically driven forcing alone could represent the real residual circulation. Even in these months transient wave activity is responsible for driving lower stratospheric flows from the equator to pole implying that again the diabatically driven circulation alone is insufficient. In some other months including November, October, September and July the eddy forcing is most obvious in the high latitudes and throughout

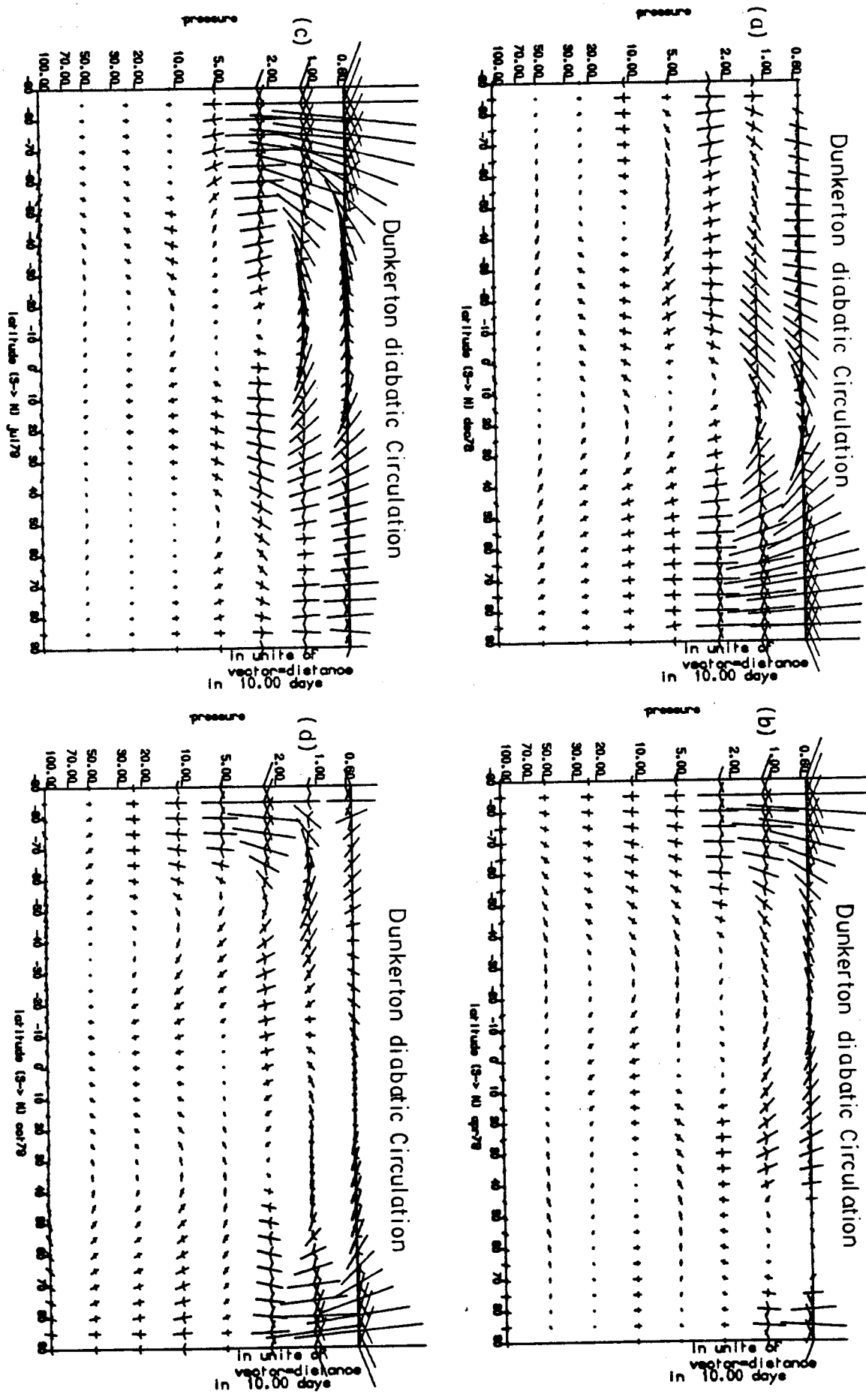

Figure F5.24 The 'Dunkerton- diabatic' circulations evaluated using the [Q]'s from the present study for; (a) December 1978, (b) April 1979 , (c) July 1979 & (d) October 1979.

the lower stratosphere but during highly active months such as December to February the entire winter hemisphere is affected. If Dunkerton's method is generalised to include $\partial T/\partial t$ in the evaluation then both it and the fully implemented residual circulation are merely different techniques of examining the same reality. Therefore they should give the same answer for Ψ to within experimental error. However the Dunkerton circulation as defined in Dunkerton (1978) does not include $\partial T/\partial t$ and so cannot represent the total circulation. The differences between these circulations therefore requires some consideration and discussion. Apart from the acceleration term, $[u]_t$, not included in the Dunkerton's circulation definition, the circulation represents a circulation forced by a mean state which is the atmospheres response to all past forcing and so inherently includes gravity wave forcing. This is not present in the residual circulation's evaluation as the resolution of the small scale fluxes due to such waves is impossible using the LIMS and SSU satellite data. Another reason for the differences involves the evaluation of [Q] which is critical to the Dunkerton circulation, as it is to the diabatically driven component of the residual circulation, and so a correct calculation of the total circulation is highly dependent upon the accuracy of the approximations used in calculating [Q]. Thus the different manipulation techniques used upon [Q] to obtain the different circulations are likely to introduce different errors.

5.6: DAILY CIRCULATIONS.

5.6.1 : THE RESIDUAL CIRCULATION DURING A SUDDEN WARMING.

The following section describes the events during the sudden warming of February 1979: this forcing evolution has also been described by several authors including Palmer (1981a&b), whose analysis is based upon SSU data. The following analysis thus serves in part to compare the diagnostics available from the LIMS & SSU data sources and to give confidence that the quantities such as EP-fluxes used in this thesis are broadly correct. In conjunction with this is a description of the daily evolving residual circulation throughout the period of the major warming. This allows bi-daily residual circulations to be examined to assess the variation occuring on this shorter time scale and during a highly active and interesting wave event. A

comparison can also be made with the monthly averaged circulation for February to examine some of the consequences and differences between a monthly averaged circulation and a flow description using a shorter interval average.

The sudden warming of February 1979 evolved over the period from the 17th to the 28th as described by Palmer (1981a). On the 17th of February a strong wave number two disturbance had developed from within the upper troposphere and was propagating into the stratosphere affecting the atmosphere throughout the majority of the northern hemispheric stratosphere by the 19th. Figures F5.25 & F5.26 illustrate the EP-flux and wave acceleration terms derived using the present data set allowing a comparison with the description by Palmer (1981a & b) of the above event. Examination of the results for the 15th and 17th of February, seen in figures F5.25a & b, shows there is evidence of weak wave activity propagating up and equatorward below 10 mbar. By the 17th the flux is more evidently vertically oriented extending beyond 10 mbar. By the 19th figure F5.25c shows that the wave propagation has changed, with EP-flux convergence occuring throughout the middle stratosphere, being particularly strong in the high latitudes at $\approx$ 10 mbar. The direction of the EP-flux has also changed as some flux is now directed poleward. By the 21^{st}, (see figure F5.26a), the pattern of convergence shifts and intensifies, the maximum convergence having moved lower in the atmosphere and slightly equatorward.

The event then appears to pause, as on the 23rd, (see figure F5.26b), the EP-flux divergence field changes significantly with the appearance of a divergent region of F at 5 mbar & above, & $> 60^{\circ}$N, and the return of the main EP-flux stream to an equatorward direction. By the 25th as is seen in figure F5.26c however the pattern is more like the 19th again with a region of convergence of F returning to the upper stratosphere. The only area of divergence occurs at high latitudes below $\approx$ 20 mbar. Then as the event begins to die down, around the 27th (see figure F5.26d) , the flow reverts to similar conditions to the 15th with a region of divergence of F dominating the high latitude stratosphere and the wave activity funnelling equatorward and flattening out, though still reaching up to

≈ 3 mbar.

This sequence is basically a repitition of that described in Palmer (1981a) and as such it provides a very useful confirmation of the LIMS, SSU data and diagnostics derived therefrom. Noticeable differences are evident when figures F5.25 & F5.26 are compared with figure F5.27 from Palmer (1981a). These include large positive values of D_F at >80°N in the present study. Also on the 23rd the mid-latitude convergence values are generally larger than those described in Palmer(1981a). However the general qualitative nature of the sequence of wave activity which comprises the sudden warming does compare well between the two. Simultaneous to these events the residual circulation has been evolving and changing in conjunction with the wave forcing and wave, mean-flow interaction.

Figures F5.28 & F5.29 show the residual circulation every two days from the 15th to the 27th of February 1979, covering the period discussed by Palmer (1981a) and Butchart et al (1982) which illustrates the onset and development of a stratospheric sudden warming. Figures F5.28a & b show the circulations for February the 15th and 17th, and are very similar exhibiting an indirect cell close to the pole centered at ≈ 5mbar. This diminishes thereafter and on the 19th, (see figure F5.28c), it has vanished leaving, except for a small deviation at ≈ 5mbar, a flow which descends over the polar region. The descent from the upper stratosphere has weakened whereas the lower stratospheric confluence from mid-latitudes has become more significant. Throughout mid-latitudes the flow between equator and pole, as seen in figure F5.29a, has remained in general unchanged. On the 21st the upper flow once again experiences an indirect equatorward motion at a height similar to that observed earlier but it is now confined very close to 90°N, and below, the lower stratospheric poleward and descending motion has grown larger. By the 23rd this has once again disappeared, (see figure F5.29b), but evidence of a slowing of the flow and a stagnation at approximately 5mbar, above the pole, is still present. The lower descent has weakened and there is motion away from the pole at ≈ 105mbar. By the 25th, (see figure F5.29c), there is no evidence of any indirect flow and the flow in high latitudes is very much simplier, consisting of air descending almost

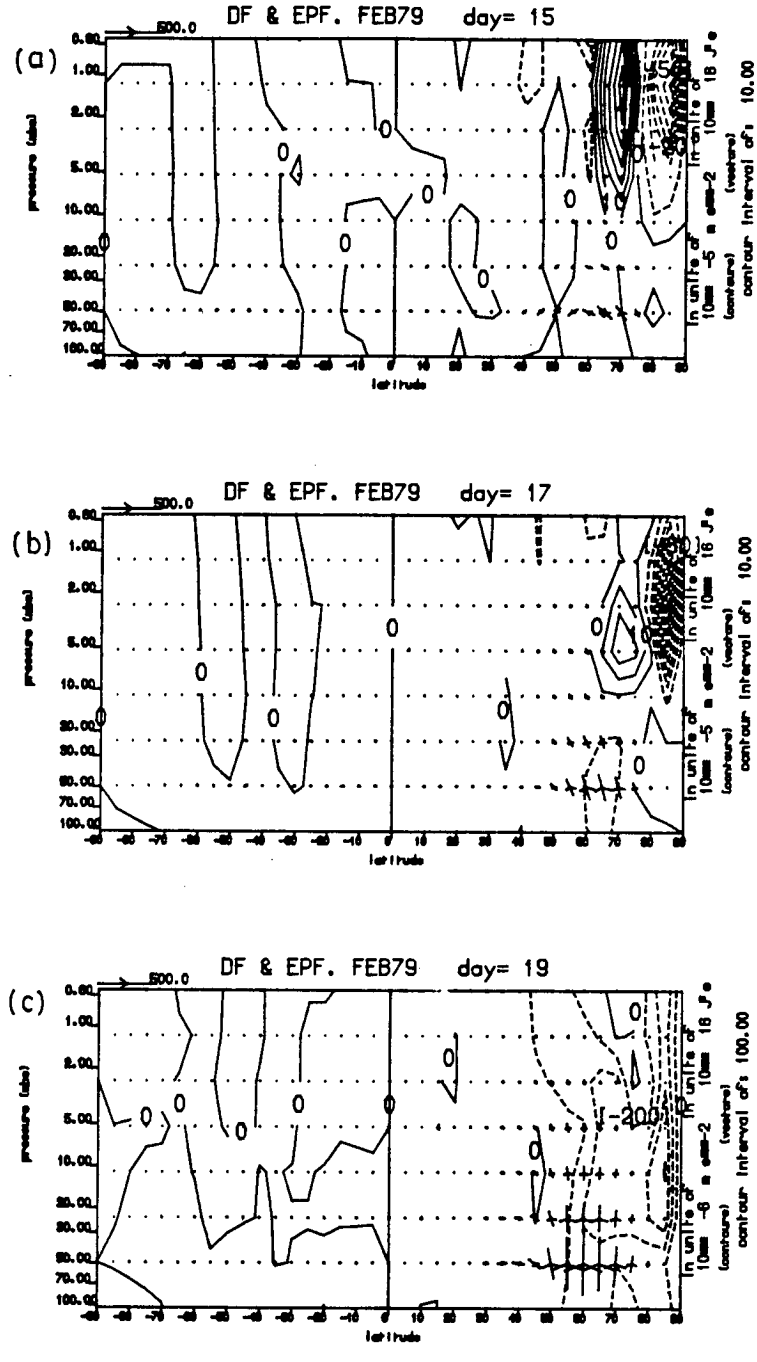

Figure F5.25 Contours of D_E (ms^{-2}) combined with EP-Flux vectors for (a) the 15th, (b) the 17th & (c) the 19th of February 1979. The arrow scales are such that a vector whose length is the horizontal distance 10° on the diagram represents a value of $(5\pi/18)n$ of F^{φ} in {J's} & a vector whose length is the vertical distance 1 interval of η represents a value n of F^{η} in {J's}; where n is the scale arrow magnitude at the top right of the figure multiplied by the vector scale factor at the left edge (top) of the diagram. F^{φ} & F^{η} are defined as in Appendix C. $n = 500.10^{16}$.

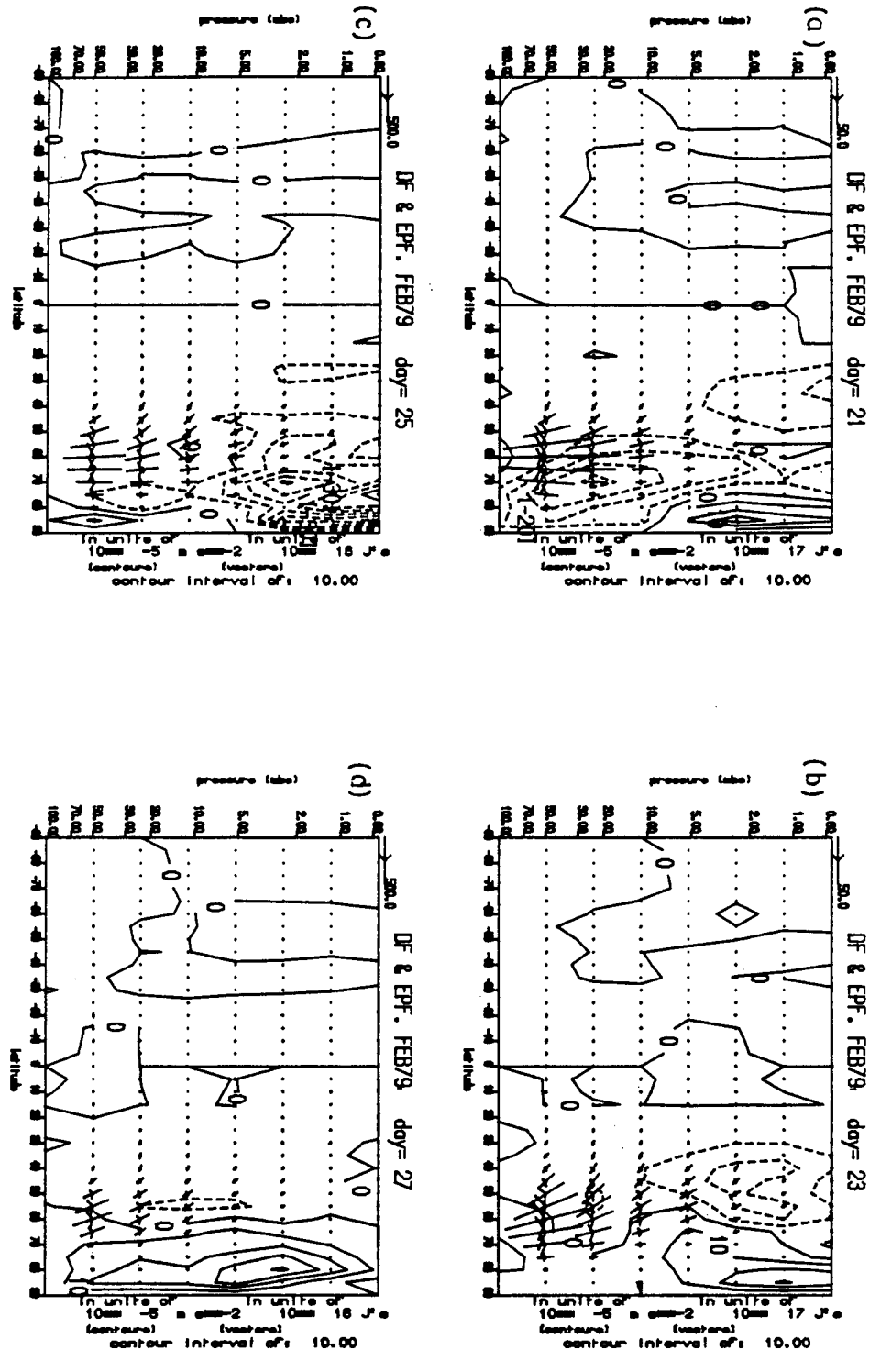

Figure F5.26 as F5.25 but for (a) the 21st ,(b) the 23rd ,(c) the 25th & (d) 27th. Vector scaling as in Figure F5.25.

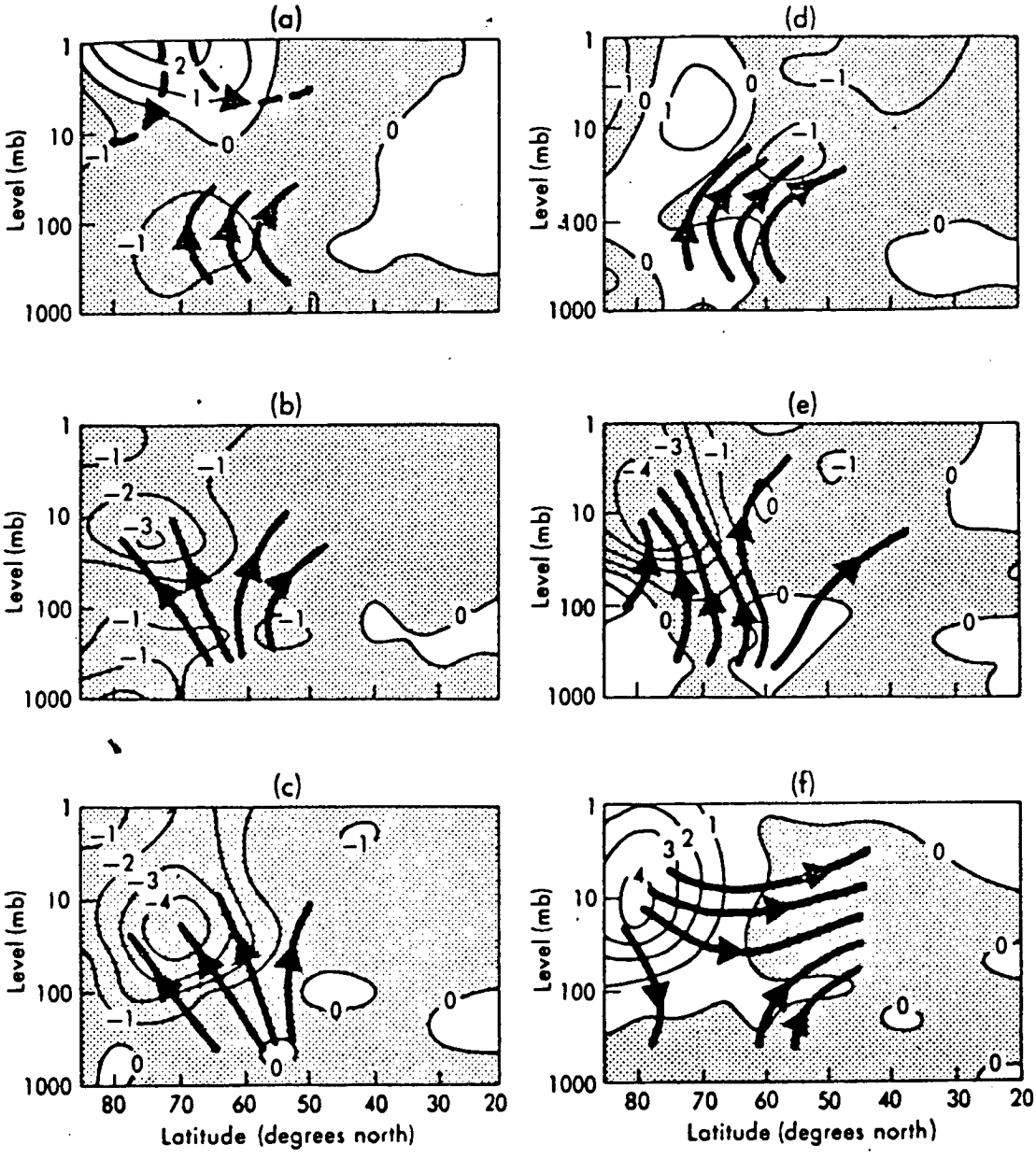

Figure F5.27 Contours of D_F in units of $10^{-4} ms^{-2}$ together with some integral curves of F, for the (a) 17th, (b) 19th, (c) 21st, (d) 23rd, (e) 26th & (f) 28th of February 1979 from Palmer (1981a). (negative values are stippled.)

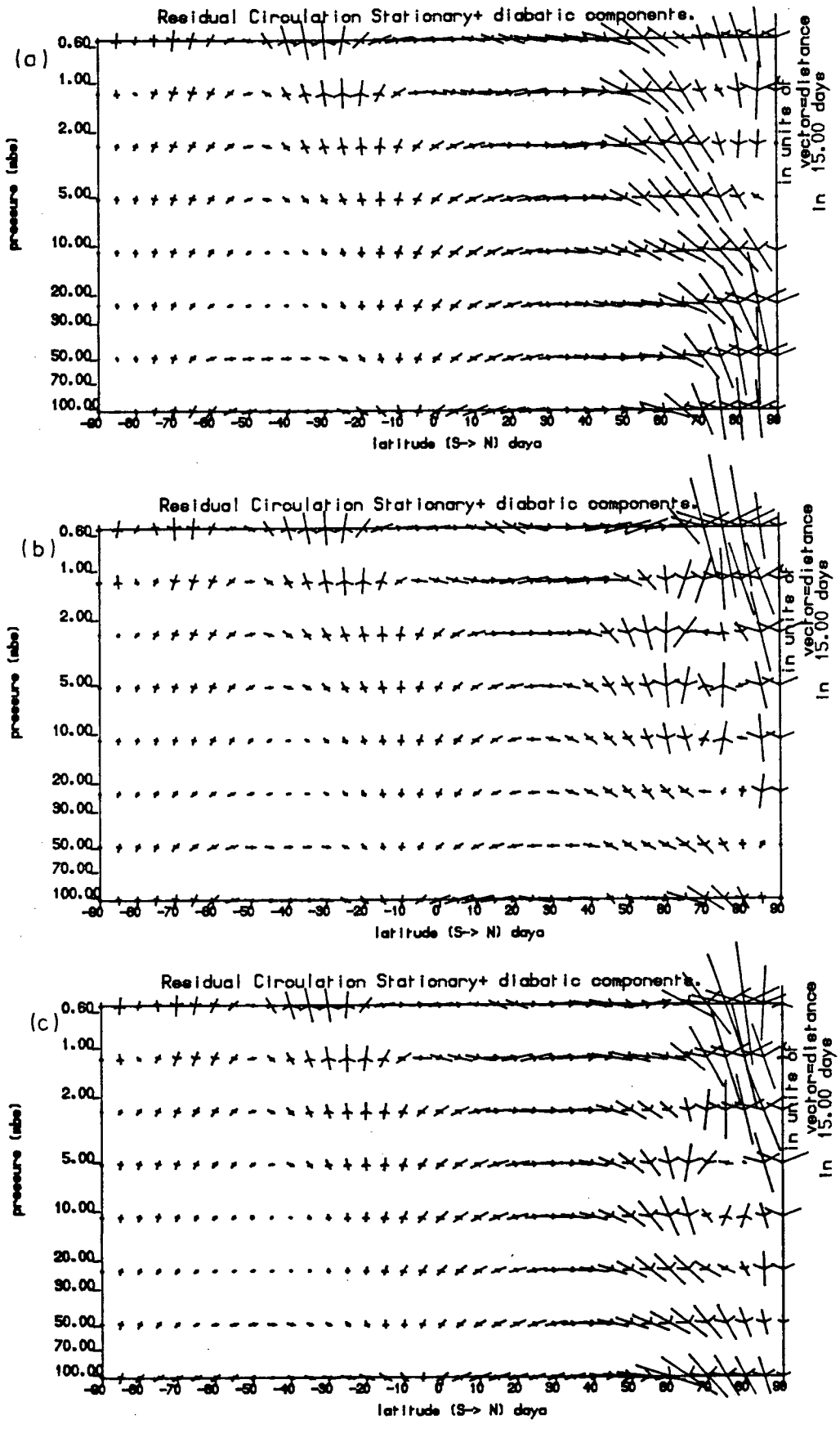

Figure F5.28 The total daily residual circulation's for the; (a) 15th, (b) 17th & (c) 19th of February 1979.

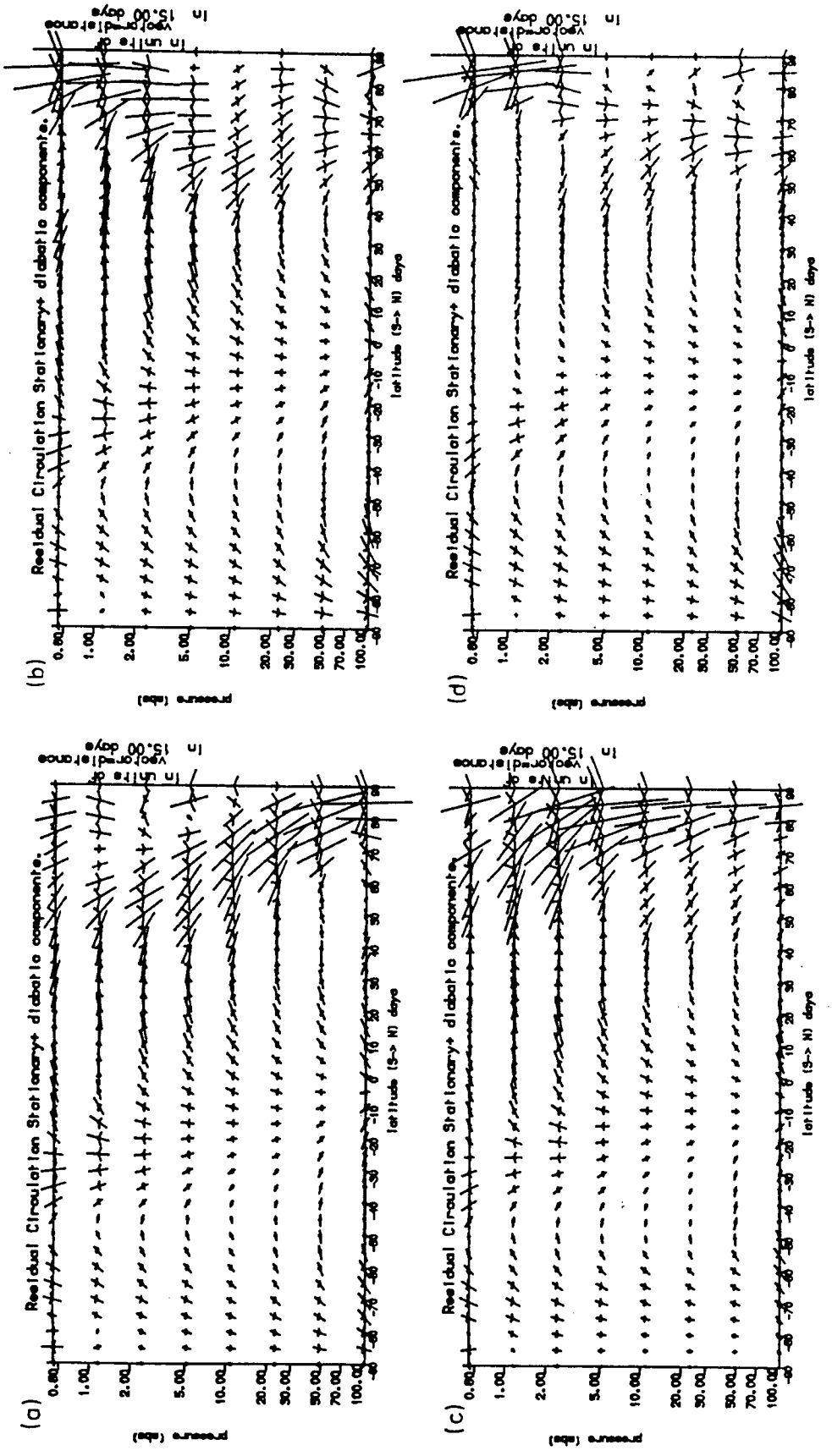

Figure F5.29 as F5.28 but for; (a) 21st, (b) 23rd, (c) 25th & (d) 27th of February 1979.

vertically from the upper stratosphere right down through the entire depth of the stratosphere, with the largest velocities being confined to > 80°N. Figure F5.29d shows the 27th of February is very different, with the maximum descent having shifted to approximately 70°N, which has also decreased in magnitude considerably compared with the 25th. A large reversed cell is now seen close to the pole moving air equatorward with no return flow in the stratosphere.

As would be expected the rest of the atmosphere excluding the high latitude northern hemisphere region remains fairly constant in flow direction and the southern hemisphere remains constant in magnitude and sense. In the northern hemisphere mid-latitudes and throughout the upper stratosphere, although the flow sense remains constant as a northward flux, it exhibits an acceleration with the flow reaching its maximum strength on the 25th in the upper stratosphere and on the 21st in the middle and lower stratosphere.

This discussion adds a detailed examination of the parallel development of the residual circulation during the evolution of the sudden warming in February 1979 as described by Palmer (1981a&b) and others. This description of the residual circulation throughout the sudden warming highlights the strong and variable flow occuring which shows features similar to those described in Dunkerton et al (1981)'s model experiments but in this case based upon diagnostics derived from observational data taken during a real sudden warming.

Several authors indicate that the regions of large EP-flux convergence as shown by Figures F5.25 & F5.26 will give rise to a poleward residual circulation due to the necessity to maintain the quasi-geostrophic balance (Eliassen (1951)). This in turn can, result due to continuity, in two (or possibly one) cells, one above and one below the region of EP-flux convergence. The upper cell consists of rising motion at the poleward side of the region with a return flow above and sinking at the equatorward side, while the lower cell has sinking motion at the poleward side with an equatorward return flow below and rising at the equatorward side of the convergence region to close the cell. As a result of the density decrease with height, the upper cell requires very strong velocities to balance totally the mass flux and

it appears that the atmosphere preferentially drives a larger lower cell compared with a small upper cell. This will be a further flow structure superimposed upon the slowly varying diabatically (radiatively) driven circulation.

Reversing this argument, a region of divergence, for example as occurred on the 17th (figure not shown) with a maxima at p≈ 5mbar in the high latitudes, should drive an equatorward flow, with accompanying cells above and below. The cell above should exhibit rising motion at the equatorward end of the divergence region and then flow poleward and sink near the poleward end. The cell below on the other hand should consist of sinking motion at the equatorward end of the divergence region, rising motion near the poleward end and poleward flow inbetween. The lower cell is very evident in the observations, (see figure F5.28c), but the upper cell is not visible. It is interesting to examine the daily and monthly averaged circulations for February to look for this form of induced eddy driven circulation as described by the theory. (Matsuno & Nakamura 1979, Eliassen 1951).

Examining the separated eddy, and diabatically driven components of the residual circulations derived, allows a better means of analysing the purely eddy driven circulation structures, by removing the diabatically driven flow which is superimposed upon this dynamically forced circulation. On the 17th therefore it is clear from figure F5.30 that the eddies are driving a large component of the flow especially in mid-latitudes and it is only in the upper stratosphere that the influx is of diabatically driven origin. Figure F5.30 shows that the eddies do drive an upper and lower cells due to the EP-flux divergence with the two cells linking at the level of the divergence maxima at (p=5 mbar. The upward branch at ≈ 60°N is indistinct while the downwelling is interrupted and almost vanishes suggesting a reversal. During the periods when the EP-flux convergence dominates, the cells are more difficult to identify. But on the 19th as seen in figure F5.28c a weak upper cell occurs above p= ≈ 5mbar, while below a large descent shows no sign of turning equatorward within the stratosphere. Figure F5.29 shows that on the 21st the two-cell structure is again not evident partly due to the presence of divergence and convergence close in high latitudes on this day which combine to produce a complex

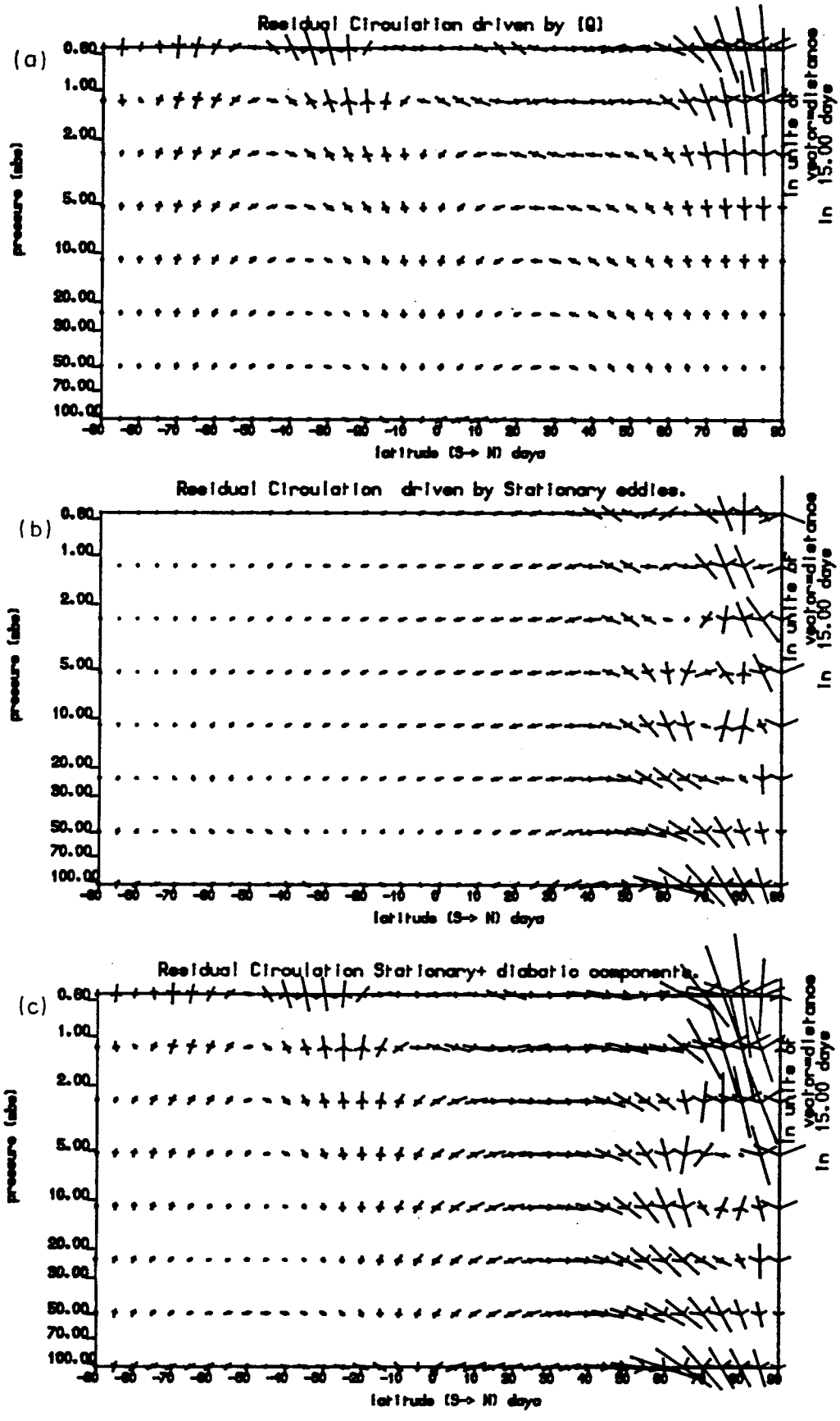

Figure F5.30 The daily residual circulations driven by (a) the [Q] forcing, (b) the eddy forcing, & (c) the total forcing for the 17th of February 1979.

pattern. However it is possible to see both an upper and lower cell with equatorward flow reversal near p=105mbar, centered on ≈p= 11mbar at ≈ 60°N. The flow of the 23rd does not exhibit a two-cell structure with its axis at ≈p=11mb but on this day the forcing is large and divergent which is contrary to the pattern of forcing observed earlier in the warming. What is noticeable however is a large reduction and reversal of the flow in the lower stratospheric high latitudes compared with the flow on the 21st, implying that the forcing has been diminished rather than reversed compared with the large forcing on the 21st. On the 25th the large convergence at high levels produces a large poleward flow once again, as seen in figure F5.29c, with no reversal and a strong descent over the pole. An important aspect of the separation of the flow into eddy, and diabatically driven components, is that it reveals that not only are the obvious reversed cells a product of the eddy forcing but also that these large fluctuations in the northward flow with both the maxima on the 21st and 25th are also principally eddy driven, while the diabatic circulation component is basically very constant throughout the month. This can be seen by comparing the monthly average February flow with any of the daily diabatically driven circulations, see figures F5.30 & F5.11.

As has been described in Dunkerton et al (1981) the eddy-circulation components are basically adiabatic flows which result in the warming of the polar region due to the descending branch of the circulation which shifts the isentropic surfaces downward in a rapid motion. The description of the circulations above illustrates the rapidity of the changes of the eddy driven component and contrasts this with the diabatically driven component which changes very little and seems to change on a much longer time scale. Clearly the events as described of the oscillating circulation structure and sense, including the lull of the forcing on the 23rd and the subsequent strong variable circulation branches, contain some reversible motion which merely 'sloshes' the isentropic surfaces up and down. However during these large fluctuations eddy induced dispersion is likely to cause air parcels to be irreversibly mixed with important repercussions in terms of changes in the mean state and tracer quantities.

The fully-forced residual circulation shows during the 15th to 27th, a period of large amplitude wave activity, considerable variability throughout the northern hemisphere and into the southern hemisphere in the equatorial upper stratosphere. The variability in the flow has been described above to be produced by the rapidly varying eddy forcing throughout the extreme events of the sudden warming which these dates cover. Under such conditions to model satisfactorily the full evolution of the system and its associated transport it would be essential for the individual days variations to be included and accurately determined in any modelling if the correct advective transport is to be achieved. During the changes observed there are signs of possible reversible events which are seen to occur during the change from strong confluence into the lower stratospheric polar regions on the 19th to equatorward flow from this area by the 23rd and then weaker confluence poleward on the 25th followed by an even weaker equatorward flow on the 27th. The oscillatory nature is indicative of a reversible event but the discrepancy in the magnitudes of the lower influx and gradual diminishment of flux of either sense thereafter also points to some irreversible consequences. It is principally the northern hemisphere high-latitudes which are changing the most with the region between 30°S and 40°N remaining qualitatively constant in structure and subject only to relatively small changes in magnitude of the flow compared with the high latitudes. This flow is one of rising motion with its axis centered slightly south of the equator and tilting further south with increasing height. This vertical motion then splits to produce two cells. One turns southward producing a weak motion toward the south pole, while the other is stronger and flows northward until as described above at $\approx 40^{\circ}-45^{\circ}$N a number of variations on the flow pattern occur throughout the warming event. The use of daily circulations therefore appears to be necessary due to the complexity and rapidly changing conditions including irreversible events but any analysis using daily circulations would be complicated by the large reversible events also occuring, confusing the interpretation.

5.7: CONCLUDING REMARKS.

The above sections have examined in various ways the residual circulations and the influence of each component throughout the period studied. A description of the residual circulation in the stratosphere was obtained and has been used to study the effect and evolution of the circulation diagnostic compared with other existing circulations in both the Eulerian and the residual formulations. Despite the lack of certain forcing mechanisms such as equatorial waves and gravity wave drag forcing, a major part of the forcing of the residual circulation has been computed and can be comparatively assessed. The interhemispheric analysis provides an interesting indication that the evolution and hemispheric differences observed in the circulations of this study appear to be consistent with similar interhemispheric variations in the redistribution of a tracer throughout the year considered. Although based upon purely advective and qualitative considerations these results indicate that the advective transport due to the residual circulation is a major part of the dynamical meridional transport in the stratosphere. As has been stressed above, the transport considerations are only qualitative and so it is necessary, in the future, to test these conclusions more quantitatively in a two-dimensional chemical stratospheric model.

The use of the solution method described in chapter 4 has allowed very easy separation of a number of component circulations as defined in section (4.3.1) in order that their relative evolution and importance can be considered. A major conclusion of this analysis is that the influence of the eddy circulation's are seen to be considerable and it is clearly the wave forcing characteristics and different evolution of the wave forcing between the two hemispheres which contributes significantly to producing the interhemispheric circulation differences described in section (5.3). Both the dominance of the late winter northern hemispheric flow compared with its southern hemispheric weaker counterpart and the existence of the strong spring eddy activity in the southern hemisphere which appears to have no northern hemispheric equivalent in this analysis, are the results of the extra eddy forcing which produce the extra circulation components and consequent transport. Both are effects which produce circulation

components which seem to be consistent with the yearly evolution of the tracer concentration as was illustrated by the SBUV total ozone fields. This point will be expanded upon in chapter 6 where a fuller analysis and description of the wave forcing responsible for the extra circulation components will be discussed in relation to the zonal mean state's evolution.

The eddy forcing was further sub-divided into its time-averaged (stationary) wave and transient wave forced circulation components as defined in section (5.4.1). However this analysis proved disappointing in identifying any distinct residual circulation features uniquely defined by the separation of the eddy circulation in this manner. On the basis of the active year chosen in this study, 1978/79, the eddy fluxes due to both the transient and stationary waves are clearly seen to drive significant residual circulation components, which act both to enhance and oppose the more slowly varying diabatically driven circulation component. Further work aimed at investigating the different roles of the transient and stationary wave forcing contributions has been undertaken by means of an analysis of the eddy forcing diagnostic in chapter 6.

The daily circulation analysis illustrates on a shorter time scale a similar picture to that of the monthly averaged flows in that the more variable eddy components during active wave flux periods are important and produce significant effects in terms of transport and in maintaining the stratospheric atmospheric mean state. The diabatically driven circulation here illustrates a slowly varying but ever present flow existing because of the influence of past wave, mean interaction events in maintaining the atmosphere in its existing balance away from pure radiative equilibrium conditions. During the short period examined, from the 15^{th} to the 25^{th} of February 1979, which was subject to intensive and large wave amplitude activity, the circulation changes and evolves fairly rapidly, but a comparison of the average and daily circulations shows that the average is representative of the general features seen in the daily circulations. The clear lower stratospheric confluence, seen in both the monthly averaged flow and the daily circulations, resulting from the large wave activity convergence can be related to the accompanying adiabatic warming of the winter polar

region at this level during the sudden warming. However to model successfully the complex transport which is evident from the variability seen in the daily circulations examined it may be necessary to use daily circulation evaluations when considering vigorous wave forcing similar to the conditions of the sudden warming event period of February 1979.

As demonstrated by the brief examination of the equatorial component, the residual circulations described in the main section of this chapter were incapable of realistically representing the wave forced circulation components of the flow in equatorial regions. The role of these waves in driving a residual circulation component is small but the advective influence has been shown to be necessary if a complete description of tracers is to be accurately modelled.

In summary then the analysis in chapter 5 has provided a full years description of the residual circulation and its monthly evolution over the period December 1978 to November 1979. A year's analysis was made of the relative importance of the diabatically, transient eddy and time averaged eddy driven circulation components. The major conclusions that can be drawn from the analyses above include:-

Firstly, the result that from the analysis of the comparison of the circulation components undertaken it was seen that the eddy circulation components during a number of months of strong wave activity were a significant part of the total residual circulations calculated. These circulation components will have important repercussions upon the budgets of heat, momentum and tracers due to the extra advection of these quantities principally into the winter high latitudes thus altering the mean state distribution of all these quantities.

Secondly, part of the analysis was a interhemispheric comparison of the residual circulation which highlighted some important differences between the hemispheres in the circulations which appear to qualitatively account for the total ozone's distribution throughout the year. A close qualitative correlation can be seen between the evolution of the total ozone's redistribution and the circulations advective consequences over the year. This provides supportive

evidence for the use of the residual circulation as a stratospheric transport circulation diagnostic in two-dimensional modelling.

Thirdly, identification of some important differences in the definition and physical significance of the diabatically driven circulation and the 'diabatic' circulation as defined by Dunkerton (1978) or Murgatroyd & Singleton (1961) have been emphasised.

In Chapter 6 the component residual circulations together with the Eulerian and diabatic circulations calculated will be examined in terms of their role and consistency in the momentum and thermodynamic budget equations. Also a more detailed examination of the forcing diagnostics and evolution of the mean state throughout the period studied will be undertaken.

CHAPTER 6 : A BUDGET AND DIAGNOSTIC ANALYSIS.

6.1 : A COMPARISON BETWEEN THE EULERIAN AND TEM MOMENTUM AND THERMODYNAMIC BUDGET EQUATIONS.

Chapter 6 views the circulations in terms of their part in the atmospheric Eulerian and TEM momentum and thermodynamic conservation budgets. The TEM formulation is briefly contrasted with the Eulerian formulation and the respective eddy terms are discussed. This chapter describes the momentum and heat budgets based upon the Eulerian, Residual and diabatic circulations computed as discussed in chapter 5. This allows a comparison of the circulations to be undertaken in terms of their consistency in relation to the observed heat and momentum tendencies and also illustrates the role of the residual circulation components in contributing to these tendencies.

The budgets illustrated are based upon the combined data set as described in chapter 4 for December 1978 to May 1979. Thereafter only SSU geopotential and SBUV ozone are available. The budgets were examined for all twelve months and for a number of the η-levels throughout the depth of the data available. In the budgets shown in this chapter a mass balance corrected [Q] is displayed. This is achieved by means of correcting [Q], as calculated from the radiative heating scheme, so that no net mass transfer occurs across a zonal material surface.

i.e.

$$\int \frac{([Q] - \frac{\partial \theta}{\partial t})}{[\theta]_\eta} c\,d\varphi = 0 \quad \text{where } [Q]=[Q]_{obs}-Q_e$$

s.t. $$Q_e = \frac{\int \frac{[Q]_{obs}}{[\theta]_\eta} c\,d\varphi}{\int \frac{c}{[\theta]_\eta} d\varphi}$$

and Q_e is assumed to be independent of φ. The magnitudes of Q_e for the various months are discussed later.

The total budget analysis for all months and levels is discussed by means of a small sample showing the momentum and heat budgets for December 1978, February 1979 and September 1979. Of these December is a poor case showing some of the problems encountered, while February and September are illustrative of better cases.

Subsequent to the budget analysis, chapter 6 continues with a discussion of various aspects important to the budgets, including gravity wave forcing which is not explicitly handled, and possible inaccuracies in the calculated eddy terms due to the use of the geostrophic velocity approximation used. Finally in section 6.4 some of the main non-circulation diagnostic results are described in order to try and assess the importance of the error due to the use of geostrophic winds and to provide further background information for the assessment of the wave forcing and circulations generated in this study.

6.1.1 : EULERIAN CANCELLATION

The Eulerian momentum and heat budgets based upon the quasi-geostrophic equations as described in chapter 4 can be written as:

$$[u_t] = f[v_i] - [c^2 v_n^* u_n^*]_y / c^2$$

(1) (2) (3)

(6.1)

$$[\theta_t] = -[v_i][\theta]_y - [w_i][\theta]_\eta + [Q]$$

(1) (2) (3) (4)

$$- ([v_n^* c\theta^*]_y)/c - (\varrho_o [w_i^* \theta^*])_\eta / \varrho_o)$$

(5)

(6.2)

These can be re-formulated into their TEM counterparts as below.

$$[u]_t = f[v]^R + ((cF^{\varphi})_{\varphi}/ac + (F^{\eta})_{\eta})/(ac\varrho_o)$$

(1) (2) (3)

where $F^{\varphi} = -a\varrho_o c[v^* u^*]$ & $F^{\eta} = a\varrho_o cf[v^* \theta^*]/[\theta]_{\eta}$

(6.3)

$$[\theta]_t = -[v]^R[\theta]_y - [w]^R[\theta]_{\eta} + [Q]$$

(1) (2) (3) (4)

$$-(\varrho_o([\theta]_y[v^* \theta^*]/[\theta]_{\eta} + [w^* \theta^*]))_{\eta}/\varrho_o$$

(5)

(6.4)

The circumstance of large cancellations in the Eulerian zonally averaged momentum and heat budgets highlights the difficulties which would arise when the eddy terms of such a formulation are parametrized as the eddy terms would be very critical in determining the calculated net modification of the zonal mean state. The TEM budget should reduce this problem by simplifying the eddy terms and removing a large portion of the eddy-mean cancellation. The analysis that follows is therefore aimed at examining the extent of this simplification throughout the year under various seasonal conditions and examining the interpretational value of the TEM terms compared with its traditional Eulerian counterpart.

Basically for most months both the momentum and thermodynamic budgets for the Eulerian and TEM differ only because of the magnitude of the cancellation of the mean and eddy advection. However the TEM momentum budget still retains a cancellation between D_F and $f[v]^R$ but both terms have been reduced in magnitude compared with their Eulerian counterparts. While in the TEM thermodynamic budget the relative importance of the various terms have changed considerably from that in the Eulerian thermodynamic budget. See figures F6.1 and F6.2. In all the Eulerian thermodynamic budget plots, the values of

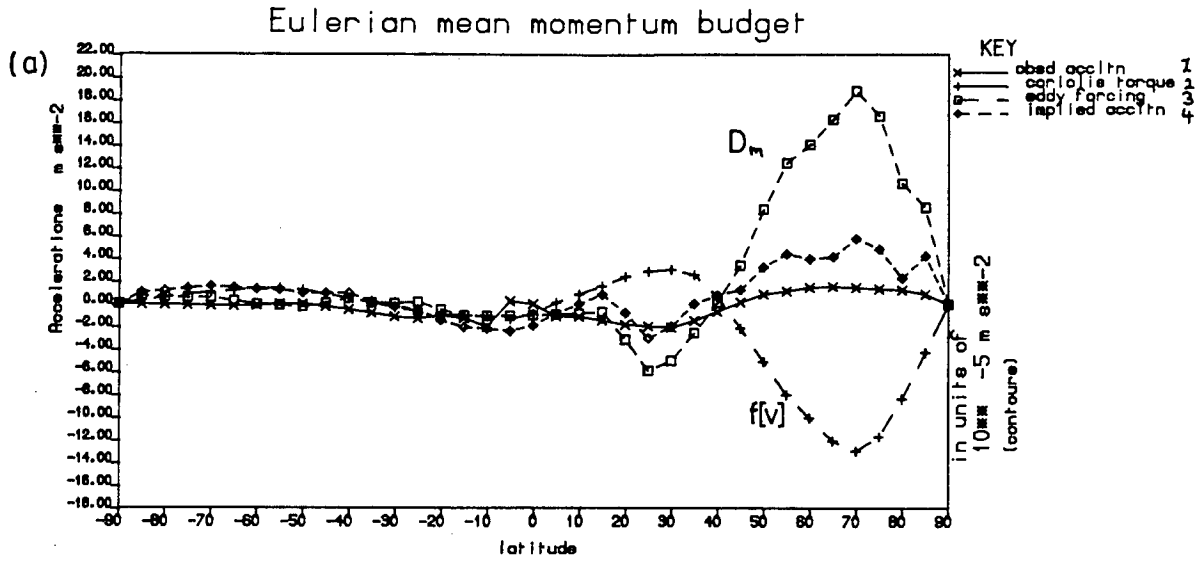

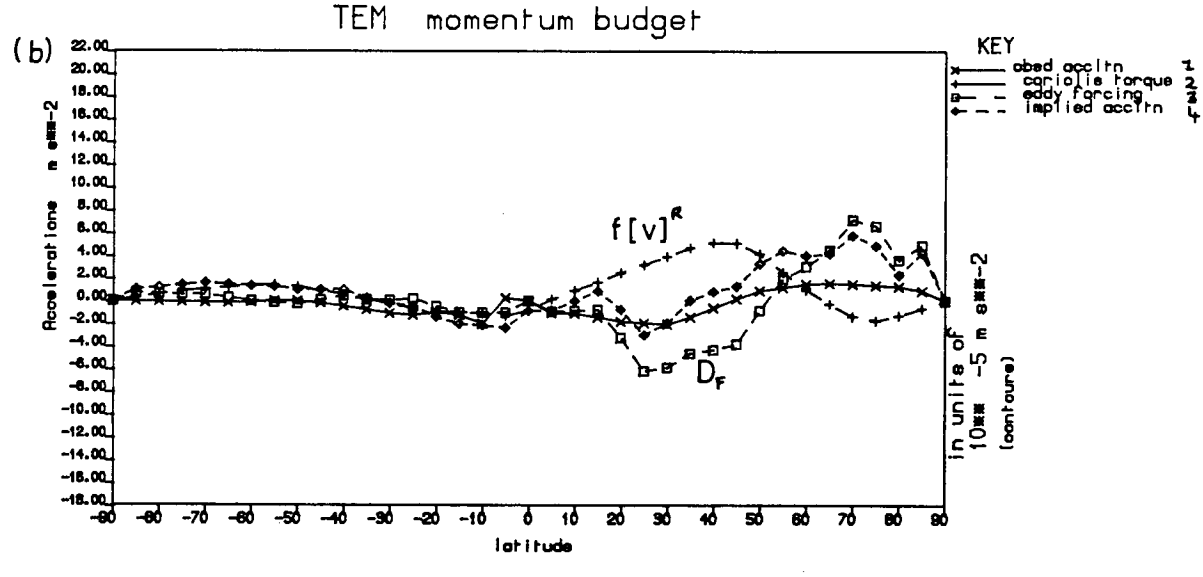

Figure F6.1 The momentum equations for; (a) the Traditional Eulerian & (b) the TEM formulations, for December 1978 at η=6, ($p \approx$ 2.5mb.) The momentum budget linegraph shows the terms from equations (6.1 & 6.3); (1) observed $[u]_t$, (2) f[v], (3) The momentum eddy term, and (4) = terms ((2)+(3)) the implied or budget calculated acceleration. Note [v] represents $[v]^R$ or [v] depending upon which formulation is displayed.

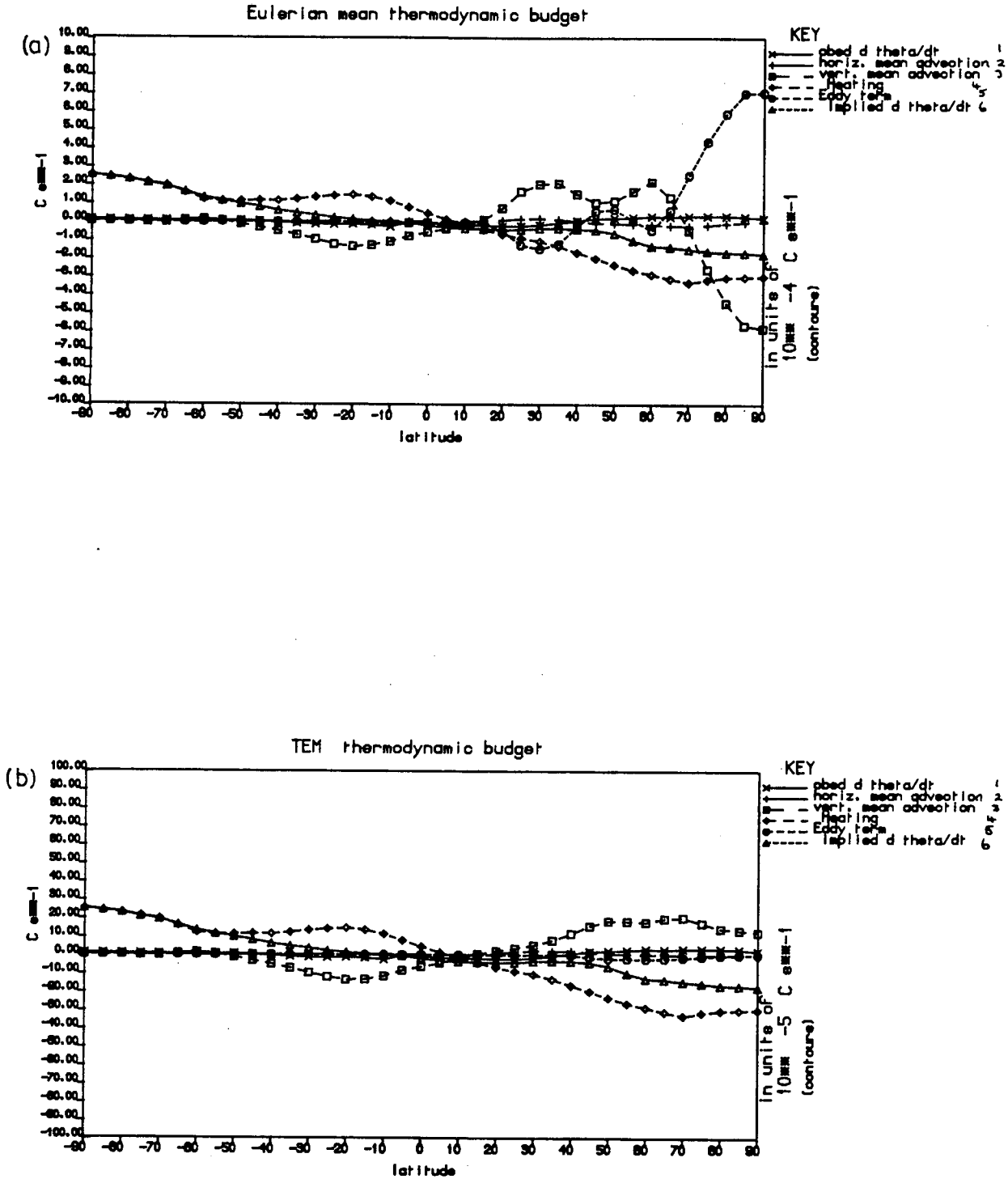

Figure F6.2 The thermodynamic equations for (a) the traditional Eulerian & (b) the TEM formulations, for December 1978 at η=6, (p≈ 2.5mb.) The thermodynamic budget linegraph shows the terms from equations (6.2 & 6.4); (1) the observed $[\theta_t]$, (2) $-[v][\theta]_y$, (3) $-[w][\theta]_\eta$, (4) [Q], (5) the thermodynamic eddy term, and (6) = terms ((2)+(3)+(4)+(5)) implied $[\theta]_t$, calculated from the budget. [v] and [w] are residual or Eulerian quantities depending upon which formulation is displayed.

the eddy forcing at the poles have been calculated by assuming $[v^* \theta^*]$ is anti-symmetric across the pole (along a great circle). For the TEM case the equivalent eddy term is zero at the pole.

In the TEM formulation the transport by steady conservative wave motions is removed and hence so is a large component of the Eulerian mean-eddy cancellation. Thus the actual acceleration tends to follow D_F more consistently than it follows the convergence of the eddy momentum flux but the forcing is redistributed by the forced residual circulation (Dunkerton et al 1981). In a TEM formulation the balance in the two-dimensional framework is therefore nolonger dominated by the eddy-mean cancellation compared with the traditional Eulerian formulation. Further examination of the magnitude and possible interpretation of the EP-flux divergence and its mass weighted equivalent forcing term, D_F, will be discussed in section (6.4.2).

During the months when the eddy driven component of the residual circulation is weak, see figures F5.12-F5.14, such as March, April and May the Eulerian formulation is seen from the budgets analysed to still retain a large cancellation between the mean and eddy components, resulting from the presence of wave activity which is close to non-acceleration conditions. The wave activity therefore produces only a small net effect on the zonal mean state but also drives a large Eulerian circulation component and eddy heat flux term, see figure F5.5b. These are predominantly in high latitudes and these are not present in the TEM formulation. Equatorward of 40^0 in May the TEM forcing term D_F is approximately equal to the eddy momentum convergence and so the residual is almost identical to the Eulerian circulation. At higher latitudes however the reversal of the sense of the circulation forced by the steady eddy forcing is not present and so the reversed circulation component or Eulerian Ferrel type cell of the residual circulation is not as large.

6.1.2 : THE NEGLECTED EDDY TERMS.

The analysis of the residual circulations shows that the eddy forcing terms are responsible for forcing a significant component of the circulation throughout a large period of the year. Therefore the non-zero eddy terms, in equations (6.3) & (6.4), responsible for this circulation component will require parameterization in a two-dimensional model, and will influence the tracer continuity equation directly, see equation (5.1). Both the TEM and traditional Eulerian formulations involve a 'Eulerian' cancellation between eddy and mean terms but the TEM provides a smaller and simpler description of the cancellation.

The reduction of D_F compared with its Eulerian counterpart, D_M, (See Andrews et al (1983), Palmer(1981a&b), O'Neill & Youngblut (1982) and Dunkerton et al (1981) for example) and hence the reduction in the cancellation between the Eulerian mean advection of momentum and the eddy momentum convergence is illustrated by figure F6.3. In high latitudes the extensive region of positive D_M has been reduced to a smaller region of D_F and in the upper stratosphere its sign has reversed to result in $D_F<0$. Only in the very high latitudes does any significant divergence occur and even here its magnitude is diminished compared with D_M. However the observations reveal that this reduction in the eddy forcing term is not universal and a balance between a residual coriolis torque and a significant D_F term remains in a number of months. In particular the difference between the monthly average values of D_F and the eddy momentum flux convergence is not considerable in high latitudes. However these estimates of D_F (and also D_M) may be subject to error introduced when calculating the eddy forcing terms from geostrophic winds (Robinson 1986). (See section 6.3). The reduction in magnitude of D_F compared with D_M (based upon geostrophic fluxes) is not sufficient to warrant the neglect of this eddy term as a forcing term of the residual circulation throughout the majority of months in the year of the study period. The above implies that the breakdown of non-acceleration is important in producing non-zero D_F and consequently driving a component of the residual circulation, as shown by (Holton (1981), Andrews et al (1983) and Dunkerton et al (1981)).

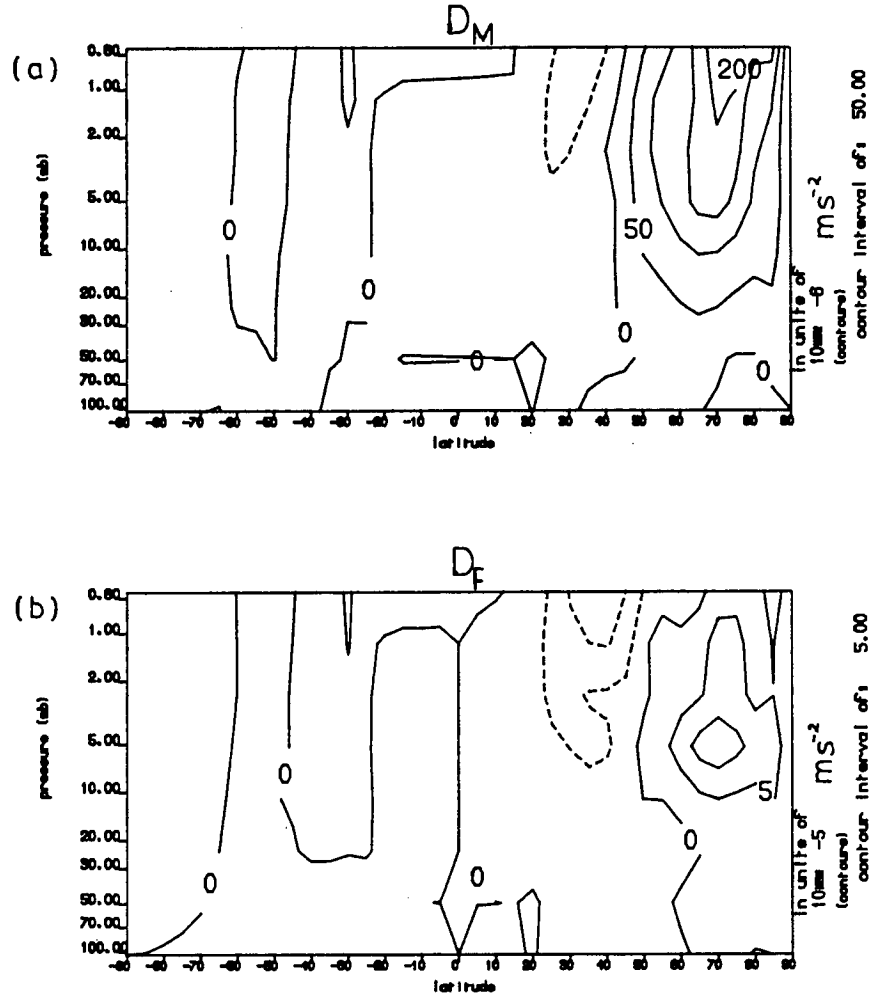

Figure F6.3 A Comparison of the right hand side eddy terms in the momentum equations (a) D_M & (b) D_F, from the Eulerian and TEM formulations respectively for December 1978.

In the TEM thermodynamic equation the eddy heat transport term as formulated and used in this thesis does not completely vanish, see appendix A and equation (6.4) above. The second right hand side term in equation (4.16) occurs as a result of the inclusion of term (5) of equation (6.4). This term is observed in the TEM budget for the majority of months used with a magnitude of $\approx$ <0.1 to 0.6° C/day. In all months except October and March it was positive reaching a maximum of typically $\approx$ 0.4° C/day at 45-65° in the winter hemisphere (the eddy active hemisphere). This striking difference between the equations is illustrated in Figures F6.2a & F6.2b, the thermodynamic budgets for p$\approx$ 2.5mbar for the month of December 1978. It is clear that from the traditional viewpoint the heat budget is principally a balance between the meridional vertical flux convergence and eddy flux convergence both with terms of the order of $\approx$ 7° C/day in high latitudes. This relegates [Q] to a less significant role. However in the TEM budget the eddy heat term has been reduced to a maximum usually in middle latitudes of $\approx$ 0.4° C/day and it is now clear that the vertical flux due to the mean vertical advection is basically in balance with the diabatic heating though this does not imply that the vertical velocity is totally driven by [Q].

In order to assess the relative importance of the separate effect of the heat flux forcing in equation (4.16), a separation of the forcing by div.$\underline{F}$, (term a) and the remaining thermodynamic term, (term b), in equation (4.16) was undertaken. Circulations were obtained from using various forcing contributions in equation (4.16) and these will be discussed below to examine in particular how large a circulation component the thermodynamic eddy terms induce.

To illustrate the affect of the TEM re-formulation upon the thermodynamic forcing term and hence the circulation it drives, consider equation (6.5) below.

$$-\frac{1}{c}\frac{\partial}{\partial y}\left([cv^{*}\theta^{*}]\right) + \left(\frac{[\theta]}{c}\eta\frac{\partial}{\partial y}\left(\frac{c[v^{*}\theta^{*}]}{[\theta]_{\eta}}\right)\right)$$

(B) (C)

$$-\frac{[\theta]}{\varrho_{o}}y\frac{\partial}{\partial\eta}\left(\varrho_{o}\frac{[v^{*}\theta^{*}]}{[\theta]_{\eta}}\right)\Big)$$

(D)

$$= -\frac{1}{\varrho}\frac{\partial}{\partial\eta}\left(\frac{\varrho[\theta]}{[\theta]}y\frac{[v^{*}\theta^{*}]}{\eta}\right)$$

(A)

(6.5)

Equation (6.5) shows a sub-division of the thermodynamic forcing term (b) in equation (4.16). The last term, term A, is the eddy term on the right hand side of equation (6.4). This is obtained from the sum of the Eulerian term, term B above or the eddy term in equation (6.2), and terms C and D. Terms C and D arise in equation (6.4) through the residual circulation's definition. Namely these terms arise in the TEM re-formulation when $[v]^{R}$ & $[w]^{R}$ are substituted into equation (6.2). Each of these terms A, B and (C+D) has been used to calculate a separate residual circulation component and these are illustrated in Figure F6.4. This was undertaken to illustrate the circulations driven by the traditional Eulerian eddy term, term B, a compensatory heat flux term introduced by the residual circulation's definition, terms C & D, and the net transport circulation of the two combined. These circulations are: an Eulerian Ferrel cell; an opposing residual circulation component; and the combined circulation component, forced by term A. By this means it is possible to illustrate the major reason for the Eulerian cancellation, namely the eddy heat flux caused by the waves which drives a component of the meridional circulation shown in figure F6.4a. When using the residual circulation, terms C & D are introduced and drive a component in the opposite sense, see figure F6.4b, thus removing a part of the 'wave' driven component of the meridional circulation. The addition of these two circulations

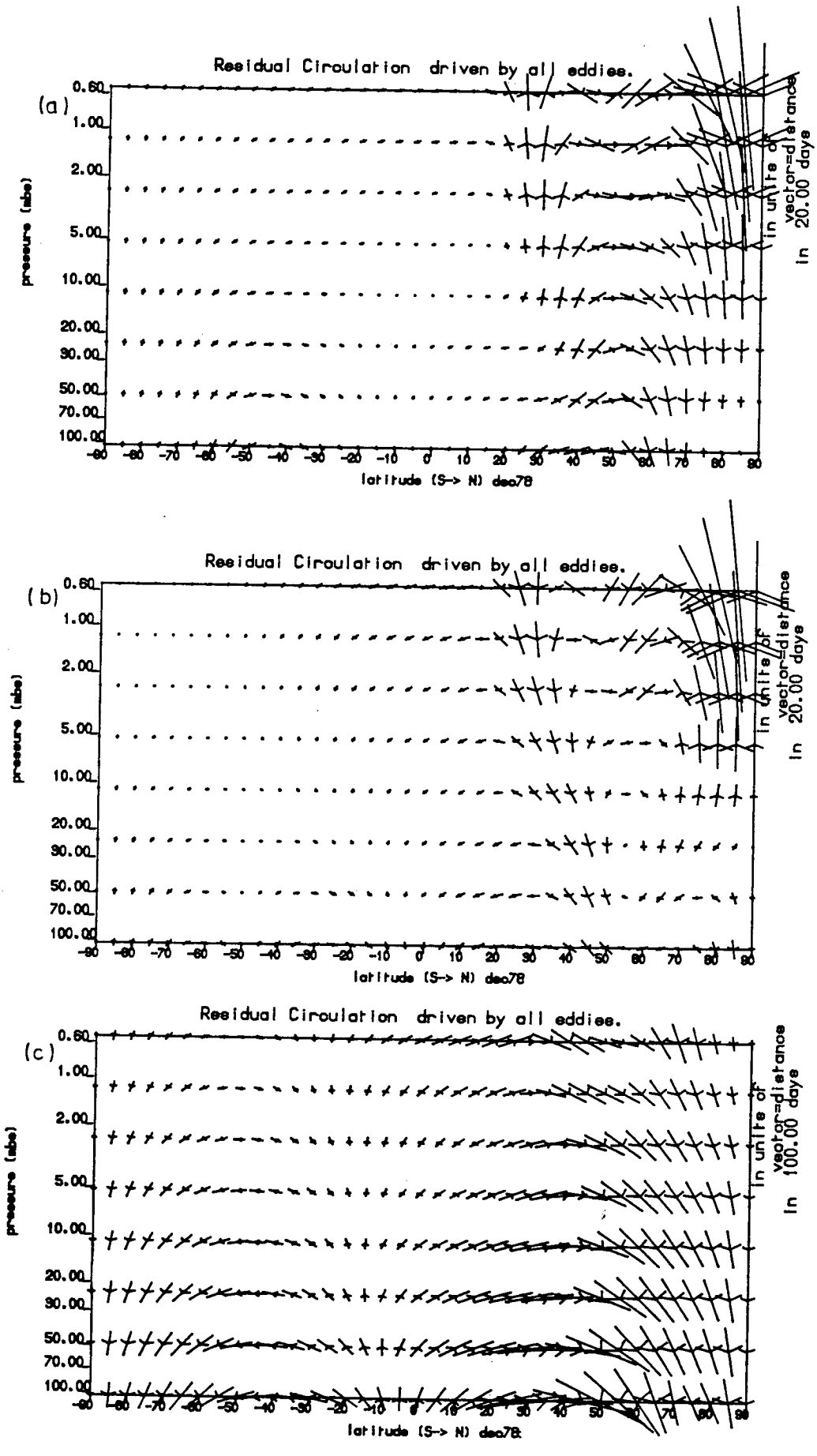

Figure F6.4 The residual circulations, for December 1978, driven by the components of the TEM thermodynamic eddy term; (a) component driven by TEM reformulated extra heat flux term, (b) component driven by the Eulerian thermodynamic heat flux term, & (c) the circulation driven by the sum of (a) and (b), the net thermodynamic eddy forcing of the residual circulation.

shows a large fraction of the Eulerian cancellation has been removed, resulting in a much reduced circulation directly forced by the thermodynamic eddy heat flux terms, see figure F6.4c, which arise in equation (4.16) from equation (6.4). It is clear that this term will not play a major role in determining the residual circulation even in active eddy winter months.

6.1.3 : THE TEM MOMENTUM AND THERMODYNAMIC BUDGET EQUATIONS.

6.1.3.1 : INTRODUCTION.

The momentum budgets analysed, samples of which will be shown later, although disappointing in their lack of consistent balance do show certain interesting features. For the months such as December, January, July and February where indirect cells were deduced in the residual circulation and were important circulation components, the budgets were poorly balanced in the regions of circulation reversal. This could imply that these large scale circulation components may not be fully realistic or that they may be over-estimated or that the eddy flux divergences evaluated forcing them are in error. From the momentum budgets it is seen that the high latitudes do exhibit acceleration as implied by $[u_g]_t$ (hereafter referred to as $[u]_t$), see figure F6.5 for example. But what is clear then is that the positive divergence close to the pole appears to be possibly exaggerated while the convergence in mid-latitudes appears to be in good agreement.

Only in the months such as September, October and for the upper stratosphere in February, where the eddy flow is strong but not indirect, do the momentum and thermodynamic budgets produce a better balance between the advection by the mean circulation and the momentum and heat transports. The month of September appears to be one month which can be described as a 'good' month in terms of well balanced momentum and heat budgets though the southern hemisphere acceleration deduced from the momentum budget is far too noisy compared with the actual $[u]_t$. It is interesting to note that this month requires for its consistency the enhancement of its diabatically driven circulation by an eddy driven residual circulation component directed into the lower atmosphere of the polar northern hemisphere, see figures F6.6 & F6.7. Also in months such as February,

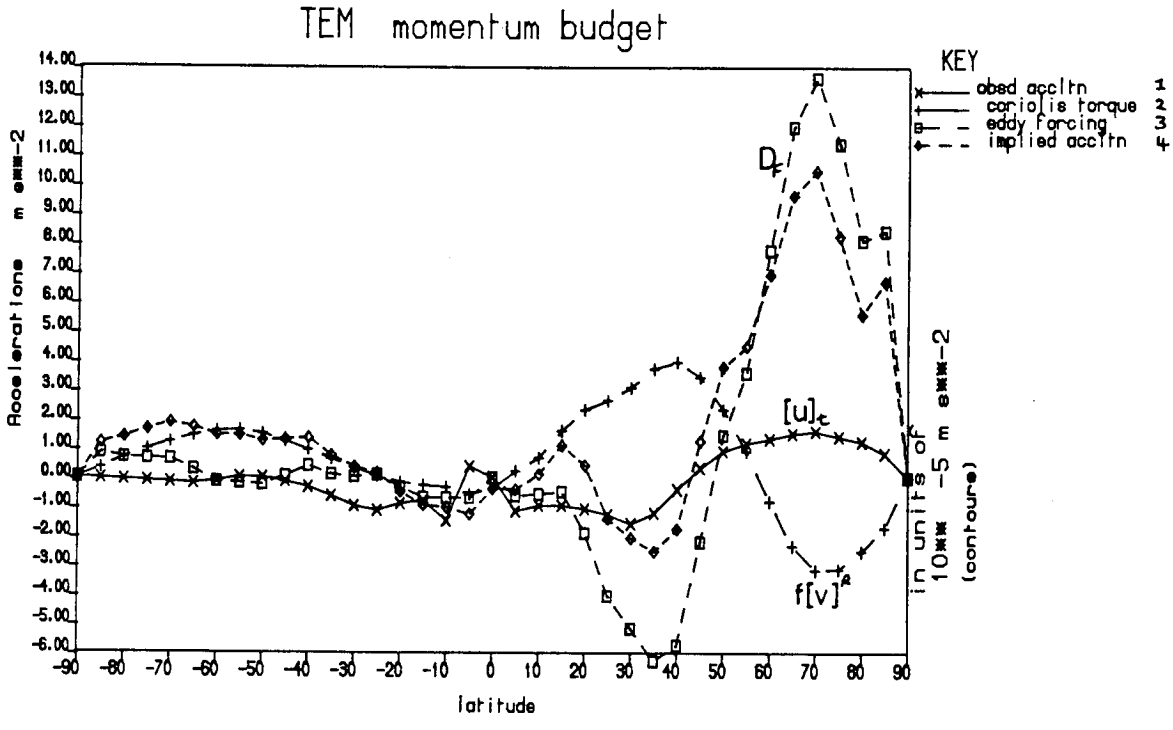

Figure F6.5 The TEM momentum budget terms for December 1978 at η=5.25, (p≈ 5 mb.) Linegraph key as Figure F6.1

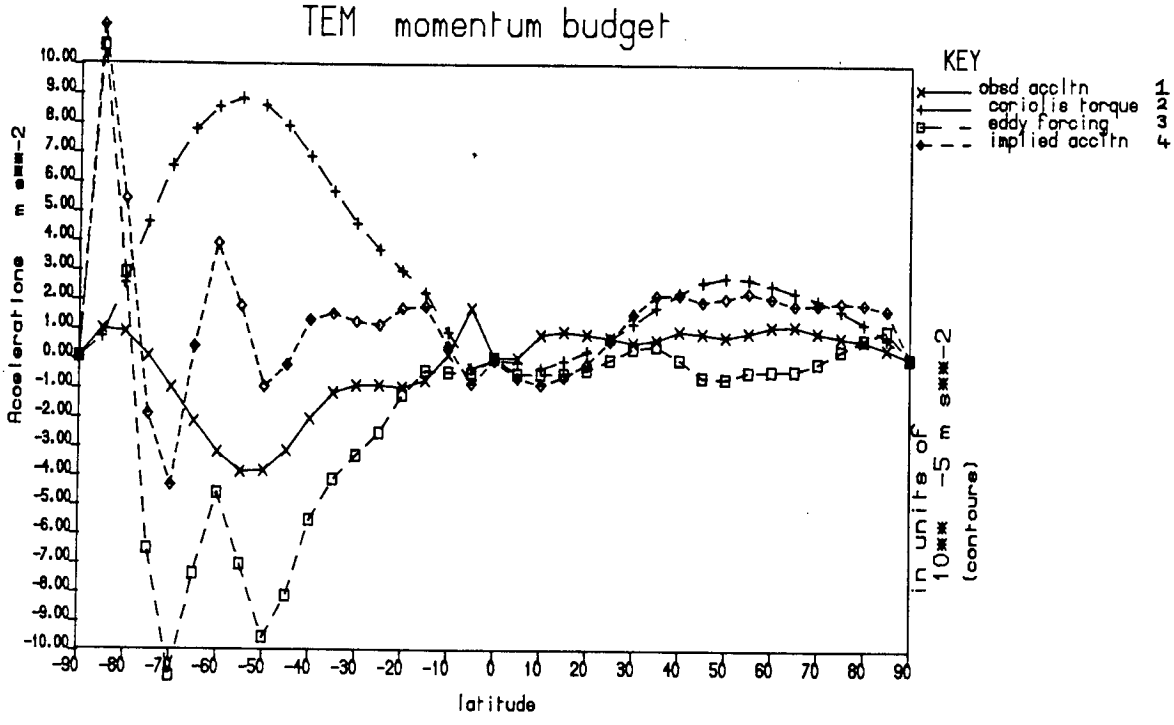

Figure F6.6 The TEM momentum budget terms for September 1979 at η=6, (p≈ 2.5 mb.) Linegraph key as Figure F6.1

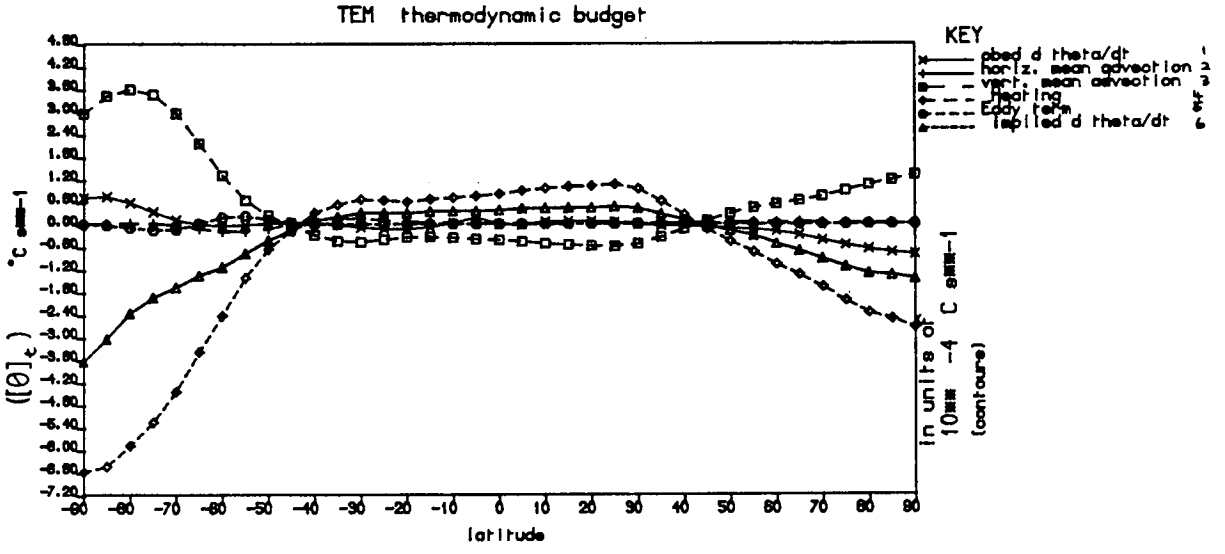

Figure F6.7 The TEM thermodynamic budget for February 1979 at η=6,(p≈ 2.5mb) Linegraph key as Figure F6.2

October and December, in regions where the high latitude divergence is not so important, better balances of heat and momentum occur in the northern hemisphere, see figures F6.8 & F6.9.

The analysis of the northern hemisphere February quasi-geostrophic momentum budget at p≈ 2.5mbar provides one of the best cases where the difference between the implied acceleration and $[u]_t$ observed was low. At this level the diabatically driven flow is enhanced by an eddy flow descending over the north pole from the upper atmosphere and mid-latitudes. A smoother eddy forcing in latitudes >60°N would give rise to a very close momentum balance and the sign of the acceleration implied by the full TEM terms follows the observed acceleration very closely although the magnitude is exaggerated. However at lower levels in the atmosphere the degree of the imbalance between the implied acceleration and $[u]_t$ observed increases. This improvement in balance with height is seen in several months although the exaggeration of the acceleration implied by the momentum budget still occurs at ≈>50°N and in some cases exaggeration of the implied deceleration is also seen in middle latitudes.

Lower in the stratosphere, below p≈ 24mbar, the budgets show a large coriolis torque due to the strong poleward cells basically driven by transient eddies at these levels. These torque values produce large imbalances in the momentum budgets at these levels. However the $[w]^R$ required at these levels to balance the thermal budgets are insufficient especially if $[w]^R$ decreases toward the pole due to the effects of high latitude divergence of the EP-flux. The use of the Dunkerton diabatic circulation in the budget analysis also prove inadequate at these levels. However the Dunkerton circulation is far weaker in magnitude at this level and therefore produces a smaller coriolis torque and hence a smaller difference between the implied and observed accelerations. The reason for the imbalance, arising due to the large transient eddy driven circulation component in the upper troposphere and lower stratosphere in the fully-forced residual circulations, is not clear though it appears that the tropospheric representation is possibly poor and in error.

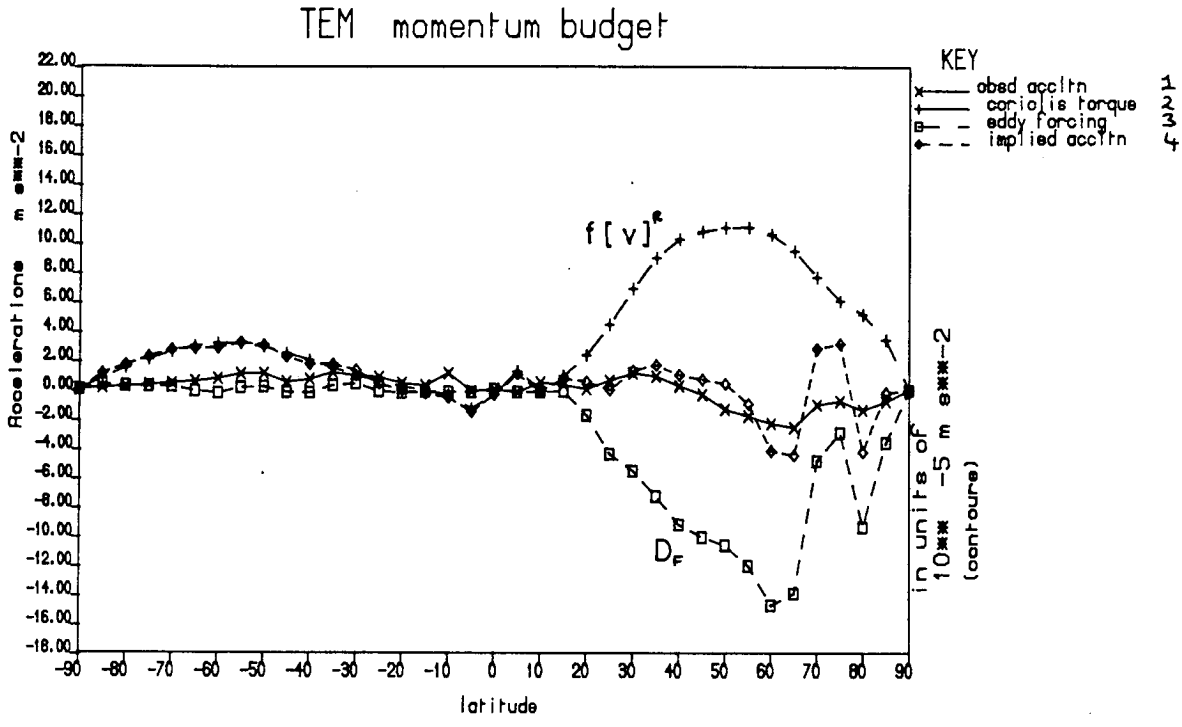

Figure F6.8 The TEM momentum budget terms for February 1979 at η=6, (p≈ 2.5mb.) linegraph key as Figure F6.1

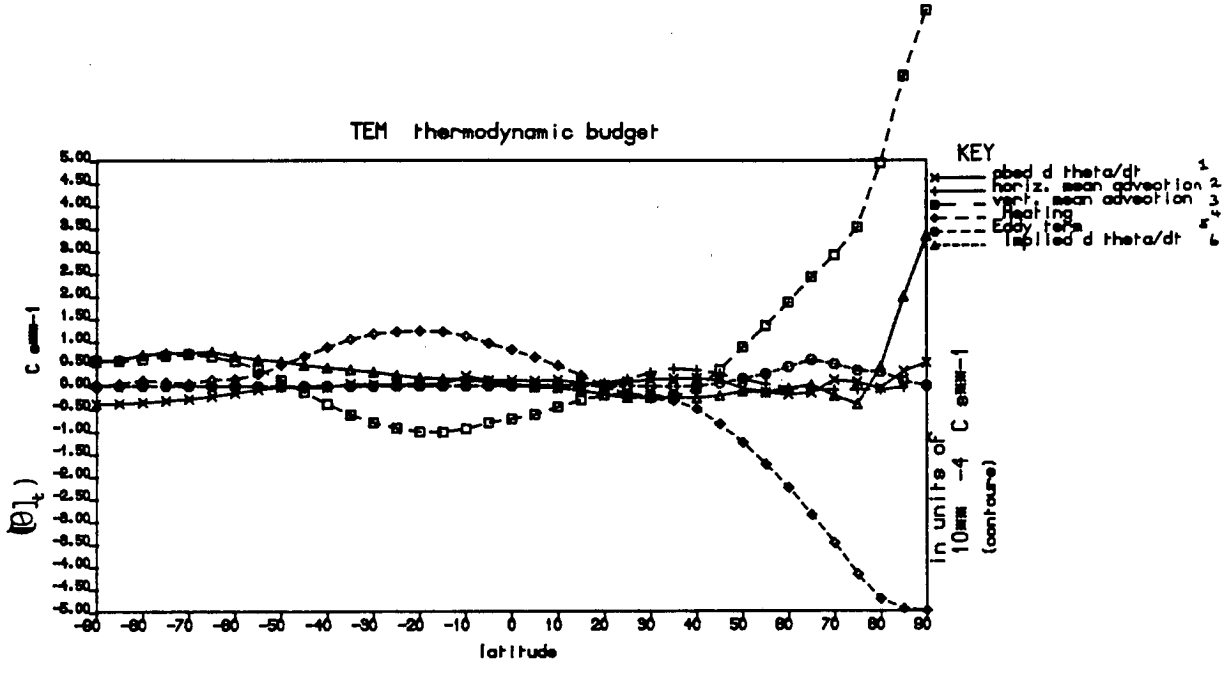

Figure F6.9 The TEM thermodynamic budget for February 1979 at η=6,(p≈ 2.5mb) Linegraph key as Figure F6.2

6.1.3.2 : A COMPARISON OF THE TEM AND DUNKERTON DIABATIC MOMENTUM AND HEAT BUDGETS.

Figures F6.8, F6.9, F6.10 & F6.11 show the TEM thermodynamic and momentum budgets for February using the fully forced residual circulation, the diabatically driven component of the residual circulation and a Dunkerton circulation at ≈ 42km, ≈p=2.5mbar. In the full residual case, in the northern hemisphere, except near the pole, the predicted and actual potential temperature change differs by only ≈ $<1.6^{\circ}$ C/day. Of the three, the fully-forced residual vertical advection shows a good cancellation between the vertical advection and the diabatic heating terms and so appears to satisfy the thermodynamic budget well. However the Dunkerton velocity, $[w]^{D}$, results in a smaller error between implied and actual net heating, $[\theta]_{t}$, but this is a trivial case as this balance is to be expected due to the nature of the definition the Diabatic circulation.

The diabatically driven residual circulation component, as seen in Figure F6.10a, is inadequate to fully balance the radiative cooling in the polar night and throughout high latitudes. An extra enhancement of the diabatically driven vertical component of the residual circulation is necessary above that forced by the the zonal mean diabatic forcing and this is apparently provided by the eddy forcing, D_{F}, due to the breakdown of non-acceleration conditions. The diabatically driven residual circulation case illustrated should not be considered in the same sense as the 'fully-forced' and Dunkerton budget cases, as this case is not a complete picture but it is used here to illustrate the error of misinterpreting the diabatically driven residual circulation as a 'Diabatic circulation' and also shows by comparison with the fully-forced budget figures, F6.7 & F6.8, that the eddy components to the various thermodynamic terms are important.

The Dunkerton vertical component is clearly as good, the net global cooling arising due to the readjustment necessary to $[w]^{D}$ to ensure continuity of mass across a log-pressure surface and because of the variation in $[\theta_{\eta}]$ with latitude. The Dunkerton circulation was calculated from a knowledge of [Q] and $[\theta]_{\eta}$ alone and does not include $[\theta]_{t}$ which may have improved the thermodynamic balance for

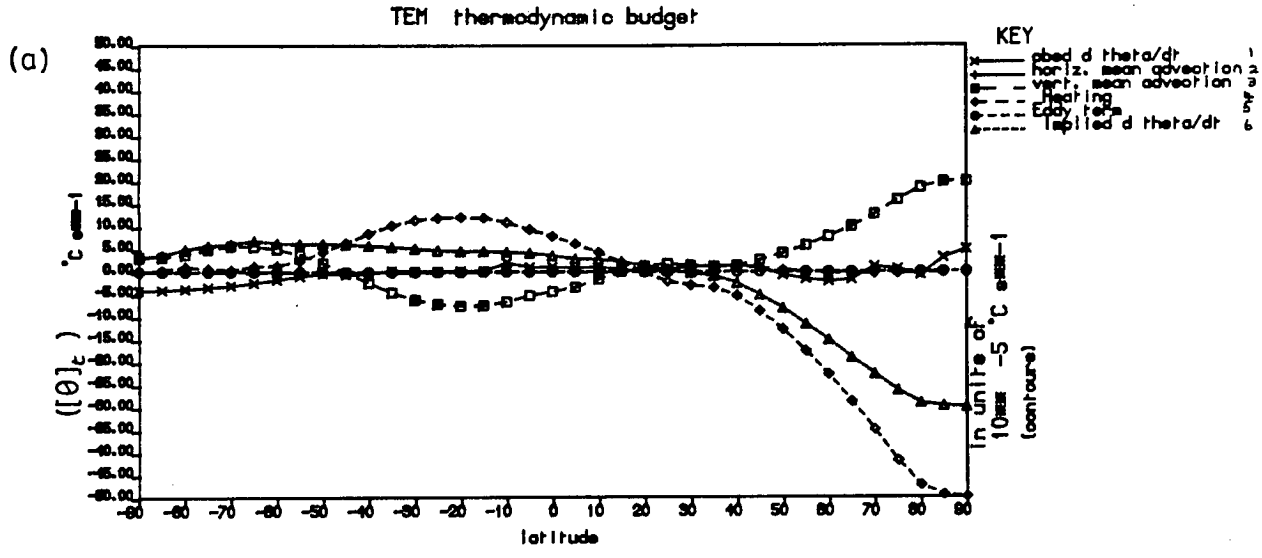

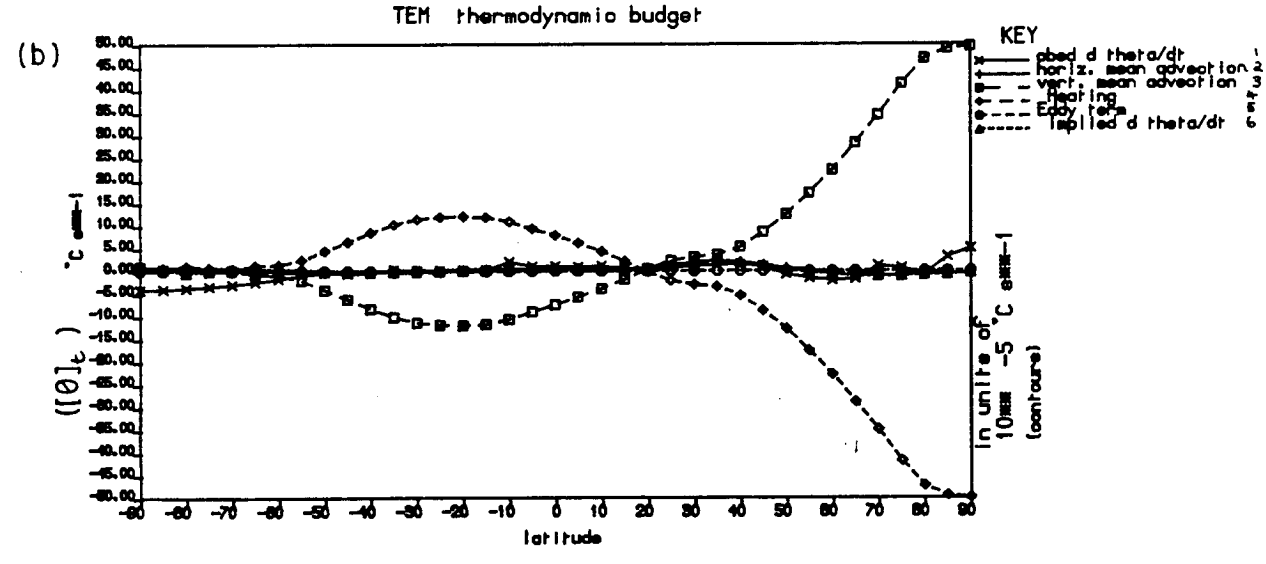

Figure F6.10 The TEM thermodynamic budget terms for February 1979 at η=6, (p≈ 2.5 mb.) using as $[v]^R$ & $[w]^R$; (a) The diabatically driven component of the residual circulation & (b) the 'Dunkerton-diabatic' circulation. Linegraph key as Figure F6.2

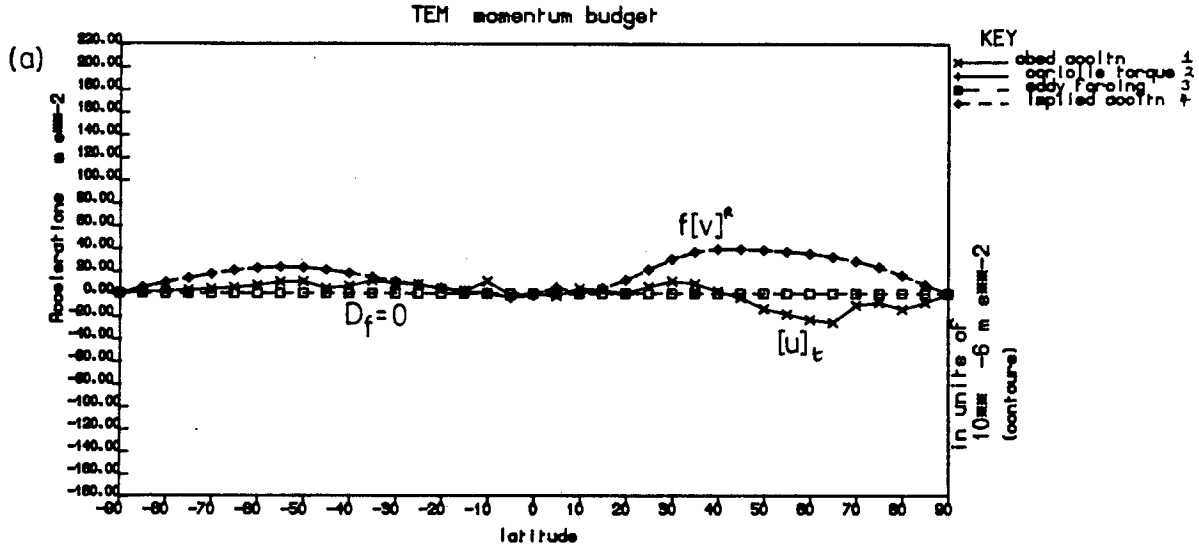

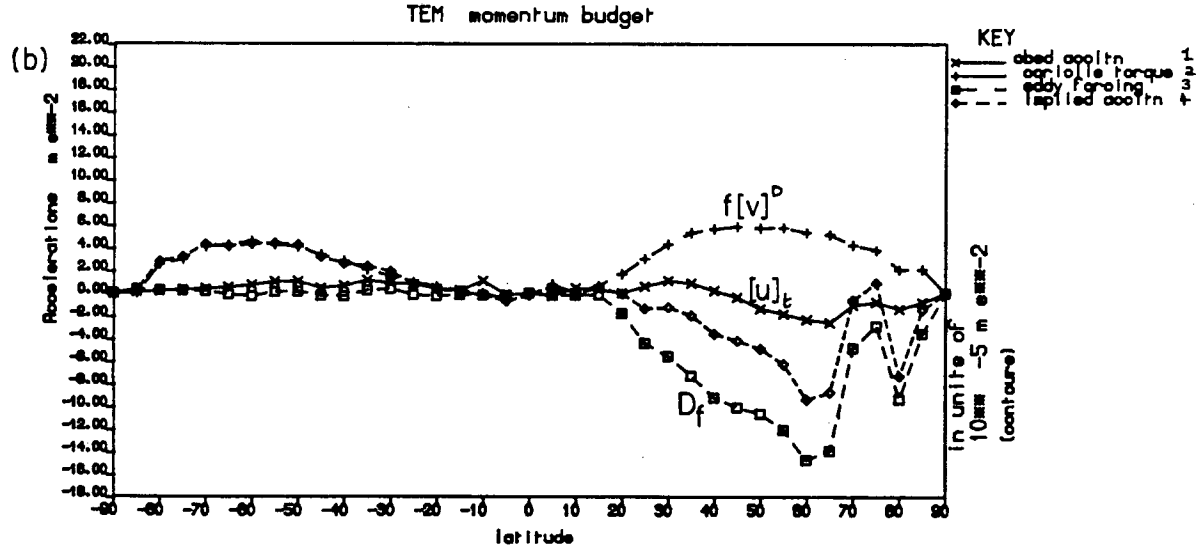

Figure F6.11 The TEM momentum budget for the same occasion as figure F6.10. Linegraph key as Figure F6.1

this circulation so non-zero heating and cooling could have been identified by the Dunkerton based thermodynamic budget. Thus the thermodynamic budget using the Dunkerton flow is a good approximation showing the approximate validity of the near Lagrangian flow assumed. The Dunkerton momentum balance is an interesting comparison as $[v]^D$ and $[w]^D$ do not "know" of the influence of D_F except through the indirect affect of D_F on the mean state via [Q]. However the balance shown in Figure F6.11b shows that in comparison with the fully forced case, (figure F6.8), the Dunkerton momentum balance gives a poorer description of the observed $[u]_t$ in the northern hemisphere, with both failing in the southern hemisphere. The February case illustrates one of the better cases for the residual circulation in describing the observed zonal velocity changes.

6.1.3.3 : THE SUMMER HEMISPHERE BUDGETS.

In most months examined the momentum budget of the quiet hemisphere without significant eddy activity does not achieve a balance due in part to the coriolis torque of the poleward diabatic circulations driven by cooling in both hemispheres throughout a large part of the lower and middle stratosphere, (contrasting with the single pole to pole cell which occurs only in the high upper stratosphere). Without the eddy activity there is no decelerative mechanism (observed or calculated in the present study) to prevent the diabatic circulation from modifying the heat and momentum balances. This decelerative mechanism could be occuring due to the role of breaking gravity waves in producing a source of wave drag or possibly in combination with horizontal fluxes unresolved by the present study.

Of the 'quiet' months identified in chapter 5 it was expected that the thermodynamic balances should be close to a balance because of the absence of eddy activity. In the three months of April, May and June however the balances achieved are poor. In June the eddy activity although still weak over-estimates the acceleration, while the diabatic flow near both poles is very large and possibly in error resulting in excessive cooling and warming. Both April and May are similar producing imbalances of the order of $2.10^{-5}\,ms^{-2}$ & $3\,^{\circ}C$/day at $\approx p = 2.5$ mbar.

6.1.3.4 : A DIABATIC HEATING RATE CORRECTION.

In a large number of the monthly thermodynamic balances examined there was seen to be a consistent error of $\approx 1^{\circ}$C/day when the basic [Q] calculated was used in the budget instead of the mass balance corrected version of [Q] as discussed earlier in this chapter. Most months generally exhibit a difference which is approximately constant with latitude at all latitudes except in the winter eddy active regions i.e. greater than 40-60°N. This was mostly removed by means of calculating Q_e and subtracting it from the basic [Q] calculated from the radiative scheme as described earlier, however for the purpose of solving for the residual circulation a constant [Q] error will not be important, as it is the horizontal gradient of $[Q]_\lambda$ which appears in equation (3.16). In the summer hemisphere, and close to both poles in particular, the vertical advection by the flow and [Q] are the major terms which lead to large imbalances in the thermodynamic equation if an implied $[\theta_t]$ is compared with the observed value of $[\theta_t]$. In the summer hemisphere it is particulary noticeable that the single-cell component of the circulation transfers insufficient heat from summer to winter pole to maintain a balance. The velocity components, $[w]^R$ & $[v]^R$, driven by the diabatic forcing, [Q], and weak planetary wave forcing of this region, are not sufficient to balance the heat budgets. Also noticeable is that at both poles the tendency for $[w]^R$ to decrease, as the eddy forcing vanishes and $\partial/\partial y([Q])$ tends to zero, produces large imbalances in the thermodynamic budgets. Part of the imbalance in the thermodynamic equation may be caused by the uncertainties involved in the calculation of the diabatic heating rates. (See section 4.3.6.8) Due to the closeness of the middle-lower stratosphere to radiative equilibrium, and so the small values of [Q] in this region, these sources of error are likely to introduce relatively important consequences and possibly a change in sign of [Q] at these lower levels. As [Q] is small, so is Ψ, and so the relative percentage error is larger in this region. These discrepancies therefore remain a major problem in this study.

6.1.3.5 :EDDY DRIVEN EFFECTS.

In a number of months where a large eddy driven component of the residual circulation exhibits a flow descending into the polar stratosphere, there also occurs a region of divergent EP-flux near the pole, which reduces $[w]^R$ in magnitude and sometimes reverses the sign if large enough. These situations result in a diminution of the implied adiabatic warming to the point where it cannot balance the diabatic cooling in the thermodynamic budget. For instance in December, see figure F6.2b, there is evidence of weak net heating, which must be produced by the net warming effect of the atmospheric mechanisms in this region. This situation could arise either by the vertical mean advection of heat exceeding the diabatic cooling or the existence of some other warming mechanism adding the extra heat to produce the observed warming which cannot be explained by the vertical advection as calculated in this case. This could indicate that the reversal or reduction in $[w]^R$ near the pole is incorrect, resulting from a possibly exaggerated divergent forcing near the pole. The diabatically driven component of the residual circulation is even more inadequate in acting in this role of balancing the diabatic cooling. Thus the budget implies cooling and does not account for the observed net heating. So an eddy forced component seems to be necessary but strong reversed cells near the pole do not provide the necessary thermodynamic balance observed.

Another interesting flow feature is the existence of the lower stratospheric cells from the equator to both poles which are illustrated in figures F5.1-F5.4. These are driven by both the transient and stationary fluxes but transience appears to be the most important driving mechanism. The momentum torque of these cells dominates the other terms in the momentum budgets producing a large acceleration which is not seen in the observed $[u]_t$. The vertical velocities of this transient circulation component do not produce the same relative imbalances in the thermodynamic budget, infact they appear as a necessary enhancement of the adiabatic cooling resulting from the other circulation components in the thermodynamic budgets. The budgets at these levels contain a major component due to the presence of the lower stratospheric transient circulation and the

contributions are particularly large in the winter hemisphere. The transient circulation contributes significantly to the vertical advection producing a large implied $[\theta]_t$ or anomaly in the thermodynamic budget. The $[\theta]_t$ observed for this level does not reach the same magnitudes as predicted by the implied $[\theta]_t$. The existence of such cells, but reduced in magnitude, is possible because of the agreement in terms of the sign of acceleration. The existence of some extra circulation component appears to be necessary, since the diabatically driven component of the residual circulation if used alone in the budgets produces an implied acceleration which nolonger (compared with the budget including the transient circulation component) agrees in sign with that observed, though the error in magnitude drops. Getting the magnitude of the lower stratospheric circulation component right is made more difficult because of the interaction of tropospheric cyclonic and anti-cyclonic activity complicating the fluxes in this region.

6.1.3.6 : SUMMARY.

From the above analyses of the momentum and heat transports, evidence was found to support the existence of the large eddy driven flows during the months of February and September for instance. However at levels and for months where the reversed 'indirect cells' occur, the evidence is contrary to their existence because of the imbalance implied. Since these features are direct consequences of strong regions of positive EP-flux divergence this may lend support to the hypothesis that such features obtained using the quasi-geostrophic approximation to div.F (i.e. using geostrophic velocities to evaluate $u_g v_g$ and $v_g \theta$, plus the neglect of all 'smaller' terms in its definition) are over-estimated and therefore erroneous. It is necessary therefore to assess each month which exhibits EP-flux divergent regions and determine if the divergence is totally spurious, an over-estimate or a real estimate in magnitude and sign.

The problem highlighted by these features and the imbalances in the budget results is the existence of uncertainties and errors in the derived diagnostics and in the source data fields. It introduces uncertainty into all the diagnostics and so the trustworthiness of all the diagnostics are brought into question. However this problem due to data errors in the basic data sources and the subsequent methods

of calculation will occur in all studies and so other studies must suffer from similar uncertainties.

6.2 : GRAVITY WAVE FORCING.

A major part of this thesis has centered around the problem of examining the mechanisms by which the zonal wind is decelerated to the observed values away from radiative equilibrium conditions, as discussed in Brasseur & Solomon (1984). It is div.F which must principally provide the necessary momentum balance to prevent the coriolis torque from accelerating the winds. It is argued that the strength of the mean meridional circulation in a rotating frame of reference such as the earth depends crucially on the ability of the transient, dissipating eddies as a momentum sink (or source) to balance the coriolis torque ($f[v]^R$) produced when the parcels move in the meridional direction. The balance is achieved by a wave momentum deposition or 'wave-drag' through a probable combination of mechanisms on both planetary and gravity wave scales in collaboration. More recently interest has been generated in the examination of the influence of gravity wave propagation and the effect of their breaking in the middle atmosphere.

In the upper stratosphere and mesosphere the atmospheric momentum balance appears to include a source of wave drag additional to that provided by the planetary waves which balances the coriolis torque, resulting from the meridional circulation. The physical mechanism for this strong damping is thought to be the turbulent breakdown of gravity waves near the mesopause (McIntyre 1987), generating a wave drag and so decelerating the mean wind. The total wave drag which includes both gravity wave drag and planetary wave drag, is sometimes crudely parametrized by Rayleigh friction. Only in the mesosphere however is the magnitude used of this wave drag large as it is only here that a mechanism such as simulated by this form of drag appears to be necessary so that the observed zonally averaged distributions of wind and temperature are produced in the models at significantly different values from radiative equilibrium. Except at the tropical tropopause and in the polar night, the stratosphere may be considered to be in approximate radiative equilibrium while the mesosphere is very different from radiative equilibrium conditions.

In order to crudely test the possibility of the gravity-wave contribution being the primary missing effect required to balance the momentum deficits, a further circulation test was undertaken. In this the gravity wave drag was parametrized as a Rayleigh friction and the corresponding streamfunction found. This parametrization was based upon the form described in Holton & Wehrbein (1980). The component circulation driven by this extra forcing only is shown in figure F6.12, while the addition of this forcing to the 'fully-forced' momentum and thermodynamic balances are illustrated in Figures F6.13 a&b. As is to be expected from the functional form, which gives greatest drag at large z, the only major circulation components produced were high in the mesosphere, above the region of interest. However throughout the stratosphere the wave drag drove a single-cell flow from the summer to the winter hemisphere. The horizontal velocities were generally weak and $\approx<0.1$ of the residual velocity components as described in chapter 5 except in the upper stratosphere where both $[v]_F^R$ and $[w]_F^R$, the horizontal and meridional residual velocity components forced by the parametrized gravity-wave drag, were of equal order of magnitude with the total residual velocities calculated. The effect upon the momentum budgets in the middle and lower stratosphere was on the whole small as only a small net improvement between $[u_t]$ and the implied acceleration was achieved as the extra coriolis torque and gravity wave momentum deposition are in opposition. Qualitatively however the Rayleigh friction or gravity-wave drag driven component of the residual circulation has the required single-cell branch structure of flow and the larger vertical velocities producing larger ascent over the summer pole and descent over the winter pole. These two features thus result in a reduction of the summer hemisphere positive coriolis torque and an enhancement of the vertical mean advection of heat from the heating region to the cooling, which none of the residual circulations of chapter 5 were capable of doing. In the summer hemisphere in the high latitudes, the flow toward the south pole was diminished due to a flow of the opposite sense driven by the Rayleigh friction representation of the gravity wave drag. However the reduction in the implied positive anomalous acceleration, which was seen in the momentum balance in the northern hemisphere,did not occur so significantly in the momentum balance of the southern hemisphere despite the fact that the coriolis torque was reduced by the extra

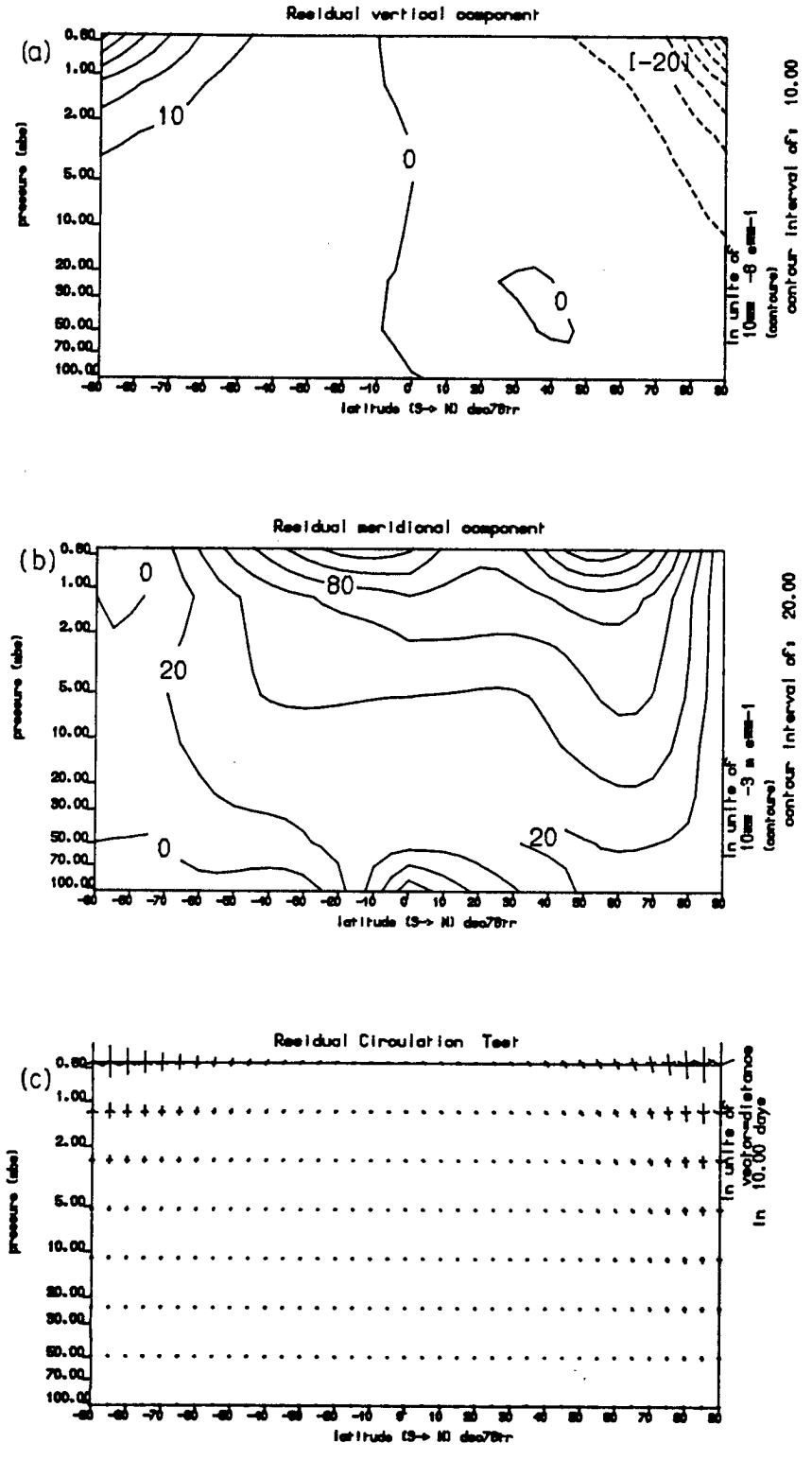

Figure F6.12 The component Residual circulation for December 1978 forced only by a parameterised Rayleigh Friction term. Its velocity components, (a) $[w]^R$ in s^{-1}, (b) $[v]^R$ in ms^{-1} and the circulation, where the vectors are velocity and represent the distance travelled by an air parcel in 10 days. (dashed lines are negative values.)

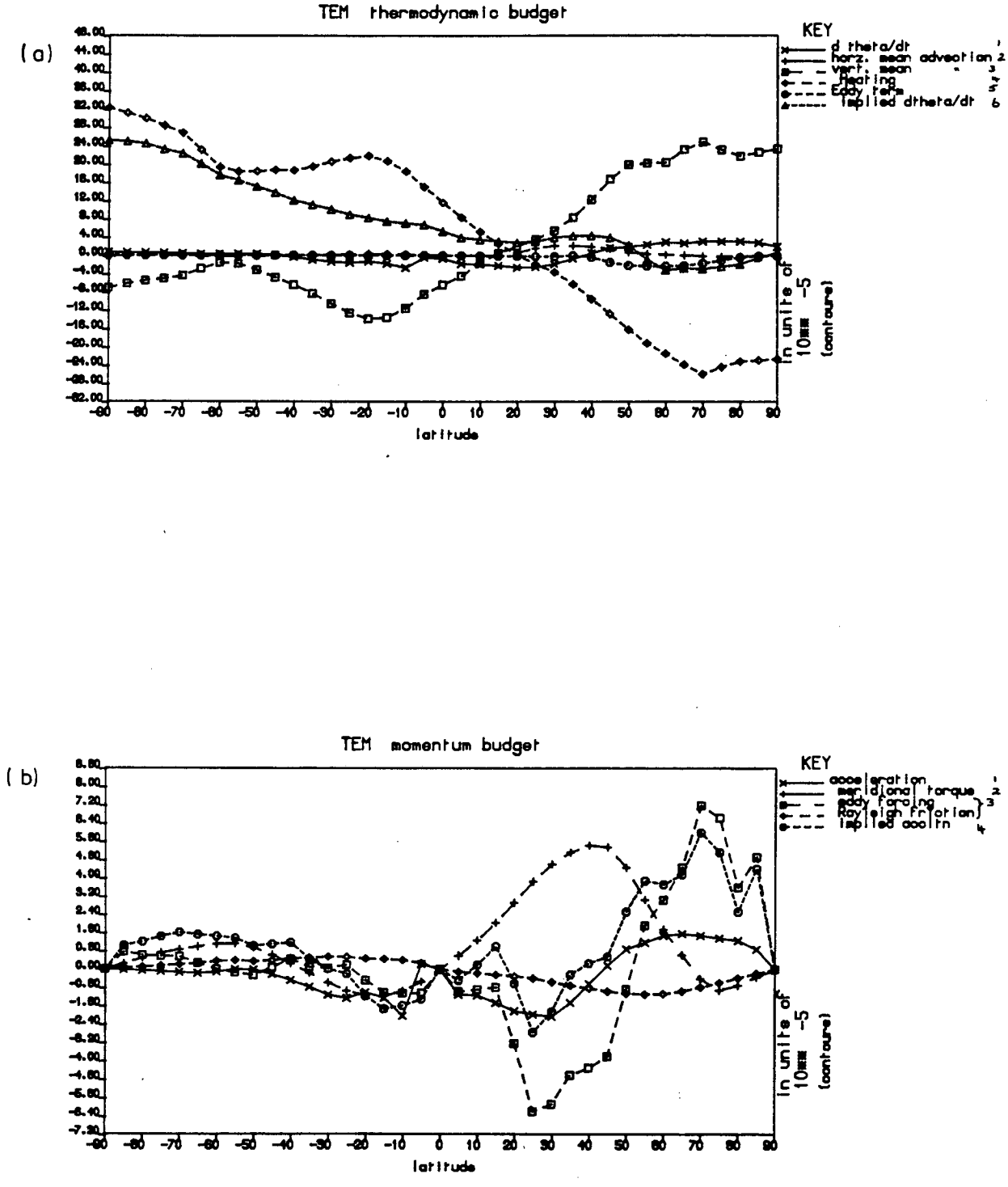

Figure F6.13 The (a) momentum and (b) thermodynamic budgets for December 1978 for the test case fully-forced Residual circulation including a right-hand side forcing term based upon a Rayleigh Friction parameterization. The Linegraph keys are as for Figures F6.2 & F6.1 respectively except that term 3 in the momentum budget above has two parts driven by a) the resolved eddy forcing and b) the Rayleigh friction parameterization.

gravity-wave driven circulation. The reason for this was that the gravity-wave momentum deposition, $(D_F)^F$, was positive in the high latitudes and so negated the decelerative effect of the reduced $f[v^R]$ by introducing a new acceleration of the mean state. In the northern hemisphere this cancellation between the circulation driven and the direct momentum deposition, is also occuring but of the opposite sign. In the northern hemisphere the coriolis torque is increased while the direct momentum deposition is easterly. However in the winter hemisphere its affect is more strikingly beneficial in mid-latitudes (due to the large zonal wind here). This suggests that the parametrization used does not provide the correct structure of gravity-wave drag and hence the necessary gradients of D_F to allow this extra momentum contribution to have the desired effect of accounting for the momentum imbalances. In the thermodynamic equation the enhancement of the vertical mean advection in high latitudes by the gravity-wave circulation component reduces the anomalous implied heating and cooling regions in the upper stratosphere considerably. An improvement of the heat balance which is very evident compared with the much smaller changes seen in the momentum budget.

The origin and magnitude of wave drag in the stratosphere, as has been seen in this study, can be partly explained in terms of the upward propagation of large scale planetary wave activity and the ultimate deposition and transfer of the wave energy to the mean state. However the momentum balances achieved in this study for the southern summer hemisphere, for example, indicate the necessity of an extra contribution to both the total momentum budget to offset the coriolis torque of the basically diabatically driven flows in the summer hemisphere and an extra 'wave-drag' forcing of a residual circulation component. Geller (1983) has suggested that gravity wave breaking may not only be important in the mesosphere but may also be important in the stratosphere and provide much of the frictional dissipation necessary for balance. However it is clear from the results in chapters 5 and 6, that the planetary wave 'wave-drag' resulting from transience and dissipation, breaking the conditions of non-acceleration, has a major role in explaining part of the momentum balance and zonal mean velocity deceleration process not only in the highly active winter months but also during the quieter equinox months such as illustrated

by the southern hemisphere of September 1979.

The relative roles of the two mechanisms throughout the middle atmosphere remains an uncertainty, and until a better knowledge of the extent of influence of gravity wave breaking is achieved, more accurate modelling will be reliant on crude parametrization schemes to fill in for this lack. It is important therefore that observations and analysis of a gravity wave climatology be given a high priority in middle atmosphere studies in the near future so that a better understanding of the role and magnitude of this form of wave drag is made available.

6.3 : POSSIBLE INACCURACIES FROM THE GEOSTROPHIC APPROXIMATION.

Recent work highlighted by the work of Robinson (1986) and Andrews (1987) indicates that the use of quasi-geostrophic theory in the evaluation of the EP-flux and divergence terms can lead to anomalous divergent regions in high latitudes due to the over-estimation of the eddy momentum flux by the geostrophic winds. The divergence calculated from a primitive equation model was undertaken by Robinson (1986) and he clearly showed the discrepancy. The magnitude of this error is also not small, with the large divergence region in high latitudes, $>55^{\circ}$N, being according to Robinson (1986) virtually entirely due to the error resulting from using geostrophic fluxes, while the convergence region seen in figure 3b, of Robinson (1986), compared with that derived using balanced winds is also considerably exaggerated. This implies that almost the entire calculated divergence in $div.F_g$ is possibly spurious compared with its primitive equation counterpart div.F which shows only a weak divergence in high latitudes. These results represent a major difficulty if this order of magnitude error is included in the EP-flux divergence evaluations used here. Due the uncertainty in these regions of divergence and a possible over estimation of the flux convergence in lower latitudes the residual circulations derived in this thesis may be affected and therefore represent over-estimations of the flow. This is suggested by the inability to balance the heat and momentum budget using quasi-geostrophic estimates. In most months the implied acceleration although generally of the right sign is seen to be excessive. This complication or error has undoubtedly led to an increase in the

interpretational difficulties of EP-flux divergence, div.**F**, and the circulations in this and in a number of other studies using these diagnostics.

In order to directly assess the affect of the extra ageostrophic velocities upon the derived circulation, the following circulation experiment was undertaken for a selection of days. The ageostrophically enhanced velocities were calculated from the following equations.

$$v_q = (f v_g + (u_g)_t + \mathbf{v_g} \cdot \nabla u_g + u_g v_g \tan(\varphi)/a)/f \qquad (6.6)$$

$$u_q = (f u_g - ((v_g)_t + \mathbf{v_g} \cdot \nabla v_g + u_g^2 \tan(\varphi)/a))/f \qquad (6.7)$$

The extra terms are non-linear terms ignored in the definition of the geostrophic wind and include the effects of the earth's curvature, local acceleration and centripetal acceleration.

The results were examined at various stages in their calculation. Firstly some sample velocity fields on particular pressure surfaces were examined. Secondly the eddy fluxes calculated from geostrophic and the enhanced velocities were compared and thirdly the resulting residual circulations and eddy forcing terms, D_F, were compared.

The u & v velocity field at 5mbar, figure not shown, was taken as a sample and showed a number of variations. Both velocity fields showed a split vortex with the high and middle latitudes dominated by two strong cyclonic vorticies. The comparison of the geostrophic and enhanced velocity fields showed that the ageostrophic velocities made the cyclones weaker. The anticyclones were weak features in both versions and as such clear differences were hard to assign or count as significant. The curvature and local acceleration produced vector differences such that the geostrophic winds were greater than the enhanced wind velocities in the cyclones as was to be expected.

An examination of the longitudinal variation of the flux $u^* v^*$, revealed that the extra contribution due to the ageostrophic velocities to the fluxes results in a general decrease in uv especially near the pole.

The resulting zonally averaged momentum flux due to the enhanced or quasi-geostrophic velocity estimates was decreased. The earth's curvature terms produced only a slight extra modification, further decreasing $[u^* v^*]$. The total quasi-geostrophic velocities resulted in a zonally averaged momentum flux whose maximum value decreased by ≈ 20 per cent, but more importantly the gradient of the momentum flux between the maximum and the pole was diminished because of the reduced maximum value of the flux and by a shallower decrease toward the pole. The heat flux was also generally decreased by all the extra ageostrophic velocity estimates, dropping by ≈ 15 percent at its maxima. The combined effect of these changes upon the eddy forcing term D_F using the two velocity sets is illustrated in figure F6.14. These show that the ageostrophic velocities have slightly increased the divergence region near the pole. However equatorward of 70°N the effect is to reduce the region of convergence in the upper stratosphere at ≈ 50°N and to produce a constriction of the divergence region confining it to an area close to the pole. The reduction in the convergence appears to be consistent with the fluxes produced by Hitchman(1985) who also compared the effect of using geostrophic and balanced winds in a similar fashion. However the retention of the strong divergence seen in figure F6.14b, is not as expected from the arguments of Robinson (1986), as it is in this region that the geostrophic fluxes are expected from his arguments to be most in error compared with fluxes based upon balanced winds.

Finally the two 'fully forced' residual circulations evaluated using the two forcing estimates in figures F6.14a & b are illustrated in figures F6.15 & F6.16. These contain a diabatically forced component and so are 'fully-forced' as defined in chapter 5. Figure F6.15 shows the residual circulation for the 23rd of February 1979 using geostrophic velocities in the evaluation of D_F, while F6.16 shows the same day's circulation but using v_q and u_q as defined in equations (6.6) and (6.7) in the evaluation of D_F. The figures show there are some

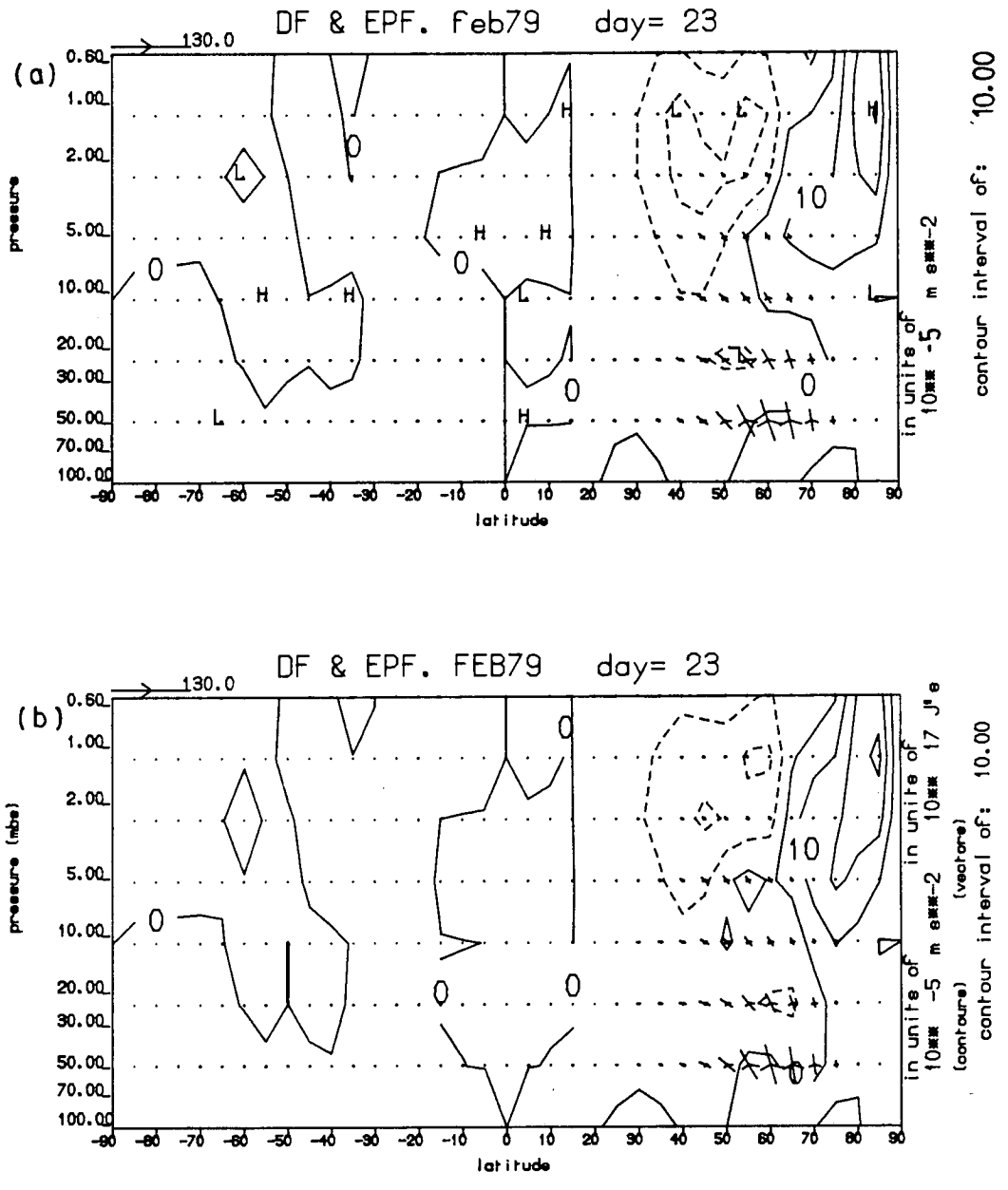

Figure F6.14 Contours of D_F (ms^{-2}) combined with EP-Flux vectors for the 23rd of February 1979 using (a) geostrophic velocities, & (b) ageostrophic enhanced velocities. The arrow scales are such that a vector whose length is the horizontal distance 10° on the diagram represents a value of $(5\pi/18)n$ of F^{φ} in {J} & a vector whose length is the vertical distance 1 interval of η represents a value n of F^{η} in {J}; where n is the scale arrow magnitude at the top right of the figure multiplied by the vector scale factor at the left edge (top) of the diagram. F^{φ} & F^{η} are defined as in Appendix C.($n= 130.10^{17}$ {J})

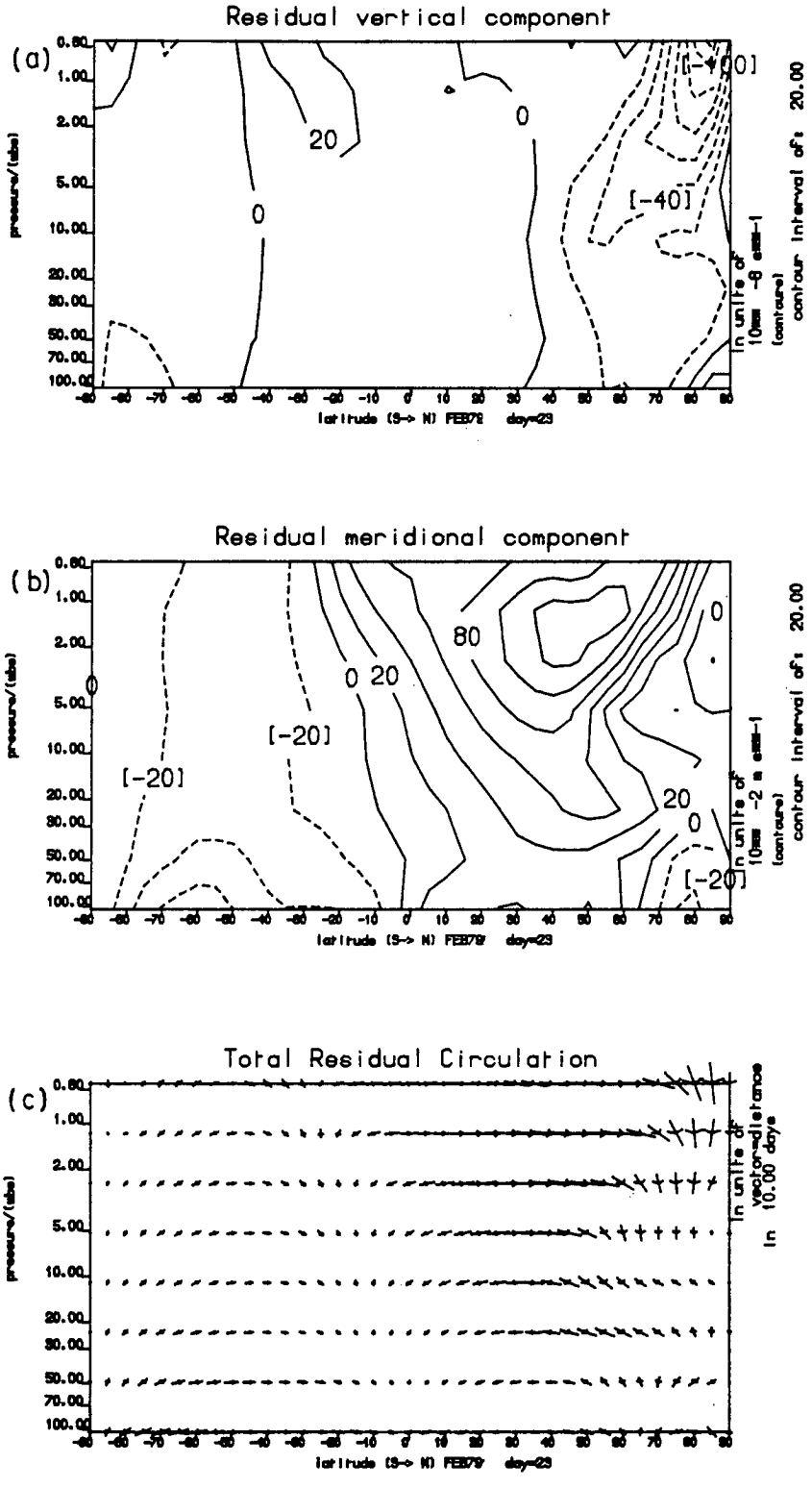

Figure F6.15 The total residual components (a) $[v]^R$, (b) $[w]^R$ and circulation, for the 23rd of February 1979 using geostrophic velocities to calculate the eddy flux terms.

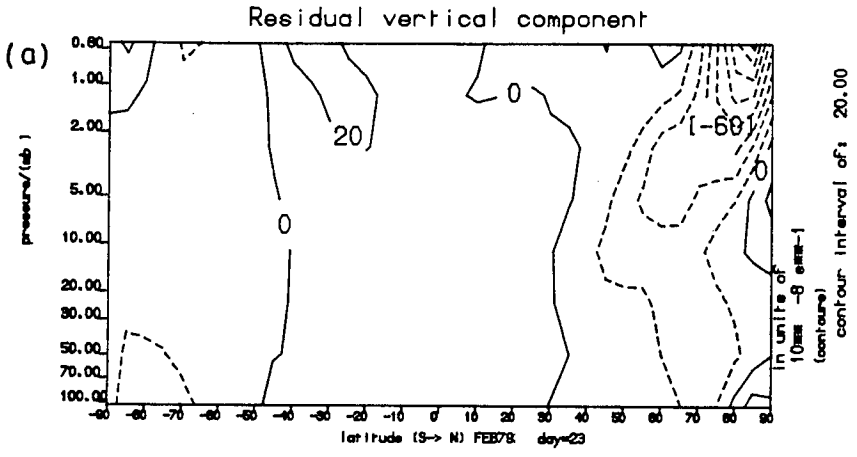

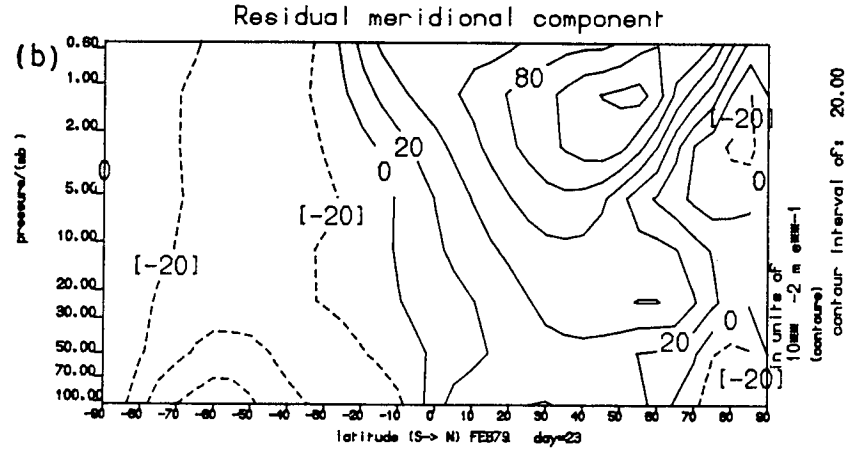

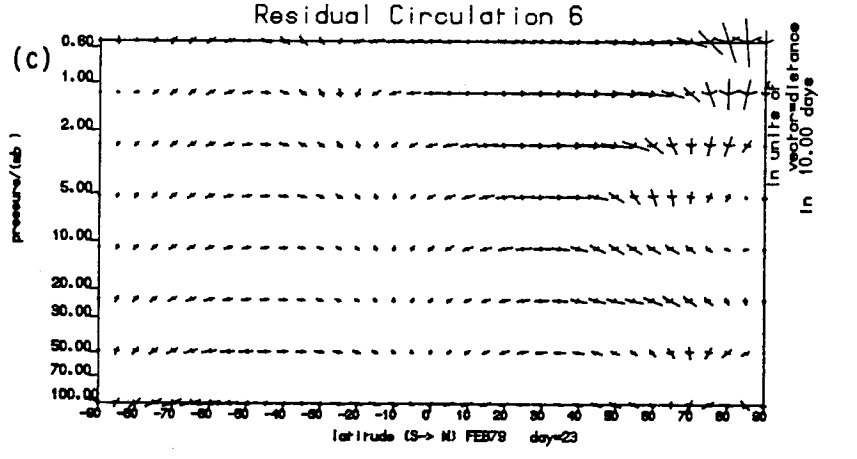

Figure F6.16 as F6.15 except using the ageostrophic enhanced velocities to calculate the eddy flux terms.

differences but these are not large enough to invalidate the flows as the changes are not large compared with the uncertainties in the magnitudes of the velocities shown here due to the other error sources examined in chapter 4. A more extensive study using non-geostrophic velocity estimates appears to be a necessary next step to provide a larger sample and alternative estimations of the ageostrophic velocity components. The inclusion of these ageostrophic velocities in a momentum budget examination for the 23rd did not provide the answer for the problems indicated earlier in this chapter and other answers for the imbalances must be sought.

6.4 : FURTHER DIAGNOSTIC ANALYSIS

In the following section a brief description will be made of the zonal mean state and its variation throughout the data period studied. This description of the monthly averaged circulation and mean state statistics for this period has also been undertaken by a number of other authors. Therefore diagrams from the present study will be compared with the climatological values from Geller et al (1984), Shiotani & Hirota (1984) and Mechoso et al (1985) which similarly describe this period. This evolution will then be used as background information as a basis for a discussion of the forcing and implied mean state changes in relation to the problem of the accuracy of the EP-flux divergence regions calculated. A number of differences are evident, between the various diagnostics from the different studies described covering the same period, which arise due to the different satellite measurements, techniques and inherent errors of the various data. The basic description of the evolution of the zonal state is based upon the SSU and LIMS data used in the present study. This is done to provide a consistent background for the assessment of the corresponding wave forcing and circulations in this study.

6.4.1 : THE SEASONAL MARCH

Section 6.4.1.1 describes the zonal mean state, its evolution (seasonal march) and the wave forcing during the period December 1978 to November 1979. This description examines the mean state and its relation to the wave forcing in order to gain confidence in the results and to provide background information for the earlier and further analysis. The derived zonal mean wind and acceleration together with the wave forcing term D_F and its associated EP-flux vectors are illustrated for each month in the figures F6.17 to F6.28.

6.4.1.1 : THE ZONAL MEAN WIND.

THE NORTHERN HEMISPHERE.

From December to January, as seen in figures F6.17 & F6.18, the upper stratospheric jet core decelerates slightly and descends from above 0.6mbar to about 1mbar, but very little poleward motion is evident. Figure F6.19 shows that the change in February is substantial with the sudden warming having dramatically modified the zonal wind field and removed the westerly jet from mid and high latitudes leaving only a weak flow with slight easterlies in the upper stratospheric polar night. The remaining jet maxima is now confined to the low latitudes in the upper stratosphere with a maximum of approximately 50 ms^{-1} at 50km. The zonal wind fields for the present study for December to January are different from those seen in Geller et al (1984) in a number of ways. Basically the main features are similar but the zonal wind based on the NMC data shows a jet maxima further equatorward in December. This is then seen to split in January, (not shown) (see Geller et al (1984)), producing one maximum high in the upper stratosphere-mesosphere near 30°N and the other which resembles the present study maxima of $\approx$ 50ms^{-1} at $\approx$ 60°N. In general the present study values were also weaker than those in Geller et al (1984), while the easterlies close to the pole in February are not seen in Geller et al (1984). The main differences occur in equatorial regions and high in the data.

In March, see figure F6.20, the westerlies are re-established throughout the northern hemisphere but the core is only slowly shifting poleward now centered at 40°N and of slightly decreased

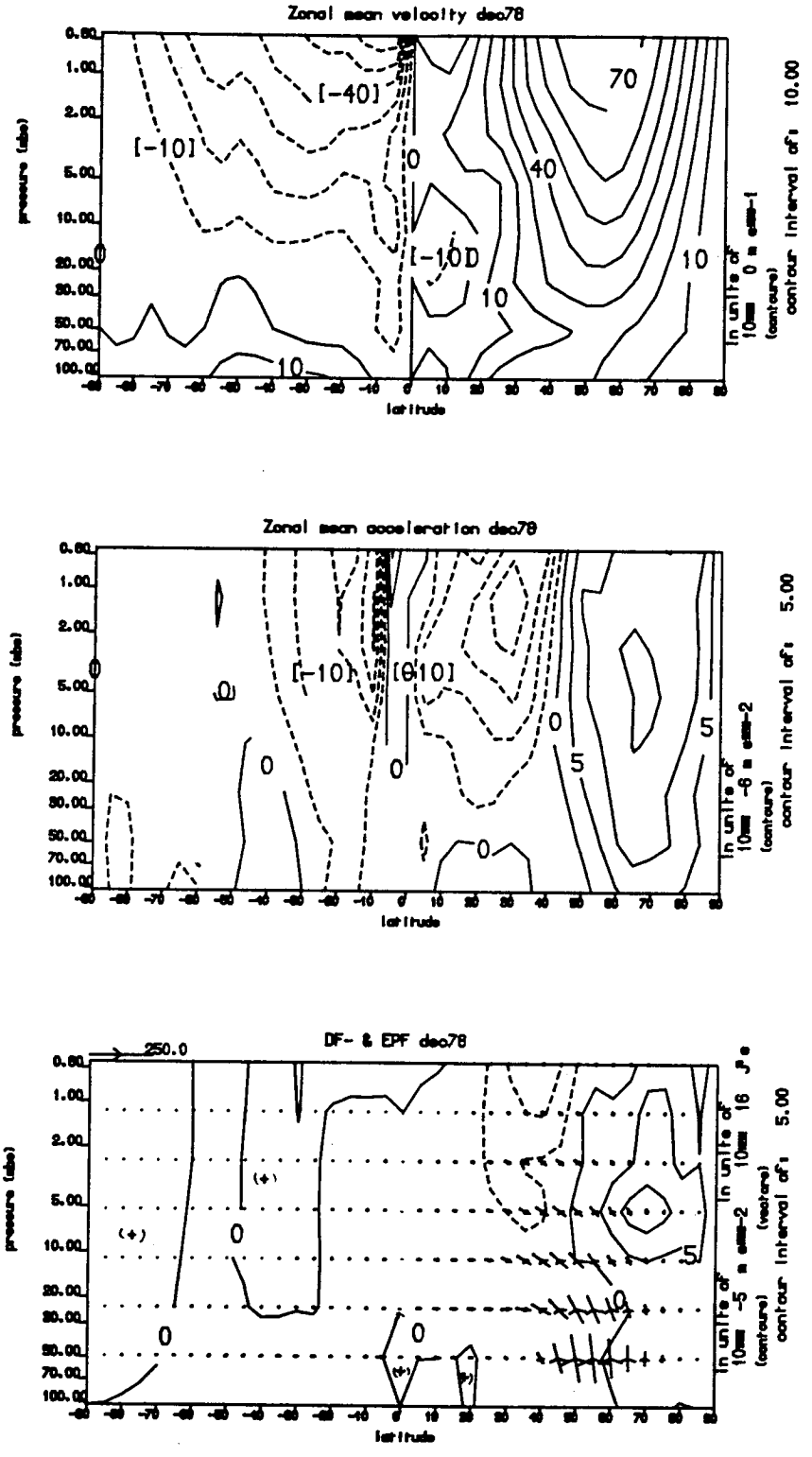

Figure F6.17 The zonal mean (geostrophic) wind, the zonal wind acceleration, $[u]_t$, and the wave forcing shown as contours of D_F (ms^{-2}) combined with EP-Flux vectors for December 1978 Vector scaling as Figure F6.14 except $n=250.10^{16}$

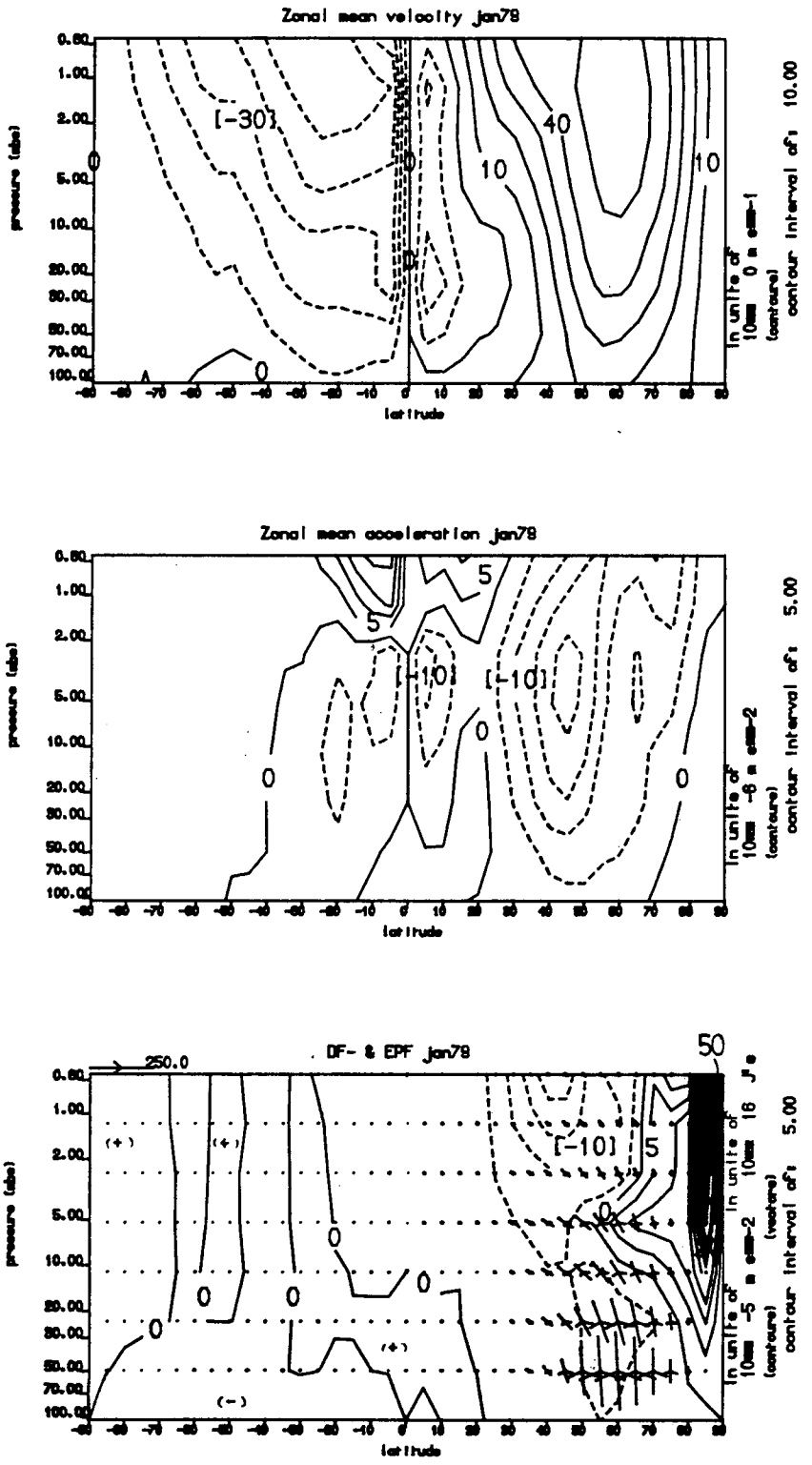

Figure F6.18 The zonal mean (geostrophic) wind, the zonal wind acceleration, $[u]_t$, and the wave forcing shown as contours of D_F (ms^{-2})combined with EP-Flux vectors for January 1979 Vector scaling as Figure F6.14 except $n=250.10^{16}$

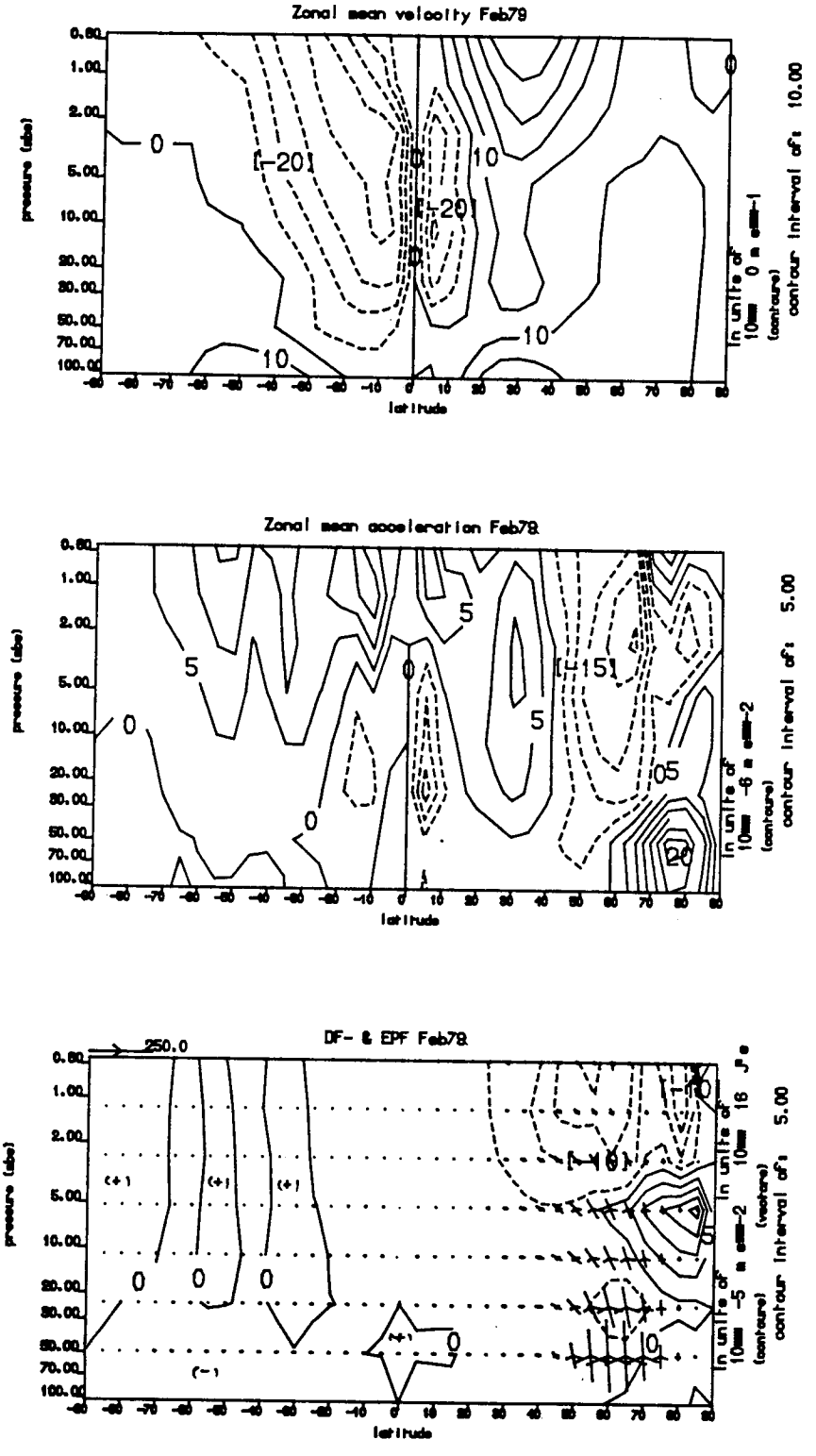

Figure F6.19 The zonal mean (geostrophic) wind, the zonal wind acceleration, $[u]_t$, and the wave forcing shown as contours of D_F (ms^{-2})combined with EP-Flux vectors for February 1979 Vector scaling as Figure F6.14 except $n=250.10^{16}$

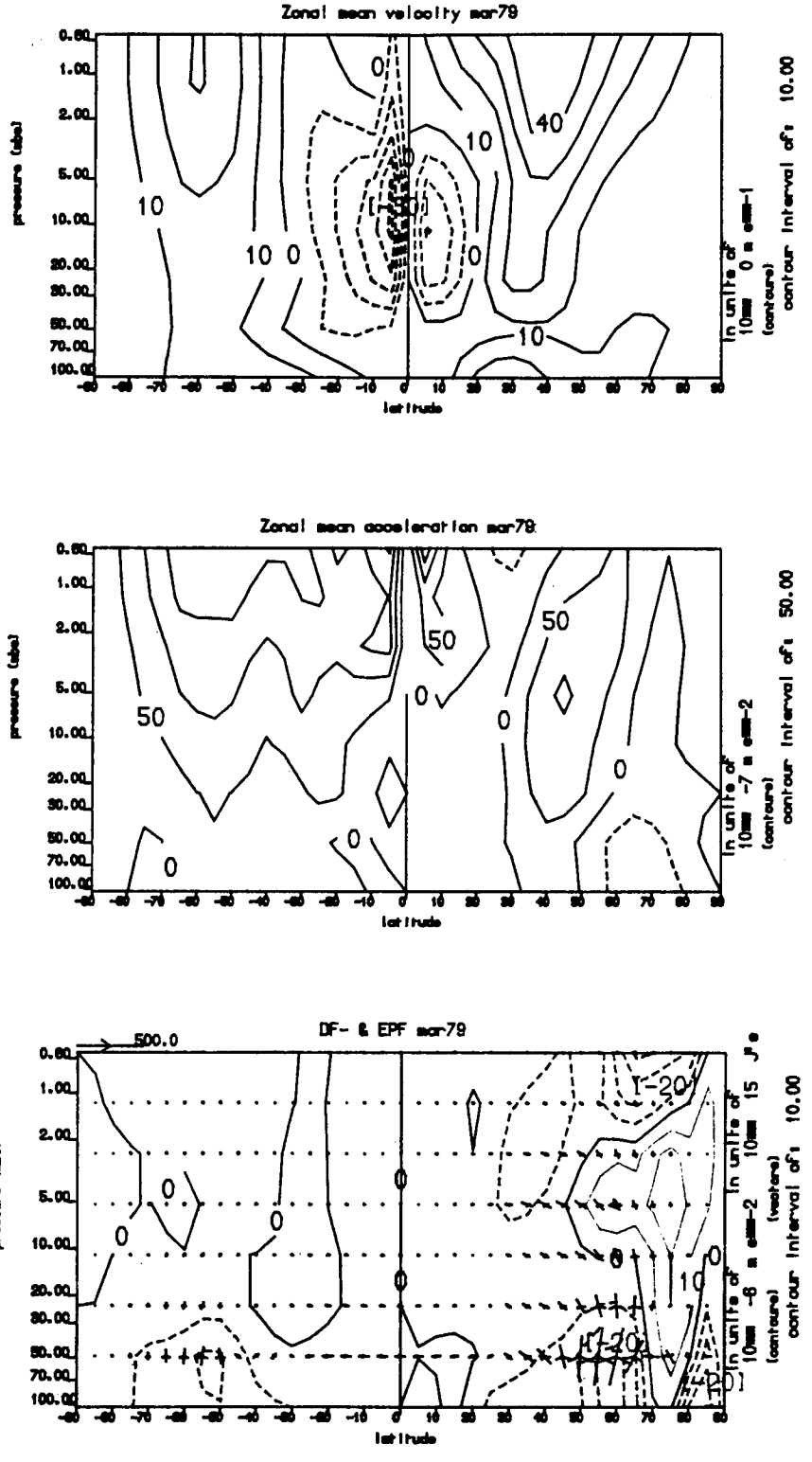

Figure F6.20 The zonal mean (geostrophic) wind, the zonal wind acceleration, $[u]_t$, and the wave forcing shown as contours of D_F (ms^{-2})combined with EP-Flux vectors for March 1979 Vector scaling as Figure F6.14 except $n=250.10^{16}$

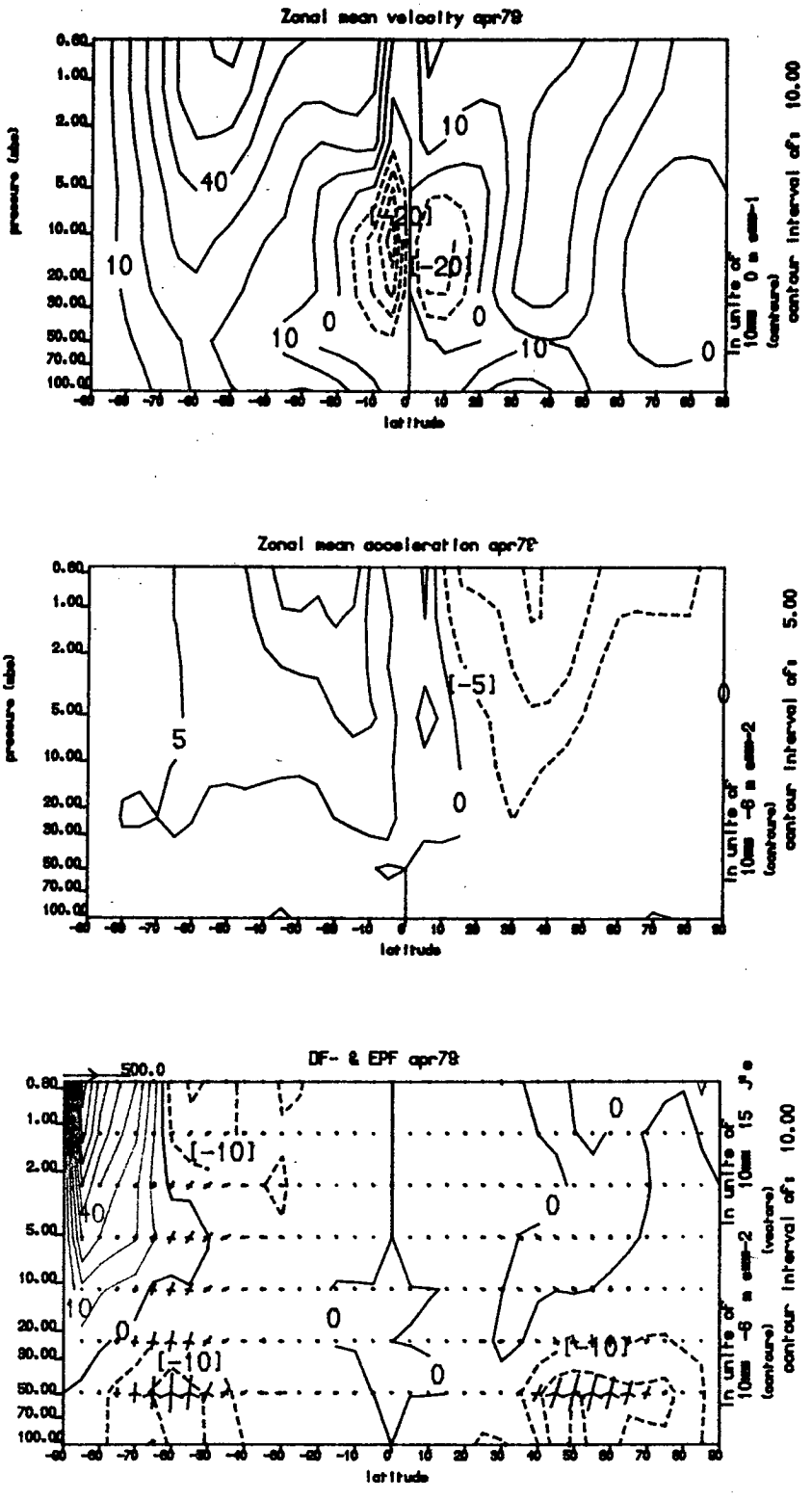

Figure F6.21 The zonal mean (geostrophic) wind, the zonal wind acceleration, $[u]_t$, and the wave forcing shown as contours of D_F (ms^{-2})combined with EP-Flux vectors for April 1979 Vector scaling as Figure F6.14 except $n=250.10^{16}$

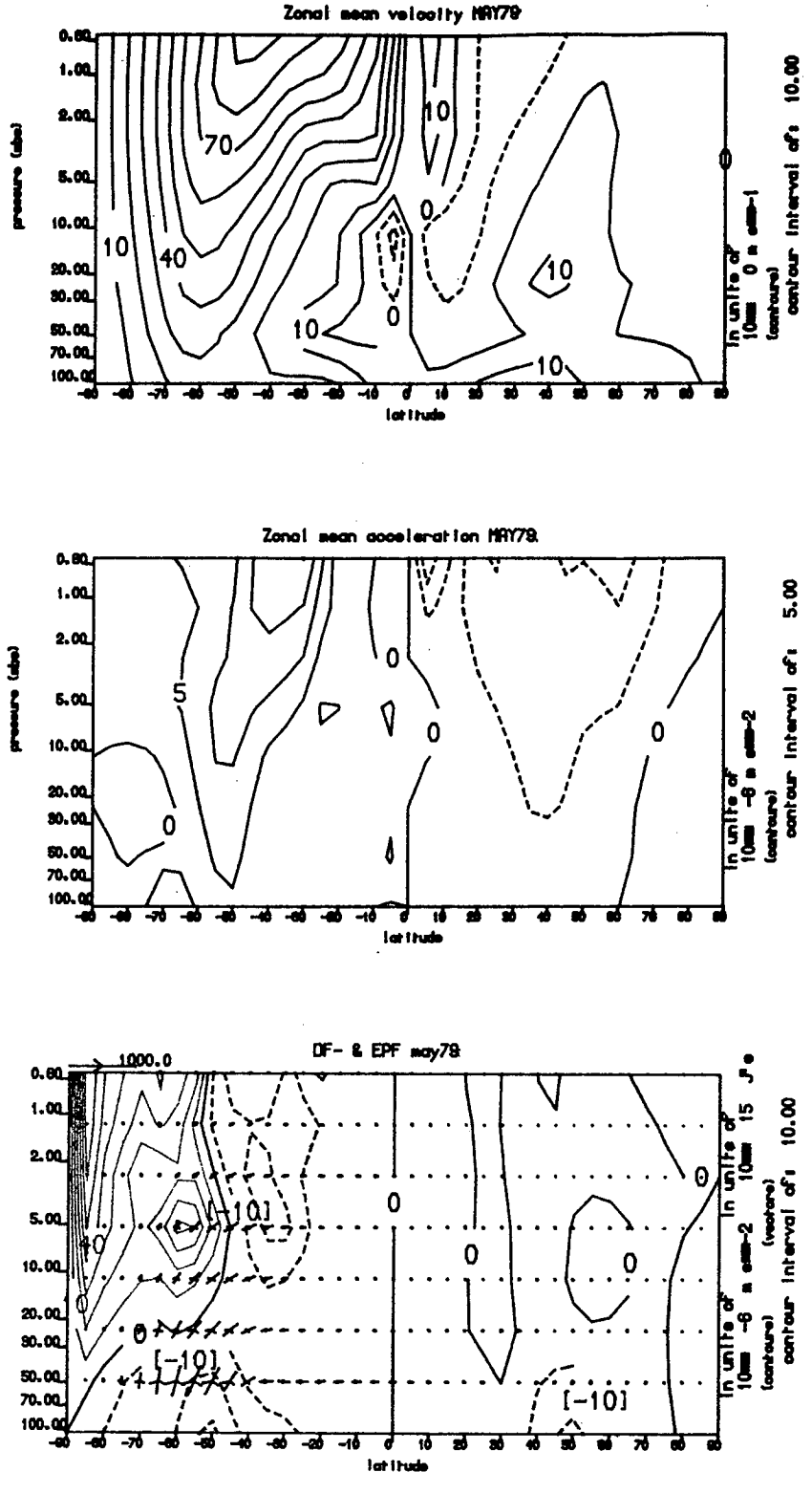

Figure F6.22 The zonal mean (geostrophic) wind, the zonal wind acceleration, $[u]_t$, and the wave forcing shown as contours of D_F (ms^{-2})combined with EP-Flux vectors for May 1979 Vector scaling as Figure F6.14 except $n=250.10^{16}$

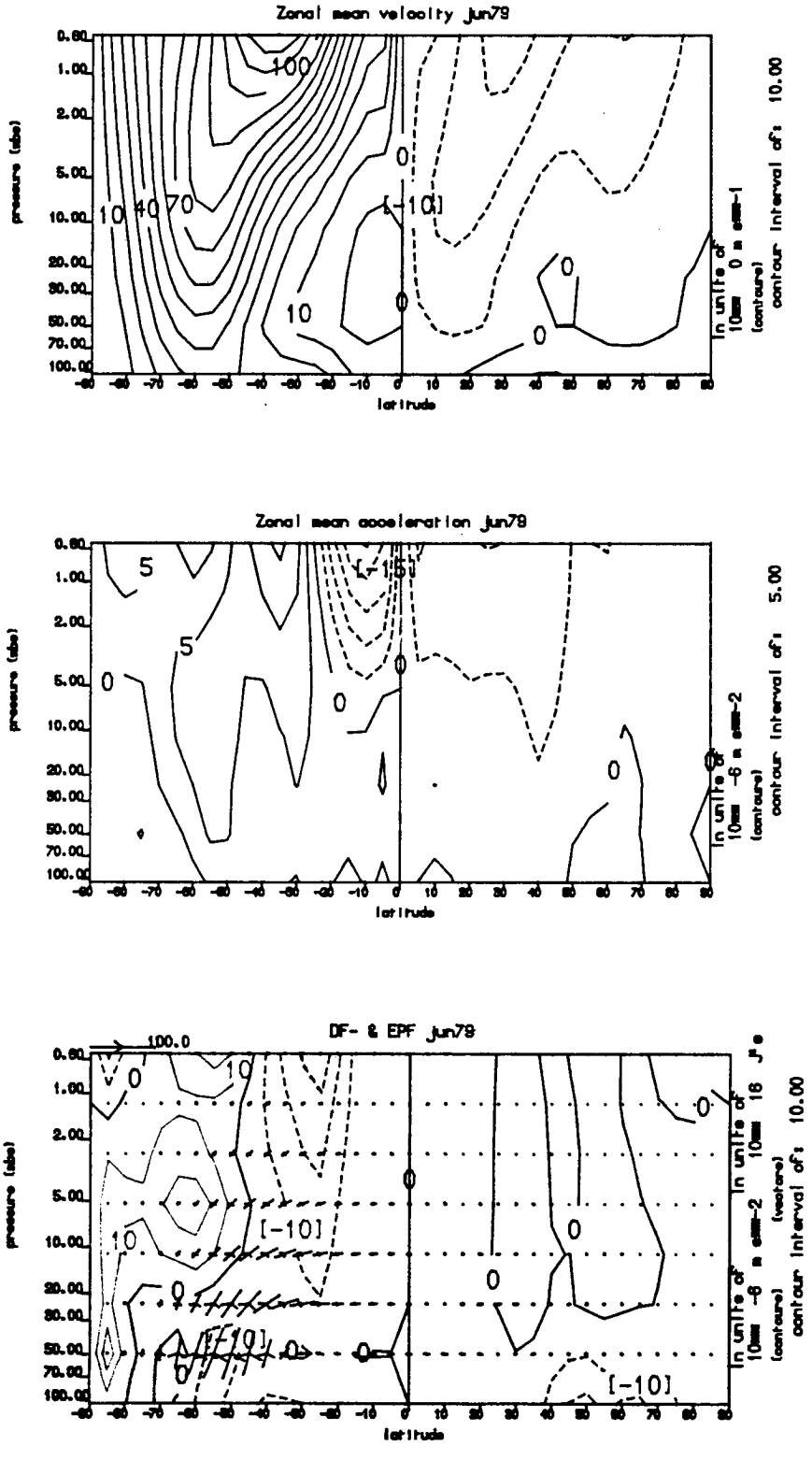

Figure F6.23 The zonal mean (geostrophic) wind, the zonal wind acceleration, $[u]_t$, and the wave forcing shown as contours of D_F (ms^{-2})combined with EP-Flux vectors for June 1979 Vector scaling as Figure F6.14 except $n=250.10^{16}$

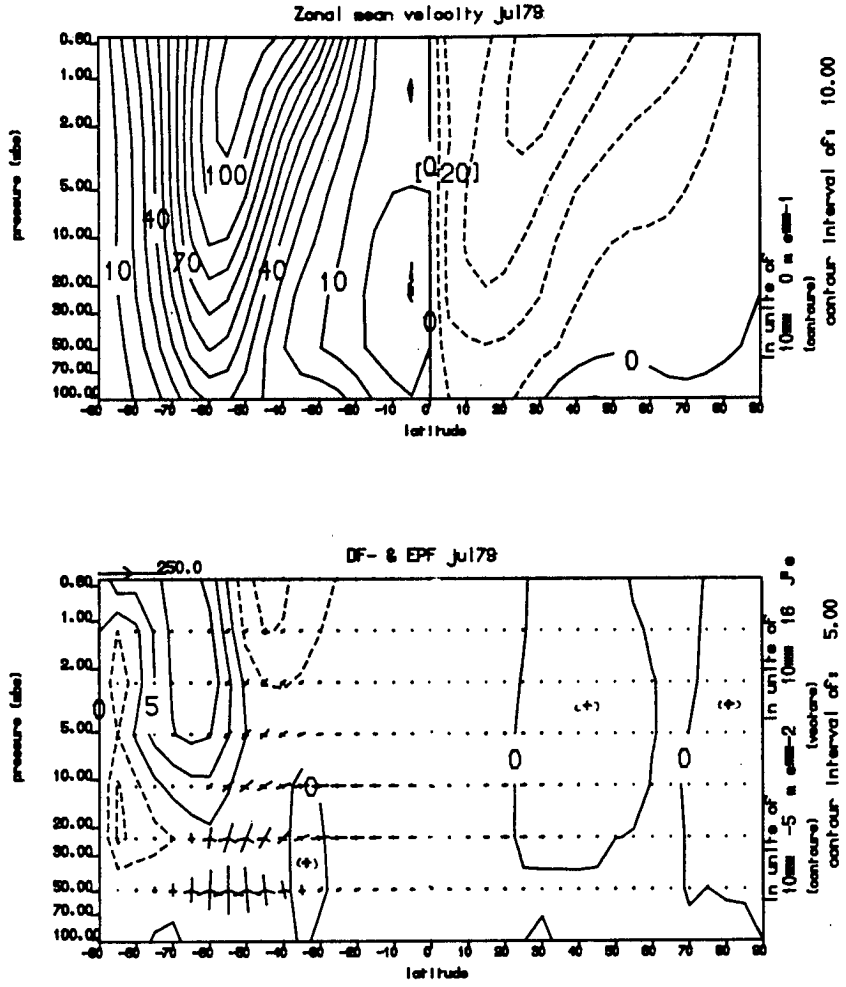

Figure F6.24 The zonal mean (geostrophic) wind, and the wave forcing shown as contours of D_F (ms^{-2})combined with EP-Flux vectors for July 1979 Vector scaling as Figure F6.14 except $n=250.10^{16}$

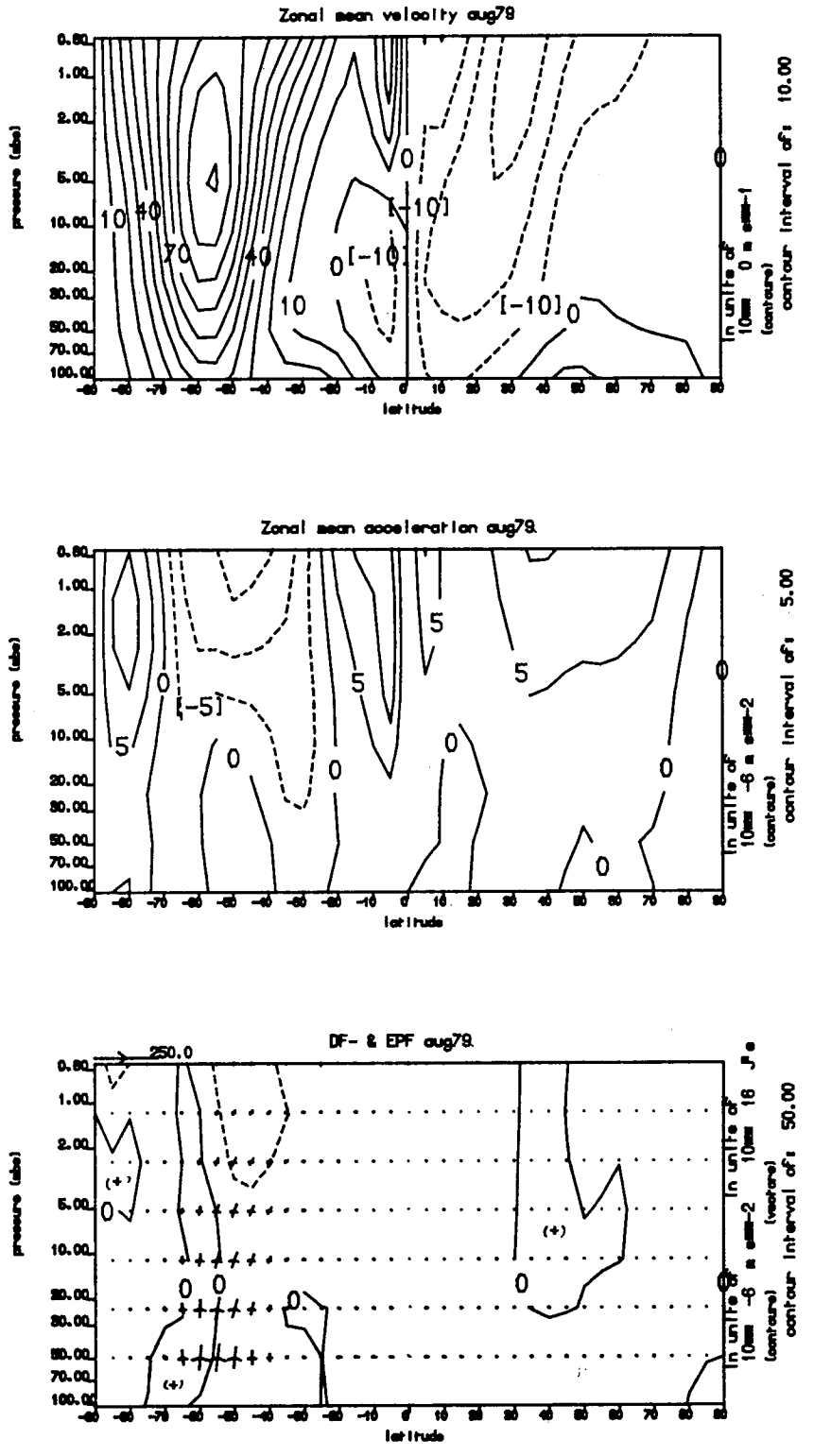

Figure F6.25 The zonal mean (geostrophic) wind, the zonal wind acceleration, $[u]_t$, and the wave forcing shown as contours of D_F (ms^{-2})combined with EP-Flux vectors for August 1979 Vector scaling as Figure F6.14 except $n=250.10^{16}$

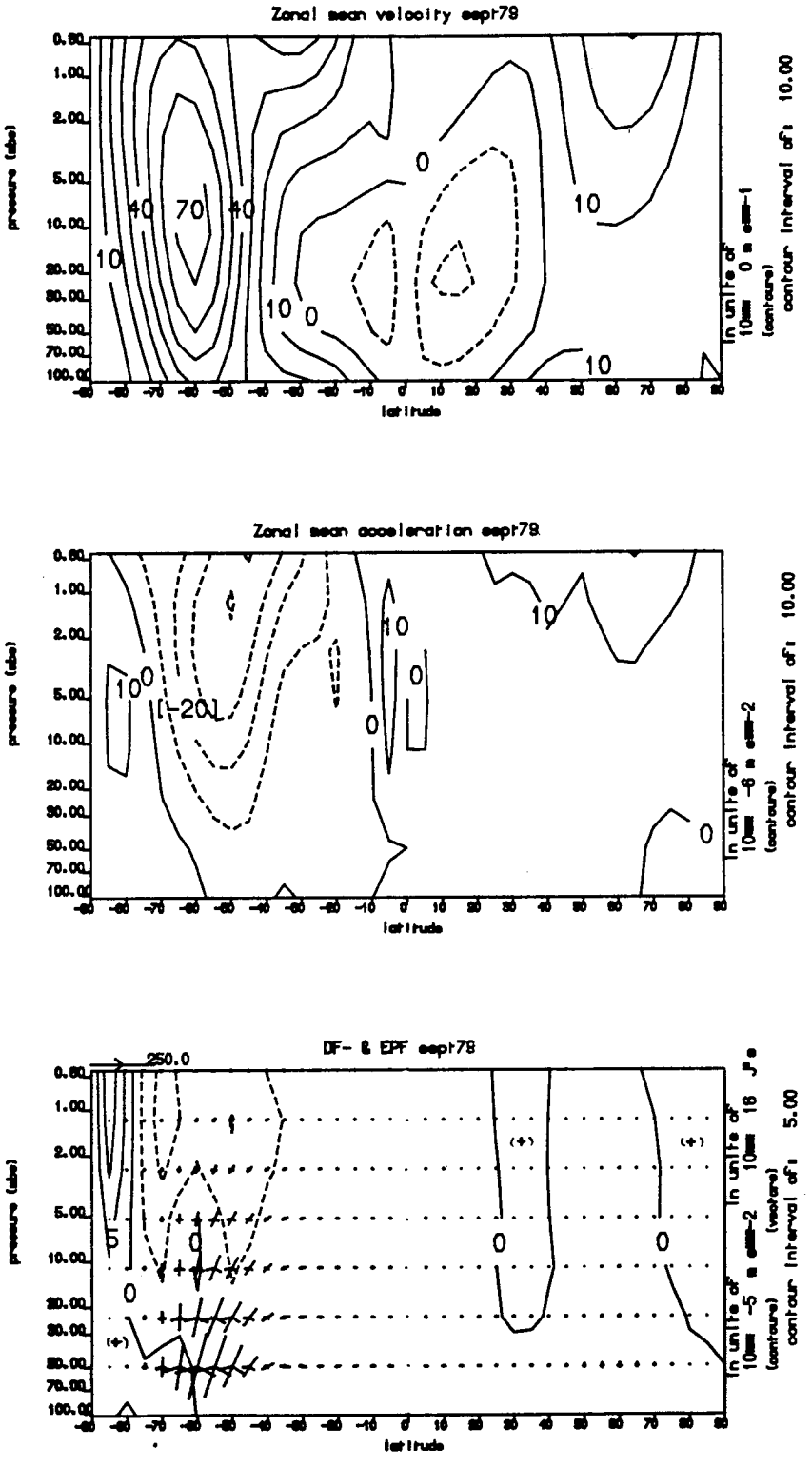

Figure F6.26 The zonal mean (geostrophic) wind, the zonal wind acceleration, $[u]_t$, and the wave forcing shown as contours of D_F (ms^{-2})combined with EP-Flux vectors for September 1979 Vector scaling as Figure F6.14 except $n=250.10^{16}$

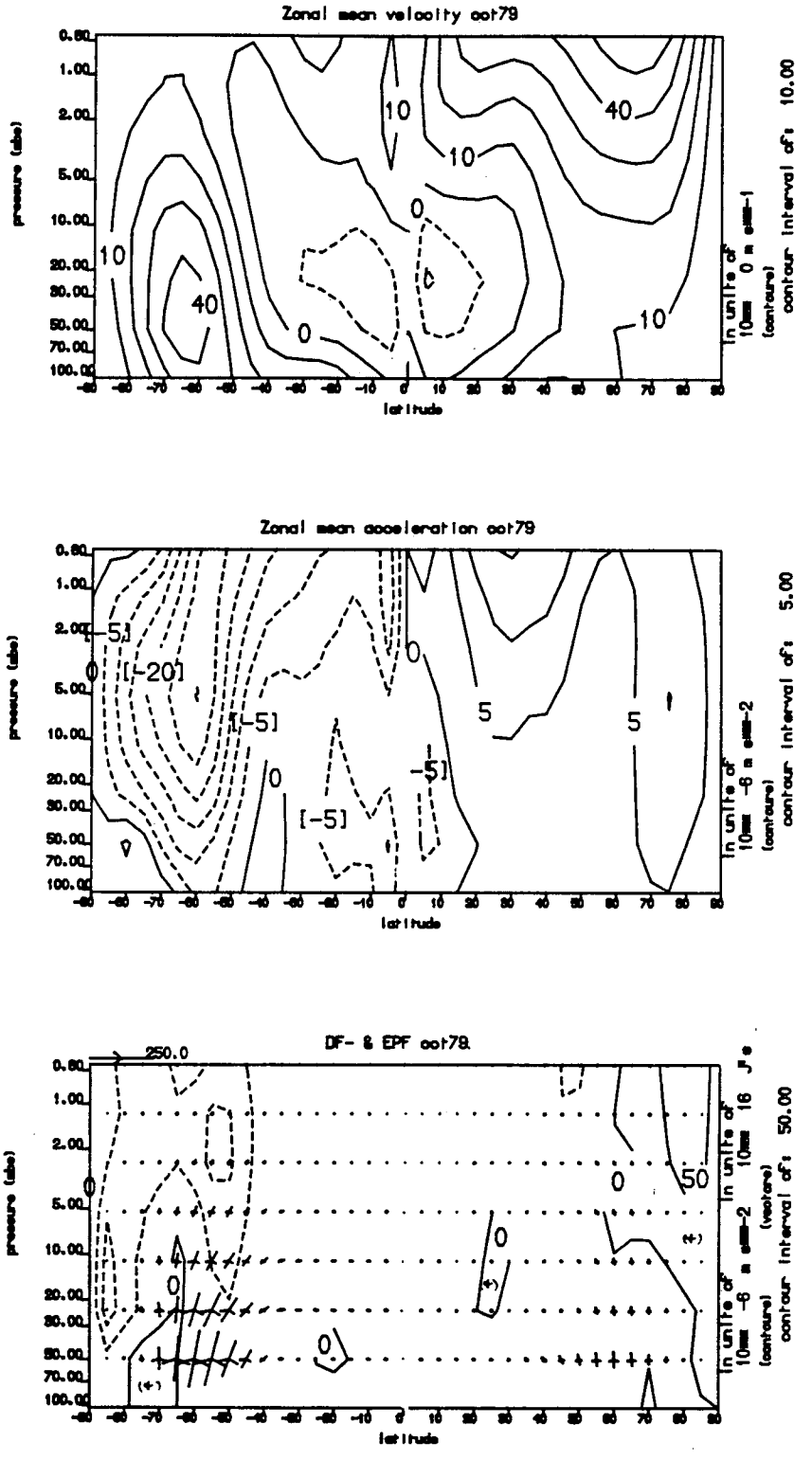

Figure F6.27 The zonal mean (geostrophic) wind, the zonal wind acceleration, $[u]_t$, and the wave forcing shown as contours of D_F (ms^{-2})combined with EP-Flux vectors for October 1979 Vector scaling as Figure F6.14 except $n=250.10^{16}$

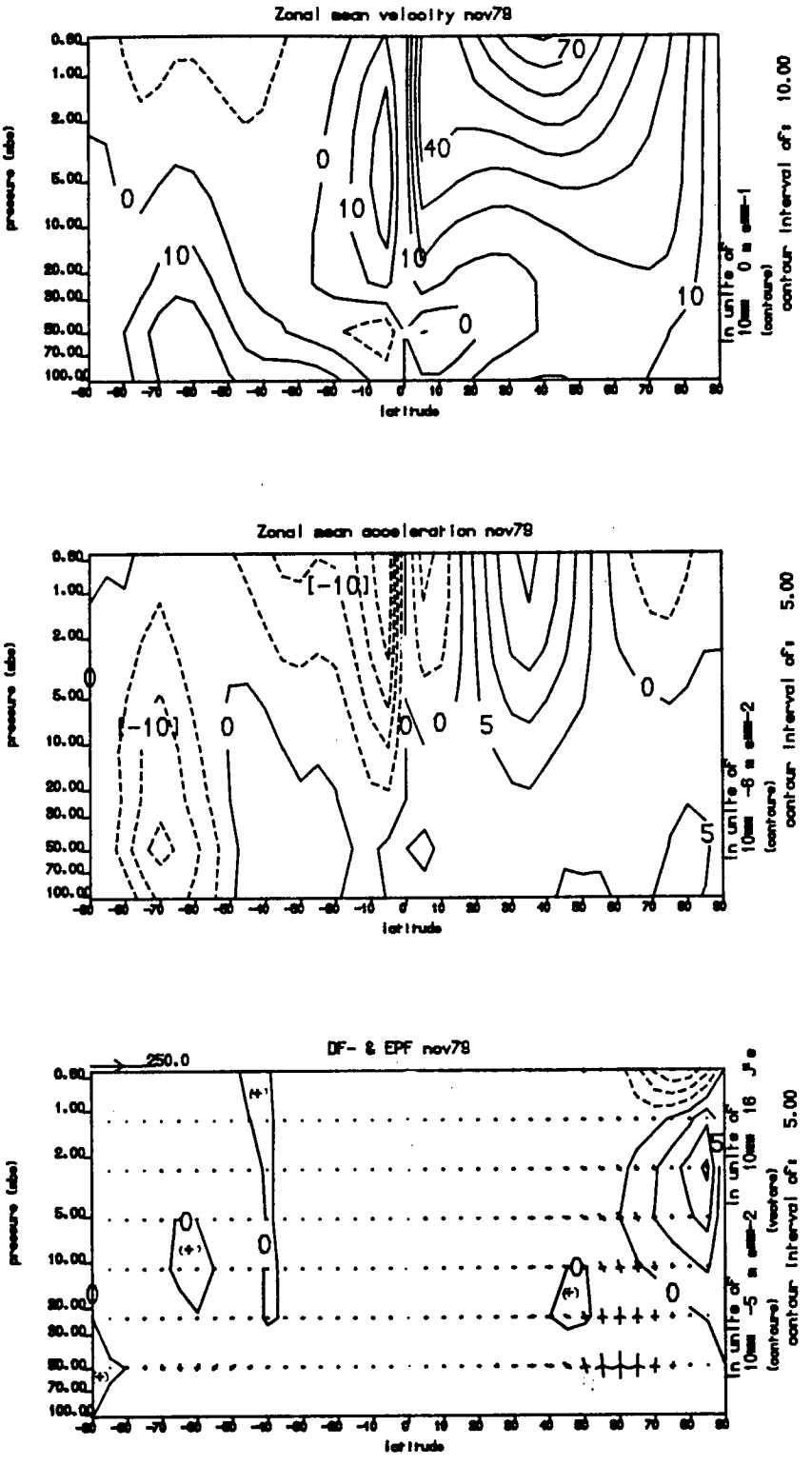

Figure F6.28 The zonal mean (geostrophic) wind, the zonal wind acceleration, $[u]_t$, and the wave forcing shown as contours of D_F (ms^{-2})combined with EP-Flux vectors for November 1979 Vector scaling as Figure F6.14 except $n=250.10^{16}$

magnitude. Not until May, see figure F6.22a, do weak easterlies appear in the upper stratosphere with a weak maximum lying close to 30°N, tilting equatorward. This easterly region grows throughout June, July and August, as seen in figure F6.23, F6.24 & F6.25, giving easterlies across the whole northern hemisphere stratosphere with a jet axis again tilted equatorward from about 30°N in the upper stratosphere. In September westerlies re-appear close to the pole, see figure F6.26, and by November, as seen in figure F6.28, the westerly jet has grown to a maximum of >70 ms^{-1} in the upper stratosphere and reaches into the mesosphere at approximately 40°N, similar to the previous December.

THE SOUTHERN HEMISPHERE

From December to February, see figures F6.17-F6.19, the southern hemisphere easterly jet, with its maximum above 0.6mbar, decreases from around 50ms^{-1} close to the equator to less than 40ms^{-1}. By March, as seen in figure F6.20, a westerly core has penetrated into the high latitude upper and middle stratosphere, of ≈ 30ms^{-1} at 65°S. The jet core at 65°S amplifies from March to May, see figures F6.20-F6.22, shifting equatorward but tilting poleward with an upper maximum of ≈ 90ms^{-1}. The motion of the jet continues into June, as seen in figure F6.23, with further shifting of the upper stratospheric jet core equatorward and an increase to ≈ 120ms^{-1} which is larger than its northern hemisphere counterpart.

In July figure F6.24a shows the movement now reverses and tends to return the jet poleward, so by August the jet maximum, as seen in figure F6.25a, has moved down to about 55°S. Figure F6.26a shows the motion of the jet continues into September with the jet diminishing and moving slowly to around 60°S. The upper stratospheric component then disappears as easterlies appear in the lower latitudes throughout the middle and lower stratosphere. By October, figure F6.27a shows, the westerly jet has decreased to ≈ 40ms^{-1} at 50-20 mbar. By November, see figure F6.28a, weak easterlies appear in the upper stratosphere and the westerlies are confined to the troposphere with only a slight penetration into the lower stratosphere. In the present study, zonal winds for June to September have been compared with those described in Mechoso et al (1985). Overall the comparison is very

good with the location and magnitude of the stratospheric zonal wind maxima being very similar over the entire period.

6.4.1.2 : THE EP-FLUX.

In December the stationary wave flux dominates the EP-flux, but the transient flux is clearly seen to diverge from 5-10mbar in the northern hemisphere high latitudes which seems to indicate some transient wave generation mechanism being responsible for its growth and propagation out of this region, see figure F6.17. Throughout this section the transient and time averaged D_F and EP-flux component vectors are discussed but only figures of the total D_F and EP-flux vectors are shown for each month.

In January and February, see figures F6.18c & F6.19c, the lower stratosphere remains dominated by the stationary flux but as February approaches the middle-upper stratosphere is largely penetrated by transient flux. In both months the divergence appears to be basically caused by the transient wave flux. Strong divergence also occurs in the lower stratosphere caused by the stationary or time-average wave conditions. This appears to be due to the shape and magnitude of the wave generation and penetration into the bottom of the stratosphere in the region 50-70°N. In both these months the transient EP-flux has originated from a narrower latitude band of ≈ 60-70°N in February compared with 50-70°N for the stationary flux. In March and April figures F6.20c & F6.21c show that the EP-flux virtually vanishes but as in December a very weak region of divergence at 5-10mbar in the high latitudes results from the amplification of the EP-flux vectors out of this region. Figure F6.22c shows that in May the southern hemisphere starts to become active in terms of wave activity penetration of the stratosphere, though the flux is small compared with the values for both January and February. However it is the transient flux which is more vertical and penetrates much higher with a smaller divergent region evident at 5-10mbar at ≈ 60°S compared with December for instance.

In the southern hemisphere winter, shown in figures F6.23-F6.25, the flux of wave activity gradually grows but it is far weaker than its northern hemisphere counterpart. In June the stationary wave flux is

slightly larger than the transient component but the transient activity penetrates higher in the stratosphere to ≈ 2-3 mbar. By July, see figures F6.23 & F6.24, the total EP-flux has increased in total magnitude with the two components being approximately equal in size, while the stationary flux appears to penetrate higher into the stratosphere. The flux is seen to split into two main branches, see figure F6.24; one almost vertical and the other turning equatorward and becoming almost horizontal thereby remaining below ≈ 5mbar. The transient EP-flux component exhibits some poleward orientation and as a result the diverging wave activity seen in the EP-flux vectors results in a region of divergence at 50 mbar. The stationary component also exhibits a divergent effect but only in high latitudes at ≈ 60° S and above 24mbar. As in December and March this feature is confirmed by the strong vector amplification and orientation implying divergence out of this region. In August, see figure F6.25, the transient flux is dominant and is almost vertical, penetrating high into the upper stratosphere with very little equatorward curvature. Very little divergence is calculated except in the lower stratosphere at≈ 50mbar at 65-70° S, where it appears to be an extension of the divergent region seen in the troposphere at these latitudes.

By September, shown in figure F6.26, the large burst of transient EP-flux activity of August has diminished but the transient EP-flux remains strong and basically vertically orientated. Now the stationary component is also important and is of equal magnitude throughout the middle and lower stratosphere. The EP-fluxes calculated by Mechoso et al (1985) likewise show an increase from June to July but the splitting of the flux orientation in July is not seen, see figure F6.24 & Mechoso et al (1985). Also in August the EP-flux values of Mechoso et al (1985) do not become almost vertical as seen in the present study but in September the activity does diminish in both studies.

October is the last month in which the southern hemisphere EP-flux is large, see figure F6.27, and as in September the stationary flux is the larger contribution in the lower and middle stratosphere with the transient flux diminishing in relative importance and now beginning to turn equatorward. The northern hemisphere wave activity in October is also important. A weaker wave presence is evident, compared with the

southern hemisphere but, the flux shows penetration into the upper stratosphere. Once again there are signs of a weak divergence near the north pole but this appears from the magnitude and orientation of the EP-flux vectors possibly to be a curvature problem rather than a real divergent effect.

Finally in November figure F6.28 shows the southern hemisphere EP-flux has virtually vanished except for a weak lower stratospheric penetration. However the northern hemisphere now has a dominant stationary wave flux component, as the transient flux remains quite weak and does not penetrate as high.

From the description of the evolution of the monthly averaged and transient fluxes in the stratosphere, it is clear that significant hemispheric differences occur between the northern and southern hemispheric winter eddy-active periods. The northern hemisphere exhibits a predominant stationary (time-averaged) flux throughout November to February, while in the equivalent southern hemisphere winter months of May to August the eddy forcing exhibits more variability. In the latter months the stationary or time-averaged eddy contribution does not dominate the forcing, instead throughout most of these months both contributions, transient and time-averaged, are of similar importance while in August it is the transient forcing which is dominant. Also, whereas in the early spring month of March the northern hemispheric winter activity ceases, its southern hemisphere equivalent early spring month of September is still active in terms of eddy forcing and this continues through into October, resulting in important consequences for the southern hemisphere polar region in terms of the circulation and advective heat transport. The enhanced southern hemispheric activity in the spring months described above has also been noted by Shiotani & Hirota (1984). They observed that the winter to spring activity is more vigorous in the northern than in the southern hemisphere, whereas from spring to summer the wave activity is more vigorous in the southern than the northern hemisphere. Their comments are based upon data for the period June 1981 to May 1982, when June and July were observed to be quiet eddy months and it was only after August that the southern hemisphere exhibits strong wave activity penetration into the middle and upper stratosphere. In

the present study July was observed to be fairly active and this difference could have arisen because of the earlier shifting of the westerly jet polewards during July in 1979 compared with late July early August in 1981, thus allowing the flux to penetrate higher earlier in the year. The northern hemispheric dominance in the winter to spring period was also seen in the present study but this is principally because of the major and minor warming events in the northern hemisphere which results in the order of magnitude of flux activity being greater in the northern compared with the southern hemisphere. These differences in hemispheric forcing have repercussions upon the evolution of the eddy driven circulation components during these months. The southern hemispheric flows in July and August, see Figures F5.20 & F5.21, clearly show the atmospheric response to the wave, mean interaction and disturbance of the momentum and heat balances. Also the strong eddy driven descent into polar regions during September and October arises due to this southern hemispheric forcing which has no equivalent in the northern hemisphere. The structure of the forcing asymmetries in time are seen to be part of the reasoning for the hemispheric differences in transport discussed earlier in chapter 5.

6.4.2 : WAVE, MEAN-FLOW INTERACTION.

6.4.2.1 : INTERPRETATION AND VALIDATION OF THE EP-FLUX DIVERGENCE :- INTRODUCTION

The use of the quasi-geostrophic EP-flux divergence term div.F as the basis of the forcing of the zonal mean state, [u] & [T], in this study and its evaluation using geostrophic velocities has in previous sections been shown to be subject to a degree of uncertainty. Therefore this section is intended to assess the validity of the eddy forcing observed using div.F, by relating the regions of divergence to physical mechanisms where possible and to observed complementary evidence available from the other diagnostics. To correctly examine in detail the full relationship between $[u_t]$ and D_F it is necessary to solve the elliptic equation (2.32), described in section (2.8.2). This complex analysis has not been undertaken in this study, instead, the following descriptive assessment is given as a simple alternative. The observed accelerations and D_F calculated are illustrated in figures

F6.17-F6.28. However it must be noted that the results of the brief experiments on the circulation which incorporated ageostrophic velocity components into the evaluation of the EP-flux divergence produced only small changes. The circulations remained qualitatively similar to those produced when using only geostrophic fluxes and so the error which may be present due to the use of geostrophic eddy fluxes does not invalidate the circulations presented in chapter 5.

THE NORTHERN HEMISPHERE.

In December, see figure F6.17, the westerly jet is subject to a gradual deceleration and a shifting of its core poleward and downward. This is associated with a dipole acceleration pattern with decreasing westerlies in middle and lower latitudes and acceleration in high latitudes. This tendency is also reflected in the eddy forcing term D_F, which also indicates a high latitude positive acceleration for all latitudes greater than $\approx 50^{\circ}$N. The wave energy transport, as expressed by the EP-flux vectors, see figure F6.17, shows a strong flux upward between 40° and 70°N, which turns equatorward but penetrates to $\approx$ 3mbar and above. D_F, $[u]_t$ and the EP-Flux vectors all suggest that the likelihood of significant divergence of the EP-flux is probable and is occuring in the winter high latitudes. However the magnitude of this eddy forcing at $\approx$ 5mbar is possibly an over-estimate of the actual forcing because of the large imbalance seen for this level in the momentum budget, resulting in an exaggerated implied acceleration, see Figure F6.1b. Geller et al (1984) also show D_F positive in high latitudes extending out to $\approx 60^{\circ}$N and the magnitudes are of similar if not larger values than those calculated in the present study for December 1978.

In stark contrast the January comparison, see figure F6.18, is not so straightforward. The zonal mean wind is seen to be decelerated throughout the stratosphere as a result of the pre-warming event in late January. There is no evidence for high latitude accelerations, based upon $[u_g]_t$, whereas the eddy forcing, D_F, is very large and positive indicating a mean acceleration at 85°N. A qualitative assessment of the EP-flux vectors gives no clear indication or confirmation either way regarding the existence of the divergence. However from the study of Palmer & Hsu (1983) there is evidence of

in-situ wave generation due to nonlinear wave interactions resulting in positive divergence regions close to the pole during a sudden cooling period which was observed in this month. It may be that this real divergence is exaggerated because of the time-average split in an event which is continuing into February but both the Geller et al (1984) and Palmer & Hsu (1983) studies show divergence regions in approximately the same areas of the atmosphere and it is only the values at latitudes greater than 80°N that are very different from the magnitudes seen in these other studies. The problem seems to be very large due to the very strong local gradient of eddy momentum flux calculated using geostrophic velocities. This makes the finite difference calculation prone to error because it produces a situation where the EP-flux distribution will be such as to result in a small balance between large convergent and divergent EP-Flux vectors curving from a vertical orientation to an equatorward sense. The small net balance between these large terms is subject to error and has in this case produced a spuriously large divergence region close to the pole. However this month because of the extreme magnitude of divergence at ≈ 85°N & 5mbar, has been tested to see the effect of the existence of the divergence feature upon the residual circulation. See section (3.3.6.7). Important to the aim of this study is the conclusion found from these tests, that the very high latitude features as observed in the January case are not significantly modifying the residual eddy driven components of the circulation.

In February, see figure F6.19, there is evidence of weak acceleration at 3mbar which grows in magnitude as p increases into the troposphere, the maxima occuring at about 50mbar. In terms of wave forced acceleration the maxima is once again located at 5mbar which is too high compared with the observed change in the mean state. However its magnitude is considerably smaller than in January, the value for February being smaller by a factor of 5. Also the direction and magnitudes of the EP-flux vectors are once again very difficult to interpret, but the transient vectors do appear divergent at 5mbar & ≈ 60°N, but this is countered by a strong 'time-averaged' wave convergence which restricts the divergence to >70°N where the divergence is more difficult to assess and more likely to error. Evidence of divergence is seen, in figure F6.19c, only below 50mbar in

the high latitudes. It must be borne in mind that the events in February provide ample conditions for the existence of real divergence. The conditions include the non-linear, large amplitude, highly transient wave activity occuring during the sudden warming in the latter part of February, but it appears that the problem region at 5mbar in the high latitudes may well also be at least exaggerated. Comparison with the D_F values from Geller et al (1984) in January and February is good. In January there is evidence of a narrow net divergent EP-flux region in high latitudes which correspondes with that seen in the present study with similar magnitudes. However the peak values at latitudes greater than 80°N are not seen. In February in both studies a region of divergence is seen at ≈ 10mbar while convergence is dominant in the middle latitudes of the upper and middle stratosphere.

In March the zonal mean state of the northern hemisphere is relatively unchanged, see figure F6.20, with a small low latitude deceleration region high in the stratosphere/mesosphere and some acceleration in the middle and high latitudes of the middle-upper stratosphere. Here too although the magnitude is considerably smaller i.e. factor of 1/5 compared with the February values, a region of divergence occurs around 5mbar from 50-90°N with an extension at 75°N into the lower stratosphere. However one alternative explanation is that the divergence occurs as a result of the time averaging which subdivides one event between the months of February and March. Wave activity occuring during the end of February and into the beginning of March will be split between the two months. This is suggested in these months by the orientation and evolution of the EP-flux vectors, possibly implying that a reversible transient event has been split between the two months, February and March. The split of one wave event between the two monthly averages will lead to a possibly false interpretation of the trend of the mean state's acceleration. The reversible nature arises because a wave packet appears to have passed through the region and so in February it is seen entering and so converging while in March it is exiting and so diverging. In this case however the magnitudes involved are sufficiently small as to have very little effect on the residual circulation as seen in figure F5.16, see section (5.2).

In April D_F and $[u_t]$, as seen in figure F6.21, are basically consistent since the majority of the stratosphere is being decelerated and D_F's major influence is in the troposphere. The region of divergence which occurs is very small and once again the eddy driven circulation is not significant compared with the diabatic component.

In May, see figure F6.22, the situation is similar except for a lower to middle stratospheric acceleration region near the north pole, which coincides with a similar divergent region of D_F. The wave flux for this month and hemisphere is very small, as too is the acceleration feature, i.e. $[u_t] < 5.10^{-6}$ ms^{-2}. In both June and July the extent of the wave propagation is also small as seen in figures F6.23 & F6.24. Under these circumstances where there is only a small direct wave forcing term, the evolution of the zonal mean-flow must be determined by other forcing terms. An assessment of the reasoning for the forcing needs a fuller explanation via the solution of the partial differential equation in $[u_t]$ to be properly described. The activity in August and September, see figures F6.25 & F6.26, is similar, with the upper stratospheric acceleration having no link to the northern hemisphere troposphere as the wave flux is very small and does not penetrate into the stratosphere.

In October however, see figures F6.27, the EP-flux activity in the northern hemisphere is more important and penetrates to ≈ 5mbar. This month exhibits a dipole structure in D_F in the upper stratosphere with a strong divergence centre at $>80^{\circ}$N. The EP-flux activity is small at this level, but the flux orientation is virtually totally vertical and does penetrate into this region. The zonal wind however shows acceleration throughout the majority of the stratospheric northern hemisphere. This suggest the high latitude acceleration is real but that the convergence in mid-latitudes is not consistent with the observed acceleration at this level across the whole hemisphere, requiring an acceleration due to a large meridional circulation for instance to enhance the westerlies.

In November, see figure F6.28, the EP-flux is much larger with a strong curvature of the EP-Flux vectors at $50\text{-}60^{\circ}$N and evidence of

divergence poleward of this turning. The high latitude positive values of D_F at 5 mbar, coincides with this propagation and a real acceleration in the lower stratosphere. However the acceleration maximum in the upper stratosphere has no clear D_F counterpart.

THE SOUTHERN HEMISPHERE.

In December and January figures F6.17 & F6.18 show, despite the strong deceleration throughout the lower stratosphere, that the wave forcing, D_F, is small. The deceleration must be principally driven by the readjustment of [θ] by [Q] or due to the residual circulation torque and gravity wave deceleration mechanisms. Also in February, see figure F6.19, the net weak stratospheric acceleration has only weak divergence to account, locally in terms of D_F, for its presence. This acceleration, $[u]_t$, continues into March, see figure F6.20, penetrating down throughout the stratospheric southern hemisphere. However the D_F forcing and wave activity shows very little resemblance to the acceleration, $[u]_t$, throughout these summer to autumn months.

In April as seen in figure F6.21 this changes, with the upper stratospheric maximum acceleration being increased and confined to the lower latitudes. However, both D_F and the EP-flux orientation indicate a region of implied forcing, and so the existence of acceleration in the upper stratospheric high latitudes. The effect of this wave forcing must be redistributed considerably across the hemisphere to account for the acceleration pattern observed. The forcing, shown in figure F6.21c, has a peak at $\approx$ 0.6mbar of $\approx 8.10^{-5} ms^{-2}$.

In May, see figure F6.22, the high latitude divergence, although slightly diminished, remains and has now spread to produce a secondary maxima at 55° S, $\approx$ 5mbar. In this region the EP-flux divergence is still present but as noted in section 6.4.1.2 there are clear signs of the transient EP-flux being divergent at 5-10mbar in the latitude band 50- 70° S. The acceleration in May is fairly consistent with this except it is not so weighted to the high latitudes. The maximum wave forcing, D_F, in the upper stratosphere is at $\approx$ 30° S, see figure F6.22, but a lower ridge bends to $\approx$ 55° S at 5mbar, which overlaps the implied acceleration region.

Figure F6.23 shows that in June the structure of the wave forcing region throughout the upper and middle stratosphere is qualitatively similar to that in May and is coincident with the observed acceleration $[u_t]$. Also the equatorial deceleration and $D_F < 0$ are in agreement. Once again it is only in the high latitudes that the magnitude of the positive wave forcing is considerably larger than the observed acceleration, $[u_t]$.

In July, see figure F6.24, another strong divergence or $D_F > 0$ forcing is calculated in the upper stratosphere, centered at 60° S. This coincides with $[u_t] > 0$ but this is positioned further poleward centered at 70° S. However the observed $[u]_t$ values calculated for this month are poor and are not shown in figure F6.24. The EP-flux vectors, again exhibit at ≈ 2-5 mbar some enhanced wave activity which results in a region of divergence above 5-10 mbar at ≈ 60° S.

In comparison figure F6.25 shows that August is a far more complex month with a divergent forcing at 60-65° S but with a maximum lower in the stratosphere and stretching throughout the stratosphere in a thin column. The upper extension is not seen in the observed zonal acceleration which is negative in this region and is only positive close to the pole i.e. >75° S. This dipole structure is also seen in the total forcing, D_F, but principally only in the transient component of D_F. However the EP-flux vectors are very strong and vertically orientated. Moreover they exhibit an apparent divergent tendency throughout the stratosphere with the poleward flanking vectors pointing slightly poleward to considerable heights (see Fig F6.25c). This strong vertical orientation with contraction of the flux column from the lower to middle stratosphere and expansion thereafter, is responsible for the divergent column of positive D_F throughout the stratosphere. Equatorward of 55° S, the large convergence appears to dominate and to be responsible for the strong deceleration observed in the upper-middle stratosphere. It is this convergence, which has the greatest influence in determining the meridional circulation, swamping the effect of the divergent forcing region.

September, as seen in figure F6.26, is another month which exhibits a dipole pattern, with acceleration observed throughout the

stratosphere close to the south pole and deceleration throughout the remainder of the stratosphere. This is reflected by the wave forcing, see Fig F6.26c, which shows a similar pattern of D_F. As in other months, it is possible that the large divergence at high latitudes is overestimated but real, since acceleration is observed. This pattern is also confirmed by the wave activity propagation with the EP-flux vectors again resulting in a strong penetration of the stratosphere. The divergence higher in the atmosphere is difficult to assess but appears to arise because of the transient wave activity flux terms. Comparison of the D_F values in Mechoso et al (1985) with the present study southern hemisphere wave forcing shows that in June and July the qualitative structure of the features are very similar but the magnitudes in the present study are in general larger. While the divergence region seen in Mechoso et al (1985) is considerably larger in August and September in extent and the general pattern of the divergence extends further into the mid-latitudes than in the present study results.

Figure F6.27 shows that in October the mean state is subject to a large wave forced deceleration throughout the majority of the stratosphere and this is reflected by the deceleration of the [u] field observed, except in the lower stratospheric high latitudes. By November the southern hemispheric wave activity has all but vanished and the deceleration observed cannot be totally accounted for by the wave, mean-interaction mechanism alone. The deceleration must basically arise because of the seasonal variation in diabatic forcing which in the summer southern hemisphere during November is warming the upper stratosphere, and so via the thermal wind balance, requires a residual torque to readjust and decelerate [u] in this hemisphere.

6.5 : SUMMARY AND DISCUSSION

In conclusion, Chapter 6 has examined the TEM budgets of momentum and heat with particular attention to the eddy forcing term D_F. The latter was undertaken to examine the validity and accuracy of the EP-Flux divergences obtained and to examine the relative contribution throughout the year and for the different hemispheres of the transient and stationary EP-Flux terms.

The separate analysis of the zonal mean wind field, principal eddy forcing term and the EP-flux vectors have provided a firmer basis from which to scrutinize the effects and physical reality of the EP-Flux divergence and its consequence upon the meridional circulation and mean state. As described above part of the divergence features calculated is thought by certain authors (Robinson 1986) to be partly spurious, however in a number of months the divergent forcing has been shown to be very probably a real atmospheric response and it remains to be established by what magnitude the divergent forcing for these months are exaggerated if at all. A fuller examination of the relationship between $[u]_t$, $f[v]^R$ & D_F can only be obtained by the solution of the elliptic operator for $[u]_t$ described in section (2.8.2). Firstly it has been noted before that in general the magnitude of D_F does not compare well with the numerical magnitude of $[u]_t$, since often the coriolis term, $f[v]^R$, is significant. However regions of EP-flux divergence can usually be associated with positive $[u]_t$ and vice versa. Secondly, the Eulerian viewpoint of the wave, mean-flow interaction process involves understanding and interpreting correctly the relative contributions spatially and the sequence of the cause and effect of the individual terms in the budgets.

A further area of discussion which has arisen from the analysis above involves the question of the accuracy of using geostrophic velocities, in the evaluation of the momentum and heat fluxes, compared with the use of velocities obtained from the solution of the non-linear balance equation. Such a comparison is presently under study. The brief experiment in section 6.3 describes a more limited attempt at calculating the ageostrophic enhanced or quasi-geostrophic, balanced winds for use in calculating D_F more accurately. The experiment shows that the active conditions of February 1979 produce differences which are observed to be important and will result in a modification to the residual circulations deduced. However although the changes are significant, the circulations with and without these changes are still qualitatively very similar and so do not invalidate the circulations based upon geostrophic fluxes, described in chapter 5 which approximate the fuller forced version. The EP-flux vectors and their separation into transient and stationary flux components have proved very useful in assessing the true divergence and in determining

that in a large number of cases the major influence in generating the divergent effect may have been irreversible transience. In section 6.4.2.1 by checking the consistency and evolution of these diagnostics together with the momentum and heat budget data the forcing and consequent zonal mean wind accelerations and the validity of the divergence computations were assessed. The examination of the time variations gave some information on the irreversibilty of the forcing, indicating instances where the evolution of particular wave events were split between the time averaged and transient flux statistics by the monthly averaging used. The possible split of the event can result in misinterpretation of the influence on the zonal mean wind acceleration of the total wave forcing for two (or more) months. The separation of the diagnostics, (F & D_F), into transient and time averaged components in section 6.4.1.2, also helps identify the lifetime of the divergent features over the month since the time-averaged diagnostics favour the more permanent features. The analysis of the total and separated, transient and time-averaged (figures not shown), EP-Flux and D_F diagnostics in section 6.4.1.2 included a number of important conclusions. The evolution described showed significant hemispheric differences occuring in the timing and nature of the wave forcing. The winter eddy-active periods exhibited a distinct inter-hemispheric difference in character of the EP-Flux, with the northern hemispheric flux being principally a stationary flux while the southern hemisphere EP-Flux contains a far larger and important component due to the transient flux. The two early spring periods are also very distinct, as in the northern hemisphere the wave forcing activity diminishes considerably (in March), whereas in the southern hemisphere the strong wave activity of July and August does not diminish in September and October. During the months of September and October, as shown in figures F6.26 & F6.27 compared with F6.20 & F6.21, the eddy forcing continues and even possibly amplifies in the lower stratosphere. The enhanced southern hemispheric spring wave activity and the hemispheric differences described above have also been observed by Shiotani & Hirota (1984), however it has also been possible in this thesis to split the eddy forcing into its transient and time averaged fluxes and so illustrate the hemispheric differences also apparent in the nature of the forcing events throughout the year. More importantly the

hemispheric differences in the eddy forcing can be related to the circulations in chapter 5, showing the consequences of the differences in terms of the year's evolution of the residual circulation and its transport. From the analyses in chapters 5 & 6 it can be seen that the hemispheric differences observed in the circulations and the transport effect postulated, are a direct consequence of the eddy forcing differences described above. There is also evidence of possible exaggerated divergence in high latitudes as suggested by Robinson (1986) and therefore the results from this thesis must be analysed with this problem in mind when interpreting the circulation and forcing diagnostics in high latitudes of the stratosphere.

As discussed in section 6.1.3.3 the values of the implied $[u_t]$ and $[\theta]_t$ for the summer hemispheres examined, calculated from the momentum and thermodynamic budgets, in general show a poor correspondence with the observed values of $[u_t]$ and $[\theta_t]$. The summer hemispheres show minimal wave activity and so any deceleration or acceleration must be a response to the diabatically driven residual circulation component in this hemisphere and/or a response to a mechanism unresolved or neglected in this analysis. The imbalances seen in the summer hemisphere budgets has not been satisfactorily explained.

One important mechanism which is not included in the right hand side forcing of the 'total residual' circulations described, is that produced by the momentum deposition due to gravity-wave breaking and their interaction with the mean state in the stratosphere. The experiment described in section (6.2) and the recently increasing number of studies by middle atmospheric workers indicates that this mechanism will be important and should be studied more in order to understand its role in the total forcing and interaction with the stratosphere and the residual circulation component thereby produced.

CHAPTER 7

CONCLUSIONS

A principal aim of this thesis was the evaluation and analysis throughout one year of the global evolution of the residual circulation of the stratosphere. Monthly averaged residual circulations, evaluated using an omega equation method for the year December 1978 to November 1979, have been presented and their seasonal evolution described. From this information certain general features of the flow were evident. The characteristic development and evolution of the flow in the upper stratosphere, from summer to winter, is seen with equator-to-pole cells occuring during equinox conditions but also present in both hemispheres in the middle and lower stratosphere all year round. The vertical extent of these are higher than in other published studies of this type of circulation, e.g. Dunkerton (1978), Garcia & Solomon (1983) and Pitari & Visconti (1985). The dominant pole-to-pole upper stratospheric and mesospheric flow is not very strong within the region (e.g. below 0.6 mbar) examined; but this may be due to the absence of any gravity wave drag forcing, which is likely to be important at the top of the region examined.

In chapter 5 transport by the residual circulations was examined. It was found that the residual circulation requires the inclusion of an eddy driven component to describe the mean meridional transport, and hemispheric asymmetries associated therewith, of the trace species in the stratosphere. The diabatically driven component as defined in chapter 5 should not be used on its own as the total circulation in a transport model, as used in Rogers & Pyle (1984) and Pyle & Rogers (1984). Such a circulation has been shown in this thesis to underestimate the total transport as it does not include the the significant eddy driven component and will fail to incorporate the eddy driven hemispheric asymmetries through the seasons. Thus the residual circulation contains an important circulation component throughout the majority of the year which is directly driven by the eddies. Since the influence of transience and dissipation gives rise to a wave driven component of the residual circulation whose net influence upon the transport and the mean state is important.

However, these findings were not wholly corroborated at all levels in the stratosphere by the budget analyses. Although the momentum and heat balances derived from the budget analyses were poor, they provided evidence that the eddy driven velocity terms in the budgets were necessary to maintain the momentum and thermal balances. Note, for example, that the summer hemispheres were poorly described and the very lowest stratospheric levels exhibited problems in terms of very large meridional poleward-directed velocities which, through the coriolis torque, resulted in accelerations when $[u_t]$ was calculated from the momentum budget. These large implied accelerations were considerably larger than the observed accelerations. On the other hand in high latitudes the vertical velocities associated with this flow component appeared to be too small to transport the necessary heat required to offset the diabatic forcing of [Q]. Hence the observed warming and cooling regions, seen in $[\theta]_t$, at particular latitudes were not reproduced in the implied thermal tendency obtained from calculating $[\theta_t]$ as a residual of the thermodynamic budget terms.

The year December 1978- November 1979 was an active year in terms of eddy motions. This is shown in the diagnostics presented for a sequence of years by Geller et al (1984). They show that the eddy activity varies a great deal from year to year in both its extent and magnitude and in terms of its effect upon the stratosphere, with significant variations in the location and intensity of the wave forcing features evident over the period. Due to this large variability in wave activity seen in different year's analyses the analysis of any particular year (e.g. December 1978- November 1979) can only be considered as a case study.

The variability in the extent of the wave activity in the stratosphere is partly due to extreme events in late January and in mid February of 1979 when the stratosphere was subject to minor and major warmings. A period of strong wave activity has been examined in more detail by calculating daily D_F, $[v]^R$ and $[w]^R$ to view the influence on the residual circulation throughout the peak warming period of late February 1979. In section 5.4 the residual circulations for the period 15^{th} to the 27^{th} of February were calculated every second day based upon single day's data. These were analysed together

with the TEM forcing diagnostics also produced bi-daily. This case study was undertaken for several purposes. Firstly it enabled a direct comparison of the forcing diagnostic terms to be made with those of Palmer (1981). This comparison showed that, apart from errors in high latitudes due to a possible over-estimation in D_F, there was good correspondence between the results. Since the basic data is the same, this result is to be expected and merely corroborates the analyses. Secondly, an assessment of the variability of the residual circulation on a shorter time scale than the period used in the rest of the study could be made. This allowed the monthly averaged circulations to be justified as representative of the month considered and not just as chance statistical residues of a highly variable set. Finally it provided a sequence of bi-daily circulations during a sudden warming, illustrating the application of this diagnostic and its relation to the large amplitude wave effects during these extreme conditions. This analysis illustrated the strong eddy driven flows and large degree of variability of the flow, involving both reversible and irreversible events, during the sudden warming period. The flow illustrated in figures F5.28 & F5.29 exhibit strong eddy driven poleward and descending motions throughout the majority of the warming similar to the model analysis of Dunkerton et al(1981).

These adiabatic motions were seen to be important during the evolution of the sudden warming. The separated eddy and diabatic forcings show that the adiabatic motions evolve as a result of the rapidly changing wave forcing, significantly dominating the slowly varying diabatic component illustrated in figure F5.30. The patterns of EP-Flux divergence and convergence and the consequent eddy driven residual circulations were seen to conform to the dynamical theory of Eliassen (1951). The analysis in Chapter 5 also showed the desirability of daily circulation evaluations during the sudden warming period and the complexity of interpretation when such a rapidly changing and complex event is being analysed.

The circulations have also been used to investigate the role of the mean meridional circulation in the generation of observed tracer asymmetries between the hemispheres. The examination in chapter 5 provides useful insight into the direct relevance of the residual

circulation to the redistribution of chemical tracers with long lifetimes. This is illustrated by the application of the circulations to the transport and hence seasonal and global evolution of the total ozone column distribution. Although a number of uncertainties exist, namely, in the data used and in the interpretation of the mean advective contribution to the total transport without a knowledge of non-negligible eddy transports, the results do show the good correspondence between observed tracer evolution and that which is qualitatively implied by advection by the residual circulations.

As discussed in chapter 5, a complete analysis of the evolution of a tracer requires knowledge of the TEM tracer eddy transport term and the source term for the tracer χ, see equation (5.1). The TEM eddy terms which were neglected in the qualitative tracer redistribution analysis in chapter 5 should be parametrized in a complete two-dimensional model analysis.

A brief experiment was undertaken to examine in more detail the residual circulation in equatorial regions. The experiment used a parametrized forcing of the flow, based on the work of Gray & Pyle (1986), to achieve an approximate SAO representation. This produced a similar flow response to that described in Gray & Pyle (1986) but was found to be of small magnitude compared with the flow forced by the other mechanisms and was therefore found to be insignificant in the budget analyses.

Another aim of this study was to examine the magnitude and variability of the eddy terms in the TEM formulation, so that an assessment of the remaining nature of required parametrization could be made. Clearly the magnitude of D_F using the quasi-geostrophic approximation is not negligible throughout the whole year and, as has been shown in chapter 5, term (3) in equation (6.3) drives a significant component of the residual circulation so that the term D_F must be evaluated. The examination of the momentum and thermodynamic budgets has allowed assessment over a one year period of the re-formulated eddy terms of the TEM equations, equations (6.3) & (6.4). This reveals the virtual elimination, as compared with the traditional Eulerian viewpoint, of the thermodynamic eddy term but affirms the

importance of the retention of the 'body force' accelerating term on the right hand side of the momentum equation. An examination was also made of the momentum and heat budgets using several other circulations which are presently used as stratospheric circulations in models. These included the 'Dunkerton' or diabatic circulation whose definition assumes steady state and is derived from a knowledge of the current instantaneous diabatic forcing in the atmosphere. The diabatic circulation includes the effect of adiabatic influences through its evaluation of [Q],since [Q] is partly determined by adiabatic effects.

Also the residual circulation and its various separable components, defined by the streamfunction terms Ψ_Q, Ψ_S, & Ψ_T as described in chapters 4 & 5, were examined. For each of the residual component circulations the relevant forcing terms (see chapter 4) have been computed from the satellite data.

In chapters 5 and 6 these circulations were compared and their budget and transport consequences discussed. The various circulations, although they include circulation components which resemble the Brewer-Dobson cell, are not the same, and show major differences in magnitude and evolution throughout the year. Using these various circulations in the budget analysis it can be seen that in general the fully-forced residual circulation is the best circulation to use to describe the temporal changes in the zonal mean state, in both the momentum and heat budgets, because it best represents the sign of the mean state changes, $[u]_t$ and $[\theta]_t$. The Dunkerton circulation produces smaller magnitude imbalances in the thermodynamic equation but it gives no information about $[\theta]_t$ and fails to determine the sign of $[u]_t$. However, all the circulations have unresolved imbalances in the momentum budget arising from both errors in method and data and from other inadequacies. The fully-forced or total residual circulation appears more consistent with the budget information compared with both the Dunkerton and [Q]-driven component only, because of the eddy contributions. These enhance the winter poleward cells and help balance the thermodynamic equation and prevent [Q] from disturbing the balance. However none of the circulations derived are totally satisfactory in representing the necessary meridional flow which is required to balance the observed budgets of heat and momentum.

For the period December 1978 to November 1979 the zonal mean wind, its acceleration and the wave forcing have been presented and discussed in terms of EP-flux vectors and the equivalent mass weighted body force. This was done in order to provide further information on the wave, mean interaction occuring throughout the year and to examine the validity and accuracy of the divergence regions calculated in high latitudes. The examination of the seasonal evolution of the EP-flux, in chapter 6, revealed a distinct hemispheric difference in the relative importance of the contributions of the time averaged and transient flux forcing to the residual circulations. The data show a continuous and hence predominantly time-average wave flux in the northern hemisphere, driving most of the circulation but with a highly variable transient eddy flux component also of importance. The separate roles of the transient and time averaged flux components are not the same in the southern hemisphere where the active months, during the period July to September, indicate that it is the transient or highly variable nature of the propagation and subsequent influence of the wave flux which is responsible for a major component of the strong wave forcing throughout the months. These active eddy months during the spring in the southern hemisphere have no similar northern hemispheric equivalent and the analysis described in chapter 6 has allowed this seasonal variation in the forcing, D_F, and EP-flux penetration to be noted. Similar seasonal evolution and hemispheric asymmetries are described by Shiotani & Hirota (1984). Prolonged spring eddy activity in the southern hemisphere could be responsible for part of the differences seen in the evolution of the residual circulations and in the resulting transport differences as described in chapter 5.

The calculations of the EP-flux divergence appear to be especially prone to error in high latitude regions in the upper-middle stratosphere. The EP-flux vectors do indicate a number of occasions, as described in chapter 5, when the possibility of errors resulting from the near cancellation between the convergence of the vertical components and the divergence of the horizontal components is likely. This is partly due to the sensitivity of such a situation close to the pole where error magnification and hence misinterpretation can occur due to the inverse cosine weighting. The results from Robinson (1986) must be considered and any conclusions must be tempered with a

knowledge of the uncertainties he discussed. His work however is based upon idealised model conditions and so it is possible that the values obtained in the present study occur at least in part due to real physical mechanisms observed as a result of the atmosphere breaking the ideal conditions he describes. These mechanisms include wave-wave interactions, instabilities, in-situ wave generation, ageostrophic influences and nonlinear effects (Andrews (1987)). Positive EP-flux divergence may also arise via the action of non-wave like synoptic actions and the associated non-linear dynamics as described by O'Neill & Pope (1988).

In order to assess further the importance of the ageostrophic velocity components upon the EP-flux divergence a single day's circulation was examined. The analysis of the residual circulation for this single day based upon estimated velocities including ageostrophic effects, does indicate that there are differences from the eddy driven circulations calculated geostrophically and hence in the transport which results. Further study based upon the same lines but undertaken more extensively throughout a year is required to assess the full impact of these differences upon the residual circulations deduced. A next step would be to use ageostrophic winds calculated from a non-linear balance equation to assess more precisely the magnitudes of the D_F terms throughout the year and the consequent modifications to the residual circulation. This step was investigated but no satisfactory method of solution of the non-linear balance equation using the real data sets described here was found.

The analysis has shown that the distribution and magnitude of both the transient and time-averaged eddy forcing components are important. Consequently the first three terms on the right-hand side of equation (4.16) and term (d) in equation (5.1) will remain a necessary part of two-dimensional modelling which uses the residual circulation. Parametrization or specification using observational data will be required. Moreover, further parametrization of the smaller scale fluxes not resolved by the model grid, including gravity waves, is an important aim and its satisfactory representation in two-dimensional modelling is an important task if the models are to represent the atmosphere accurately.

The results achieved in investigating the momentum and thermodynamic balances over the year were on the whole poor. However one consequence of the imbalances even in the better months is that the satellite-derived fluxes may prove insufficient to resolve the total flux required for balance and that smaller scale fluxes could provide an important extra decelerative drag upon the mean circulation. The existence and possibly important role of gravity waves has become more evident recently and it is clear that more work is necessary to understand and incorporate their effect in models of the stratosphere and mesosphere (Hunt (1986)).

The use of the traditional Eulerian equations are known to complicate the analysis and interpretation of the true state of the middle atmosphere. By decomposing the residual circulation and using a spherical geometry quasi-geostrophic equation set this thesis has examined, to what extent the residual circulation is influenced by the eddy forcing above and beyond radiative forcing.

It is clear that a number of major unknowns and uncertainties remain as obstacles to the understanding and successful modelling and prediction of the stratospheric system.

A number of important further questions and comments arise from the study including: Is D_F significantly different when calculated using geostrophic velocities compared with a calculation using velocities including ageostrophic components? Are gravity waves significant in the stratosphere? It would also be very illuminating to examine these residual circulations in an operational two-dimensional model. This could be achieved by using the residual circulations calculated in this thesis as 'climatology' for input into a two-dimensional model written in a TEM formulation. The transport effects of the mean circulation components and a TEM eddy parametrization could be examined simultaneously. Alternatively the eddy and diabatic forcing data only, could be used as input for a TEM formulated two-dimensional model to solve for the residual circulations allowing the model circulations to feedback on the mean state and hence subsequent circulations throughout the year. In both the above suggested analyses, some means of handling the eddy transports e.g. the use of eddy transport

coefficients or specifying data (for instance using LIMS data), suitable for the TEM equation set would be needed.

It would also be interesting to use these circulations to solve a tracer conservation equation. This would require the calculation of the mean and eddy flux terms for the tracer, e.g. ozone, using for instance the LIMS data.

The ideas proposed above are several of the most obvious ways in which the present study could be extended. At present no one eddy parametrization and diffusion coefficient set can be rigorously validated. Many models rely therefore on a continual input from observational data of eddy transports. Alternatively in the case of a diabatic circulation, explicit eddy transports are not considered but are included indirectly through the use of some other observational data input i.e. temperature. The role of eddies can be incorporated in some form into two-dimensional models in a diagnostic manner, but they cannot generally be included prognostically.

Further experiments using realistic gravity wave parametrizations could be undertaken to examine the influence and magnitudes of gravity waves in the momentum and heat budgets. As noted above one important area requiring further research is the observation and understanding of the role of gravity waves in the middle atmosphere. Further work is also needed to further assess the importance of the ageostrophic components in the evaluation of div.$\underline{F}$.

APPENDIX A

The full derivation of the residual circulations streamfunction.

$$\frac{\partial}{\partial t}\nabla^2\psi = -J(\psi,\nabla^2\psi + f) + \nabla\left(f\,\nabla\cdot\left[\frac{\partial\chi}{\partial p}\right]\right) + \nabla\cdot(\underline{F}_r \times \underline{k}) \qquad \text{(I)}$$

$$\frac{\partial\theta}{\partial t} = -J(\psi,\theta) + \sigma_e\,\omega + \frac{J}{c_p}\left[\frac{p}{p^s}\right]^{\kappa} \qquad \text{(II)}$$

where $\omega = \nabla^2\chi = \frac{Dp}{Dt}$, $\qquad \sigma_e = -\frac{\partial\theta}{\partial p}$

ψ, is the quasi-geostrophic streamfunction

& $-\frac{\partial\chi}{\partial p} = X$ the velocity potential,

s.t. $v_i = \nabla X$

Frictional force = F_r,

Jacobian, $J(a,b) = \nabla\, a.(\nabla\, b_x \underline{k})$

expanding out and with a little manipulation these basic equations can be written as:

$$\frac{\partial\xi}{\partial t} + v_n.\ \nabla(\xi+f) + v_i.\ \nabla f + f\ \nabla v_i = 0 \qquad \text{(III)}$$

$$\frac{\partial\theta}{\partial t} = -u\frac{\partial\theta}{\partial x} - v\frac{\partial\theta}{\partial y} - \omega\frac{\partial\theta}{\partial p} + Q$$

$$= -u_n\frac{\partial\theta}{\partial x} - v_n\frac{\partial\theta}{\partial y} - u_i\frac{\partial\theta}{\partial x} - v_i\frac{\partial\theta}{\partial y} - \omega_i\frac{\partial\theta}{\partial p} + Q \qquad \text{(IV)}$$

$$\frac{\partial\xi}{\partial t^n} = -u_n\frac{\partial\xi}{\partial x^n} - v_n\frac{\partial}{\partial y}(\xi_n + f) - \mathrm{div}(fv_i) \qquad \text{(V)}$$

multiplying by cosφ and using equations (VIa) & (VIb).

$$\frac{\partial}{\partial x}(u_n c) + \frac{1\partial}{c\partial y}(v_n c) = 0 \qquad \text{(VIa)}$$

$$\frac{\partial}{\partial x}(u_i c) \quad \frac{1\partial}{c\partial y}(v_i c) = -\frac{\partial}{\partial p}(\omega_i c) \qquad \text{(VIb)}$$

which are the non divergent and irrotational flow continuity equations, it is then possible to rewrite the thermodynamic equation as:

$$\frac{\partial}{\partial t}(c\theta) = -\frac{\partial}{\partial x}(u_n c\theta) - \frac{\partial}{\partial y}(v_n c\theta)$$
$$-\frac{\partial}{\partial x}(u_i c\theta) - \frac{\partial}{\partial y}(v_i c\theta) - \frac{\partial}{\partial p}(\omega_i c\theta) + c[Q]$$

(VII)

It is convenient to then write this in the form which when zonally averaged gives

$$\frac{\partial}{\partial t}(c[\theta]) + \frac{\partial}{\partial y}([v_i]c[\theta]) + \frac{\partial}{\partial p}([\omega_i]c[\theta]) + \frac{\partial}{\partial y}([v_n]c[\theta])$$
$$= -\frac{\partial}{\partial y}([v_n{}^* c\theta^*]) - \frac{\partial}{\partial y}([v_i{}^* c\theta^*]) - \frac{\partial}{\partial p}([\omega_i{}^* c\theta^*]) + c[Q]$$

(VIII)

Similarly for the vorticity equation we can write

$$\frac{\partial}{\partial t}(c\xi_n) = -\frac{\partial}{\partial x}(cu_n(\xi_n + f)) - \frac{\partial}{\partial y}(cv_n(\xi_n + f))$$
$$-\text{div.}(fv_i) + (\xi_n + f)\left(\frac{\partial(cu_n)}{\partial x} + \frac{\partial}{\partial y}(cv_n)\right)$$

(IX)

Next zonally averaging we get

$$\frac{\partial}{\partial t}(c[\xi_n]) = -\frac{\partial}{\partial y}(fc[v_i]) \quad -\frac{\partial}{\partial y}(c[v_n^* \xi_n^*]) \qquad \text{(X)}$$

Since

$$\text{div}(f[v_i]) = \frac{1\partial}{c\partial y}(fc[v_i]) \qquad \text{(XI)}$$

next as

$$\xi_n = \nabla_x v_n = \frac{\partial v}{\partial x^n} \quad -\frac{1\partial}{c\partial y}(cu_n) \qquad \text{(XII)}$$

we get

$$\text{So } \frac{\partial^2}{\partial t \partial y}(c[u_n]) = \frac{\partial}{\partial y}(fc[v_i]) + \frac{\partial}{\partial y}(c[v_n^* \xi_n^*]) \qquad \text{(XIII)}$$

which if we integrate with respect to y gives

$$\frac{\partial}{\partial t}(c[u_n]) = fc[v_i] + c[v_n^* \xi_n^*] \qquad \text{(XIV)}$$

The constant of integration vanishes because of the $\cos\psi$ factor tending to zero at both poles. Next consider the zonal mean balance equation.

$$\nabla^2 \phi = \nabla(f \quad \nabla\psi) \qquad \text{(XV)}$$

where $\phi = gZ$

Thus

$$g\,\text{div}.\nabla[Z] = \text{div}(f\nabla[\psi_n]) \qquad \text{(XVI)}$$

where $\nabla[\psi_n] = (0, [\psi_y])$ & $\underline{v} = \underline{k}_x \nabla\psi_n$

Hence

$$g\frac{\partial}{\partial y}(c\frac{\partial[Z]}{\partial y}) = \frac{\partial}{\partial y}(fc\frac{\partial[\psi]}{\partial y}_n) \qquad \text{(XVII)}$$

So integrating w.r.t. y gives

$$gc\frac{\partial[Z]}{\partial y} = fc\frac{\partial[\psi]}{\partial y}_n = -fc[u] \qquad \text{(XVIII)}$$

The hydrostatic equation can be written as:

$$\frac{\partial Z}{\partial p} = \frac{-1}{\varrho g} = \frac{-RT}{pg} = \frac{-R\theta}{pg}\left(\frac{p}{p_o}\right)^K \qquad \text{(XIX)}$$

So combining equations (XVIII) & (XIX) we get:

$$g\frac{\partial[Z]}{\partial y \partial p} = -g\frac{\partial}{\partial y}\frac{R[\theta]}{pg}\left(\frac{p}{p_o}\right)^K = -f\frac{\partial[u]}{\partial p} \qquad \text{(XX)}$$

differentiating equation (XX) w.r.t t and then substituting this into $\partial/\partial p$ of equation (XIV) we then get:

$$f\frac{\partial^2}{\partial t \partial p}(c[u]) = \frac{\partial}{\partial p}(f^2 c[v_i]) + fc\frac{\partial}{\partial p}([v_n^* \xi_n^*])$$

$$-\frac{\partial^2}{\partial t \partial y}\frac{R[\theta]}{p}\left(\frac{p}{p_o}\right)^K = -\frac{\partial}{\partial p}(f^2 c[v_i]) - fc\frac{\partial M}{\partial p} \qquad \text{(XXI)}$$

Where $M = ([v_n^* \xi_n^*])$

Returning to equation (VIII) we can rewrite it as:

$$c\frac{\partial[\theta]}{\partial t} + c[v_i]\frac{\partial[\theta]}{\partial y} + c[\omega_i]\frac{\partial[\theta]}{\partial p} = H_e + c[Q] \qquad \text{(XXII)}$$

Since $[\theta]\frac{\partial}{\partial y}(c[v_i]) + [\theta]\frac{\partial}{\partial p}(c[\omega_i]) = 0$

where $H_e = -\frac{\partial}{\partial y}([v_n^* c\theta^*]) - \frac{\partial}{\partial y}([v_i^* c\theta^*]) - \frac{\partial}{\partial p}([\omega_i^* c\theta^*])$

It is now possible to eliminate $\frac{\partial^2[\theta]}{\partial y \partial t}$ in

equation (XXI) by substituting equation (XXII) into equation (XXI) to give:

$$-f^2\frac{\partial[v_i]}{\partial p_i} - f\frac{\partial M}{\partial p} = -\frac{R}{p_o}\left(\frac{p}{p_o}\right)^{K-1}\{-[v_i]\frac{\partial^2[\theta]}{\partial y} - \frac{\partial[v_i]}{\partial y_i}\frac{\partial[\theta]}{\partial y}$$

$$-\frac{\partial[\omega_i]}{\partial p_i}\frac{\partial^2[\theta]}{\partial y\partial p} - \frac{\partial[\omega_i]}{\partial y_i}\frac{\partial[\theta]}{\partial p} + \frac{\partial}{\partial y}\left(\frac{H_e}{c} + [Q]\right)\} \qquad \text{(XXIII)}$$

It is at this point that it is necessary to replace the meridional velocities with the streamfunction which was defined as:

$$[v^R] = [v] - \frac{\partial}{\partial p}\left(\frac{[v^*\theta^*]}{[\theta_p]}\right) = -\frac{1\partial p\Psi}{c\partial p}$$

$$\& \quad [\omega^R] = [\omega] + \frac{1\partial}{c\partial y}\left(\frac{c[v^*\theta^*]}{[\theta_p]}\right) = \frac{1\partial}{c\partial y}(p\Psi)$$

note: $$[\omega^R]=\frac{dp}{dt} \quad \& \quad [w]^R = \frac{d\eta^R}{dt} = -\frac{1\partial\Psi}{c\partial y} \qquad \text{(XXIV)}$$

note: Since the equations will ultimately be transformed to log pressure coordinates the streamfunction is given here in both coordinate systems.

Before proceeding, it is possible to illustrate the elliptic nature of the equation for the streamfunction without a change of coordinates. So substituting this streamfunction definition into equation (XXIII) we get:

$$-\frac{f^2}{c}\frac{\partial^2}{\partial p^2}(p\Psi) + f^2\frac{\partial^2}{\partial p^2}\left(\frac{[v^*\theta^*]}{[\theta_p]}\right) + f\frac{\partial M}{\partial p}$$

$$= A_1\{\frac{\partial^2[\theta]}{\partial y}\frac{\partial(p\Psi)}{\partial p} - \frac{\partial^2[\theta]}{\partial y}\frac{\partial\left(\frac{[v^*\theta^*]}{[\theta_p]}\right)}{\partial p}$$

$$+\frac{\partial[\theta]}{\partial y}\frac{\partial}{\partial y}\left(\frac{1\partial(p\Psi)}{c\partial p}\right) - \frac{\partial[\theta]}{\partial y}\frac{\partial^2}{\partial y\partial p}\left(\frac{[v^*\theta^*]}{[\theta_p]}\right)$$

$$-\frac{\partial}{\partial y}\left(\frac{1\partial}{c\partial y}(p\Psi)\right)\frac{\partial[\theta]}{\partial p} - \frac{1\partial}{c\partial y}(p\Psi)\frac{\partial^2[\theta]}{\partial y\partial p}$$

$$+\frac{\partial}{\partial y}\left(\frac{1\partial}{c\partial y}\left(\frac{c[v^*\theta^*]}{[\theta_p]}\right)\right)\frac{\partial[\theta]}{\partial p} + \frac{\partial^2[\theta]}{\partial y\partial p}\frac{1\partial}{c\partial y}\left(\frac{c[v^*\theta^*]}{[\theta_p]}\right)$$

$$+ \frac{\partial}{\partial y}\left(\frac{H}{c^e} + [Q]\right) \quad \} \tag{XXV}$$

Where $A_1 = \frac{R}{p_o}\left(\frac{p}{p_o}\right)^{K-1}$

The leading terms of this conical equation give us the information to classify the equation type.

$$ab - h^2 = \left(A_1 \left[\frac{\theta}{c^y}\right]\right)^2 + \frac{4[\theta_p]f^2}{c^2} A_1 \tag{XXVI}$$

So the equation is elliptic as required if the following conditions hold

$$[\theta_p] < 0 \quad \text{and} \quad \frac{4[\theta_p]f^2}{A_1[\theta_y]^2} > 1 \tag{XXVII}$$

Finally rewriting this in log pressure coordinates and rearranging the terms we get equation (XXVIII)

$$-\frac{f^2}{c}\frac{\partial^2 \Psi}{\partial \eta} + \frac{f^2}{c}\frac{\partial \Psi}{\partial \eta} - A_1 p \frac{\partial [\theta]}{\partial y}\frac{\partial}{\partial y}(\Psi) c$$

$$+A_1 p \frac{\partial [\theta]}{\partial y}\frac{\partial}{\partial y}\left(\frac{1}{c}\frac{\partial \Psi}{\partial \eta}\right) + \frac{A_1}{c} p \frac{\partial^2 [\theta]}{\partial y}\left(\frac{\partial \Psi}{\partial \eta} - \Psi\right)$$

$$-A_1 p \frac{\partial}{\partial y}\left(\frac{1}{c}\frac{\partial [\theta]}{\partial \eta}\frac{\partial \Psi}{\partial y}\right)$$

$$= \frac{1}{c}\{ \frac{f}{a}\{\frac{\partial}{\partial \eta}\left(\frac{1}{\rho_o}\frac{\partial}{\partial \eta}\left(a\rho_o \frac{[v^* \theta^*]}{[\theta_\eta]} fc\right) - \frac{1}{c}\frac{\partial}{\partial y}(ac^2[u^* v^*])\right) \}$$

$$-A_1 pc \frac{\partial}{\partial y}\left(\frac{\partial [\theta]}{\partial y}\frac{\partial}{\partial \eta}\left(\frac{[v^* \theta^*]}{[\theta_\eta]}\right) - \frac{\partial [\theta]}{c \partial \eta}\frac{\partial}{\partial y}\left(\frac{c[v^* \theta^*]}{[\theta_\eta]}\right)\right)$$

$$-A_1 pc \frac{\partial}{\partial y}\left(\frac{1}{c}\frac{\partial (c[v^* \theta^*])}{\partial y} - [Q]\right) \} \tag{XXVIIIa}$$

the right hand side can also be written as

$$= \frac{1}{c}\{ \frac{f\partial}{a\partial\eta}(\frac{1}{\varrho_o}\nabla.\underline{F})$$

$$-A_1 pc\frac{\partial}{\partial y}(i\times\frac{\nabla\theta}{\varrho_o}.\ div(\varrho_o[\underline{v^*\theta^*}]))_{[\theta_\eta]}$$

$$-A_1 pc\frac{\partial}{\partial y}(\frac{1\partial}{c\partial y}(c[v^*\theta^*]) \quad - [Q] \quad) \}$$

(XXVIIIb)

The full partial differential equation of the residual circulation using a quasi-geostrophic equation set applicable to the spherical earth.

A more common reformulation of these terms is as follows:

$$= \frac{1}{c}\{\frac{f\partial}{a\partial\eta}(\frac{1}{\varrho_o}\nabla.\underline{F}\ )$$

$$-A_1 pc\ \frac{\partial}{\partial y}(\frac{1}{\varrho_o}\frac{\partial}{\partial\eta}[\theta_y]\ \varrho_o\frac{[\underline{v^*\theta^*}]}{[\theta_\eta]}\ )\ -[Q] \quad) \}$$

(XXIX)

At the equator it is necessary to evaluate the streamfunction differently, since at this point only does the equation go hyperbolic due to a singularity at $\varphi=0$ arising from a $(\tan\varphi)^{-1}$ term in the equation. Therefore returning to equation (XXII) and differentiating w.r.t. y we get:

$$\frac{\partial^2[\theta]}{\partial t\partial y} + [v_i]\frac{\partial^2[\theta]}{\partial y^2} + \frac{\partial[v_i]}{\partial y}\frac{\partial[\theta]}{\partial y} + \frac{\partial[\omega_i]}{\partial y}\frac{\partial[\theta]}{\partial p}$$

$$+ [\omega_i]\frac{\partial^2[\theta]}{\partial y\partial p} = \frac{\partial}{\partial y}(\frac{H}{c^e} + [Q]\ )$$

(at $\varphi = 0$) (XXX)

By assuming

$$\frac{\partial[\theta]}{\partial y} = 0 \quad \text{at} \quad \varphi=0 \quad (\text{but} \quad \frac{\partial^2[\theta]}{\partial y^2} \neq 0)$$

Equation (XXX) reduces to

$$[\underline{\theta}_{yy}]\frac{1}{c}\frac{\partial\Psi}{\partial\eta} - [\underline{\theta}_{yy}]\frac{\Psi}{c} - [\underline{\theta}_{\eta}]\frac{\partial}{\partial y}\left(\frac{1}{c}\frac{\partial\Psi}{\partial y}\right)$$

$$-[\underline{\theta}_{y\eta}]\frac{\partial\Psi}{\partial y} = \frac{\partial}{\partial y}\left(\frac{H}{c^e} + [Q]\right) \qquad \text{(XXXI)}$$

A second order parabolic equation for Ψ with no singularity. This equation is only used at the equator.

APPENDIX B

Following on from appendix A the two streamfunction equations which are to be solved numerically are:

$$\frac{f^2}{c}\left(\frac{\partial\Psi}{\partial\eta} - \frac{\partial^2\Psi}{\partial\eta^2}\right) + \frac{A_1}{c}p[\theta]_{yy}\left(\frac{\partial\Psi}{\partial\eta} - \Psi\right)$$

$$+\frac{A_1}{c}p[\theta]_y\left(\frac{\tan\varphi}{a}\left(\frac{\partial\Psi}{\partial\eta} - \Psi\right) + \frac{\partial}{\partial y}\left(\frac{\partial\Psi}{\partial\eta} - \Psi\right)\right)$$

$$-\frac{A_1}{c}p[\theta]_\eta\left(\frac{\tan\varphi}{a}\frac{\partial\Psi}{\partial y} + \frac{\partial^2\Psi}{\partial y^2}\right) - [\theta]_{\eta y}\frac{A_1}{c}\frac{\partial\Psi}{\partial y} = RHS \qquad \text{(XXXII)}$$

$$\frac{[\theta]}{c}_{yy}\left(\frac{\partial\Psi}{\partial\eta} - \Psi\right) - \frac{[\theta]}{c}_\eta\left(\frac{\partial^2\Psi}{\partial y^2} + \frac{\tan\varphi}{a}\frac{\partial\Psi}{\partial y}\right) - \frac{[\theta]}{c}_{\eta y}\frac{\partial\Psi}{\partial y} = RHS_e \qquad \text{(XXXIII)}$$

For the equator (XXXIII), and the remaining gridpoints (XXXII). Each differential operator has been approximated using a simple second order centered difference scheme as follows.

$$\Psi_{\eta\eta} = \frac{\Psi_{i\,j+1} - 2\Psi_{i\,j} + \Psi_{i\,j-1}}{h_z^2} \qquad \Psi_\eta = \frac{\Psi_{i\,j+1} - \Psi_{i\,j-1}}{2h_z}$$

$$\Psi_{yy} = \left(\frac{\Psi_{i+1\,j} - 2\Psi_{i\,j} + \Psi_{i-1\,j}}{h_\varphi^2}\right) \qquad \Psi_y = \left(\frac{\Psi_{i+1\,j} - \Psi_{i-1\,j}}{2h_\varphi}\right)$$

$$\Psi_{\eta y} = \left(\frac{\Psi_{i+1\,j+1} - \Psi_{i+1\,j-1} - \Psi_{i-1\,j+1} + \Psi_{i-1\,j-1}}{4h_\varphi h_z}\right) \qquad \text{(XXXIV)}$$

The following finite difference stencil form has been used with i increasing from 90° S to 90° N and j increasing with η increasing. h_φ and h_z are the horizontal and vertical finite difference intervals used for the numerical integration being determined by the grid used of $d\eta = 0.75$ and $d\varphi = \pi/36$ (rad's). i & j are indices in the φ and η directions.

$P_{i\,j+1}$

× × ×

$P_{i-1\,j}$ × × × $P_{i+1\,j}$

$P_{i\,j}$

× × ×

$P_{i\,j-1}$

Substitution of these equations into (XXXII) & (XXXIII) gives the two equations of the form:

$$AP_{i\,j} + BP_{i\,j+1} + CP_{i\,j-1} + DP_{i+1\,j} + EP_{i-1\,j}$$

$$+ FP_{i+1\,j+1} + GP_{i+1\,j-1} + HP_{i-1\,j-1} + JP_{i-1\,j+1} = RHS \qquad \text{(XXXV)}$$

$$AAP_{i\,j} + BBP_{i\,j+1} + CCP_{i\,j-1} + DDP_{i+1\,j} + EEP_{i-1\,j} = RHS_e \qquad \text{(XXXVI)}$$

where here the coefficients are:

$$A = \left(\frac{2f^2}{ch_z^2} - \frac{A_1\rho}{c}\left(\frac{[\theta]_y}{a}\tan\varphi + [\theta]_{yy} - \frac{2[\theta]_\eta}{h_\varphi}\right)\right)$$

$$B = \frac{f^2}{c}\left(\frac{1}{2h_z} - \frac{1}{h_z^2}\right) + \frac{A_1\rho}{h_z}\left([\theta]_y\frac{\tan\varphi}{a} + [\theta]_{yy}\right)$$

$$C = \frac{-1}{ch_z}\left(f^2\left(\frac{1}{2} + \frac{1}{h_z}\right) + \frac{A_1\rho}{2}\left([\theta]_y\frac{\tan\varphi}{a} + [\theta]_{yy}\right)\right)$$

$$D = -\frac{A_1\rho}{h_\varphi}\left(\frac{[\theta]_y}{2} + \frac{[\theta]_{y\eta}}{2} + [\theta]_\eta\left(\frac{1}{h_\varphi} + \frac{\tan\varphi}{2a}\right)\right)$$

$$E = \frac{A_1\rho}{h_\varphi}\left(\frac{[\theta]_y}{2} + \frac{[\theta]_{\eta y}}{2} + [\theta]_\eta\left(\frac{\tan\varphi}{2a} - \frac{1}{h_\varphi}\right)\right)$$

$$F = \frac{A_1\rho[\theta]_y}{4ch_\varphi h_z}, \quad G=-F, \quad H=F, \quad J=-F$$

$$AA = \frac{2[\theta]_\eta}{ch_\varphi^2} - \frac{[\theta]_{yy}}{c}, \quad BB = \frac{[\theta]_{yy}}{2ch_z}$$

$$CC = -BB$$

$$DD = -\left(\frac{[\theta]}{ch_\varphi}{}_{2\eta} + \frac{[\theta]}{2h_\varphi c}{}_{y\eta}\right), \quad EE = \left(\frac{[\theta]}{2h_\varphi c}{}_{y\eta} - \frac{[\theta]}{h_\varphi^2 c}{}_{\eta}\right)$$

(XXXVII)

Note:

RHS = as defined in appendix A.

$$RHS_e = \left(\frac{\partial}{\partial y}\left(\frac{H}{c^e}\right) + \frac{\partial [Q]}{\partial y}\right)$$

Each coefficient has been calculated at all points on the grid as has the RHS_{ij} term. This is then solved using the SOR method so that Ψ_{ij} is iteratively approached using an upper error bound, delta=Δe_{ij}, of $\Delta e_{ij} = 1.10^{-6}$. The SOR procedure works by assuming that the m^{th} guess of the tendency at the point (i,j) is $\Psi_{ij}{}^m$. So equation (XXXV) for example, is written in the form.

$$\Psi_{ij}{}^{m+1} + \left(\frac{B}{A}_{ij}\right)\Psi_{ij+1}{}^m + \left(\frac{C}{A}_{ij}\right)\Psi_{ij-1}{}^m + \left(\frac{D}{A}_{ij}\right)\Psi_{i+1j}{}^m$$

$$+\left(\frac{E}{A}_{ij}\right)\Psi_{i-1j}{}^m + \left(\frac{F}{A}_{ij}\right)\left(\Psi_{i+1j+1}{}^m - \Psi_{i+1j-1}{}^m\right.$$

$$\left. -\Psi_{i-1j+1}{}^m + \Psi_{i-1j-1}{}^m\right)$$

$$-\left(\frac{RHS}{A}_{ij}\right) = E_{ij}{}^m$$

(XXXVIII)

Here $E_{ij}{}^m$ is a measure of the error of the guess. The relaxation reduces the E's, until they are all below the prescribed accuracy chosen, Δe. This is achieved by on each iteration and evaluation of $\Psi_{ij}{}^m$, that $\Psi_{ij}{}^m$ is modified by the quantity $(1+\alpha)E_{ij}{}^m$ which will gradually reduce the E's to zero at this particular point. However this has to be repeated for all the points on the grid and adjacent points do not necessarily improve by the

reduction of E at the point (i,j). Nevertheless each iteration represents progress and the method converges (for suitable differential equations.) toward the true solution for the tendencies, Ψ.

The above method uses an over relaxation by including the $(1+\alpha)$ multiplier in its modification on each re-evaluation of Ψ_{ij}^{m+1}. This reduces the time required for convergence. Also the Ψ^{m+1} is implemented immediately in a method known as sequential relaxation which also leads to a more rapid convergence. So that equation (XXXVIII) is strictly written as:

$$\Psi_{ij}^{m+1} + \left(\frac{B}{A_{ii}}_{ij}\right)\Psi_{ij-1}^{m} + \left(\frac{C}{A_{ij}}_{ij}\right)\Psi_{ij-1}^{m+1} + \left(\frac{D}{A_{ij}}_{ij}\right)\Psi_{i+1j}^{m}$$
$$+\left(\frac{E}{A_{ij}}_{ij}\right)\Psi_{i-1j}^{m+1} + \left(\frac{F}{A_{ij}}_{ij}\right)\left(\Psi_{i+1j+1}^{m} - \Psi_{i+1j-1}^{m+1}\right.$$
$$\left.-\Psi_{i-1j+1}^{m} + \Psi_{i-1j-1}^{m+1}\right) - \left(\frac{RHS}{A_{ij}}_{ij}\right) = E_{ij}^{m} \qquad \text{(XXXIX)}$$

where

$$\Psi_{ij}^{m+1} = \Psi_{ij}^{m} + (1+\alpha)E_{ij}^{m} \qquad \text{(XXXX)}$$

The calculation is undertaken for all internal points, a dirichelet condition is used for the external grid points, Ψ is assumed as equal to zero on all boundaries. i.e. at 90°S, 90°N , η=0 and η=12.0.

Having solved for Ψ it is possible using the definition the streamfunction to calculate the residual and Eulerian velocity fields, since the residual velocities have been defined in terms of Ψ by equations (XXIV), see appendix A. The fields are calculated using numerical finite difference forms as per equations (XXXIII), to

approximate the gradients in equations (XXIV). Thus centered difference finite difference forms are used whenever possible, except at boundaries. (see below) At both both poles [w] and $[w]^R$ are obtained by considering

$$\lim_{\varphi \to \pm\pi} \quad -\frac{1}{c}\frac{\partial \Psi}{\partial y} = \frac{a}{\sin\varphi}\frac{\partial^2 \Psi_2}{\partial y^2}\Big|_{\varphi=\pm\pi} \qquad \text{(XXXXI)}$$

It is assumed that Ψ is symmetrical across the pole and that $\Psi=0$ at both poles, then we can write:

$$\frac{\partial^2 \Psi}{\partial y^2}\Big|_{\varphi=\pm\pi} = 2\Psi/\Delta y^2 \;|_{\,85^\circ}$$

$$\Rightarrow \; [w]^R \;|_{90^\circ N} = 2\Psi/a h_\varphi^2 \;|_{85^\circ N}, \; [w]^R \;|_{90^\circ S} = -2\Psi/a h_\varphi^2 \;|_{85^\circ S} \qquad \text{(XXXXII)}$$

[v] and $[v]^R$ at the top and bottom of the grid are calculated using a one sided difference scheme. i.e.

$$f'_{btm} \quad +O(a^2) = \frac{(4f(x+h)-3f(x)-f(x+2h))}{2h}$$

$$f'_{top} \quad +O(a^2) = \frac{(3f(x)+f(x-2h)-4f(x-h))}{2h} \qquad \text{(XXXXIII)}$$

Ψ_E is defined by the relation

$$\Psi = \Psi_E - c\frac{[v^* \theta^*]}{[\theta]_\eta} \qquad \text{(XXXXIV)}$$

So Ψ_E and hence [v] & [w] can be calculated knowing Ψ.

APPENDIX C

EP-FLUX VECTOR DIAGRAMS: GRAPHICAL CONVENTIONS.

The EP-flux cross section displays are defined by the spherical geometry formulas:

$$F_{\varphi} = -a\cos\varphi[v^{*}u^{*}]\varrho_{o} \qquad \{kgs^{-2}\} \qquad (C1)$$

$$F_{\eta} = fa\cos\varphi[v^{*}\theta^{*}]\varrho_{o}[\theta_{\eta}] \qquad \{kgs^{-2}m^{-1}\} \qquad (C2)$$

where φ is latitude, a- the radius of the earth, and f is $2\Omega\sin\varphi$ where Ω is the angular velocity; $[\theta_{\eta}]$ is taken as a function of latitude and log-pressure.

The EP-flux divergence is therefore written as:

$$\nabla.F = \frac{1}{ac\partial\varphi}(F_{(\varphi)}) + \frac{\partial}{\partial\eta}(F_{(\eta)}) \qquad \{kgs^{-2}m^{-1}\} \qquad (C3)$$

The following graphical conventions for representing F and its divergence pictorially will be adopted along the lines of Edmon et al (1980) & Dunkerton, Hsu & McIntyre (1981). The volume element for integrating (C3) over a zonally symmetric portion of the atmosphere is in η-coordinates

$$dV = 2\pi a^{2}H\cos\varphi d\varphi d\eta \qquad (C4)$$

So from (c3) and (c4)

$$\int \nabla.F \; dV = \int \Delta d\varphi d\eta$$

where

$$\Delta = \frac{\partial}{\partial y}(2\pi a^2 H \cos\varphi F_{(\varphi)}) + \frac{\partial}{\partial \eta}(2\pi a^2 \cos\varphi F_{(\eta)} H) \qquad \text{(C6)}$$

$$\{kgm^2 s^{-1} \equiv J\}$$

Here Δ is the natural form of the divergence of F for contouring in the (φ,η) plane, since by (C5) the volume between the plane and a surface at a distance $\Delta(\varphi,\eta)$ from it equals

$$\int \nabla.F \; dV$$

The arrows will be drawn with the horizontal and vertical components proportional to the quantities in brackets above, in (C6), viz.,

$$\{F_{(\varphi)}, F_{(\eta)}\} \equiv 2\pi a^2 H \cos\varphi \; (\underline{F}_{a(\varphi)}, \underline{F}_{(\eta)}) \qquad \text{(C7)}$$

$$\{ \text{ J, energy } \}$$

expressed in terms of scale units for φ and η in the diagram. So the horizontal and vertical arrow components as measured on the diagrams to obtain SI units must be multiplied by factors proportional to the distance occupied on the diagram by one radian of latitude and one log-pressure interval.

This determines the direction and relative magnitudes of the arrows uniquely and so equation (C6) then implies that the pattern of arrows will look non-divergent if and only if div.F = 0.

APPENDIX D

SYMBOL LIST

a Radius of the earth.

A_1 $= \frac{R}{p_o}(p/p_o)^{K-1}$

c_p Specific heat capacity of air.

c abbreviation for cosine(φ)

D_F div F/($a\varrho c$)

f Coriolis parameter.

f_o Coriolis parameter assumed constant on the f-plane.

F_r Frictional force.

$F, \underline{F}$ EP-flux vector.

g Acceleration due to gravity.

h_φ Latitudinal grid interval in relaxation finite differencing equations.

h_z Vertical grid interval in the relaxation finite differencing equations.

H Atmospheric scale height.

H_e Eddy Heat flux terms.

$J()$ Jacobian operator.

J diabatic source function

k vertical coordinate vector.

N^2 Brunt Vaisala frequency.

M Eddy momentum flux.

p Pressure.

p_s , p_o	=1000mb pressure.
Q	Diabatic source function.
Q_x	Quantity X source function.
q	quasi geostrophic potential vorticity.
R	Gas constant.
S	Source function.
T	Temperature.
t	time.
u,U	x-component velocity.
v	y- component velocity.
V_o	basic state velocity.
w	vertical velocity, $\partial\eta/\partial t$.
w_o	correction velocity to w^D due to mass balance.
x	E-W horizontal distance co ordinate.
x	position vector.
y	S-N horizontal distance co ordinate.
z	Vertical distance co ordinate.
Z	Geopotential height.
a	notation for vector quantity of variable a.
χ	arbitary variable.
λ	longitude
π	pi
δ	delta- small increment.
θ	potential temperature.
φ	latitude.
ω	vertical velocity, $\partial p/\partial t$.

ϕ Geopotential height

ψ geostrophic streamfunction.

ϱ, ϱ_o density

ϵ displacement vector.

ξ absolute vorticity.

η log pressure vertical co ordinate.

Γ Lapse rate.

Γ_d Dry adiabatic lapse rate.

σ_e static stability.

κ R/c_p

Ψ The residual meridional circulation streamfunction.

Ψ_E The Eulerian meridional circulation streamfunction.

Ω Omega, the planetary vorticity.

Δ is the natural form of the divergence of **F** for contouring in the (φ,η) plane. See appendix C. Units of joules.

e Upper error bound used in Numerical relaxation calculation.

div Divergence operator

∇ Grad operator

Superscripts

I	Lagrangian disturbance associated quantity.
L	Lagrangian average
ξ	disturbance related variable.
s	Stokes correction
R	residual component
D	Diabatic circulation component.
'	perturbation from the time mean.
—	overbar- time-average.
[]	zonal average.
*	perturbation from zonal average.

Subscripts

j,k	tensor notation.
,jk	differentiated in directions j & k tensor notation.
x,y,p,t	differentiated by
ψ	ψ is the geostrophic streamfunction so that $u_\psi=-\psi_y$ and $v_\psi=\psi_x$.
n	Non-divergent vector component. $V=V_n+V_i$.
i	Irrotational component.
$X_{(\varphi)}$	φ component of vector variable X.

APPENDIX E

THE DUNKERTON DIABATIC CIRCULATION.

The Dunkerton diabatic circulation was calculated based upon the formulation in Dunkerton (1978), but using a different data set. The vertical velocity is defined as :

$$[w]^D_1 = \frac{[Q]}{[\theta_\eta]} \left(\frac{p}{p_o}\right)^{R/c_p} \{s^{-1}\} \qquad \text{(E1)}$$

Each level was adjusted to maintain no net mass flux across a surface by modifying $[w_\varphi]^D_1$ as follows:

$$w_o = \frac{\Sigma_{\varphi=-90}^{\varphi=90} [w_\varphi]^D_1 c_\varphi}{\Sigma_{\varphi=-90}^{\varphi=90} c_\varphi} \qquad \text{(E2)}$$

and so setting $[w]^D = [w]^D_1 - w_o$. (E3)

The continuity equation was then integrated to obtain $[v]^D$.

$$[v]^D = -\frac{1}{c}\int_{\varphi}^{\varphi+\delta\varphi} \left(\frac{ac}{\varrho_o}\right) \frac{\partial}{\partial\eta}\left([w]^D \varrho_o\right) d\varphi \; . \qquad \text{(E4)}$$

$[v]^D$ at both poles was set to zero.

APPENDIX F
REFERENCES

Al-Ajmi,D.N., R.S.Harwood, & T.Miles (1985) A Sudden warming in the middle atmosphere of the southern hemisphere. Quart. J.R. Met. Soc., **111**, 359-389

Andrews,D.G.& M.E.McIntyre (1976) Planetary waves in horizontal and vertical shear: the generalised Eliassen-Palm relation and the zonal acceleration. J.Atmos.Sci., **33**, 2031-2048

Andrews,D.G.& M.E.McIntyre (1978a) An exact theory of nonlinear waves on a Lagrangian mean-flow. J.Fluid Mech., **89**, 609-646

Andrews,D.G. & M.E.McIntyre (1978b) Generalised Eliassen-Palm & Charney-Drazin Theorems for waves on axisymmetric mean-flows in compressible atmospheres. J.Atmos.Sci., **35**, 175-185

Andrews,D.G. J.D.Mahlman & R.W.Sinclair , (1983) Eliassen-Palm Diagnostics of Wave, mean-flow Interaction in the GFDL 'SKYHI' GCM. J.Atmos. Sci., **40**, 2768-2784

Andrews,D.G. (1983) A conservation law for small amplitude quasi- geostrophic disturbances on a zonally asymmetric basic flow. J.Atmos.Sci., **40**, p85-90

Andrews,D.G. (1987) On the interpretation of the EP-flux divergence Quart. J.R. Met. Soc., **113**, 323-338

Austin,J. & A.F.Tuck (1985) The calculation of stratospheric air parcel trajectories using satellite data. Quart. J.R. Met. Soc., **111**, 279-307.

Barnett,J.J. & M.Corney (1985) Middle atmosphere reference model derived from satellite data. Middle atmosphere program handbook for M.A.P. Vol **16**, 47-85

Brasseur,G. & S.Solomon (1984) Aeronomy of the middle atmosphere. Chemistry and Physics of the stratosphere and mesosphere. D.Reidel 441pp

Brewer,A.W (1949) Evidence for a world circulation provided by measurement of helium and water vapour distribution in the stratosphere. QUART.J.R. Met. Soc., **75**, 351-363

Butchart,.N, S.A.Clough, T.N.Palmer & P.J.Trevelyan (1982) Simulations of an observed stratospheric warming with quasi-geostrophic refractive index as a model diagnostic. Quart.J.R.Met.Soc., **108**, 475-502

Charney,J.G.& P.G.Drazin, (1961) Propagation of planetary scale disturbances from the lower into the upper atmosphere. J.Geophys.Res., **66**, 83-109

Clough,S.A., N.S.Grahame, & A.O'Neill (1985) Potential vorticity in the stratosphere derived using data from satellites. Quart. J.R. Met. Soc., **111**, 335-358.

Crane,A.J., J.D.Haigh, J.A.Pyle & C.F.Rogers (1980) Mean meridional circulations of the stratosphere and mesosphere. Pure Appl. Geophys., **18**, 307-328

Cunnold,D.M., F.N.Alyea & R.G.Prinn (1975) Preliminary calculations concerning the maintenance of the zonal mean ozone distribution in the northern hemisphere. Pure Appl. Geophys., **118**, 329-354

Dickinson,R.E (1969a) Theory of planetary wave-zonal flow interaction. J.Atmos.Sci., **26**, 73-81

Dickinson,R.E. (1969b) Vertical Propagation of planetary Rossby waves through an atmosphere with newtonian cooling. J.Geophys. Res., **74**, 929- 938

Dopplick (1971) The energetics of the lower stratosphere including radiative effects. Quart.J.R.Met. Soc., **97**, 207- 237

Dunkerton,T.J (1978) On the mean meridional mass motions of the stratosphere and mesosphere. J.Atmos.Sci., **35**, 2325-2333

Dunkerton,T.J (1980) A Lagrangian mean theory of wave, mean-flow interaction with application to non-acceleration and its breakdown. Rev.Geophys. Space Phys. **18**, 387-400

Dunkerton (1981) Wave transience in a compressible atmosphere. Part I. Transient internal wave, mean- flow interaction. J.Atmos.Sci., **38**, 281-297

Dunkerton,T.J,C-P.F.Hsu & M.E McIntyre (1981) Some Eulerian and Lagrangian diagnostics for a model stratospheric warming. J.Atmos.Sci., **38**, 819-843

Edmon,H.J. jr (1980) Study of the general circulation over the northern hemisphere during the winters of 1976-1977. Mon. Weath. Rev., **108**, 1538-1553

Edmon,H.J jr,B.J. Hoskins & M.E.McIntyre (1980) Eliassen-Palm cross-sections for the troposphere. J.Atmos.Sci., **37**, 2600-2616

Eliassen,A (1951) Slow thermally or frictionally forced meridional circulations in a circular vortex. Astrophysica Norv., **5**, 19-60

Eliassen,A & Palm,E (1960) On the transfer of energy in stationary mountain waves. Geofys. Publ. **22** No 3,1-23

Fels,S.B. (1985) Radiative-dynamical interactions in the middle atmosphere. Advances in Geophysics, **28A**, Academic Press, Edited by Saltzmann & Manabe.

Garcia,R.R. & S.Solomon, (1983) A numerical model of the dynamical and chemical structure of the middle atmosphere. J.Geophys. Res., **88** No. C2, 1379-1400

Geller,M.A. (1983) Dynamics of the middle atmosphere. Space Science Rev., **34**, 359-375

Geller,M.A., Mao-Fou Wu, & M.E.Gelman (1983b) Troposphere-Stratosphere (surface to 55km) monthly winter general circulation statistics for the northern hemisphere - four-year averages. J.Atmos. Sci., **40**, 1334-1352.

Geller,M.A., Mao-Fou Wu, & M.E.Gelman (1984) Troposphere-Stratosphere (surface to 55km) monthly winter general circulation statistics for the northern hemisphere - interannual variations. J.Atmos. Sci., **41**, 1726-1744.

Gille,J.C. J.M.Russell III,P.L.Bailey, L.L.Gordley, E.E.Remsberg, J.H.Leinesch, W.G.Planet, F.B.House, L.V.Lyjak, & S.A.Beck. (1984a) Validation of Temperature retrievals obtained by the limb infra-red monitor of the stratosphere experiment on Nimbus 7. J.Geophys.Res., **89**, 5147-5160

Gille,J.C. J.M.Russell III, P.L.Bailey, E.E.Remsberg, L.L.Gordley, W.F.J.Evans, H.Fischer, B.W.Gandrud, A.Girard, J.E.Harries, S.A.Beck. (1984b) Accuracy and precision of the nitric acid concentrations determined by the LIMS experiment on Nimbus 7. J.Geophys.Res., **89**, 5179-5190

Gille,J.C. & J.M.Russell (1984) The Limb infra-red monitor of the stratosphere: experiment, description, performance and results. J.Geophys.Res., **89**, 5125-5140

Gray,L.J. & J.A.Pyle (1986) The semi-annual oscillation and equatorial tracer distributions Quart.J.R. Met. Soc., **112**, 387-407

Green,J.S.A (1970) Transfer properties of the large scale eddies and the general circulation. Quart.J.R. Met. Soc., **96** 157-185

Haigh,J.D. (1984) Radiative heating in the lower stratosphere and the distribution of ozone in a two-dimensional model. Quart.J.R. Met. Soc., , **110**, 167-185

Hamilton,K. (1982) Stratospheric circulation statistics. NCAR technical note NCAR/TN -191 + STR, Boulder, Colorado.

Hamilton,K. (1983) Diagnostic study of the momentum balance in the northern hemisphere winter stratosphere. Mon. Weath. Rev., **111**, 1434-1441

Hartmann,D.L. (1976) The dynamical Climatology of the stratosphere in the southern hemisphere during late winter 1973. J.Atmos.Sci., **33**, 1789-1802

Hartmann,D.L., C.R.Mechoso, & K.Yamazaki (1984) Observations of wave-mean flow interaction in the southern hemisphere. J.Atmos. Sci., **40**, 351-362.

Harwood,R.S. & J.A.Pyle, (1975) A two- dimensional mean circulation model for the atmosphere below 80km. Quart.J.R. Met. Soc., **101**, 723-747

Harwood,R.S. & J.A.Pyle (1980) The dynamical behaviour of a two-dimensional model of the stratosphere. Quart. J.R. Met. Soc., **106**, 395-420

Hess,P.G. & J.R.Holton (1985) The origin of temporal variance in long-lived trace constituents in the summer stratosphere. J.Atmos.Sci., **42**, 1455-1463

Hirota,I. & Y.Sato (1969) Periodic variation of the winter stratospheric circulation and intermittent vertical propogation of planetary waves. J.Met.Soc. Japan **47**, 390- 402

Hitchman,M.H. (1985) An observational study of wave, mean-flow interaction in the equatorial middle atmosphere. PhD Thesis. University of Washington.

Holopainen,E.O., L.Rontu & N.C.Lau (1982) The effect of large scale transient eddies on the time mean-flow in the atmosphere. J.Atmos.Sci., **39**, 1972-1984

Holton,J.R. (1974) "Forcing of mean flows by stationary waves". J.Atmos.Sci., **31**, 942-945

Holton,J.R. (1975) "The dynamic meteorology of the stratosphere and the mesosphere". Meteorology Monograph NO 37 vol **15** 216pp

Holton,J.R. (1979) An introduction to Dynamic Meteorology. Volume 23 IGS, 2nd Edition. Academic Press. 391pp

Holton,J.R. (1980) Wave propagation and transport in the middle atmosphere. Phil.trans.R.S.London. **A296**, 73-85

Holton,J.R. (1981) An advective model for two-dimensional transport of stratospheric trace species. J.Geophys.Res., **86** 11989-11994

Holton,J.R. (1982) The role of gravity waves induced drag and diffusion in the momentum budget of the mesosphere. J.Atmos.Sci., **39**, 791-799

Holton,J.R. & T.Dunkerton (1978) On the role of wave transience and dissipation in the stratospheric mean-flow vacillations. J.Atmos.Sci., **35**, 740- 744

Holton,J.R. & W.M.Wehrbein, (1980a) A Numerical model of the zonal mean circulation of the middle atmosphere. Pure Appl. Geophys., **118**, 284-306

Holton,J.R. & W.M.Wehrbein (1980b) The role of forced planetary waves in the annual cycle of the zonal mean circulation in the middle atmosphere. J.Atmos.Sci., **37**, 1968-1983

Hunt,B.G. (1986) The impact of gravity wave drag and diurnal variability on the general circulation of the middle atmosphere. J. Met. Soc. Japan., **64**, 1-16.

Kanzawa,H. (1982) Eliassen - palm flux diagnostics and the effect of the mean wind on planetary wave propagation for an observed sudden stratospheric warming. J.Met.Soc. Japan **60**, 1063 - 1073

Kiehl,J.T. & S.Solomon (1986) On the radiative balance of the stratosphere J.Atmos. Sci., **43**, 1525-1534

Kurzeja,R.J. (1983) The transport of trace chemicals by planetary waves in the stratosphere part II: transport of O_3 & N_2O by transient waves. J.Atmos.Sci., **40**, 2036-2054

Lau,.N.C. & A.H.Oort (1981) A comparitive study of observed northern hemisphere circulation statistics based on GFDL and NMC analyses. Part I: The time mean fields. Mon. Weath. Rev., **109**, 1380-1403

Lau,.N.C. & A.H. Oort (1982) Part II: Transient eddy statistics and the energy cycle. Mon. Weath. Rev., **110**, 889-906.

Leovy,C. (1964) Simple models of thermally driven the mesospheric circulation. J.Atmos. Sci., **21**, 327-341

Leovy,C.B., C-R.Sun, M.H.Hitchman, E.E.Remsberg, J.M.Russell,III, L.L.Gordley, J.C.Gille & L.V.Lyjak (1985) Transport of ozone in the middle stratosphere: Evidence for planetary wave breaking. J.Atmos.Sci., 42, 230-244

Lorenz,E.N. (1960) Energy and numerical weather prediction. Tellus **12**, No 4, 364-373

Mahlman,J.D.& W.J.Moxim (1978) Tracer simulation using a global general circulation model: results from a mid-latitude instantaneous source experiments. J.Atmos.Sci., **35**, 1340-1374

Mahlman,J.D., H.Levy II & W.J.Moxim (1980) Three-dimensional tracer structure and behaviour as simulated in two ozone precursor experiments. J.Atmos.Sci., **37**, 655-685

Mahlman,J.D. & J.L.Umscheid (1984) Dynamics of the middle atmosphere: success and problems of the GFDL SkyHi GCM. From 'Dynamics of the middle atmosphere' Editors J.R.Holton & T.Matsuno, Terrapub., Tokyo, 501-525.

Mahlman,J.D. D.G. Andrews, H.U.Dutsch, D.L.Hartmann, T.Matsuno, R.J.Murgatroyd, & J.F.Noxon (1981) Transport of trace constituents in the stratosphere. Rep. study grp.2 ,Middle atmosphere program handbook for M.A.P. Handbook vol **3**, 14-43

Matsuno,T. (1971) A dynamical model of the stratospheric sudden warming. J.Atmos.Sci., **28**, 1479-1494

Matsuno,T. (1980) Lagrangian motion of air parcels in the stratosphere in the presence of planetary waves. Contributions to current research in geophysics **-9**, "The Middle atmosphere" 189-216 { editors: S.V.Venkateswaran & N.Sundararaman.}

Matsuno,T. & K.Nakamura (1979) The Eulerian and Lagrangian mean meridional circulations in the stratosphere at the time of a sudden warming. J.Atmos.Sci., **36**, 640-654.

McIntyre,M.E. (1980a) An introduction to the generalised Lagrangian mean description of wave, mean-flow interaction. "The middle atmosphere" Contributions to current research in geophysics **-9**, 152-176

McIntyre,M.E (1980b) Towards a Lagrangian-mean description of stratospheric circulations and chemical transports. Phil.trans.R.S.London. **a296**, 129-148

McIntyre,M.E.& T.N.Palmer (1983) Breaking planetary waves in the stratosphere. Nature **305**, 593-600

McIntyre,M.E. (1987) Dynamics and Tracer transport in the middle atmosphere: an overview of some recent developments. From 'Transport Processes in the Middle atmosphere' D.Reidel Pu.Co., Edited by G.Visconti & R.Garcia., p267-296.

McPeters,R.D., D.F.Heath, & P.K.Bhartia. (1984) Average ozone profiles for 1979 from the Nimbus 7 SBUV instrument. J.Geophys.Res., **89**, D4, 5199-5214

Mechoso,C.R., D.L.Hartmann, & J.D.Farrara (1985) Climatology and interannual variability of wave, mean-flow interactions in the southern hemisphere. J. Atmos. Sci., **42**, 2189-2206

Murgatroyd,.R.J. & F.Singleton (1961) Possible meridional circulations in the stratosphere and mesosphere. Quart.J.R. Met. Soc., **87**, 125-135

Newell,R.E., D.G.Vincent, T.G.Dopplick, D.Ferruzza, & J.W.Kidson. (1969) The energy balance of the Global atmosphere, from 'The Global Circulation of the Atmosphere', 42-90, Edited by Corby,R., Met. Soc. London.

O'Neill,A & C.E.Youngblut (1982) Stratospheric warmings diagnosed using the TEM equations and the effect of the mean state on wave propagation. J.Atmos.Sci., **39**, 1370- 1386
v5

O'Neill,A. & V.D.Pope (1988) Simulations of disturbances in the stratosphere. Quart. J.R. Met. Soc., **114**, 1063-1109.

Oort,.A.H. (1964) On the energetics of the mean and eddy circulations in the lower stratosphere. Tellus **16**, 309-327

Oort,.A.H. & Rasmussen (1971) Atmospheric circulation statistics. NOAA Professional paper **5**, U.S. Dept. of commerce, Rockville.

Palmer,T.N. (1981a) Diagnostic study of a wavenumber two stratospheric sudden warming in a transformed Eulerian-mean formalism. J.Atmos.Sci., **38** 844-855

Palmer,T.N. (1981b) Aspects of stratospheric sudden warmings studied from a Transformed Eulerian-Mean viewpoint. J.Geophys.Res., **86**, 9679-9687

Palmer,T.N. (1982) Properties of the Eliassen-Palm flux for planetary scale motions. J. Atmos. Sci., **39**, 992-997

Palmer,T.N. & C-P.F.Hsu (1983) Stratospheric sudden coolings and the role of non-linear wave interactions in preconditioning the circumpolar flow. J.Atmos. Sci., **40**, 909-928

Pawson,S. (1987) Unpublished Ph.D. Thesis. University of Edinburgh.

Pick,D.R. & J.L.Brownscombe (1981) Early results based on the stratospheric channels of TOVS on the TIROS-N series of operational satellites. Int. Counc.Sci.Unions, Comm.Space Res., Adv. Space Res., **1**, No 4, 247-260

Pitari,G. & G.Visconti (1985) Two-dimensional tracer transport: derivation of residual mean circulation and eddy transport tensor from a three dimensional model data set. J.Geophys.Res., **90**, 8019-8032

Plumb,R.A. (1983) A new look at the energy cycle. J.Atmos.Sci., **40**, 1669-1688

Plumb,R.A. & J.D.Mahlman (1987) The zonally averaged transport characteristics of the GFDL general circulation/transport model. J.Atmos. Sci., **44**, 298-327

Pyle,J.A.& C.F.Rogers (1980a) Stratospheric transport by stationary planetary waves - the importance of chemical processes. Quart.J.R. Met. Soc., **106**, 421-446

Pyle,J.A.& C.F.Rogers (1980b) A modified diabatic circulation model for stratospheric tracer transport. Nature **287**, 711-714

Pyle,J.A. & C.F.Rogers (1984) Modelling tracer budgets in the stratosphere. Quart. J.R. Met. Soc., **110**, 1097-1106

Reed,R.J.& K.E.German (1965) A contribution to the problem of the stratospheric diffusion by large scale mixing. Mon. Weath. Rev., **93**, 313-321

Remsberg,E.E., J.M.Russell III, L.L.Gordley, J.C.Gille & P.Bailey (1984) Implications of the stratospheric water vapour distribution as determined from Nimbus 7 LIMS experiment. J.Atmos.Sci., **41**, 2934-2945

Robinson (1986) On the application of the quasi-geostrophic EP-flux to the analysis of stratospheric data. J.Atmos.Sci., **43**, 1017-1023

Rodgers,C.D. (1967) The radiative heat budget of the troposphere and lower stratosphere. M.I.T. Planetary circulation project Report A2, 99pp.

Rodgers,C.D. (1983) Clarendon Laboratory: Atmospheric Physics report upon the workshops on comparison of data and derived dynamical quantities during northern hemisphere winters. Atmospheric Physics Memorandum 84.1, Univ. of Oxford.

Russell,J.M.,J.C.Gille,E.E. Remsberg, L.L.Gordley, P.L. Bailey, S.R. Drayson, H.Fischer, A.Girard, J.E.Harries & W.F.J. Evans. (1984) Validation of Nitrogen dioxide results measured by the LIM of the stratospheric experiment on Nimbus 7. J.Geophys.Res., **89**, 5099-5107
Validation of water vapour results measured by the Limb infra-red monitor of the stratosphere experiment on Nimbus 7. J.Geophys.Res., **89**, 5115-5124

Rogers,C.F. & J.A. Pyle (1984) Stratospheric tracer transport: a modified diabatic circulation model. Quart. J.R. Met. Soc., **110**, 219-237

Rood,R.B. & M.R.Schoeberl (1983) A mechanistic model of Eulerian, Lagrangian mean and Lagrangian ozone transport by steady planetary waves. J.Geophys.Res., **88**, 5208- 5218

Rood,R.B. & M.R.Schoeberl (1983) Ozone transport by diabatic and planetary wave circulations on a beta- plane. J.Geophys.Res., **88**, 8491-8504

Shiotani,M. & I.Hirota (1985) Planetary wave, mean-flow interaction in the Stratosphere: a comparison between the northern and southern hemispheres. Quart. J.R. Met. Soc., **111**, 309-334

Schoeberl,M.R. (1981) A simple model of the Lagrangian mean-flow produced by dissipating planetary waves. J.Atmos.Sci., **38**, 1841- 1855

Schoeberl,M.R. (1982) Vacillation, sudden warmings and potential enstrophy balance in the stratosphere. J.Atmos.Sci., **39**, 1862- 1872

Schoeberl,M.R. (1983) A study of stratospheric vacillations and sudden warmings on a beta- plane. PART I : Single wave mean-flow interaction J.Atmos.Sci., **40**, 769- 787

Schoeberl,M.R. & D.F.Strobel (1978) The zonally averaged circulation of the middle atmosphere. J.Atmos.Sci., **35**, 577-591

Solomon,S., R.R.Garcia, & F.Strodal (1985) Transport processes and ozone perturbations. J.Geophys.Res., **90**, 12981-12989

Strobel,D.F. (1978) Parameterisation of the atmospheric heating rate from 15 to 120km due to O_2 and O_3 absorption of solar radiation. J.Geophys.Res., **83**, 6225-6230.

Tung,Ka Kit. (1982) On the two-dimensional transport of stratospheric trace gases in the isentropic co ordinates. J.Atmos.Sci., **39** 2330-2355.

Vincent,D. (1968) Mean meridional circulations in the northern hemisphere lower stratosphere during 1964 & 1965. Quart.J.R. Met. Soc., **94**, 333-p349

APPENDIX G
PUBLISHED PAPER.

References

Andrews, D.G., and M.E. McIntyre, Planetary waves in horizontal and vertical shear: Asymptotic theory for equatorial waves in weak shear, J. Atmos. Sci., 33, 2049-2053, 1976.

Barnett, J.J., and M. Corney, Middle atmosphere reference model derived from satellite data, in Handbook for MAP, Vol. 16, edited by K. Labitzke, J.J. Barnett, and B. Edwards, pp. 47-85, SCOSTEP Secretariat, University of Illinois, Urbana, IL, 1985.

Fels, S.B., A parameterization of scale-dependent radiative damping in the middle atmosphere, J. Atmos. Sci., 39, 1141-1152, 1982.

--------, and L.D. Kaplan, A test of the role of longwave radiative transfer in a general circulation model, J. Atmos. Sci., 33, 779-789, 1975.

--------, J.D. Mahlman, M.D. Schwarzkopf, and R.W. Sinclair, Stratospheric sensitivity to perturbations in ozone and carbon dioxide: radiative and dynamical response, J. Atmos. Sci., 37, 2266-2297, 1980.

Held, I.M., R.T. Pierrehumbert, and R.L. Panetta, Dissipative destabilization of external Rossby waves, J. Atmos. Sci., 43, 388-396, 1986.

Kiehl, J.T., and S. Solomon, On the radiative balance of the stratosphere, J. Atmos. Sci., 43, 1525-1534, 1986.

Mahlman, J.D., and L.J. Umscheid, Dynamics of the middle atmosphere: Sucesses and problems of the GFDL "SKYHI" general circulation model, in Dynamics of the Middle Atmosphere, pp. 501-525, Reidel Publishers, Dordrecht, Netherlands, 1984.

Oort, A.H., Global Atmospheric Circulation Statistics, 1958-1973, NOAA Professional Paper 14, U.S. Department of Commerce, National Oceanic and Atmospheric Administration, Rockville, MD., 1983.

Ramanathan, V., E.J. Pitcher, R.C. Malone, and M.L. Blackmon, The response of a spectral general circulation model to improvements in radiative processes, J. Atmos. Sci., 40, 605-630, 1983.

Shine, K., 1987: The middle atmosphere in the absence of dynamical heat fluxes. Quart. J. Roy. Meteor. Soc., submitted.

The residual circulation: Interhemispheric differences and heating and eddy components

S.R. Beagley and R.S. Harwood, University of Edinburgh
Department of Meteorology, JCMB,
King's Buildings, Mayfield Rd.,
Edinburgh EH9 3JZ
SCOTLAND.

Abstract. The residual circulation has been diagnosed using an "omega-equation" technique, which allows it to be split into the components driven by the various factors which are tending to destroy the thermal wind balance of the zonal mean state. This clarifies how the stratosphere is maintained away from zonal-mean radiative equilibrium conditions by the eddy heat and momentum fluxes. The "diabatic" circulation has also been diagnosed. This shows many similarities to the residual circulation, though we find the latter to be larger in the lower stratosphere.

The interhemispheric differences in residual circulation are discussed too. The differences found during months near the equinox are in the sense which is expected to result in the observed interhemispheric differences in total ozone.

1. Scope of the investigation

The introduction of the residual circulation and the related transformed Eulerian mean formalism (Andrews & McIntyre 1976, 1978) has led to a greater understanding of the processes governing the evolution of the zonal mean wind and temperature distributions. The residual circulation is also of importance in studying distributions of trace gases such as ozone, being closely related to the "diabatic" circulation and both being related to a Lagrangian mean or "transport" circulation (Dunkerton 1978). The residual or diabatic circulations have been proposed, or used, with suitable parametrizations for certain eddy effects, as the main basis for calculating constituent transport in 2-D chemical models (eg Pyle & Rogers 1980, Holton 1981, Garcia & Solomon 1983). It is to be anticipated therefore that the interhemispheric differences in such quantities as total ozone, will be clearly associated with interhemispheric differences in the residual circulation. In section 4 below, we present the stratospheric residual circulation for several months for the whole globe, tentatively noting features of the interhemispheric differences which may be related to those in the total ozone distribution.

G. Visconti and R. Garcia (eds.), Transport Processes in the Middle Atmosphere, 387–399.

In general the pattern of zonal mean (diabatic) heating and the torque produced by the divergence of Eliassen-Palm flux both disturb the thermal wind balance of the zonal mean state. The residual circulation can be regarded as the response to those disturbing tendencies, which opposes them to restore thermal wind balance. In section 3 below the relative contributions of heating and EP-flux convergence in "driving" the residual circulation for January 1979 are discussed and the total circulation compared with the "diabatic" circulation.

2. Computational details

The zonal mean momentum and thermodynamic equations may be written in the quasi-geostrophic approximation (Lorenz 1960) as

$$[u_t] - f[v_i] = -(c^2[v^*u^*])_y/(c^2) \qquad (1)$$

$$[\theta_t] + [v_i][\theta]_y + [w_i][\theta_\eta] = [Q] - (c[v^*\theta^*])_y/c - (p[w_i^*\theta^*])_\eta/p \qquad (2)$$

where $\eta = \ln(p_o/p)$; p = pressure; p_o = 1000 mbar; $w = D\eta/Dt$; subscripts t, y and η denote differentiation with respect to that variable; subscript i denotes "irrotational part"; square brackets and superscript star denote zonal mean and departure therefrom respectively and $c=\cos(\varphi)$ with φ = latitude.

Mass continuity implies the existence of a streamfunction ψ for the zonal-mean meridional circulation

$$[v] = -(p\Psi)_\eta/(pc),\ [w] = \Psi_y/c \qquad (3)$$

To this level of approximation the streamfunction ψ_R for the residual circulation (v_R, w_R) is given by

$$\Psi_R = \Psi + c[v^*\theta^*]/[\theta]_\eta \qquad (4)$$

Equations 1 & 2 are thereby transformed to

$$[u_t] - fv_R = ((cF^\varphi)_\varphi/(ac) + (F^\eta)_\eta)/(acp) \qquad (5)$$

$$[\theta]_t + v_R[\theta]_y + w_R[\theta]_\eta = [Q] - (p([\theta]_y[v^*\theta^*]/[\theta]_\eta + [w^*\theta^*]))_\eta/p \qquad (6)$$

where (F^φ, F^η) is the Eliassen Palm flux:

$$F^\varphi = -apc[v^*u^*] \ \&\ F^\eta = apcf[v^*\theta^*]/[\theta_\eta]$$

At this level of approximation, the meridional momentum equation leads to the thermal wind equation

$$[\theta]_y = -A[u]_\eta \qquad (7)$$

where $A = f(p_o/p)^\kappa/R$

Eliminating the time derivatives between 5 & 6 using 7 gives a 2nd order linear partial differential equation for ψ_R:

$$([\theta]_\eta\Psi_{R_y}/c)_y - ([\theta]_y(p\Psi_R)_\eta/pc)_y + Af((p\Psi_R)_\eta/pc)_\eta = (A/ac)((\nabla.F)/p)_\eta + [Q]_y - (p([\theta]_y[v^*\theta^*]/[\theta]_\eta + [w^*\theta^*])_y)_\eta/p \qquad (8)$$

This equation is elliptic provided the static stability exceeds a certain rather high value, which is the case for all the cases studied here.

Appropriate boundary condition at the poles are $\psi = 0$ ie $\psi_R = 0$. At the lower boundary, $\eta = 0$, $\psi = 0$ giving $\psi_R = \cos\phi\,[v^*\theta^*]/[\theta_\eta]$. The upper boundary condition is more problematical. Our approach is to impose an artificial boundary condition, viz $\psi_R = 0$ but to place the boundary sufficiently high not to affect the region of interest. Our aim is to diagnose the stratospheric circulation up to 1 mbar. Accordingly the boundary has been set at 0.006 mbar. Trial integrations show that the solution in the stratosphere is insensitive to the value of ψ_R at that height (Beagley 1987).

Equation 8 and similar ones discussed below have been solved on a y-η grid, spaced at 5 degree intervals in latitude and 0.75 in η, by a relaxation technique, with the winds temperatures and EP fluxes based on temperatures deduced from either the SSU or LIMS temperature measurements and tropospheric data supplied by the U.K. Meteorological Office, using the geostrophic and hydrostatic equations as appropriate. As the satellite data do not extend beyond 1 mbar, the E-P fluxes have been smoothly reduced above this level to reach zero at the upper boundary. A sensitivity test has shown that the solution below 1 mbar is very little affected by the values above.

The diabatic heating rates needed for the right hand side of eq. 8 have been calculated using the radiation code of Haigh (1984).

3. Processes forcing the residual circulation

Equation 8 is of the form $L(\psi_R) = R_Q + R_E$ where L is the elliptic operator, R_Q represents the term in heating and R_E represents the terms on the right involving eddy fluxes. Since L is linear, we may write $\psi_R = \psi_Q + \psi_E$ where ψ_Q and ψ_E satisfy $L(\psi_Q) = R_Q$ and $L(\psi_E) = R_E$. The boundary conditions are satisfied by specifying $\psi_E = 0$ and $\psi_Q = 0$ on all boundaries except that at the bottom boundary $\psi_E = \psi_R$. ψ_Q can be regarded as being forced by diabatic processes and ψ_E by eddies.

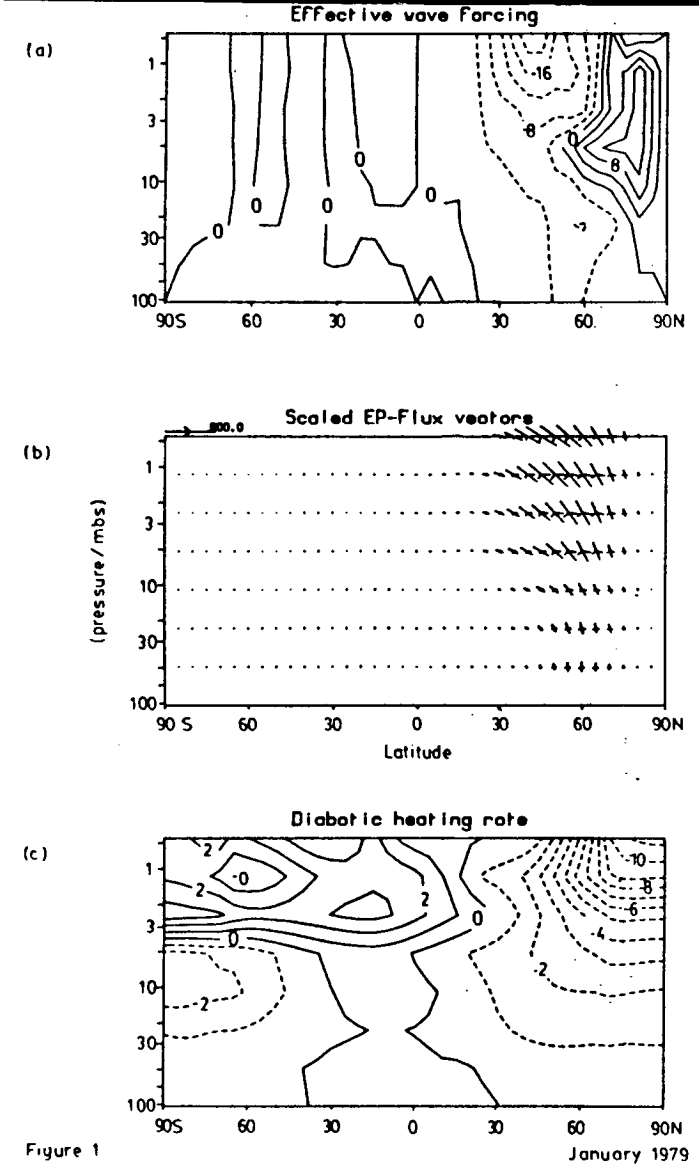

Figure 1

(a) Divergence of E-P flux expressed as a specific zonal force (equivalent acceleration).The contour interval is 4 x 10^{-5} m s^{-2}. (b) E-P flux, scaled as F/p. (c) Diabatic heating rate. The Contour interval is 1 K/day. January 1979.

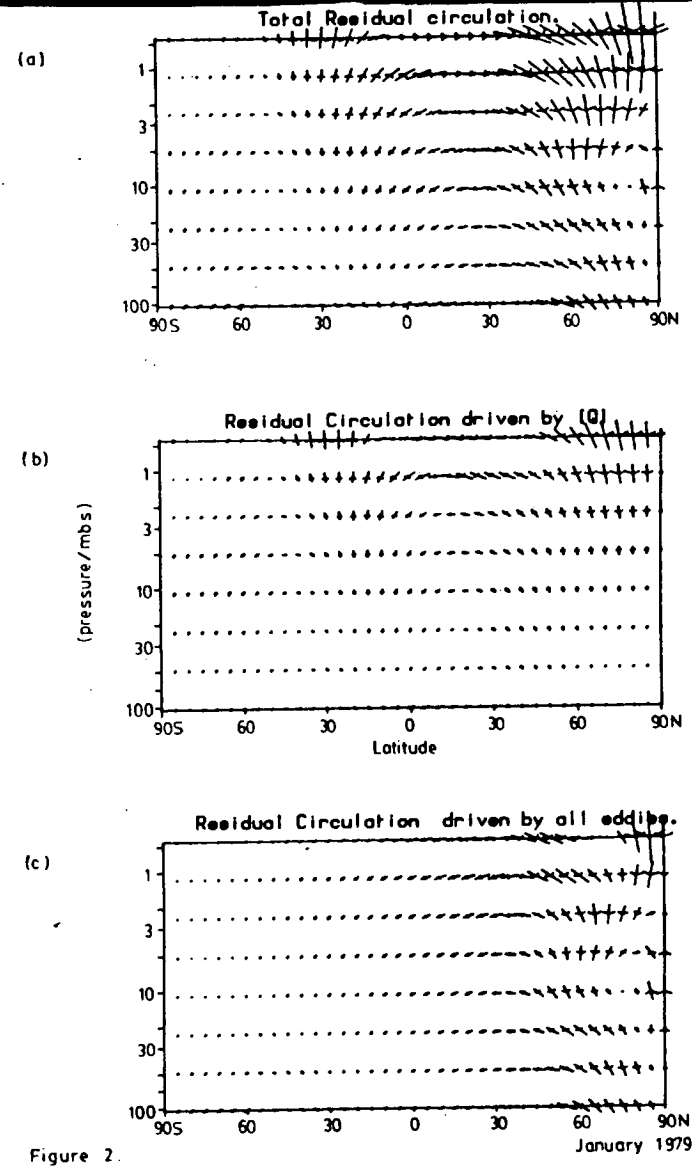

Figure 2

Components of the residual circulation for january 1979. Arrows show velocity (distance travelled in 10 days). (a) Total circulation. (b) Circulation corresponding to Ψ_Q.(c) Circulation corresponding to Ψ_E.

In this section we show some details of ψ_E and ψ_R for January 1979. The required temperatures, ozone values and eddy fluxes were taken from LIMS data, extrapolated to the south pole as appropriate. As the extrapolated area is only 8% of the globe and the eddies have small amplitudes in the summer hemisphere, this is not thought to introduce significant uncertainties.

Note that not all physical processes have been taken into account. The technique adopted here contains no estimates of the convergence of vertical fluxes of momentum associated with gravity or equatorial waves. The circulations induced by the latter are small (see fig.7 of Gray and Pyle (1986)), though they have a significant impact upon the tracer distributions. These effects add linearly to the right of equation 8.

Fig. 1c shows the diabatic heating rate. It is broadly similar to those presented by Kiehl & Solomon(1986) and Gille & Lyjak (1986) but with some differences. Some of these probably arise because no adjustments for mass-balance have been made in the calculations shown here. Fig. 1b shows the E-P flux and fig. 1a its divergence, expressed in terms of the specific force (equivalent acceleration) produced on the mean flow.

Figs. 2b and 2c show the circulations corresponding to figs. 1c and 1a respectively and Fig. 2a shows their sum. Throughout most of the winter hemisphere the eddy-driven circulation is dominant, especially in the low stratosphere where the circulation driven by heating is very small. The circulation driven by the eddies has a predominately sinking motion near the winter pole and the heating effect of this circulation can be regarded as part of the mechanism which keeps the winter pole above the radiative equilibrium temperature, leading in turn to the heating pattern (fig. 1C) and the corresponding circulation driven by the heating (which also acts in a way to warm the winter pole).

We have diagnosed a small area of rising motion near the north Pole which is reminiscent of, but at a lower height than, that found by Al-Ajmi et al (1985) in the southern hemisphere. It is possible however that this is a spurious feature, as the use of geostrophic winds is known to lead to some misrepresentation of the E-P fluxes (Robinson 1986). The strongest rising motion driven by eddies is in low latitudes of the summer hemisphere with some descent at the summer pole. Thus the general directions of the circulations driven by eddies and by heating have an overall similarity, reflecting the fact that the heating is produced by departures from radiative equilibrium which arise from the eddy induced circulations.

It is of interest to compare the residual circulation with the diabatic circulation. This is essentially the circulation diagnosed from the thermodynamic equation (6) alone usually with the time derivative set to zero and an adjustment made (equivalent to adjusting Q) to ensure mass-consistence (cf Gille et al 1987). Substituting for ψ_D (the diabatic streamfunction) and differentiating with respect to latitude gives an equation for ψ_D which may be compared with that for ψ_R or ψ_Q, namely

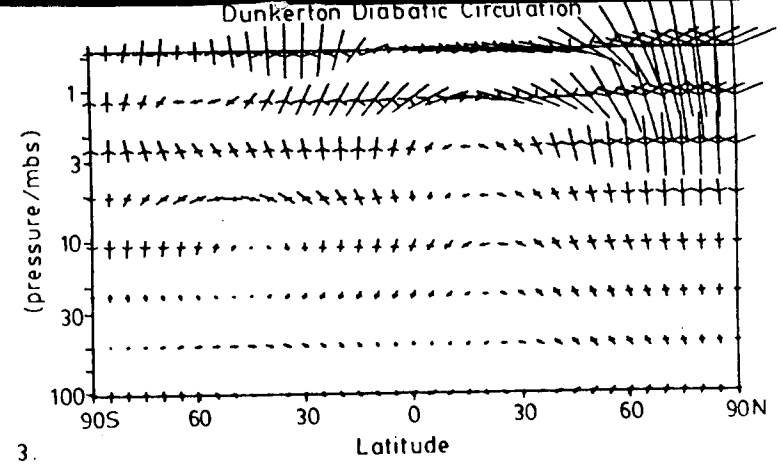

Figure 3.

Diabatic circulation (corresponding to Ψ_D) for January 1979.

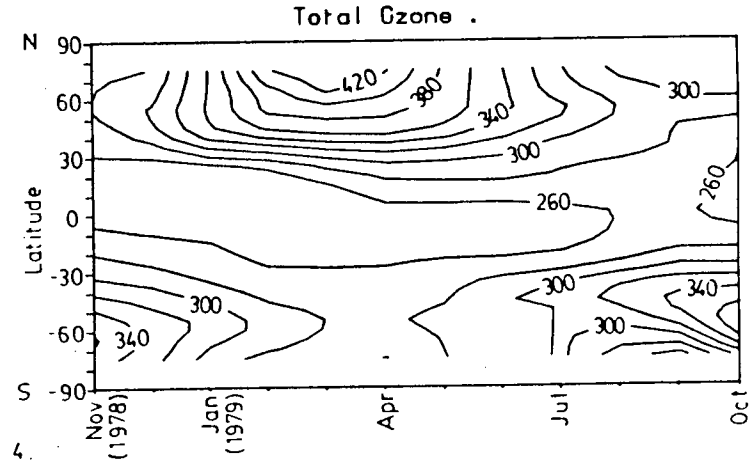

Figure 4.

Total Ozone in Dobson units based on McPeters et al 1984.

$$([\theta]_\eta \overline{v}_{\theta y}/c)_y - ([\theta]_y (p\overline{w}_\theta)_\eta/pc)_y$$

$$= -(p([\theta]_y [v^* \theta^*]/[\theta]_\eta + [w^* \theta^*])_y)_\eta/p + [Q]_y \qquad (9)$$

The diabatic circulation is in fig. 3. The relation between the sign of the vertical velocity and heating pattern is very apparent. This relationship leads to some differences from the residual circulation especially, at the summer pole where quite strong vertical velocities are diagnosed for the diabatic circulation (which depends on absolute values of the (mass-adjusted) heating), while much smaller velocities are diagnosed for the residual circulation (which involves only the gradients of heating -see equation 8).

4. Interhemispheric differences in residual circulation

The idea that the residual circulation is an approximation to a Lagrangian mean circulation (Dunkerton 1978) leads to the expectation that interhemispheric differences in the circulation should be discernible which are related to those in total ozone. Some indirect evidence for this contention comes from the (Eulerian) 2-D modelling experiment of Harwood and Pyle (1977) which produced fairly realistic interhemispheric differences in total ozone although the only differences imposed on the model were through the momentum fluxes. Accordingly we have investigated the interhemispheric differences in residual circulation for 1 year, December 1978 - November 1979.

The residual circulation has been calculated from equation 8. The ozone data for the heating rate calculations were taken from McPeters et al (1984). The dynamical fields required were taken from data supplied by the UK meteorological office based on measurements from the Stratospheric Sounding Unit on TIROS-N. The measurements are global in extent. During the period under study the upper channel of the SSU instrument was subject to considerable noise. This results in a loss of about 30 percent of data for each month, so that the results presented here are somewhat tentative. We have compared the circulations deduced using SSU data with those using LIMS data where these are available. This comparison shows the circulation deduced from the two data sets to be essentially the same below 5 mbar, but above this level the circulations based on LIMS data are stronger than those based on SSU data. (Beagley 1987). Accordingly we believe the results presented here are trustworthy for the lower 2/3 of the stratosphere, but should be treated with caution in the top 1/3.

Figs. 5-7 show a selection of three of the interhemispheric differences. Fig. 5a shows the circulation for December 1978 and fig. 5b that for June 1979. To obtain fig. 5c, the June circulation is reflected about the equator and subtracted from the December circulation. Very little difference is found between the two circulations for these months

Fig. 6 shows February and August 1979 treated in the same way. February 1979 was the occasion of a major warming in the northern

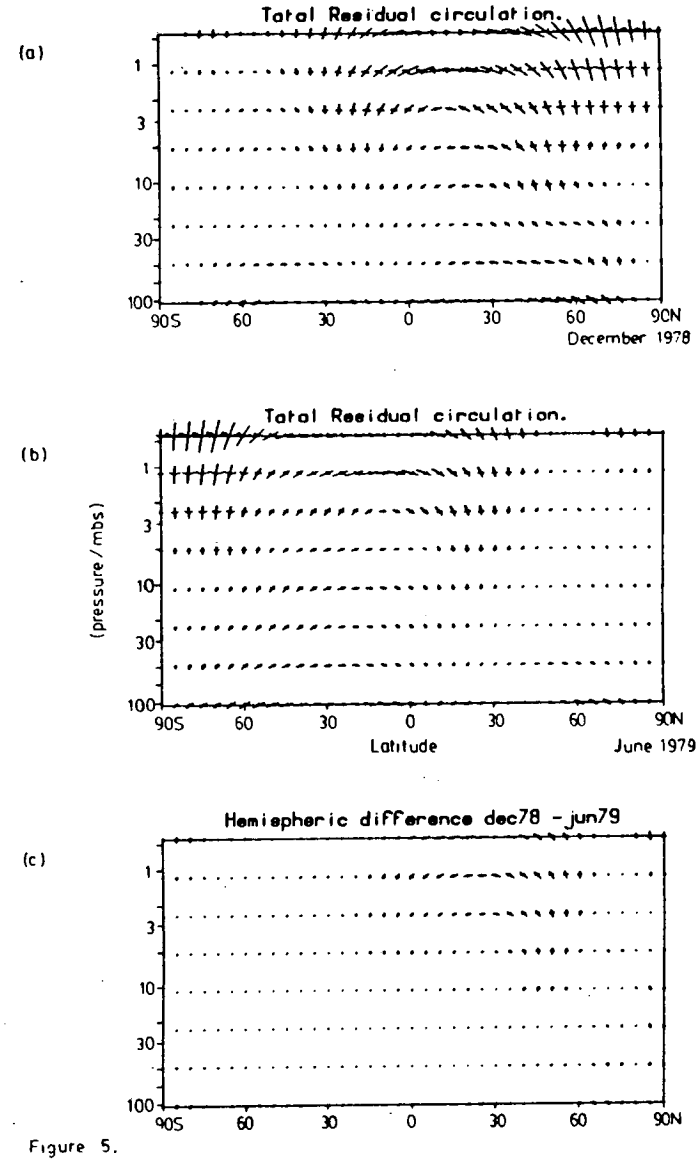

Figure 5.

Residual circulation for: (a) December 1978, (b) June 1979, (c) The difference between (a) and the reflection of (b) about the equator. The arrows are scaled as in fig 2.

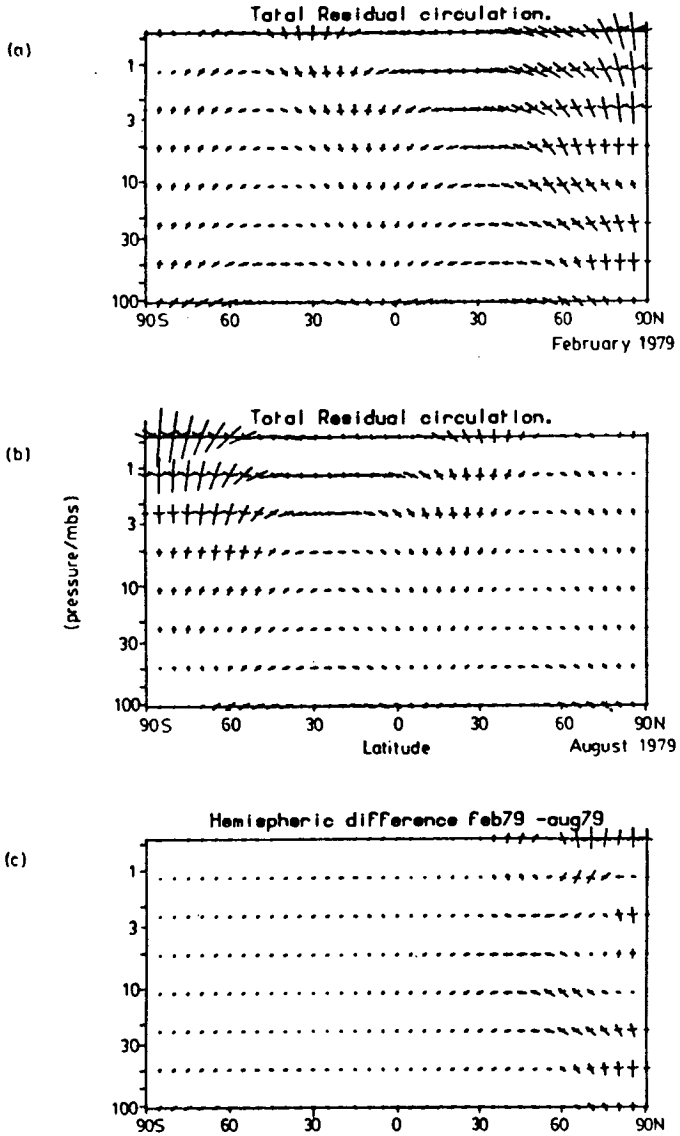

Figure 6

As fig 5 but for: (a) February 1979, (b) August 1979.

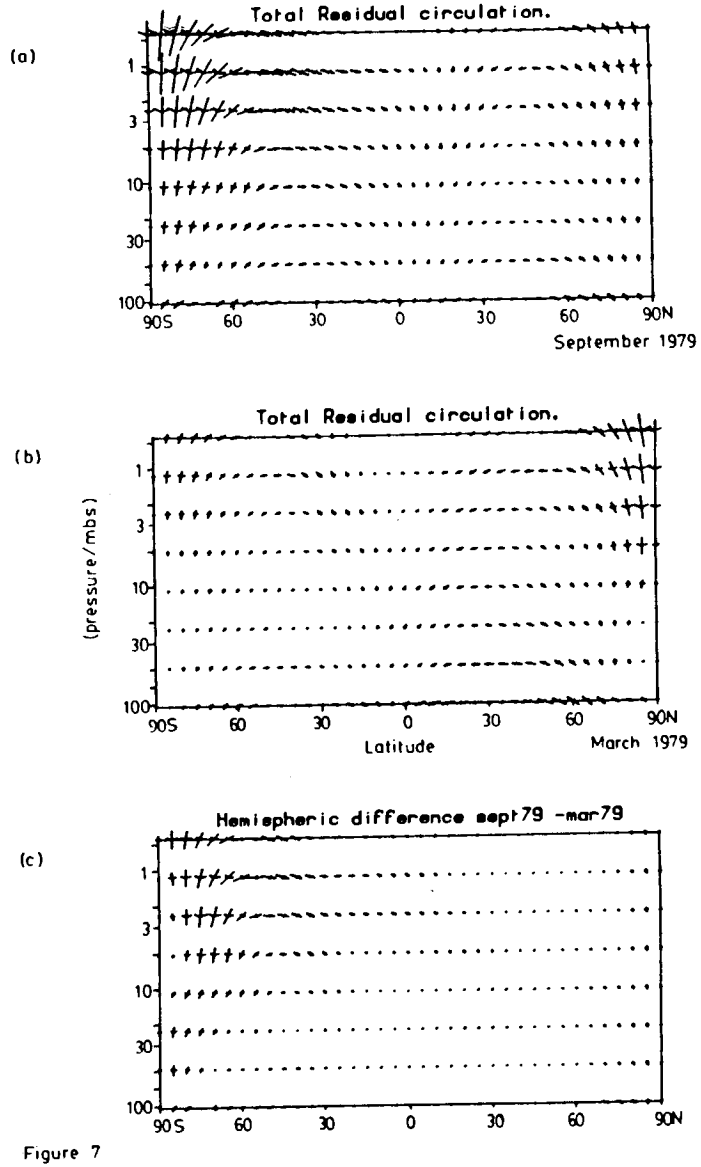

Figure 7

Similar to fig 5 except: (a) September 1979, (b) March 1979.

Hemisphere (Palmer (1981), amongst others), so it is not surprising to see the winter sinking motion is stronger in the lower stratosphere in February in the north than in August in the south. This is clearly brought out in the difference diagram (fig. 6c). It is of interest to compare the behaviour of the total ozone in these two months (see fig 4). A notable difference is the greater rate of increase of ozone at high latitudes in the north in February compared with that in the south in August. It is probable that this is related to the stronger poleward and downward motion below the middle stratosphere in February.

Fig 7 shows similar figures for March and September. Here, however the difference diagram, fig. 7c, has been obtained by reflecting the March values about the equator and subtracting them from those for September. We find much stronger sinking motion during the southern spring in high latitudes than in the northern spring. The autumnal circulations are fairly similar leading to only small differences, and are in general smaller than the vernal values. The total ozone distribution (fig 4) shows ozone increasing in September in middle and high latitudes of the southern hemisphere but declining in the north in March. These differences are consistent with what might be anticipated from the differences in motion field coupled with photochemical destruction. The ozone changes in the autumn hemisphere are less rapid. Very similar remarks apply to April/October (not shown).

These results suggest a relationship between the interhemispheric differences in behaviour of total ozone and the residual circulation, but they are not unequivocal. For instance the ozone was building up much more strongly in the north in December than in the south in June but we find little difference between the circulation for those months. A possible way to clarify the role of the residual circulation in creating interhemispheric differences in ozone is to use the circulations deduced here in a transformed Eulerian mean 2-D chemical model of stratospheric chemistry. We are currently attempting to arrange such a test.

Acknowledgements

S.R. Beagley was supported by a NERC studentship when this work was performed. We thank Dr. Haigh for supplying us with the code of the radiation calculations.

References

Al-Ajmi,D.N., R.S.Harwood and T. Miles, 1985: A sudden warming in the middle atmosphere of the southern hemisphere. Quart. J. R. Met.Soc. 111,359-389.

Andrews,D.G and M.E.McIntyre, 1976: Planetary waves in horizontal and vertical shear: The generalised Eliassen-Palm relation and the mean zonal acceleration. J.Atmos. Sci., 33 2031-2048

Andrews,D.G. and M.E.McIntyre, 1978: Generalized Eliassen-Palm and Charney-Drazin theorems for axisymmetric flows in compressible atmosphers. J.Atmos.Sci., 35, 175-185.

Beagley,S.R., 1987. Unpublished Ph.D. thesis. Edinburgh University.

Dunkerton,T., 1978: On the mean meridional mass motions of the stratosphere and mesosphere. J.Atmos.Sci., 35 2325-2333.

Gille,J.C. and L.V.Lyjak, 1986: radiative heating and cooling rates in the middle atmosphere. J.Atmos.Sci., 43,2215-2229

Gille, J.C., L.V.Lyjak and A.K.Smith, 1987: The global residual mean circulation in the middle atmosphere for the northern winter period. J.Atmos.Sci., 44, 1437-1452.

Garcia, R.R. and S.Solomon, 1983: A numerical model of the zonally averaged dynamical and chemical structure of the middle atmosphere. J.Geophys. Res., 88, 1379-1400.

Grey, L.J. and J.A.Pyle, 1986: The semi-annual oscillation and equatorial tracer distributions. Quart.J.R.Met.Soc, 112, 387-407.

Haigh, J.D.,1984: Radiative heating in the lower stratosphere and the distribution of ozone in a two-dimensional model. Quart.J.R.Met.Soc., 110, 167-185.

Harwood, R.S. and J.A.Pyle, 1977: Studies of the ozone budget using a zonal mean circulation model and linearized photochemistry. Quart. J.Roy.Meteor.Soc., 103, 319-343.

Holton, J.R.,1981. An advective model for two-dimensional transport of stratospheric trace species. J.Geophys.Res., 86, 11989-11994

Kiehl,J.T. and S.Solomon, 1986: On the radiative balance of the stratosphere. J.Atmos.Sci., 43, 1525-1534.

Lorenz,E.N., 1960: Energy and numerical weather prediction. Tellus 12, 364-373.

McPeters,R.D., P.F.Heath and P.K.Bhartia, 1984: Average Ozone profiles for 1979 from the Nimbus 7 SBUV instrument. J.Geophys.Res., 89 D4, 5199-5214.

Palmer,T. 1981: Diagnostic study of a wavenumber-2 stratospheric sudden warming in a transformed Eulerian-mean formalism. J.Atmos.Sci., 38, 844-855.

Pyle,J.A. and C.F.Rogers, 1980: A modified diabatic circulation model for stratospheric trace transport. Nature, 287, 711-714

Robinson,W.A., 1986: On the application of the quasi-geostrophic EP-flux to the analysis of stratospheric data. J.Atmos.Sci., 43, 1017-1023.